UNIVERSITY OF BIRMINGHAM

School of Biosciences

Zinc as a potential therapy for Burkitt's lymphoma

By:

Bader Ahmed Alhazmi

30 June 2022

Thesis submitted for:

The degree of Doctor of Philosophy
(PhD)

Supervised by:

Dr. Farhat Khanim

Prof. Chris Bunce

بِسۡمِ ٱللَّهِ ٱلرَّحۡمَٰنِ ٱلرَّحِيمِ

Acknowledgements

In the Name of Allah, the Most Beneficent, the Most Merciful. In the beginning, I would like to thank Allah for giving me the chance to study and complete my PhD journey and passing all obstacles and difficulties, alhamdulillah.

I would like to address my extreme grateful to my great supervisor Dr. Farhat Khanim and Prof. Chris Bunce for their continuous. I am grateful for their continuous support, advice, patience, guidance. As I will never forget having a great science with them, I will never forget their presence during my down moments to help me. Thank you Prof. Mark Drayson for sharing your experience, generous support and your valuable time.

My special thanks to my mother Fayzah who helped me during my PhD with her prays and taking off my pressures during hard times. My sincere thanks to my father Ahmed who was checking up on me daily. I wish that he is still with me at this moment, may Allah cover him with mercy, blessing and grant him heavens (Amen). My thanks also go to my life partner and my great wife Reem for standing with me during my difficult times to go through my PhD. Also, I would like to thank my brothers Bander and Turki and my sisters Doa'a and Alya'a for encouraging me during my PhD.

My big thanks to Dr. Yao Jiang and Dr. Sandro Trova for being great friends that I consider as brothers who advised me and helped me to gain many skills during my PhD. Also my thanks go to everyone in my group, Mr. Flavio Beke, Dr. Maiss Al-Amere, Dr.Elis Nitao, Dr. Zuhal Eraslan.

I would like to thank the ministry of higher education in Saudi Arabia represented by Umm Al-Qura University and Saudi cultural bureau in the United Kingdom for sponsoring my PhD scholarship. My appreciation goes to the university of Birmingham for providing all required and related facilities.

Finally, this study illustrates important scientific findings and added significant scientific points. I hope furthermore expansion for this work to help needy people around the world.

Abstract

Burkitts lymphoma (BL) is a form of non-Hodgkin lymphoma (NHL) that arises from germinal center B cells. BL is characterized by translocations of the *C-MYC* oncogene to immunoglobulin light and heavy chain loci resulting in its constitutive deregulated expression. BL shows a rapid and aggressive growth pattern. There are three different forms of BL; sporadic BL (sBL), immunodeficiency-associated BL and endemic BL (eBL) which accounts for ~50% of all paediatric cancers in Sub-Saharan Africa. Due to financial restrictions, treatment and supportive care options are limited resulting in poorer outcomes in low - middle income countries (LMICs). Thus, there is a need to develop new affordable effective low toxicity treatments for eBL.

Prior to this study, a panel of BL cell lines were tested against an in-house custom drug repurposing library developed in our lab (FMC Library) that contains ~100 approved and commonly used drug. This screen identified the nutritional supplement zinc acetate as an effective anti-BL candidate. Dose response studies showed that all BL cell lines tested had little/no response to zinc at 50 μM whereas 100 μM zinc killed all BL cell lines. In contrast, 100 μM zinc acetate induced no killing against a panel of non-BL cell lines including acute myeloid leukaemia (AML) which is a non BL cell tumour, diffuse large B cell lymphoma (DLBCL) which represent a B cell lymphoma that arise from germinal centre B cells and EBV infected lymphoblastoid cell lines (LCL) as a control cells. The latter were used as karyotypically normal B cell controls. Cell death in BL cells was associated with positive flow cytometry staining for propidium iodide and annexin V and activation of caspase 3 and 9 (western blotting) indicating cell death by apoptosis.

The proto-oncogene *C-MYC* is mutated or deregulated in >50% of cancers. In BL, deregulated expression occurs as a consequence of translocation of *C-MYC* on chromosome 8q24 to either the immunoglobulin heavy chain enhancer region on 14q32 (85% of cases) or the immunoglobulin kappa light chain or lambda loci on 2p12 or 22q11, respectively (15% of cases). Thus, the effect of zinc on C-MYC protein levels were studied. Western blot analysis showed that 100 μM zinc was able to reduce C-MYC protein levels rapidly and sustainably in BL cell lines whereas no change in C-MYC protein levels was observed in non-BL cell lines. Zinc-induced reduction of C-MYC

protein levels was time-dependent, reducing by approximately 20% after 6 hours with little/no protein detectable after 24 hours.

C-MYC protein levels were not reduced following treatment with 50 μM zinc. Quantitative real time PCR (qRT-PCR) also showed a rapid reduction in C-MYC mRNA levels in BL cell lines after 6 hours exposure to 100 μM but not upon exposure to 50 μM. Again, no reduction in C-MYC mRNA levels was seen in non-BL cell lines. Translocations of other genes to the immunoglobulin loci occur in other forms of NHL. The DLBCL cell line SU-DHL-4 has a t(14;18) translocation resulting in deregulated expression of the protooncogene *BCL2*. Western blotting showed no decrease in BCL-2 protein levels in SU-DHL-4 in response to either 100 μM or 50 μM zinc acetate after 6 or 24 hours indicating a selectivity of zinc action against *C-MYC* protein in BL cells.

To further investigate the role of altered *C-MYC* expression in zinc-mediated killing of BL cells, the eBL cell lines Raji and Namalwa were stably transfected with *C-MYC* using a piggyBac transposon system that allows gene expression under a constitutively active promoter. However, overexpression of *C-MYC* from an alternative promoter did not rescue BL cells from killing by 100μM zinc. Although western blotting showed that C-MYC protein levels were protected after 6 hours, protein reduction and loss of viability was again observed after 24 hours indicating that loss of C-MYC is important in zinc-mediated killing of BL cells. In a second approach to rescue *C-MYC* expression, the proteasome inhibitor Bortezomib was used to inhibit C-MYC protein degradation via the ubiquitin-proteasome system (UPS). Whilst increases were observed in overall ubiquitinated proteins indicating bortezomib was working, western blotting and flow cytometry showed no rescue of C-MYC protein levels. Furthermore, bortezomib did not rescue cells from zinc-mediated killing after 24 hours.

In conclusion, findings from this study have identified that 100 mM zinc is effective at killing BL cell lines selectively, and that this killing is associated with activation of apoptotic markers. Treatment with zinc resulted in a rapid and sustained reduction in C-MYC mRNA and protein levels that could not be rescued through constitutive overexpression or the use of proteasome inhibitors. Given that zinc deficiency is common in sub-Saharan Africa and that zinc supplementation is safely used to treat diarrhoeal episodes in children, the studies proposed here indicate that zinc may safely be used as an adjunctive therapy to target *C-MYC* in BL.

Table of Contents

List of Figures

List of Tables

List of abbreviation

ABL	Tyrosine-protein kinase ABL1
Abs	Antibodies
AID	Activation induced cytidine deaminase
Akt	Protein kinase B
ALL	Acute lymphoblastic leukaemia
ALP	Alkaline phosphatase
AML	Acute myeloid leukaemia
AP	Abasic DNA site
APC	Antigen presenting cells
APC	Adenomatous polyposis coli
APEX	Apurinic/apyrimidinic AP endonucleases
APOBEC	Apolipoprotein B mRNA-editing enzyme, catalytic polypeptide
ARID1A	AT rich interaction domain containing protein A1
ATP	Adenosine 5'-triphosphate
BaP	Bezafibrate and Clofibrate
BART	BamHI fragment A rightward transcript
BCR	B cell receptor
BCRp	Breakpoint Cluster Region protein
BER	Base pair excision repair
bHLHZip	Basic helix-loop-helix zipper
BL	Burkitt's lymphoma
BM	Bone marrow
BTK	Bruton Tyrosine Kinase
C3a	Complement component 3a
C3b	Complement component 3b
C5a	Complement component 5a
C5b	Complement component 5b
C6	Complement component 6
C7	Complement component 7
CA	Clofibrate
CAD	Carbamoyl-phosphate synthetase 2, aspartate transcarbamylase
CARs	Chimeric antigen receptor
CCND3	Specific cyclin D3
CD	Cluster of differentiation
CD40L	Cluster of differentiation 40 ligand
CIDR1α	Cysteine rich interdomain region 1-alpha
c-KIT	Type III receptor tyrosine kinase
CK1	Casein kinase 1
CLL	Chronic lymphocytic leukaemia
CLP	Common lymphoid progenitors
Cmax	Maximum serum does

CML	Chronic myeloid leukaemia
CRC	Reticular cell
CSR	Class switch recombination
CXCL12	CXC chemokine ligand 12
CXCR4	CXC chemokine receptor 4
DLBCL	Diffuse large B cell lymphoma
DSB	Double strand breaks
DVL	Disheveled proteins
DZ	Dark zone
E2A	E-box binding protein 2A
EBER	Epstein Barr Virus (EBV) encoded RNA
EBF	Early B cell factor
eBL	Endemic Burkitt's lymphoma
EBNA	Epstein Barr nuclear antigen
EBV	Epstein Barr virus
ERK	Extra cellular receptor kinase protein
Fab	Fragment antigen binding
Fc	Fragment crystallizable
FDC	Follicular dendritic cell
FISH	Fluorescence in situ hybridization
FL	Follicular lymphoma
Flt3	Fms-like tyrosine kinase
FOXO1	Forkhead box protein O1
FZD	Mitogenic activation of Frizzled
GATA-1	GATA-binding factor 1
GC	Germinal centre
GLUT1	Glucose transporter
GM-CSF	Granulocyte-macrophage colony-stimulating factor
GSK3β	Glycogen synthase kinase 3 β
HIC	High-income countries
HIV	human immunodeficiency virus
HK II	Hexokinase II
HL	Hodgkin lymphoma
HLA	Antigen class II
HLH	helix loop helix
HSC	Haemopoietic stem cell
ICAM-1	Intercellular Adhesion Molecule 1
ID3	Inhibitor Of DNA Binding 3
IDC	Interstitial dendritic cells
Ig	Immunoglobulin
IGF-1	Insulin-like growth factor 1
IgH	Immunoglobulin heavy chain
IgL	Immunoglobulin light chain

IKAROS	IKAROS transcription factor
IL-21	Interleukin 21
IL-4	Interleukin 4
IL-7	Interleukin 7
IL7R-α	Interleukin-7 receptor subunit alpha
JAKs	1/-2 kinases family
LCL	Lymphoblastoid cell line
LDHA	Lactate dehydrogenase A
LEF	lymphoid enhancer factor
LFA-1	Lymphocyte function-associated antigen 1
LIC	Low-income countries
LMP	Lymphoid multipotent progenitor
LRP6	Lipoprotein receptor related protein 6
LZ	Light zone
MAC	Membrane attack complex
MBR	Major breakpoint region
MCL	Mantle cell lymphoma
MCL-1	Myeloid cell leukemia-1
MCR	Minor cluster region
MDC	Myeloid dendritic cells
Meg-CSF	Megakaryocyte colony stimulating factor
MHCI	Major histocompatibility class I
MHCII	Major histocompatibility class II
MMP	Multipotent progenitor cell
MMR	Mismatch repair mechanism
MPA	Medroxyprogesterone acetate
MPC	Multipotent progenitor cells
MSH	Highly conserved MutS homologs
MUC1	Glycoproteins like mucin 1
MUC12	Glycoproteins like mucin 12
MUC4	Glycoproteins like mucin 4
MZL	Marginal zone lymphoma
NF-kB	Nuclear Factor kappa-light-chain-enhancer of activated B cells
NHE III	Nuclease hypersensitive element III
NHEJ	Non-homologous end joining pathway
NHL	Non-Hodgkin lymphoma
NOTCH	Neurogenic locus notch homolog protein 1
ODC	Ornithine decarboxylase
PAX5	Paired BOX
PI3K	Phosphoinositide 3-kinases
PPs	Peyer’s patches
Pre- B cell	Precursor B cell
Pro-B cell	progenitor B cell
PRR	Pattern recognition receptors

PU.1	Purine box factor 1
RAG1	Recombination activating gene 1
RBC	Red blood cell
sBL	sporadic Burkitt's lymphoma
SCF	Stem cell factor
SHM	Somatic hypermutation
SSB	single strand breaks
STAT	signal transducers activators of transcription
SWI/SNF	SWitch/Sucrose Non-Fermentable
T1	Transition 1
T2	Transition 2
Tat	Trans activator of transcription
TCF3	Transcription Factor 3
TCF	T-cell factor
TF	Transcription Factor
TLR	Toll like receptor
TMD	Transmembrane domains
TP53	Tumour protein P53
UDG	Uracil-DNA glycosylase
UNG	Uracil-DNA glycosylase
VCAM-1	Vascular cell adhesion protein 1
WBCs	White blood cell
Wnt	Wingless related integration site

CHAPTER ONE
INTRODUCTION

1 Introduction.

1.1 The blood components.

Blood is composed of; plasma, red blood cells (RBCs), white blood cells (WBCs) and platelets. Plasma occupies around 50% of total blood volume and water forms more than 90% of its total composition (Maton *et al.*, 1997). Due to the presence of proteins such as albumins, plasma is the delivery source of nutrients to the body's cells. Electrolytes like potassium, sodium and chloride are dissolved in plasma. Similarly, hormones required for cellular communication or growth are carried by plasma alongside with clotting proteins factors including fibrinogens, prothrombin.

Red blood cells (RBCs) are biconcave shaped, circular and non-nucleated disc cells enriched with haemoglobin which binds oxygen in the lungs and forms oxyhemoglobin, thereby transporting oxygen to all parts of the body. Oxygen is required for aerobic respiration to produce energy in the form of adenosine 5'-triphosphate (ATP) (Klinken, 2002, Organization *et al.*, 2014, Hoffbrand and Moss, 2015). Carbon dioxide, a by-product of cellular metabolism combines with haemoglobin in RBCs to form carbaminohaemoglobin which, upon transport to the lungs, release carbon dioxide. Another function carried by haemoglobin in RBCs is the regulation of acid-base balance.

Blood also consists of white blood cells (WBCs) which are important in defending against pathogens. WBCs are classified into two main groups; granulocytes which includes neutrophils, eosinophils, mast cells and basophils, and agranulocytes which includes lymphocytes and monocytes. Granulocytes differ from agranulocytes by the presence of granules that contain antimicrobial agents released as a defence response mechanism. For example, defensins, acid hydrolases and lysosomal enzyme are released from granulocytes to facilitate bacterial digestion (Organization *et al.*, 2014).

Lymphocyte are comprised of B and T cells. B lymphocytes primarily develop in the bone marrow (BM) and move to lymph nodes for further development. B cells mature into plasma cells and memory B cells that produce antibodies. Antibodies contribute to anti-microbial immunity in several ways:

1- they can bind to pathogens preventing them from entering and infecting cells or tissues.
2- They stimulate the clearance of pathogens by coating the pathogens to mark them for macrophages (Shahaf *et al.*, 2016, Cano and Lopera, 2013).
3- They stimulate other arms of the immune system such as complement proteins that create pores in the membranes of pathogens leading to cell lysis and death.

T lymphocytes have an important role in cell mediated immunity by releasing cytokines that regulate natural killer (NK) cell activity and the development of activated B cells. Although T progenitor cells are in the bone marrow, the thymus is the primary site for T cells development. Most viral infections are cleared by the help of T lymphocytes. The different types of T cells are cytotoxic T cells (CD 8) and T helper (CD 4) (Sauls *et al.*, 2018, Janeway Jr *et al.*, 2001).

Platelets are another cellular component of the blood and play an essential role in the coagulation process and wound healing through formation of blood clots (Chanarin, 1989). Platelets have a short half-life of about 7 days and normal platelet count is 150,000-450,000 cells per cubic millimetre. Platelets are produced in a process termed megakaryopoiesis which involves HSPC differentiation into megakaryocytes by the effect of megakaryocyte colony stimulating factor (Meg-CSF) (Siegal *et al.*, 1999, Bernitz *et al.*, 2017).

Cell type	Cell count / L	Cell size (μm)	Half life
Red blood cells	$4.50 – 6.50 \times 10^{12}$	7 – 8	100 – 120 days
Basophils	$0.02 – 0.10 \times 10^{9}$	10 – 14	Few hours – few days
Eosinophils	$0.1 – 0.4 \times 10^{9}$	12 – 15	5 days
Neutrophils	$1.8 – 7.5 \times 10^{9}$	12 – 14	6 hours – few days
Monocytes	$0.2 – 0.8 \times 10^{9}$	16-22	Months
Lymphocytes	$1.0 – 4.0 \times 10^{9}$	5 – 17	Hours – years
Platelets	$140 – 400 \times 10^{9}$	2 – 4	5 - 10 days

Table 1. 1 The cellular component of blood. (Rawat *et al.*, 2015, NHS, 2022).

1.2 The formation of blood cells Haematopoiesis.

The human body continually replenishes blood cells in a process termed haematopoiesis. Embryonic mammalian blood formation begins in yolk sac blood islands. Later, the site of blood formation is gradually relocated to the liver before it moves to central BM during human development (Tavian and Peault, 2003). RBCs are the first type of blood cells to be formed within the early stage of embryogenesis to support oxygen transportation which is required for tissue development (Tavian and Peault, 2003, Leffler *et al.*, 2017). After 27 weeks of development, haematopoiesis takes place within the BM which is the spongy soft part of bone tissue located in the centre of bone (Figure 1.1) (Singh *et al.*, 2019). In adult humans, haematopoiesis is concentrated in the tops of the long bones, sternum, pelvic and ribs. Haematopoiesis begins with haemopoietic stem cells (HSCs) which produce all blood cells as well as self-renewing to maintain HSCs pool (Anthony and Link, 2014). HSCs reside in the BM microenvironment niche which consists of different types of cells including adipocytes, endothelial cells, osteoblasts, neurons cells which work together and support each other by providing cell to cell interactions and soluble signals which are required for differentiation and maintaining the pool of HSCs (Morrison and Spradling, 2008, Crane *et al.*, 2017). HSCs undergo cell proliferation by regulated via pathways including the binding of stem cell factor (SCF) protein with tyrosine-protein kinase Kit (c-KIT) that expressed on HSC surface. The CXC chemokine ligand 12 or (CXCL12) also participate HSCs proliferation via interacting with CXC-chemokine receptor 4 (CXCR4). Other factors such as Insulin-like growth factor 1 (IGF-1), thrombopoietin and leptin also play a vital role in maintaining HSC pool of cells in BM microenvironment niche (Matsuoka *et al.*, 2015, Bishop *et al.*, 2000).

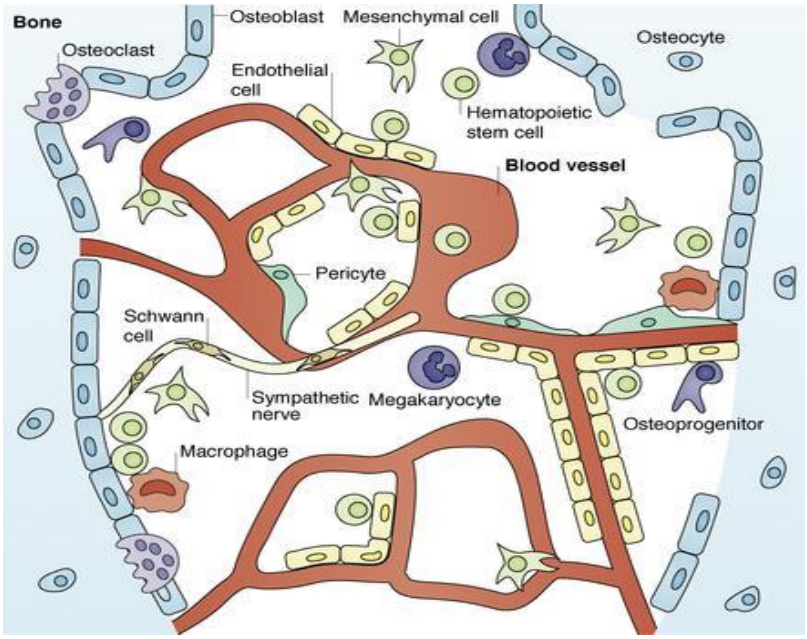

Figure 1. 1: Bone marrow microenvironment niche*. Bone Marrow is composed of different types of cells including endothelial cells, macrophages, osteoprogenitors progenitors mesenchymal cells that function and communicate in a harmonious way to provide specific cellular differentiation signals and to maintain progenitor's pool (Abarrategi et al., 2018)*

Haematopoiesis starts with the differentiation of HSCs into multipotent progenitor cells (MPCs) which then differentiate to common myeloid progenitors (CMPs) by GATA-binding factor 1 (GATA-1) transcription factor which directs CMP cells to differentiation into myeloid lineage. Alternatively, MPCs can be directed into lymphoid linage by IKAROS transcription factor (IKAROS) and Forkhead box protein O1 (FOXO1) to differentiate into common lymphoid progenitors (CLPs) (Miyai *et al.*, 2018, Zhu and Emerson, 2002).

During myeloid lineage, CMPs are stimulated to myoblast by several cytokines, regulatory proteins and activation of signalling pathways including Ras, Raf, MEK-1/-2 kinases family (JAKs), phosphoinositide 3-kinases (PI3K), granulocyte-macrophage colony-stimulating factor (GM-CSF) and signal transducers activators of transcription (STAT) which ultimately gives rise to the granulocyte, eosinophils, basophils, neutrophils or dendritic and macrophages cells (Miranda and Johnson, 2007, Ivanovs *et al.*, 2017).

In lymphoid lineage, CLP cells lead to the generation of lymphoblast cells which give rise to natural killer cells, B or T lymphocytes. Recombination Activating Gene 1 (RAG1) and Interleukin-7 receptor subunit alpha (IL-7Rα) genes are highly expressed during CLP cells differentiation (Lai and Kondo, 2006). CLP is regulated via purine box factor 1 (PU.1), interleukin-7 (IL-7), E-box binding protein 2A (E2A) proteins which are crucial in guiding lymphoid linage fate. The differentiated B and T lymphocytes cells undergo further activation in secondary lymphoid organs and B cells will continue to maturate to form plasma cells (Draper *et al.*, 2016). The different typed of blood cells are presented in Figure 1.2.

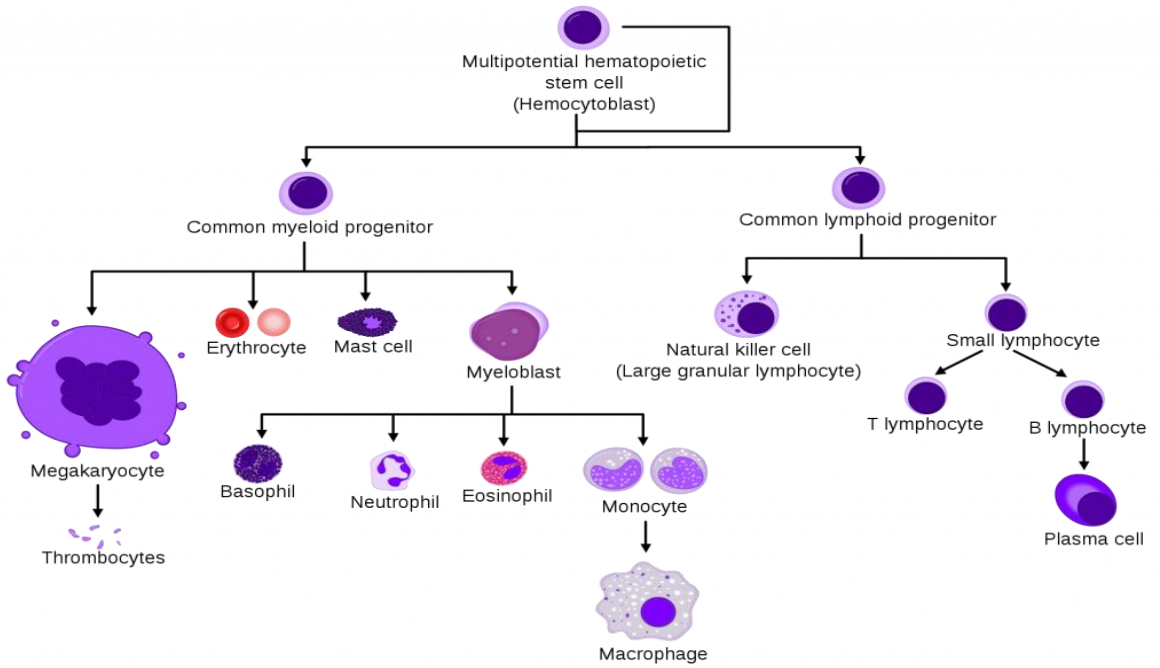

Figure 1. 2: The hierarchy of different blood cell formation*. All different cells are generated from hematopoietic stem cells (HSCs) during haematopoiesis. HSCs are differentiated into common lymphoid progenitor cells in lymphoid lineage to develop B cell, T cell and NK cells. Myeloid cells are developed from the common myeloid progenitor cells to generate granulocyte white blood cells, red blood cells and platelets during myeloid lineage of cell differentiation (Shaikh*

1.3 Introduction to the human immune system.

The human immune system has a major role in maintaining health and physiological integrity. The human body is continuously exposed to multiple pathogens including viruses, bacteria, parasites and toxic materials that can cause illness, serious

diseases or even death if not cleared. The immune system that has evolved to defend against these threats is complex and highly sophisticated (Janeway *et al.*, 2005). However, like all other mammalian immune systems the human immune system is mechanistically and functionally divided into anatomical immunity, innate immunity and the adaptive immunity. In health, both innate and adaptive immune systems work together to combat invader agents. Both of innate and apatite immune system will be reviewed.

1.3.1 Anatomical and Innate immune system.

In humans, anatomical or physiological immunity is represented by physical barrier against pathogens entry. The most important barrier is epithelium which includes skin and epithelial cells lining the surface of the lung and airways, and intestinal epithelial cells lining the oral mucosa and gut (McDonald and Levy, 2019). Besides acting as a barrier, epithelial cells are able to fight bacteria or other microbes on the skin by releasing proteins such as defensins. Defensins belong to the antimicrobial peptide group and are produced by epithelial cells and other white blood cells aiming to digest the microbes following phagocytosis (Jarczak *et al.*, 2013). The presence of mucus along the respiratory tract and gastrointestinal tract is crucial in supporting epithelial immunity by trapping and destroying microbes as it contains glycoproteins like mucin MUC1, MUC4 and MUC12 which neutralise microbes (Voynow and Rubin, 2009, Sperandio *et al.*, 2015).

The next level of immunity is the innate immune system which is a non-adaptive fast response system that includes biochemical reactions and secretion of interleukins, chemokines and activation of complement system (Sochocka and Błach-Olszewska, 2005). The complement system is divided into classical, lectin and alternative pathways and is composed of more than 25 proteins circulating within blood vessels to detect microbes. It induces incudes inflammation by anaphylatoxins via complement component 3 (C3a, and C5a) (Hugli, 1986). Complement system marks microbes with (C3b) or forms membrane attack complex (MAC) by C5b, C6,

C7 and C8 to damage the microbe's cell membrane (Figure 1.3) (Gaboriaud *et al.*, 2004).

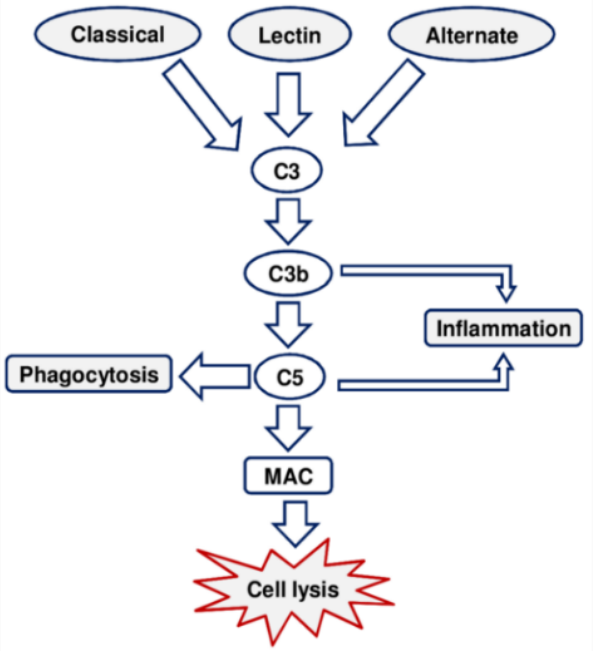

Figure 1. 3 Complement system as a part of innate immune system*. Three pathways are included in complement system activation, classical, lectin and alternative pathway. The purpose of the complement system is to activate complement 3 (C3) protein to initiate series of signalling cascades involving complement 5 (C5) to activate phagocytosis process or cell lysis via opsonisation of targeted cell via membrane attack complex (MAC) (Srivastava and Pandey, 2015).*

1.3.2 Second line of defence, adaptive immune system.

The second component of the immune system is called adaptive immunity. The term adaptive refers to the developing response to be specific to the pathogen. The adaptive immune system is comprised of the humoral response and cell mediated response regulated by B cells and T cells, respectively. Innate and adaptive immune systems are interdependent and co-regulate each other during an immune response. For example, the adaptive immune system requires innate immunity to contain pathogens specific responses to the specific pathogen are developing. The adaptive immune response provides long-term protection to reduce reinfection (Alberts, 2017).

The fundamental feature of the adaptive immune response is that upon encountering a pathogenic antigen, the immune system is able to create pathogen specific molecules called antibodies (Murphy and Weaver, 2016). Unlike the innate response, adaptive immunity takes longer to start producing high affinity antibodies by plasma cells. Besides providing adaptive immunity, this remarkable system also creates cellular immunological memory in the form of memory B-cells, allowing for a quicker and more efficient protective response on re-exposure to the same attack. This ability to 'recall' pathogens is the biology that underpins vaccination and immunisation strategies including the recent campaigns to immunise against COVID-19.

1.3.2.1 Cellular component of the adaptive immune system.

The adaptive immune system can be classified into two classes: cell mediated responses (T cells) and humoral responses (B cells). T and B lymphocytes are white blood cells derived from common progenitors during haematopoiesis (Wood, 2004). Humoral immunity is comprised of antibodies (Abs) produced by activated B cell in response to an antigen. In cell mediated immune response, pathogenic antigen is recognized by antigen presenting cells (dendritic cells and macrophages) and presented to immune cells like helper T cells that stimulate other immune cells like cytotoxic T cell to destroy the antigen by releasing cytokines and perforin molecules (Golstein and Griffiths, 2018, Metchnikoff, 1905).

1.3.2.2 Antigen presenting cells (APCs).

Antigen presenting cells or (APCs) have an important role in recognising foreign antigens and present them to T cells. APCs are dendritic cells, macrophages, and B cells. Dendritic cells are developed from myeloid progenitor cells. During development, immature dendritic cells are divided into follicular, interstitial and myeloid subsets. Follicular dendritic cells (FDC) are found mainly in the lymphatic system within lymphatic nodes while interstitial and myeloid dendritic cells (IDC,

MDC) are circulating in the blood. IDCs escape the peripheral circulation and predominantly locate in tissues including the skin, lung and intestines (Shen and Louie, 2014).

Epithelial skin migrant DCs are termed Langerhans cells and they recognise viral or bacterial surface molecules through pattern recognition receptors (PRR) before engulfing the microbe (Maverakis *et al.*, 2015). The engulfed pathogen is then degraded to produce small peptide chains composed of up to 30 amino acids that are presented to T cells in lymph nodes via DC major histocompatibility I/II complex (MHC I/ MHCII) surface proteins (Flaherty, 2014). In response to the presented pathogen, T cells have a wide range of responses, they can release chemokines and interleukins recruiting Abs or macrophage to neutralise pathogenic effect or possibly they directly cause cell death of virus infected cell (Bakshi *et al.*, 2014). Macrophages are also capable of processing pathogens to present them for adaptive immunity. Moreover, B cells at certain stage of activation express MHC I/MHCII and present antigen fragments to a specific type of T cell termed T helper cell which modulates the development of B cell to produce specific Ab molecules (Chen and Jensen, 2008).

1.4 The stages of B cell development.

1.4.1 BM development stage.

B cell development begins by the commitment of HSCs into lymphoid lineage (Decker, Hoffman *et al.*, 2017). HSC initiates the process when it is divided to multipotent progenitor cell (MPP). At this stage, the MPP is stimulated by external signals and proliferate into lymphoid multipotent progenitor cells (LMP). The transcription factor PU.1 regulates cellular differentiation by facilitating expression of Fms-like tyrosine kinase 3 (Flt3) which preserves lymphocyte production in precursor progenitors upon activation (Tobón *et al.*, 2013, Patton *et al.*, 2014). The fate of B cell development requires the expression of other regulatory proteins including IL-7 accompanied by vascular cell adhesion protein 1 (VCAM-1) which is released from BM stromal cells.

Common lymphoid progenitors (CLP) develop at this stage and receive further stimulation with E2A and early B cell factor (EBF) to enhance the development of progenitor B cell (Pro-B cell) which is regulated by Ikaros (John and Ward, 2011). This stimulatory series helps in committing the fate of B cell differentiation (Lai and Kondo, 2008). Afterwards, EBF regulates PAX5 expression which is crucial in Pro-B cell differentiation to precursor B cells (Pre-B cell). Studies showed that PAX5 is a key regulator of B cell fate considering its ability in silencing T cell and NK cells genes during maturation stages by co-stimulation with SCF (Lai and Kondo, 2008, Hoffman *et al.*, 2017).

At the pre-B cell stage, B cell gene expression is directed towards the key stage of immunoglobulin (Ig) gene maturation (Mårtensson *et al.*, 2010). Rearrangement and recombination of B cell Ig genes is an essential part of cell maturation allowing the expression of surface B cell receptor (BCR) or surface immunoglobulin. BCR on B cells will undergo positive and negative selection where it will be tested to avoid interaction with self-antigen to prevent autoimmune reactions. Later, B cells exit the BM for further development as an immature B cell (Klein *et al.*, 2014). Figure 1.4 shows the different stages of B cell development journey.

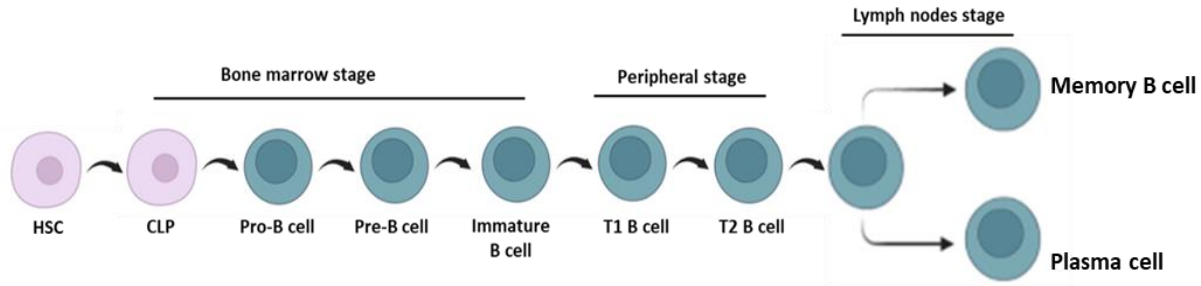

Figure 1. 4 The different stages of B cell development in bone marrow, prepheral and lymph node. *Haematopoietic stem cells (HSC) are differentiated inside BM to common lymphoid progenitor (CLP) and maintain the commitment of B cell lymphocyte development fate into progenitor B cell (pro-B cell) and precursor B cell (pre-B) cells before exported to peripheral blood at transitional stage (T1 – T2 B cells) where B cells undergo further development in the lymph node.*

1.4.1.1 Immunoglobulins (Igs).

Immunoglobulins (Igs) or antibodies (Abs) are proteins produced by B cells to fight against infections or pathogens. They are heterodimeric proteins with different molecular weights ranging from 150 to 900 kDa based on their specific class. Igs

are complexes of two types of proteins, Ig heavy chain (IgH) and Ig light chain (IgL). *IgH* chain gene is located on chromosome 14 whereas *IgL* chain genes are located on chromosome 2 or 22 (kappa (κ) or lambda (λ)) respectively (Tobón *et al.*, 2013). Ig protein structure consists of two sections; (i) Fab section which is comprised of variable (V) region of *IgL* and *IgH* genes and (ii) Fc part which is made by constant (C) region of *IgH* gene. Variable region is defined as the antigen binding site of the Ab. The constant region of heavy chain determines the class or isotype of the Ab (Janeway *et al.*, 2005).

During B cell development, *IgH* and *IgL* genes undergo class switch recombination and somatic hypermutation to produce high specificity Igs with different binding specificity (Dorshkind and Rawlings, 2018). Crystallography (Figure 1.5) results showed that heavy and light chains are structurally linked together by disulphide bonds forming a Y shape morphology.

There are five different Ab isotypes: IgG (Igγ), IgA (Igα), IgE (Igε) IgD (Igδ) and IgM (Igμ) classes. B cells first express IgM isotype and then class switch into the other isotypes as part of the maturation process when complexed with antigen (Dorshkind and Rawlings, 2018, Schroeder Jr and Cavacini, 2010, Tobón *et al.*, 2013).

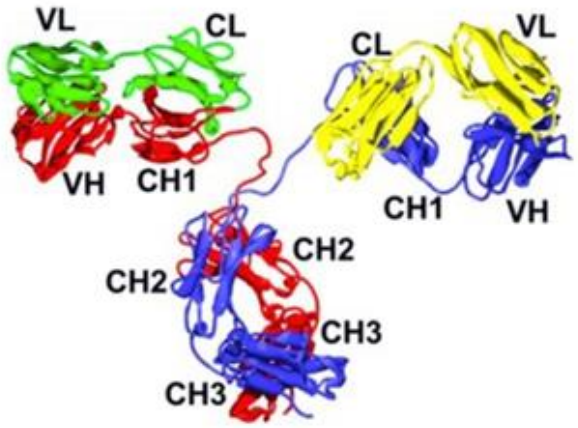

Figure 1. 5 Crystal model of IgG isotype macromolecule*. Ig is a protein molecule complex that is made by immunoglobulin heavy chain (IgH) and immunoglobulin light chain (IgL) genes. Two IgH (red and blue) and two IgL (green and yellow) proteins make the constant (C) and variable (V) region of the Ig structure and are linked together by disulphide bond (Jay et al., 2018).*

1.4.2 Post marrow development stage.

To complete their maturation, immature B cells migrate from the BM into the spleen as transitional B cells with limited numbers of immature B cells entering the peripheral system. Migrant B cells enter secondary lymphoid tissues like lymph nodes, mucosa associated lymphoid tissue (MALT) or the spleen. They are termed as transitional B cells because they have to pass through stages T1 and T2 of development (Good-Jacobson, 2014). Once they enter the spleen they are referred to as T1 B cells. T1 B cell will transform into T2 B cells in the spleen and differentiate into marginal zone or follicular zone B cells depending on BCR signalling (Good-Jacobson, 2014). The marginal B cells represent naïve B cells in the spleen when compared to follicular B cells with IgM^{high}, IgD^{low}, $CD21^{high}$, $CD1^{high}$ and express high levels of B7-1 and B7-2 ligands (Shabir *et al.*, 2015). Most B cells are found in primary follicles. Upon activation with pathogenic antigens, B cells enter the secondary follicles and form germinal centres. In the secondary follicles, somatic hypermutation and class switching takes place which will ultimately result in formation of memory B-cells and plasma cells which are vital for cellular mediated immunity in humans (Shabir *et al.*, 2015).

1.4.3 T cell dependent activation.

Naïve B cells recognise the presented antigen through binding with BCR (Schmitz *et al.*, 2014). After antigen binding with BCR, B cell starts its activation process where it engulfs the antigen via endocytosis and presents part of the antigen on its surface with major MHC II. Further activation signals from helper T-cell via IL-21, IL-4 and CD40 ligand (CD40L) interaction with B cell (Kurosaki *et al.*, 2015, Schmitz *et al.*, 2014). B cells begin to colonise and form germinal centres within lymph nodes and secondary lymphoid organs including spleen, Peyer's patches (PPs) for further activation process (Schmitz *et al.*, 2014).

1.4.4 Germinal centre (GC) B cells.

The germinal centre (GC) is a critical site for enhancing humoral immunity in human through diversification and Ig affinity maturation process (Figure 1.6). B cells receive signals from follicular T-cells to replicate and differentiate into plasma cells which produce high numbers of antibodies. GC are divided into two compartments anatomically, the dark zone (DZ) and light zone (LZ) (Figure 1.7). The LZ is for antigen driven selection while the DZ is for B cell proliferation and hypermutation. Within the DZ, CXCL12 expressing Reticular Cells (CRCs) are presented with a tight cluster of highly proliferative B cells called centroblasts that have the chemokine receptor CXCR4. Other supportive proteins that are required including CD28 which interacts with B7 on the B cell alongside Lymphocyte Function-Associated antigen 1 (LFA-1) located on the surface of T cell that interacts with Intercellular Adhesion Molecule 1 (ICAM-1) on B cells to produce plasma cells. Moreover, CD40L must interact with the surface protein CD40 continually to stimulate the differentiation of B cells to antibody producing plasma cells (Schmitz *et al.*, 2014). The LZ is less compact but diversified with GC B cells and naïve B cells with a smaller population of T follicular helper cells (Mesin *et al.*, 2016).

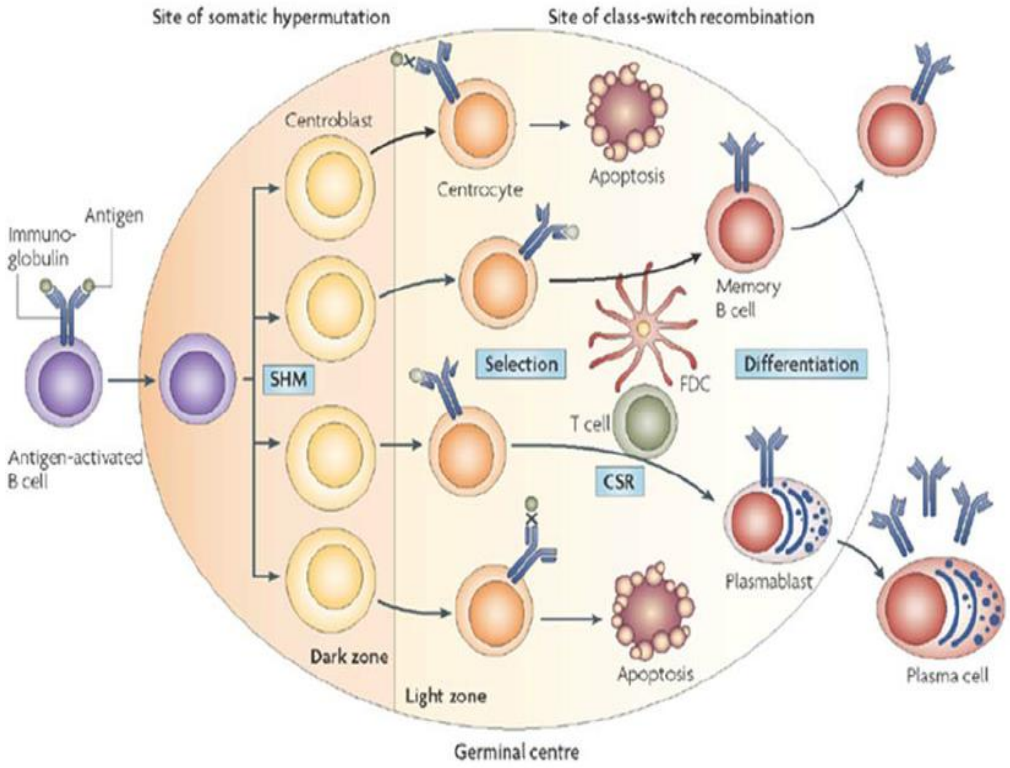

Figure 1. 6 The development of B cells during GC reaction. *Activated B cells initiate the formation of GC in the secondary lymph nodes where B cells proliferate at high rate. The formation of centroblast occurs inside the dark zone where B cells undergo somatic hypermutation (SHM) to produce high affinity Ig that is challenged by selection mechanism with dendritic cells in the light zone with follicular helper T cell to regulate and guide the maturation of B cell Ig by class switch recombination (CSR) to produce plasm cells. During class switch recombination, B cells Ig gene undergoes genetic mutation aimed to change the class of antibody produced by B cells to increase antibody affinity and specificity. The follicular dendritic cells FDC act antigen presenting cells to the affinity of the new surface antibody produced on B cells (Gibson-Corley, 2010).*

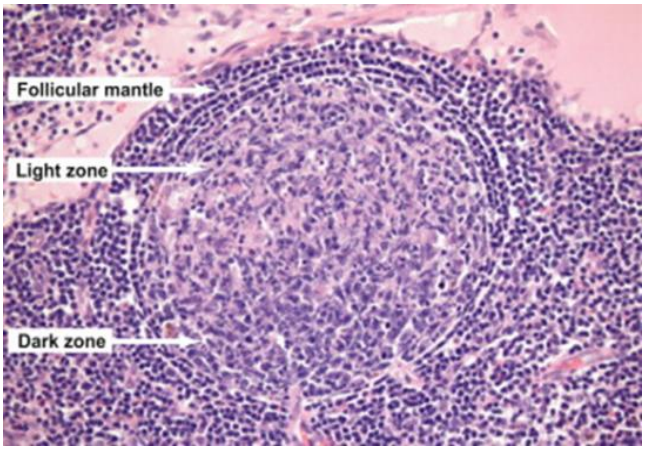

Figure 1. 7 The formation of GC in lymph nodes*. The microenvironment formation of GC in lymph node is characterized by dark zone and light zone surrounded by follicular mantle. Inside GC, B cells undergo antibody maturation and class switching to produce antibody secreting plasma cells (TW Mak, 2014).*

1.4.5 Activation-induced cytidine deaminase.

Activation-Induced Cytidine Deaminase (AID) is a 24 kDa enzyme composed of 198 amino acid residues which is encoded by the *AICDA* gene located on chromosome 12 in humans (King and Larijani, 2017, Barreto and Magor, 2011, Conticello, 2008). AID belongs to the group of zinc-dependent proteins called the AID/APOBEC deaminase family (Budzko *et al.*, 2013). AID is a natural mutator enzyme that facilitates the deamination process of cytosine (C) base converting it into uracil (U) in single strand DNA of the Ig gene during class switch recombination and somatic hypermutation (Ramiro and Barreto, 2015). The structure of the AID protein is characterized by the presence of a DNA binding catalytic domain which contains a zinc atom binding two cysteines and histidine (Budzko *et al.*, 2017).

1.4.6 Somatic hypermutation (SHM).

Somatic hypermutation (SHM) and Class Switch Recombination (CSR) are carried out by AID in GC B cells to design specific Ab against specific antigen. AID causes multiple and repeated nucleotide conversions of cytosine into uracil on Ig gene locus aimed to generate different DNA sequences that consequently produce different Ig genetic codes (Di Noia and Neuberger, 2007, Lumsden *et al.*, 2004). AID activity on the V region of the light and heavy chain Ig gene is termed as SHM focusing on V, D and J segments while CSR events occur on the C region of Ig heavy chain on switch (S) segments. In activated GC B cells, AID is expressed and catalyses the conversion of cytosine (C) to uracil (U) (Hwang *et al.*, 2015).

In SHM, V region mutations occur on bases located 200bp downstream of the promoter and up to 2 kb before reaching the Eμ enhancer and C region of the Ig gene. Studies suggested that the Ig promoter is vital during SHM to direct and position AID which is initiated before CSR (Rada and Milstein, 2001, Odegard and Schatz, 2006). In activated GC B cells, AID mediated mutation rates at each base pair located in V region during SHM can be up to 10^{-3} per cell. The main point is to create single point mutations that give transversion or transition mutations of base pairs thereby remodelling V regions to enhance Ab specificity (Casali *et al.*, 2006).

In one scenario, the newly produced mutated uracil base is recognised as thymine (T) during cell division by DNA replication pathways which gives U-A base pair in one of the daughter cell and C-G base pair in the other one. The U-A base pair is converted into T-A base pair during subsequent replication cycles (Zeng *et al.*, 2001, Simpson and Sale, 2003). The other scenario is that Uracil-DNA glycosylase (UDG or UNG) will detect U base through DNA repair machinery and excises U base leaving a basic site on the DNA (AP). The presence of AP sites leads to random nucleotide insertion during DNA replication in the newly synthesised DNA in subsequent cell generations (Casali *et al.*, 2006, Neuberger *et al.*, 2005a).

In another mechanism, DNA base pair excision repair (BER) is involved to recruit Apurinic/apyrimidinic AP endonucleases (APEX1 and APEX2) to create a single strand DNA nick which is later processed with DNA polymerases to fill the gap with nucleotides (Casali *et al.*, 2006). AP sites provoke the recruitment of mismatch repair (MMR) to direct MSH 2, MSH 3 and MSH 6 proteins to form DNA nicks where the exonuclease 1 pathway is activated and digest DNA strand around nick sites. DNA synthesis is followed by error-prone DNA polymerase to replace missing nucleotides (Maul and Gearhart, 2010, Rada *et al.*, 2004). The high speed of nucleotide replacement during BER and MMR pathways increases the chances of base pair mismatch leading to DNA sequence changes in daughter cells and results in protein diversity (Figure 1.8) (Casali *et al.*, 2006, Rada *et al.*, 2004, Neuberger *et al.*, 2005b).

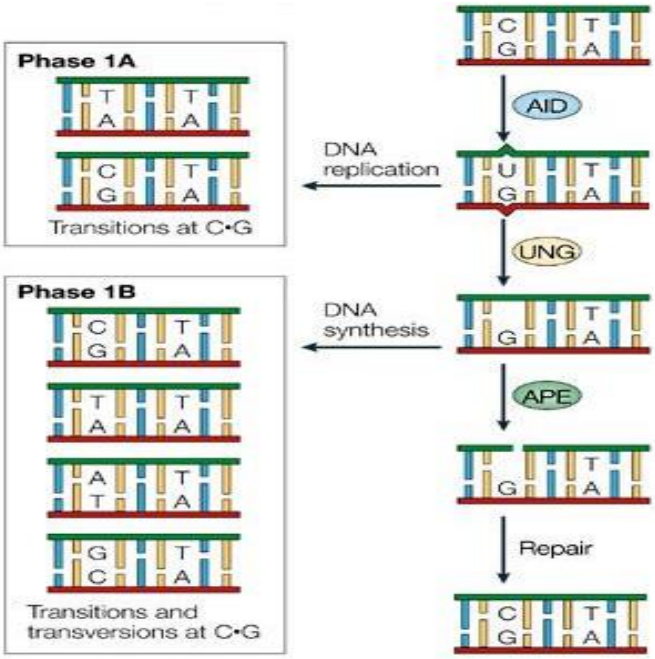

Figure 1. 8 The role of AID enzyme in deaminase cytosine base in DNA in SHM. *AID mutate C base into U base during SHM mechanism to induce transversion or transition mutation subsequently in daughter cells during cell division and DNA replication. DNA absaic sites generated by UDG/UNG could eventually give transversion or transition mutation in subsequent cells. Alternatively, BER – MMR activation is expected leading sequence changes in daughter cells (Neuberger et al., 2005a).*

1.4.7 Class switch recombination (CSR).

AID induces multiple single strand breaks (SSBs) which are developed into double strand breaks (DSBs) in specific DNA segments called the switch region (S) located upstream of isotype determining Ig segments such as: Igμ, Igα, Igδ, Igε and Igγ. Multiple DSB occur in two different S regions leading to the cleavage of both DNA strands (Iwasato *et al.*, 1990). C region is re-joined together bringing the new class determinant segment near the V region to have a new class modified Ig gene (Manis *et al.*, 2002). Similar to SHM, AID mutated U base pairs in S region are recognised by the UDG system and excised to create AP sites which are processed later with BER DNA repair mechanisms to create DNA nicks. MMR interfere as well to create SSD. The chance of having two adjacent SSBs in both DNA strands in opposite proximity results in DSBs (Figure 9) (Honjo *et al.*, 2002). Afterwards, DNA strands breaks are recognised by the Mre11, Rad50 and Nbs1 (MRN) complex pathway

which repairs DNA double strands breaks by non-homologous end joining pathway (NHEJ) using the Ku protein family (Ku70, Ku80) (Figure 1.9) (Fear, 2013, Casellas *et al.*, 1998).

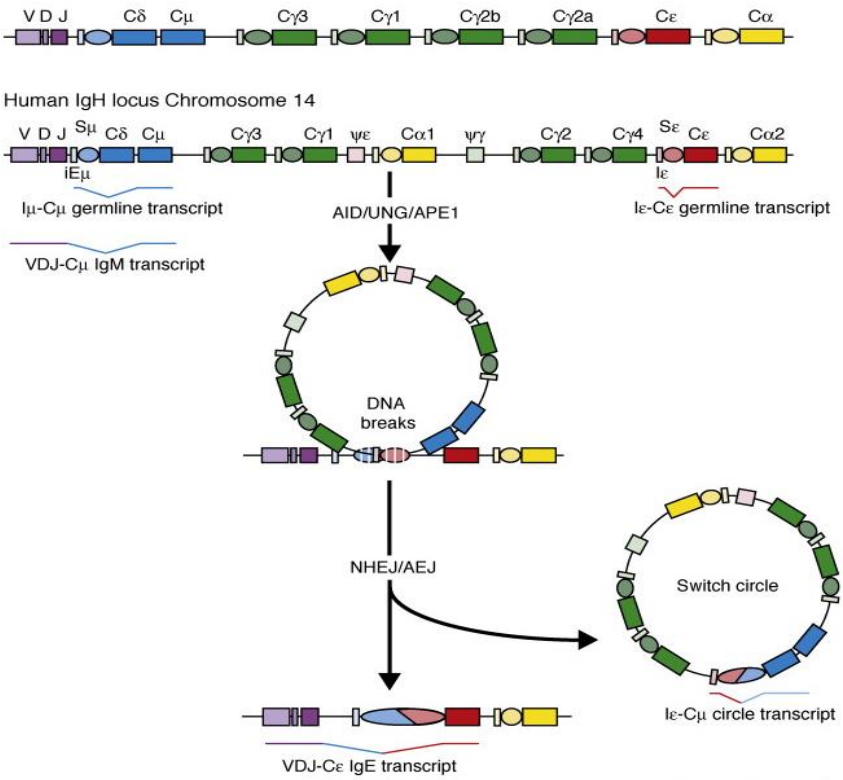

Figure 1. 9 Ig class switching in CSR mechanism mediated by AID*. IgH chain gene comprised of V and C region which is separated by switch (S) segments positioned upstream each individual DNA coding exon that is responsible to give Ab its specific class. AID deaminases C bases in S segments to cause SSB and DSB eventually. DNA DSB occur in two different S segments and DNA circle portion is excised. Non-homologous end joining (NHEJ) pathway re-join DNA strands producing new DNA sequence (Fear, 2013)*

1.5 Haematological malignancies.

Leukaemia is a malignant blood cancer associated with a rise in white cell counts within the BM or in the peripheral blood and lymphatic system. The major classifications are acute lymphoblastic leukaemia (ALL), acute myeloid leukaemia (AML), chronic lymphocytic leukaemia (CLL) and chronic myeloid leukaemia (CML)

(Rodriguez-Abreu *et al.*, 2007). The acute types are defined as a rapid proliferation of immature cells in BM leading to the suppression of other cell development and proliferation. The chronic form is defined by gradual increased proliferation rate of mature cells that result in increase of the number of white blood cell counts in the peripheral blood (Mesin *et al.*, 2016).

Leukaemias including ALL, AML, CLL and CML progress from abnormal precursor or primitive cell differentiation and proliferation when DNA synthesis checkpoint mechanism fails during cell cycle leading to aberrant proliferation and accumulation of blast cells in BM and peripheral blood. Leukaemia aetiology is multifactorial including genetic and environmental factors (Bispo *et al.*, 2020). The accumulation of blast cells in the BM causes marrow failure (Julien *et al.*, 2016). About 95% of CML patients are diagnosed with Philadelphia chromosome abnormality due to translocation of Breakpoint Cluster Region protein (*BCRp*) to tyrosine-protein kinase *ABL1* gene (ABL) on chromosome 9 and chromosome 22, respectively (t(9;22)) (Wapner, 2014). The resulting *BCR-ABL* fusion gene codes for a protein that has constitutive tyrosine kinase activity in triggering the formation of cancer by promoting abnormal cell proliferation.

Lymphomas are cancers that originate from lymphoid tissues and are divided into two major groups; Hodgkins Lymphoma (HL) or Non-Hodgkins Lymphoma (NHL). HL is characterized by the presence of Reed Sternberg cells as a hallmark (Figure 1.10).

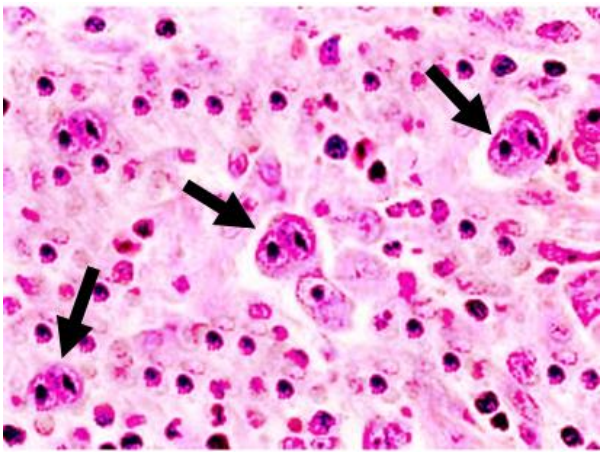

Figure 1. 10 Reed Reed-Sternberg cells*. Microscopic image showing the of Reed-Sternberg cells (black arrow) that are the hallmark in HL represented with owl eye morphology (Aggarwal and Limaiem, 2019).*

NHL are classified as low- or high-grade cancers based on proliferation rate. Low grade NHL divide very slowly and can last for months before being diagnosed. However, high grade NHL cancer cells are rapidly dividing and often diagnosed within a few weeks.

There are different types of low-grade NHLs including; follicular lymphoma (FL), marginal zone lymphoma (MZL), mantle cell lymphoma (MCL). These types of NHL are characterised by the slow growth pattern (Bende *et al.*, 2007, Ferreri and Zucca, 2007, Barista *et al.*, 2001). The high-grade NHL are Burkitt's lymphoma and diffuse large B cell lymphoma (DLBCL) which are characterized by the rapid growth pattern (Li *et al.*, 2018).

It is estimated that 30% of all B cell lymphoma cases are DLBCL making it the most common type seen in lymphoma patients around the world (Hunt and Reichard, 2008). DLBCL originates from the GC B cells stage similar to Burkitt's lymphoma (BL). However, the mechanisms involved in its lymphomagenesis are still unknown (Xie *et al.*, 2015). Several studies have suggested the mechanism to be related with BCL-2 translocation to IgH locus t(14;18) (Iqbal *et al.*, 2004). Different HL and NHL types and related characteristics are presented in Table 1.2.

	Subtypes	Causes/ aetiology	Median Age (years)	Male : female ratio	Cell type affected	Presentation sites	Additional notes
HL	Nodular sclerosing	Bothe HL and NHL: - Have no specific etiology. - Risks increase with DNA mutations, aging, viral infections and weak immune system.	--	1:1.05	B lymphocyte	- Swollen nick and lymph nodes.	- HL: Shows a Bimodal age distribution: ▪ 15 to 35 years. ▪ 50 years and older. - Insidious progression onset. - Generally localized. - Presence of Reed-Sternberg cells.
	Mixed cellularity		38	2.8:1	B lymphocyte	- Swollen lymph nodes of the armpits and neck with Splenic infiltration.	
	Lymphocyte depletion		37	2:1	B lymphocyte	- Localised bellow diaphragm in abdomen region and can reach bone marrow.	
	Lymphocyte rich		38	2:1	B lymphocyte	Painless swollen peripheral lymph nodes.	
	Nodular lymphocyte		37	3:1	B lymphocyte	Painless swollen lymph nodes of the neck and groin sites.	
NHL	Burkitt's Lymphoma		- eBL~8. - sBL ~40-50	4:1	B lymphocyte	- eBL: swollen lymph nodes and distorted jaw bones. - sBL: enlarged abdomen, liver and spleen.	NHL: - develops at any age. - Represents a sudden onset - Slow or rapid pattern of growth. - Absence of Reed-Sternberg cells.
	Mantle cell Lymphoma		68	3:1	B lymphocyte	- Swollen lymph nodes and spleen	
	Follicular lymphoma		65	1.2:1	B lymphocyte	- Swollen lymph nodes of the armpits and the neck	
	Diffuse large B cell lymphoma		64	2:1	B lymphocyte	- Swollen lymph nodes of the neck and the abdomen.	
	Adult T-cell lymphoma		62	No gender preponderance	T lymphocyte	- Development of Skin lesions, hypercalcemia, and enlarged lymph nodes.	
	Anaplastic large cell lymphoma		30	1.5:1	T lymphocyte	- Swollen lymph nodes of the neck, armpit and groin.	

Table 1. 2 ***The different types of HL and NHL with associated characteristics, gender incident rates and ages***. (Mukhtar et al., 2017, Hapgood and Savage, 2015, Medeiros and Greiner, 1995, Falko Fend, 2018, Konkay et al., 2016, Feldman et al., 2006, Ferri, 2021, Abbasi, 2022, Sapkota and Shaikh, 2020, Schnitzer, 2012, Thida and Tun, 2021, Shimabukuro-Vornhagen et al., 2005, Eichenauer and Engert, 2017, Correia et al., 2015, Adıyaman et al., 2019, Gogia et al., 2018, Wessells and Brown, 2012, Kao et al., 2018, Shamoon et al., 2018)

1.6 Burkitt's lymphoma (BL).

BL is a malignancy of B lymphocytes that originates in GC B cells. BL was firstly discovered in 1956 in Africa (Uganda) among children by the surgeon Denis Burkitt who noticed a rapid progression of jaw tumour in children (Ferry, 2006, Crombie and LaCasce, 2021). Following its discovery, world health organization (WHO) classified BL as a NHL (Thomas *et al.*, 2011). BL is described as a high grade and fast-growing type of lymphoma which can double within two days.

BL is characterized by the translocation of the *C-MYC* protooncogene from chromosome 8 to one of the Ig genes located on chromosome 14, 22 or 2 where *C-MYC* is juxtapositioned to *IgH* or *IgL* (Lambda or Kappa) chain (Figure 1.11). This translocation results in constitutive *C-MYC* gene expression leading to dysregulated C-MYC protein activity and uncontrolled cell proliferation (Schmitz *et al.*, 2014, Nossal, 2003). Molecular investigations have identified that the frequency of *C-MYC* gene translocation to *IgH* is 70% more than *C-MYC* translocation to *IgL* which makes it the most common type of *C-MYC* translocation in BL (Ferry, 2006, Graham and Lynch, 2021).

A

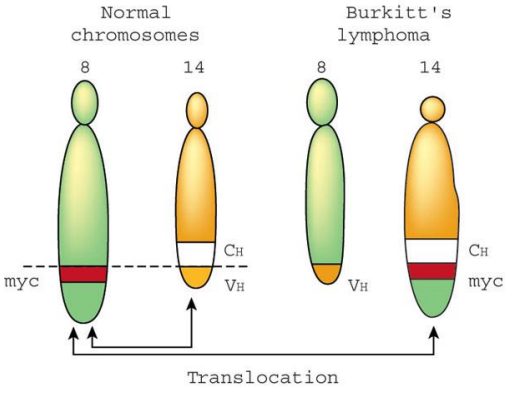

B

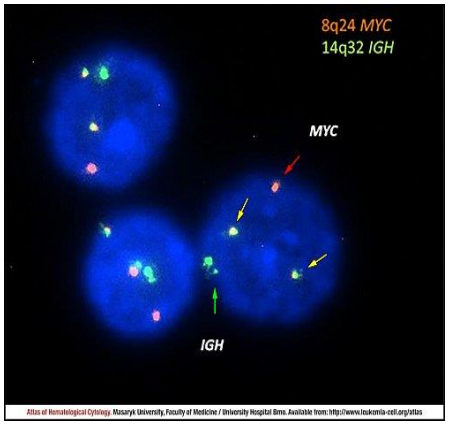

Figure 1. 11 C-MYC translocation in BL

(A) The hallmark of BL is the translocation of C-MYC to either heavy or light chain Ig gene located on chromosome 14, 22 or 2. As showed in the figure, C-MYC is normally located on chromosome 8 and the normal location of IgH is on chromosome 14. In BL, C-MYC is translocated to IgH in chromosome 14 during B cell developmental next to constant region (CH) replacing variable region (VH) which is moved to C-MYC wild type location. (Nossal, 2003). (B) Fluorescence in situ hybridisation (FISH) shows C-MYC translocation in BL cells. C-MYC breakpoint at 8q24 and translocation to IgH at 14q32 breakpoint. Red arrow is pointing to C-MYC gene wild type location and green arrow shows IgH gene wild type location. Yellow arrow shows the C-MYC/IgH fusion in BL cell (Cytology)

Based on epidemiological differences, BL is divided into 3 subtypes: endemic, sporadic, and immune deficiency BL type. BL is curable with managed long-term course of chemotherapy (Molyneux *et al.*, 2012, Bishop *et al.*, 2000, Dunleavy, 2018).

Generally, there are several methods involved in BL diagnosis which include microscopic cellular morphological evaluation, cytogenetic analysis and immunophenotyping. Under the microscope, BL cells exhibit a medium sized lymphocyte shape with increased nuclear size. BL cells are also characterized by the presence of multiple vacuoles distributed in the cytoplasm and clumped chromatin with multinuclear appearance. High apoptosis rate is one of the main characteristics of BL giving tumours a "starry sky" appearance (Figure 1.12) (Kelemen *et al.*, 2010, Faramarz Naeim, 2013).

A

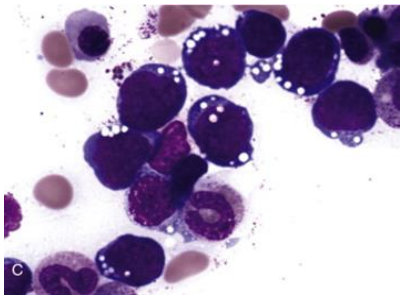

B

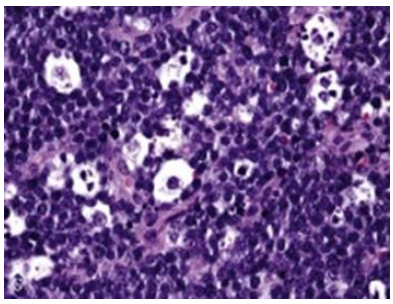

Figure 1. 12 Microscopic presentation of BL cell*. (A) BM sample from BL patients show that BL cells are characterized by the presence of increased nuclear to cytoplasm ratio with multiple vacuoles around the basophilic cytoplasm. (B) microscopic image of the lymph node sample taken from BL patient shows the starry sky pattern of BL cells (Faramarz Naeim, 2013)*

As a cancer of GC B cells, immunophenotyping with flow cytometry showed that BL cells express the classical B cell marker CD19, CD20, CD22, CD79a and surface IgM receptor. BL cells are also positive for both CD10 and BCL-6 and negative for CD5 and terminal deoxynucleotidyl transferase (Bispo *et al.*, 2020, Kelemen *et al.*, 2010).

1.7 BL epidemiology and the different BL subtypes.

As mentioned earlier, the first type of BL discovered was endemic or African BL. Endemic BL (eBL) occurs commonly in malaria endemic regions including Sub-Saharan Africa (SSA) and Papua New Guinea where BL account for more than 50% of cancer cases among children (Stefan *et al.*, 2017, Bouda *et al.*, 2019a). There is a tight relationship between the incidence of BL and malarial infection in malaria endemic regions in Africa especially with Plasmodium falciparum malaria species. Epstein–Barr virus (EBV) infection was also detected in nearly all eBL cases (Stefan *et al.*, 2017, Mbulaiteye, 2013, Hämmerl *et al.*, 2019). More than 60% of eBL patients present at clinics with enlarged spleen and lymph nodes around the abdominal area. Almost 50% eBL patients presented with facial and jaws bones distortion due to enlarged lymph nodes in advanced stages (Orem *et al.*, 2007, Shapira and Peylan-Ramu, 1998, De Coninck *et al.*, 2021).

The incidence of eBL is notably higher in males compared to females with a ratio of 4:1. The highest incidence of eBL were seen in patient around 5-9 years old (Hämmerl *et al.*, 2019, Mwanda, 2004, Mwanda *et al.*, 2004, Oguonu *et al.*, 2002). Due to the shortage of medical supportive care which is required to overcome the tumour lysis syndrome seen in patients administered with chemotherapeutic drugs, the survival rate in SSA is not very high and it is estimated to fall between 30% and 50% (Ozuah *et al.*, 2020, Magrath, 2009, Lombardo *et al.*, 2017).

The second subtype of BL is sporadic BL (sBL) which is mostly found in non-African regions and accounts for about 2% of all NHL cases in adults in the United States and Western Europe. Like eBL, sBL incidence rate is higher in children than in adult and accounts for about 30-50% of NHL cases among children with a high male to female ratio (Philip, 1985, Molyneux *et al.*, 2012, Mukhtar *et al.*, 2017). Unlike eBL cases, EBV infection is not highly associated with sBL cases as the infection rate of EBV in sBL is lower than 30% (Thomas *et al.*, 2011, Hämmerl *et al.*, 2019). More than 60% of sBL patients present with enlarged abdomens. BM tumour invasion is associated with sBL patients in 20% the cases and in advanced stages central nervous system invasion is likely (Mbulaiteye, 2013, Dozzo *et al.*, 2017).

The survival rate in patients with sBL is strongly related to early diagnosis of the disease and individual's age. At early stage, survival rate in sBL patients can be up to 60%, especially among young individuals. However, survival rates decline in older patients, especially those with a late diagnosis (Costa *et al.*, 2013). It is estimated that in the United Kingdom, the annual reported cases of BL is around 210 every year with median age of 55.4 years at diagnosis stage (Figure 1.13) (Cancer-Research-UK, 2022, (HMRN), 2022).

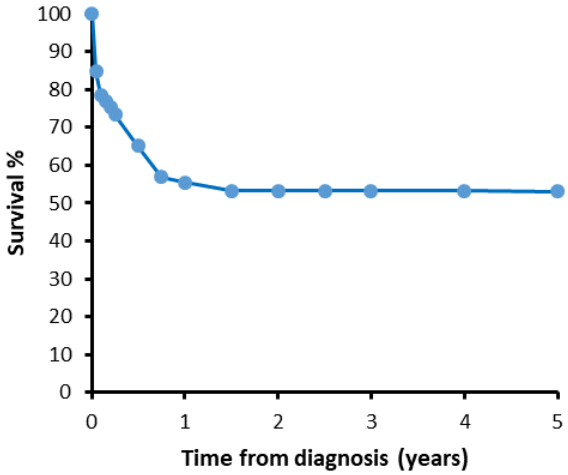

Figure 1. 13 Survival rate percentage of BL patients in United Kingdom*. Average BL survival rate in BL (male and female) patients showed to be highly dependent to diagnosis time. Over 70% and higher survival rate can be seen if patient achieved diagnosis in a time earlier than 1 year of BL development. Provided data are obtained from The Haematological Malignancy Research Network website (HMRN, 2022).*

The third BL subtype is known as immune deficiency BL type. This subtype is commonly seen in patients infected with human immunodeficiency virus (HIV) and in organ transplantation patients on immunosuppressive therapy (Thomas *et al.*, 2011, Orem *et al.*, 2007). The increased risk of BL development in HIV immunocompromised individuals is related to EBV infection and its role in lymphomagenesis. It was reported that HIV increases the risk of BL development 57 times more in when compared to the other BL groups (Birlutiu *et al.*, 2020, Dozzo *et al.*, 2017). Additional reports mentioned that BL account for 15-40% of lymphoma developed in individuals with HIV and acquired immune deficiency syndrome (AIDS). The incidences of BL lymphomagenesis are 86.7% higher in males with HIV

infection than in females with general median age of 39 years (Komatsu *et al.*, 2013, Alderuccio *et al.*, 2021, Verdu-Bou *et al.*, 2021). Table 1.3 summarises the differences between BL subtypes.

	Endemic BL (eBL)	**Sporadic BL (sBL)**	**Immunodeficiency BL**
Geographical distribution and epidemiological factor	- Mostly in African region with endemic malaria infection. - More common in children than adult.	- Worldwide. - Very rare in adult with NHL. - 25-30% in children with NHL.	- HIV infected patients worldwide. - Risk increases with HIV progression. - Most common in adult.
Incidence/ population	- 5-10 / 100000.	- 2-3 / 1000000.	- 6-23 / 1000 individuals with AIDS
Co-factor infection	- Malaria and EBV.	- EBV.	- HIV. - Immunocompromised.
Genetic mutations	- *C-MYC* (100%). - *ID3 / TCF3* (40-70%). - *CCND3* (1.8%).	- *C-MYC* (92%). - *ID3 / TCF3* (40-67%). - *CCND3* (38%).	- *C-MYC* (100%). - *ID3 / TCF3* (67-40%). - *CCND3* (1.8%).
Involved tissues	- Face. - Jaw bones. - Abdomen. - Gonads. - Central nervous system in late stage.	- Ileocecal valve. - Bone marrow. - Central nervous system. - Kidney and breast.	- Lymph nodes.
EBV incidence rate	- 95-100%	- 30%	- 50%

Table 1. 3: The differences and the characteristics of the different BL types *(Orem et al., 2007, Verdu-Bou et al., 2021, Dunleavy et al., 2016, Birlutiu et al., 2020, Schmitz et al., 2012, Huang et al., 2015, Chuang et al., 2008).*

BL represents an aggressive proliferation pattern, it can invade the BM and metastasise to the central nervous system. Early diagnosis and early treatment administration are important to avoid clinical complications seen with tumour progression during later disease stages.

Signs and symptoms of BL include nausea, vomiting, gastrointestinal bleeding, intestinal obstruction or perforation, renal failure because of retroperitoneal disease and tumour lysis syndrome. Cancer diagnosis is primarily based on pathologic evaluation of the tissue biopsy. Lymph node biopsy is crucial for managing treatment and evaluate BL stage (Molyneux *et al.*, 2012). A BM biopsy is needed for cases where there is a suspicion that the cancer has metastasised to bones.

1.8 The role of EBV in BL pathogenesis.

EBV is a member of the DNA herpes virus family. It infects human B lymphocytes and persists inside the cell lifelong. It is considered that 90% of total world population is infected with EBV (Gequelin *et al.*, 2011, Smatti *et al.*, 2018). The mechanism of EBV infection in B cell begins with infecting oropharyngeal epithelial cells. EBV enters B cells by viral glycoprotein gp350 binding to CD21 expressed on the B cell surface and glycoprotein gp42 antigen binding to major histocompatibility complex II (MHC II) (Odumade et al., 2011, Chesnokova and Hutt-Fletcher, 2014). Upon infection, EBV undergoes two different stages of viral life cycle known as the latent and lytic phases. In the latent phase, viral episomes in immunocompetent individuals remain silent and confined to infected memory B cells evading immune system and specifically cytotoxic T cells (CD4) which suppress the infected B cells (Young and Rickinson, 2004, Mawson and Majumdar, 2017, Rezk and Weiss, 2007). EBV replicates via host cell DNA polymerase during host cell replication. EBV reactivation happens when latent EBV is triggered by triggering of the B cell receptor. This initiates the lytic viral phase to produce more infectious virions (Kenney and Mertz, 2014, Odumade *et al.*, 2011).

The contribution of EBV in B cell lymphomagenesis are via regulating and controlling B cell proliferation by expressing viral transforming proteins such as Epstein Barr nuclear antigens (EBNA) 1, 2 and 3 and Latent Membrane Proteins (LMPs). Later, EBV was used in laboratories as a useful tool in generating immortalized lymphoblastoid cell lines (LCL) B cells that have helped in understanding more about B cell lymphoma (Dugan *et al.*, 2019, Saha and Robertson, 2019, Hui-Yuen *et al.*, 2011, Sall *et al.*, 2023).

EBV gene products are different and are dependent on the actual activity and the viral latency stage as referred in Table 1.4 which also shows the associated disease. As mentioned before, there is an association between EBV and BL. Different EBV gene products were found in BL including; EBNA1, Epstein Barr virus encoded small RNA (EBER 1 and EBER 2) and BamHI fragment A rightward transcript (BART) micro-RNA (Pannone *et al.*, 2014, Ambrosio *et al.*, 2014, Saha and Robertson, 2019).

Latency phase	Gene products	Associated disease
Latency phase 1	- EBNA1 protein - sRNA-EBERs -miR-BARTs	- Burkitt's Lymphoma. - Gastric cancer.
Latency phase 2	- EBNA1 protein - sRNA EBERs - miR-BARTs - LMP (1, 2A and 2B) proteins - BARF1 protein	- Diffuse large B cell lymphoma. - NK/T cell lymphoma. - Nasopharyngeal carcinoma.
Latency phase 3	- miR-BHRF1 - miR-BARTs - EBNA (1, 2, 3A,3B, 3C and LP) proteins - LMP (1, 2A and 2B) proteins - sRNA-EBERs	- Infectious mononucleosis. - Diffuse large B cell lymphoma. - Lymphoblastoid cells (LCLs). - AIDS related lymphoma.
W promoter (Wp)-restricted latency	- BHRF1 protein - EBNA (1,3A, 3B and 3C) proteins - sRNA-EBERs - miR-BARTs	- Burkitt's Lymphoma.

Table 1. 4: EBV gene expression profiles during the different latency phases with associated diseases. *EBV gene expression includes; Epstein–Barr nuclear antigen (EBNA), EBV-encoded small RNA (sRNA-EBER), micro RNA BamHI A region rightward transcript (miR-BART), Latent Membrane Proteins (LMP), micro RNA BamHI fragment H rightward open reading frame (miR-BHRF) and BamHI-A rightward frame (BARF). Acquired immune difeceincy syndrome (AIDS). EBV gene expression is different and is related to viral phase of latency (Wyżewski et al., 2022, Yang et al., 2020, Price and Luftig, 2015, Lassmann et al., 2011, Grömminger et al., 2012, Kelly et al., 2013, Murata et al., 2021, Shechter et al., 2022).*

BL cells are known for their ability to proliferate rapidly and it was observed in vivo that even with this rapid proliferation, BL cells also showed an increased and rapid pattern of apoptosis which is driven by the activity of irregular *C-MYC* expression and absence of *BCL2* expression (Milner *et al.*, 1993, Gregory and Milner, 1994).

The role of EBV in the progression of BL lymphomagenesis has been shown to be by inhibiting apoptosis in BL cells via EBV gene products during latency I stage (Xu *et al.*, 2001). Apoptosis is normally carefully regulated in the cellular microenvironment by different genes. The tumour suppressor gene *TP53* or tumor protein p53 has a major role in regulating apoptosis and in inducing cell cycle arrest. It was found that EBNA1 protein destabilizes P53 protein and facilitates its

degradation. This mechanism involves the binding of EBNA1 to ubiquitin specific protease (USP7) to block the binding of P53 leading to the increased ubiquitination and degradation (Frappier, 2012). In vitro, it was observed that inhibiting EBNA1 significantly reduced cell viability and increased apoptosis among BL cell lines (Kennedy *et al.*, 2003) Thus, the role of EBV infection in the transformation of B cells was clearly illustrated to increase cell survival by targeting apoptosis.

The BCL-2 protein family regulates the intrinsic pathway of apoptosis which is mediated by the mitochondria and caspases. BCL-2 protein family is divided into anti-apoptotic proteins (BCL-2, MCL-1 and BFL1) which block apoptosis, proapoptotic proteins (BAX and BAK) which increase apoptosis and BH3 only proteins (BAD, BIM and PUMA) that also induce apoptosis (Kale *et al.*, 2018). EBV has a significant role in targeting BIM and PUMA proteins to supress apoptosis in BL during latency 1 stage of infection. However, there is another route used by EBV to induce more apoptosis resistance which involves the Wp viral promoter regulating: EBNA2, EBNA3A, EBNA-LP and BHRF1 protein expression (Mabuchi *et al.*, 2021, Cartlidge, 2015, Kelly *et al.*, 2009, Fitzsimmons *et al.*, 2020). The increased resistance to apoptosis seen in 15% BL cases is due to the activity of the viral BHRF1 which is a BCL-2 homologue protein that blocks apoptosis. The anti-apoptotic mechanism induced by EBV via BHRF1 protein was reported to be due to the interaction of BHRF1 with BIM, PUMA, BID, and BAK protein to prevent mitochondria permeabilization and maintain mitochondrial integrity and prevent further apoptotic signalling (Cartlidge, 2015). In addition, the impact of viral BHRF1 in blocking apoptosis and increasing cell survival in BL was tested in vitro using an inducible plasmid system and it was shown that the mutant form of BHRF1 protein was not able to protect the cells against apoptosis when compared to WT BHRF1 (Fitzsimmons *et al.*, 2020, Kvansakul *et al.*, 2010).

1.9 The contribution of Malaria in BL progression.

Plasmodium falciparum is one of six different *falciparum* malaria species that accounts for more than 75% of malarial infections amongst children in SSA

(holoendemic region) (Figure 1.14). (Nkumama *et al.*, 2017, Thorley-Lawson *et al.*, 2016, Pannone *et al.*, 2014). Studying the role of the Plasmodium falciparum parasite in developing BL has provided strong link to the pathogenesis of the disease. Malaria starts by infecting RBCs which triggers B cells to increase the production of polyclonal antibodies (Magrath, 2012).

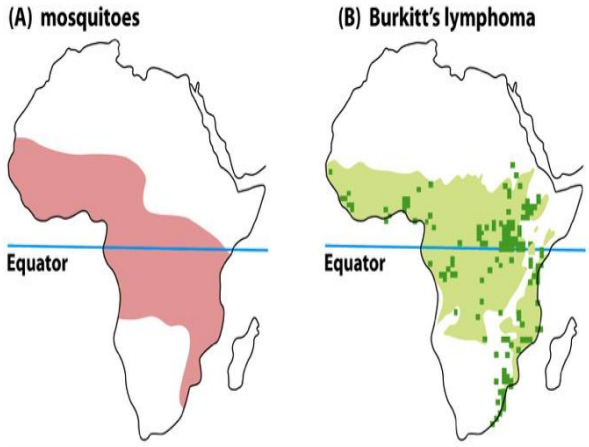

Figure 1. 14 Equatorial region in Africa is endemic with malarial infection. *Equatorial region in Africa is endemic with malaria infection with high mosquito spread across the region (green). The same region with malaria infection showed to share the distribution mapping of eBL across equatorial Africa (Mwanda et al., 2004).*

Interestingly, malarial infection was shown to prolong B cells at GC stage of development which triggered AID enzyme activity by releasing haemozoin from digested hemoglobulin. Studies showed that haemozoin binds to toll-like receptor (TLR9) on B lymphocytes causing deregulated AID activity and increased the risk of DNA breaks and MYC translocation (Edry *et al.*, 2008).

Tonsillar GC B cells collected from individuals infected with *P. falciparum* were shown to have a higher level of AID. This finding was linked to the study that showed an increased activity levels of AID in GC B cells as a response to haemozoin which was extracted from *P. falciparum* infected individuals. All these findings suggest that malarial infection can participate in the development of BL by inducing high levels of AID and increase the risk of genes breaks and translocations in GC B cells with high EBV infection rate (Thorley-Lawson *et al.*, 2016).

In response to malarial infection, RBCs infected with malaria express a protein known as cysteine rich interdomain region 1-alpha (CIDR1α). This protein was found to interact with memory B cells and increase the reactivation process of EBV virus.

Also, malaria parasite was reported to reduce T cell responses against EBV-infected B cells which increase the risk of BL developing (Magrath, 2012, Rochford, 2016).

1.10 The role of HIV in BL progression.

BL lymphomagenesis in HIV infected people is related to the immunocompromised status of the individuals (Dozzo *et al.*, 2017). Weakness of the immune system exposes the body to infection and increases the chance of having dysregulated cytokine actions which support the pathogenic effect of pathogens such as EBV (Grogg *et al.*, 2007). The immunocompromised state of HIV individuals has been linked to activation of latent EBV infection and abnormal proliferation of B cells (Galanis and Levis, 2015). HIV virus encodes trans-activator of transcription (Tat) protein which was found to bring chromosome 8 and the *C-MYC* gene in close proximity to the *IgH* gene on chromosome 14 for prolonged periods of time. This phenomenon was shown to increase the risk of the AID enzyme inducing a *C-MYC* translocation (Germini *et al.*, 2017). In HIV associated BL, there is a direct effect of Tat protein that promotes high proliferation rate in B cells thus increasing the chance of *C-MYC* translocation (Galanis and Levis, 2015). B cell development in HIV individuals is affected by inadequate and irregular cellular signalling which increases abnormal proliferation and metabolism in immature B cells, thus contributing to cancer development.

1.11 The genetics of BL.

As discussed earlier, BL is characterised by the translocation of *C-MYC* gene to immunoglobulin genes (either heavy or light chain gene). In addition to this particular translocation, other genetic mutations have been reported in different studies to be found in BL including endemic, sporadic and HIV related type. The development and progression of BL is not dependent on deregulated *C-MYC* gene expression only. Lymphoma progression requires multiple genomic mutations to evade apoptosis and proceed with cell cycle. Thus, genes that are responsible for

maintaining or regulating cell cycle, apoptosis, gene expression and cellular communications were found to participate in the progression of BL.

Genomic investigation studies used RNA sequencing, DNA sanger sequencing and whole exome sequencing reported that BL showed a *TP53* mutation in endemic and sporadic BL subtypes (Newman *et al.*, 2022, Abate *et al.*, 2015). The encoded P53 protein from the tumour suppressor gene *TP53* gene has a significant role in regulating different aspect of cellular events including cell cycle, apoptosis and DNA repair process. Irregular P53 function are linked to cancer progression which was found in almost 50% of cancers (Wang *et al.*, 2022). The mutation of *TP53* was reported in ~15% endemic BL whilst in sporadic BL, the mutation was present in about 50% of cases. Irregular P53 function and its contribution to BL progression was due to missense and or loss of gene heterozygosity causing protein failure to induce apoptosis and inhibit cell growth (Newman *et al.*, 2022, Abate *et al.*, 2015, Zhou *et al.*, 2019).

In addition to *TP53* mutations, furthermore genomic investigations of BL via whole genome sequencing showed that the neurogenic locus notch homolog protein 1 or (*NOTCH1)* was mutated in some BL cells (Love *et al.*, 2012a). Notch1, which is a member of the NOTCH protein family, functions as a transmembrane receptor that is important in cell communication. Upon activation with specific ligand, Notch1 initiates multiple cellular cascades that are important for cell development and gene expression. Thus, *NOTCH1* mutations can lead to irregular continuous signalling involved in cancer progression (Arruga *et al.*, 2014). In a study conducted on 70 different BL samples, mutation of *NOTCH1* was reported in 5 BL samples which accounts for 7.1% where *NOTCH1* was showing a truncating mutation (Love *et al.*, 2012a, Dozzo *et al.*, 2017).

Cell proliferation and the cell cycle are regulated by cell cycle proteins that facilitate cell cycle priming and progression during the different phases (Otto and Sicinski, 2017). Cell cycle regulator proteins are known as cyclin and cyclin dependent kinases. Irregular cyclin and cyclin dependent kinase activity is strongly related to cancer development in different cancers (Otto and Sicinski, 2017, Casimiro *et al.*, 2012). Upon cell development and activation with mitogens, cyclin D3 (*CCND3)*

expression levels begin to increase and complex with other cyclin dependent kinases to stimulate the phase transition of the cell cycle from G1 to S phase (Ketzer *et al.*, 2022). In BL, studies have observed that there are mutations in *CCND3* that play a role in BL progression that was commonly reported in multiple BL samples (Rohde *et al.*, 2017, Richter *et al.*, 2012). In sporadic BL, *CCND3* was mutant in 38% while HIV related BL showed a higher percentage of 68%. Although *CCND3* mutations were reported in endemic BL, it was low with 1.8% compared to other BL subtypes (Schmitz *et al.*, 2012). Genomic investigations of *CCND3 performed by Sanger sequencing of the DNA of different BL cells* showed missense, nonsense and frameshift mutations which were responsible for increasing protein stability and maintained activity by removing 41 amino acids. The mutation was reported to target the conserved PEST domain (proline, glutamic acid, serine and threonine) that regulates protein stability and degradation (Schmitz *et al.*, 2012, Nguyen-Khac *et al.*, 2021).

Another approach that can be used to stimulate cancer progression is to target the activity of the transcription factor gene *TCF3* and its negative regulator gene which is known as Inhibitor of DNA Binding 3 (*ID3*). The TCF3 protein is a transcription factor that belongs to the helix loop helix (HLH) protein family that has the ability to complex with other HLH transcription factors and binds to DNA to initiate multiple cellular events and programming. The regulation of TCF3 protein activity is controlled by ID3 protein that heterodimerises with TCF3 and inhibits its ability to bind DNA (Bakr *et al.*, 2021, Yamazaki *et al.*, 2020). In BL, the TCF3 and ID3 pathway was reported to be involved in cancer pathogenesis with mutations in both *TCF3* and *ID3 genes*. The TCF3 isoform (E47) mutation is very common in BL where N551K, V557E/G, D561E/V/N, M572K amino acid residues are affected. *ID3* nonsense and frameshift mutations were also reported in BL leading to the inability of ID3 protein to recognise and bind TCF3 and resulting in constitutive TCF3 activity. Mutations of *TCF3/ID3* genes are very common in BL and reported in 67%, 70% and 40% of sporadic, endemic and HIV related BL samples, respectively (Yamazaki *et al.*, 2020, Schmitz *et al.*, 2012).

The transcription factor Forkhead Box Protein O1 (*FOXO1)* which plays an important role in cellular metabolism, was reported to be mutant in different sporadic

(29%) and endemic (54%) BL cases where missense and nonsense mutations of *FOXO1* were reported using Sanger sequencing. In addition, *FOXO1* mutations were commonly reported in the binding domain of AKT serine-threonine protein kinase at T24 and S22 causing protein retention (Zhou *et al.*, 2019).

Gene expression of the different proteins recruited during cell proliferation can be controlled by chromatin remodelling which results in easier gene access by other transcription factors and DNA binding proteins. Thus, it is crucial for chromatin remodelling to be maintained and regulated to avoid irregular cell proliferation. The SWitch/Sucrose Non-Fermentable (SWI/SNF) protein complex is a chromatin remodeller that targets nucleosome regulation. The *ARID1A* gene is responsible for producing AT rich interaction domain containing protein A1 which is a sub unit protein that belongs to SWI/SNF complex and found to be mutated in different cancers (Wu *et al.*, 2014). In BL, truncating *ARID1A* mutations were found in 17.2% – 25% of endemic BL samples as reported by RNA sequencing (Abate *et al.*, 2015, Wu *et al.*, 2014). Additionally, in a study that was conducted for paediatric BL, nonsense *ARID1A* mutation was reported in 32% of total pediatric BL samples tested (Burkhardt *et al.*, 2022). The anti-apoptotic Myeloid Leukemia 1 (*MCL1)* gene is a hot spot that inhibits apoptosis upon its upregulation in BL.

The MCL-1 protein prevents mitochondrial cytochrome c release which is released as a consequence of BAK and BAX protein pathway. Increased MCL-1 protein activity was linked to cancer pathogenesis (Wang *et al.*, 2021). Fluorescence in situ hybridization (FISH) analysis showed *MCL1 gene* amplification which causes *MCL1* overexpression in over 20% of tested BL samples. Additionally, increased MCL-1 protein stability was reported due to point mutations found in the *FBWX7* gene which produces a ubiquitin ligase protein that controls MCL-1 protein degradation (Roth *et al.*, 2012, Klanova *et al.*, 2022).

All gene mutations discussed are listed in the following Table 1.5 which describes the different genetic mutations involved in BL.

Gene name	Gene function	Reported mutations in BL
- Inhibitor Of DNA Binding 3 (*ID3*) **- Transcription Factor 3 (*TCF3*)**	- ID3 protein is a negative regulator and suppressor of the transcription factor TCF3.	- Missense and frameshift mutations in eBL (70%), sBL (67%) and HIV related BL (40%). - Mutations involve ID3 and/or TCF3 protein binding domain.
Specific cyclin D3 (*CCND3*)	- Cell cycle driver and regulator. - Facilitate G1/S phase transition.	- Mutations reported in sBL (38%), eBL (1.8%) and HIV related BL (68%). - Missense and nonsense mutations of PEST domain causing increased protein half-life.
Neurogenic locus notch homolog protein 1 (*NOTCH1*)	- Membrane receptors. - Regulates cellular development and proliferation and cell to cell interaction.	- Truncating mutations in 7.1% of tested BL samples. - Increased NOTCH1 protein activity and continuous proliferation signalling pathway.
AT rich interaction domain containing protein A1 (*ARID1A*)	- Subunit protein in the SWI/SNF complex. - Important in chromatin remodelling. - Involved in DNA replication and repair process.	- Truncating mutations in 17.2 - 25% of BL cases. - Nonsense mutations in 32% of paediatric BL.
Tumor protein (*TP53*)	- Regulates cell cycle progression and apoptosis. - Guards cellular DNA via DNA repair process upon DNA damage.	- Loss of gene heterozygosity in 25 – 50% of sBL and 15% of eBL. - Missense mutation with inactivated protein function.
Myeloid cell leukemia-1 (*MCL1*)	- Belongs to BCL-2 protein family that regulates apoptosis. - Prevents cytochrome c release from mitochondria.	- Gene amplification in over 20% of tested BL samples. - Point mutations of ubiquitin ligase. - Overexpression in some of BL samples.
Forkhead box protein O1 (*FOXO1*)	- Transcription factor belongs to forkhead protein family. - Regulates different gene expression.	- AKT binding site mutations in 29% sBL and 54% of eBL tested samples.

Table 1. 5 The different names of mutated genes reported in BL and their cellular function. *(Bouska et al., 2017, Rohde et al., 2017, Klumb et al., 2001, Love et al., 2012b, Zhou et al., 2019, Roth et al., 2012, Kelly et al., 2014, Nguyen-Khac et al., 2021, Dozzo et al., 2017, Dozzo et al., 2016, Amato et al., 2016, Preudhomme et al., 1995, Schmitz et al., 2012, Love et al., 2012a, Abate et al., 2015, Roschger et al., 2017, Newman et al., 2022, Burkhardt et al., 2022)*.

1.12 *C-MYC* gene and its role in regulating multiple cellular mechanism.

Gene expression is regulated by specific groups of proteins known as transcription factors (TFs) that bind the promoter region of target genes and regulate transcription (Chial, 2008, Wang *et al.*, 2015). One of the most important transcription factors is called C- MYC protein. Besides being an oncogene, C-MYC is known to be involved in a wide network of molecular pathways as a master gene expression regulator (Chanu and Sarkar, 2014, Miller *et al.*, 2012). *C-MYC* gene is located on chromosome 8 and encodes a protein with 439 amino acids that belongs to the basic helix-loop-helix zipper (bHLHZip) family (Sammak *et al.*, 2019, Conacci-Sorrell *et al.*, 2014). C-MYC protein has a vital role in regulating cell cycle progression, cellular metabolism, cell division, DNA synthesis and repair and apoptosis (Figure 1.15) (Conacci-Sorrell *et al.*, 2014).

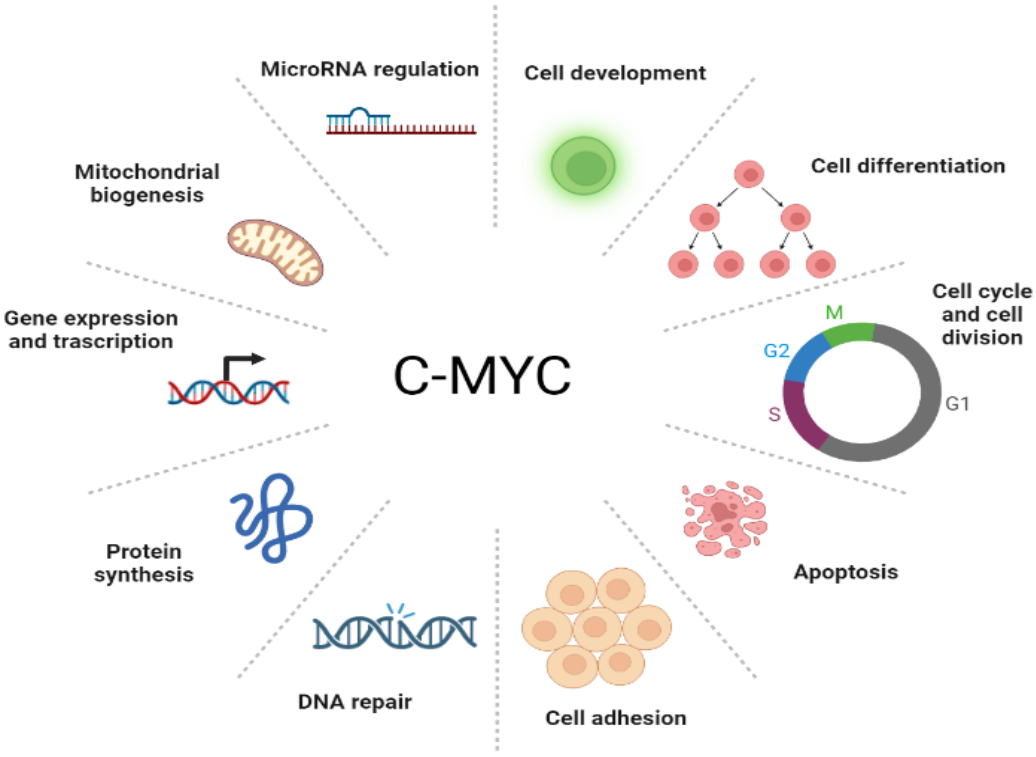

Figure 1. 15 The complex cellular functions that are regulated by C-MYC protein inside the cell. *C-MYC is involved in multiple cellular pathways and mechanism including microRMA pathways, cell cycle phases where C-MYC regulates the expression of multiple cyclin proteins. C-MYC plays a major role in gene expression by functioning as a transcription factor, controls cellular development and differentiation. C-MYC also, participates in DNA synthesis and repair mechanism and engages in protein synthesis and programmed cell death by regulating P53. This figure was created using BioRender platform (www.BioRender.com).*

C-MYC protein has the capacity of regulating between 10% and 15% of the whole genome from drosophila through to humans. *C-MYC* gene expression mediated activation is achieved via different mechanisms which includes; DNA methyltransferases, histone acetylases recruitment and proteins that modulate chromatin (Dang, 1999). C-MYC protein binds with a transcription factor MAX or MAD (Figure 1.16) to form a heterodimer protein complex forming a DNA binding motif that looks like scissors to activate or supress gene expression (Amati and Land, 1994).

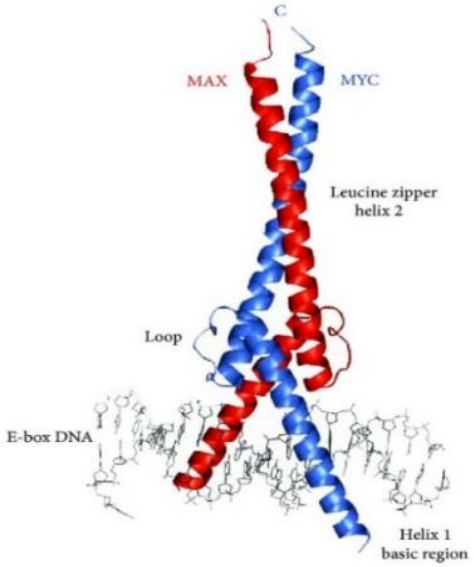

Figure 1. 16 MYC-MAX dimerization. *Crystallography structure of MYC-MAX dimerization at leucine zipper region of each protein. MYC-MAX complex binds DNA at E box initiating the transcription process of the gene (Tansey, 2014).*

Upon complexing with MAX or MAD, C-MYC binds to the E box sequence (5'-CANNTG-3') in DNA which acts as a gene expression regulator region that is known as a binding site for (bHLHZip) family (Figure 1.17). Once bound to an E box, C-MYC regulates the targeted genes transcription via chromatin remodeling complex and histone acetyl transferase or repressing the expression via regulating histone deacetylases 1 and 2, Paired amphipathic helix protein Sin3a (Sin3), and Nuclear Receptor Corepressor (N-CoR) (Kharazmi *et al.*, 2012, Dang, 1999, Chanu and Sarkar, 2014, Terme *et al.*, 2009).

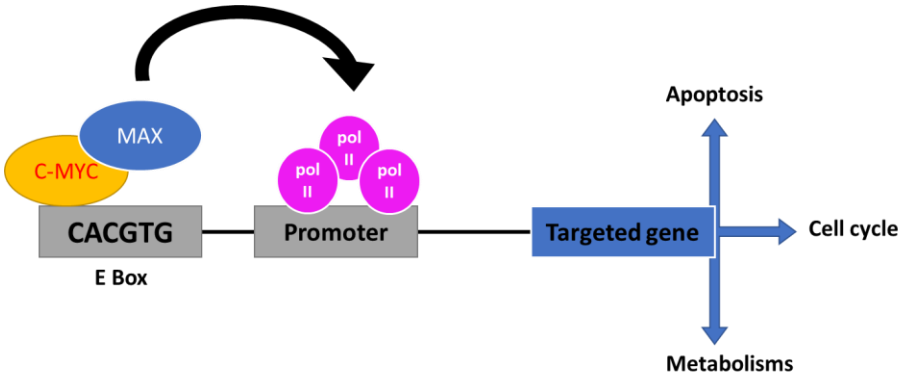

Figure 1. 17 Gene expression regulation by C-MYC- MAX heterodimerization. *C-MYC- MAX complex binds to E Box region (CACGTG) of targeted gene and recruits RNA polymerase II for gene transcription.*

MYC regulates other transcription factors involved during cell cycle and differentiation including cyclin A2, cyclin D2, cyclin dependent kinases 4 and 6, P21 and Integrin, etc (Miller *et al.*, 2012, Conacci-Sorrell *et al.*, 2014, Bretones *et al.*, 2015). Studies have shown that C-MYC regulates glucose metabolism via glucose transporter gene (GLUT1), lactate dehydrogenase A (LDHA) and hexokinase II (HK II) genes highlighting the function of C-MYC in the modulation of glycolysis and glucose uptake (Li *et al.*, 2020). C-MYC is also significant in regulating different networks of microRNAs (miRNA) by stimulating miRNA-17-92 to block different miRNAs including miRNA precursor Let-7 (Li *et al.*, 2014, Olive *et al.*, 2010). C-MYC also mediates the suppression of genes through the control of targeted genes by the Miz-1 pathways (Tansey, 2014, Van Riggelen *et al.*, 2010)

Earlier reports have demonstrated the involvement of C-MYC in energy metabolism and in mitochondrial biogenesis. C-MYC stimulates glycolysis and oxidative phosphorylation via transcription. At the DNA level, C-MYC targets aspartate transcarbamoylase (CAD) and ornithine decarboxylase (ODC1), that are involved in the repair and biosynthesis of DNA (Eberhardy and Farnham, 2001, Tsuji *et al.*, 2007, Bello-Fernandez *et al.*, 1993). In terms of apoptosis, C-MYC was expressed in fibroblast and myeloid cell line and induced apoptosis by inhibiting P21 and activating TP53 (S, 2019, Ho *et al.*, 2005).

C-MYC belongs to MYC protein family which includes; L-MYC and N-MYC. Functionally, there are no major differences among MYC members. They are similar in the way they affect cell proliferation and death except for potency differences (Nesbit *et al.*, 1998). Each member is expressed variously based on cell type and mutations in the different MYC proteins are associated with different diseases. Studies focused on *MYC* and tumorigenesis revealed that *C-MYC* was found to be mutant in solid and other blood cancer such as lymphomas. On the other hand, *L-MYC* and *N-MYC* were associated with lung cancer and neuronal cancer in brain, respectively (Tansey, 2014). Due to restricted understanding of how L-MYC and N-MYC functions and expression mechanisms, most *MYC* gene related studies in human are focused on *C-MYC* (Malynn *et al.*, 2000).

1.13 *C-MYC* expression and phosphorylation.

C-MYC protein level is increased or decreased differentially through the cell cycle. For instance, C-MYC levels are increased when cells are approaching G1 phase. C-MYC levels are regulated by different mechanisms starting with transcription rate, mRNA stability and post translational modification such as phosphorylation which plays a major role in regulating C-MYC (Sears, 2004). A key mechanism regulating C-MYC levels is protein degradation via the ubiquitin proteasome system.

Protein phosphorylation is required for C-MYC activation and RAS proteins are involved in this process. RAS is a signal transducers protein found in the cell (Goodsell, 1999). During cell cycle, growth factors induce a series of signalling events leading to activation of RAS protein which stimulates extra cellular receptor kinase protein (ERK) leading to phosphorylation of C-MYC at Serine 62 in the N-terminus and protein stabilisation. C-MYC degradation requires phosphorylation at Threonine 58 through GSK3β pathway alerting ubiquitination proteasome system to degrade C-MYC. Phosphatidylinositol-3-OH kinase also participated in regulating C-MYC stability by inhibiting Threonine 58 phosphorylation via inhibiting GSK3β (Figure 1.18) (Sears, 2004).

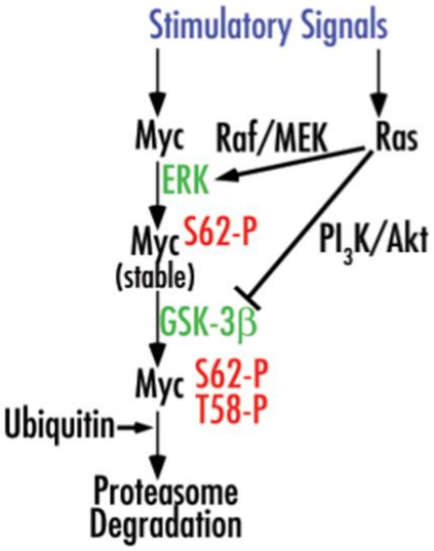

Figure 1. 18 The role of phosphorylation in C-MYC stability*. C-MYC stabilization and degradation is controlled by phosphorylating Serine 62 (S62-P) and Threonine 58 (T58-P) via rat sarcoma (Ras) pathways involving rapidly accelerated fibrosarcoma (raf)/mitogen-activated ERK kinase (MEK)/extracellular signal-regulated kinase (ERK) and glycogen synthase kinase 3 β (GSK3β) phosphorylation pathways. GSK3β phosphorylation via phosphoinositide 3-kinase (PI3K)/protein kinase B (Akt) increases C-MYC stability via inhibiting T58 phosphorylation (Sears, 2004).*

Mutations at Serine 62 or Threonine 58 will affect the normal process C-MYC regulation and increase the risk of aberrant C-MYC activity and cancer progression. *C-MYC* mutations were observed in some types of leukaemia and lymphoma such as BL where C-MYC protein was continuously elevated (Salghetti *et al.*, 1999, Sears, 2004, Thomas and Tansey, 2011). Additionally, *C-MYC* expression rate is monitored in a sophisticated genetic mechanism preventing gene abnormalities which is reflected by the fact that C-MYC protein half-life is determined to be around 30 - 20 minutes (Dang, 2012).

C-MYC expression is controlled by the wnt signalling pathway where mitogen and wnt ligand bind to G protein coupled receptor Frizzled (FZD). This interaction induces the phosphorylation of Low-density lipoprotein receptor related protein 6 (LRP6) and GSK3β thus recruiting adenomatous polyposis coli (APC) to activate β-catenin which enters the nucleus to progress with different gene expressions including *C-MYC* transcription (Figure 1.19) (Niehrs and Acebron, 2012, You *et al.*, 2002b, Jeong *et al.*, 2018).

C-MYC oncogenicity does not depend on *C-MYC* gene mutations only, it can occur due to irregular or uncontrolled activation via signalling pathways. Mutations in signal transducer genes contribute to continuously activating gene transcription and increase *C-MYC* oncogene transformation (Dang, 2012)

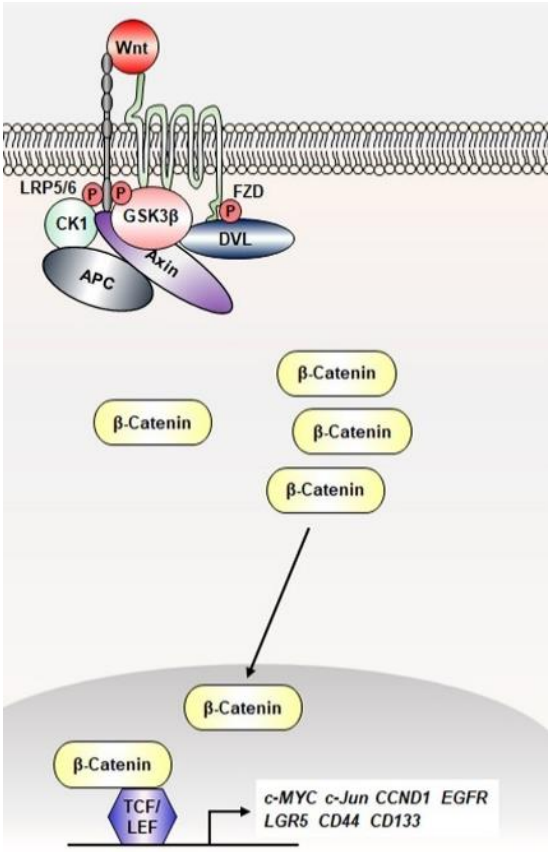

Figure 1. 19 The role of wnt pathway in C-MYC expression. *Wingless related integration site (wnt) signalling pathway plays a major role in regulating C-MYC expression. Mitogenic activation of Frizzled (FZD) receptors causing Low-density lipoprotein receptor-related protein 6 (LRP6) phosphorylation to activate β-catenin cascade via Adenomatous polyposis coli (APC) through T-cell factor (TCF)/lymphoid enhancer factor (LEF) transcription factors and induce C-MYC transcription. Multiple proteins are interacted in this process including glycogen synthase kinase 3 β (GSK3β), axis inhibition (Axin), Disheveled proteins (DVL) and Casein kinase 1 (CK1) (Jeong et al., 2018).*

1.14 The architecture of *C-MYC* breakpoints and the role of Ig enhancer elements in BL

The *C-MYC* gene is composed of 3 exons with four different promoters that initiate *C-MYC* transcriptions process; P0, P1, P2 and P3 with most transcripts initiating from the P2 promoter (Nguyen *et al.*, 2017, Levens, 2008). The first exon is a non-

coding exon which includes both C-MYC promoters; P1 and P2. Exon 2 and 3 are the protein coding exons that have about 90% of sequence identity among different species (Figure 1.20) (Spencer and Groudine, 1991).

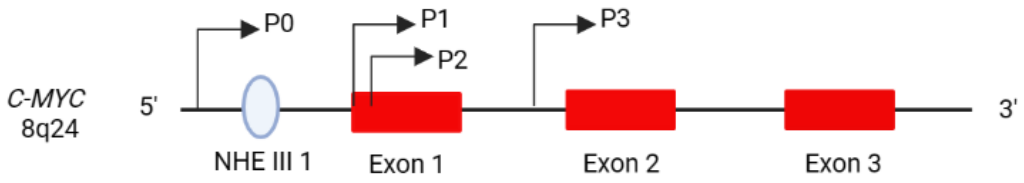

Figure 1. 20 the structure of C-MYC gene on chromosome 8 q24. *C-MYC consists of 3 exons (red) and possesses 4 promoters; P0, P1; P2 and P3 (black arrows) that facilitate transcription sites. Nuclease hypersensitive element III 1 (NHE III 1) (light blue) is a C-MYC regulatory element that regulates C-MYC expression and induces transcriptional suppression. This figure was generated using BioRender platform (www.BioRender.com).*

As previously introduced, the *C-MYC* gene (8q24) is the driving force of BL progression and proliferation due to translocation to one of the Ig genes; *IgH* (14q32), *IgK* (2p12) and *IgL* (22q11). Depending on the translocation breakpoint, *C-MYC* translocation falls into 3 different types classified as, class I, class II and class III. In class I translocations, the breakpoint is located within the *C-MYC* first exon in which *C-MYC* transcription is initiated from a cryptic sites located in the first intron (Levens, 2008). Class II translocations involve the 5' end breakpoint of *C-MYC* resulting in head-to-head (5'–5') translocation with Ig gene heavy or light chain ones. Class III translocation is characterized by a breakpoint that is located distantly from *C-MYC* up to 100 kilobases away (Nguyen *et al.*, 2017, Boxer and Dang, 2001). Despite what BL subtype is, the common translocation of *C-MYC* was found to be related with *IgH* t(8;14)(q24;q32) where it is evaluated to be around 70-80% of BL cases (Ferry, 2006, Graham and Lynch, 2021). In eBL, the common *C-MYC* breakpoint type was class II whilst in sBL class I translocations occasionally occurs. For eBL, it is common for the breakpoint to be located in the variable region in either (V), diversity (D) or joining (J) segments of the *IgH* with respect to *IgK* and *IgL* that lack (D) segment. In addition, breakpoints can also occur in the constant region of Ig gene which is common in HIV related BL and sBL (Nguyen *et al.*, 2017, Boxer and Dang, 2001).

Upon translocation, *C-MYC* expression is regulated via Ig intronic and the distal enhancer elements located at the constant region of the Ig gene causing *C-MYC* upregulation and shifting transcription to be initiated from P2 rather than P1 in an unknown mechanism (Boxer and Dang, 2001, Nguyen et al., 2017). The intronic enhancers of the *IgH* gene is referred to as Eμ and the 3' distal enhancers are (HS1-2, HS3 and HS4). Intronic enhancers of *Igk* and *IgL* are Ek and Eλ2-4 respectively while distal enhancers for *Igk* and *IgL* are 3'Ek and Eλ3-1 respectively (Bruzeau *et al.*, 2022). When the breakpoint is located in the V(D)J region of the Ig gene, both of intronic and distal 3' enhancers are likely to be present which is common in eBL cases. If the breakpoint is located in the constant region of the Ig gene, there is a high chance of losing the activity of intronic enhancer element which gives the advantage of the distal enhancer to deregulate *C-MYC* expression which is seen often in sBL. Figure 1.21 demonstrates the possible breakpoints involved in *C-MYC* translocation to *IgH, Igk* and *IgL* genes.

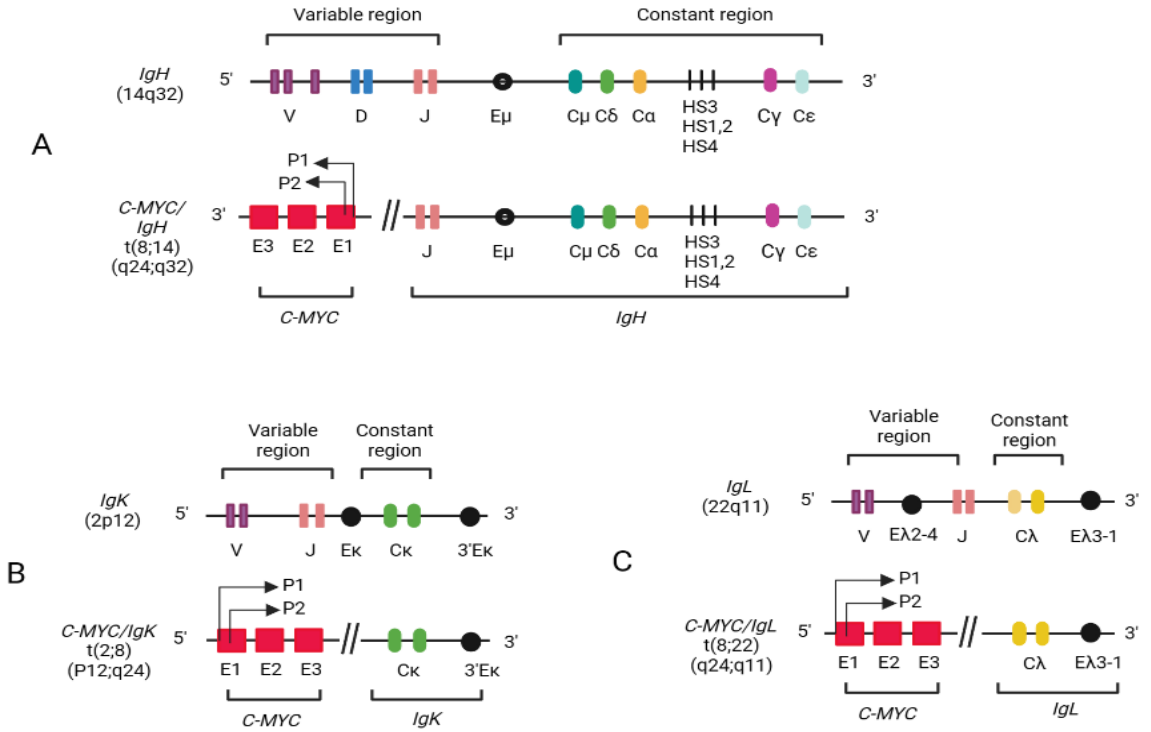

Figure 1. 21 Different C-MYC/Ig breakpoints involved in BL. *(A top) IgH gene structure on 14q32 which is composed of the variable region V(D)J, constant region (Ig isotype determinant). Enhancer elements; Eμ, HS1-2, HS3 and HS4 are shown in black. (A bottom) head-to-head C-MYC translocation to IgH t(8;14) (q24;q32) where breakpoint (//) is involved within V(D)J region. (B top) IgK gene structure on 2p12 showing variable VJ region, constant region. Enhancer elements; Ek and 3'EK are shown in black. (B bottom) C-MYC translocation to Igk t(2;8) (p12;q24) where breakpoint (//) is placed in variable region. (C top) IgL gene structure of variable VJ, constant region. Enhancer elements; Eλ2-4 and Eλ3-1 are shown in black. (C bottom) breakpoint (//) involved where C-MYC is translocated to IgL t(8;22) (q24;q11). Figure was generated using BioRender platform (www.BioRender.com).*

1.15 BL treatment and the current therapies for BL in low- and high-income countries.

BL can be treated under a controlled and scheduled regime that involves multiple drug combinations alongside supportive care protocols. It is also important to evaluate the cancer stage to determine which drug to be indicated at which dose and course. Treatment course must be progressed as soon as possible after diagnosis and evaluation of the stage of the cancer. Ann Arbor system or St Jude or Murphy staging system are usually used to stage BL and help in identifying the minimum therapies required depending on how aggressive the tumour is and identifying if there is an involvement of the central nervous system or BM (Linch, 2012, Hasse *et al.*, 2020).

The combination of chemotherapy, radiation and surgical interventions are considered as the general protocol used in treating BL worldwide (Swerdlow *et al.*, 2016). The initial diagnosis step of BL in both high-income countries (HICs) and LMICs starts by performing fine needle analysis (FNA) which help in identifying lymphoma type (Gopal and Gross, 2018). Radiography tests and PET scans are also used but are not widely affordable in LMICs (Molyneux *et al.*, 2012). Further clinical assessments routinely used to stage individuals with BL are required including general physical status, chest radiograph, abdomen ultrasound and cerebrospinal liquid analysis, followed by Ann Arbor and St Jude staging system for adults and children patients, respectively (Graham and Lynch, 2021). Lumbar puncture and bone marrow samples are collected from adults presenting with aggressive BL. Once diagnosis is completed, cytotoxic chemotherapeutic agents will be indicated with continuous evaluation which is vital to reduce mortality rate and to manage the general therapy related toxicity of the therapy. Unfortunately, due to irregular patient follow up and medical checks accompanied by limited access to advanced clinical facilities, eBL patients in SSA mostly reported with tumor lysis syndrome. High-risk group of BL patients are given a regimen of prednisone for up to 7 days (Graham and Lynch, 2021).

For BL patients, cyclophosphamide is used with intrathecal therapy in a purpose of avoiding leptomeningeal recurrence. Applying this protocol improved survival rates

up to 60% in patient receiving the treatment for 1 year with only 10% mortality rate (Gopal and Gross, 2018). In HICs, surgical intervention and radiation therapy accompanied by a treatment course which combines doxorubicin, vincristine, etoposide and cytarabine play a significant role in curing and treating advanced BL stage (Olivotto *et al.*, 2020, Molyneux *et al.*, 2012).

Survival rate is dependent on multiple factors that affect therapy outcome (Olivotto *et al.*, 2020, Gupta *et al.*, 2015). In SSA, BL individuals often present with advanced cancer that requires anthracycline to be added to the treatment plan and this reduced the general survival rate down to 40-50% after 1 year of receiving BL therapy. Methotrexate is another candidate drug that can be used in treating more advanced BL (Gopal and Gross, 2018). In comparison in HICs, the survival rate is increased to 75% after 1 year of receiving therapy. This percentage increase is due to medical resources availability, routine patients' check-ups with early access to haematologist and oncologist consultations (Gopal and Gross, 2018).

During BL therapy, tumour lysis syndrome is a problem. Thus, continuous blood analysis is necessary as part of the treatment protocol to avoid renal failure (Senbanjo, 2009). Hereto, Allopurinol is useful in treatment management alongside continuous hydration to reduce the increased uric acid production from lysed cells and to prevent kidney damage.

Intravenous antibiotics are also another part of BL therapy management and is used in neutropenic fevers related with chemotherapeutic administration. Blood transfusions are also needed where patients develop anaemia and/or low platelet counts (Ferri, 2021). As part of BL treatment, patients are required to visit the clinical facility routinely in a period that lasts 2 years to perform medical follow-ups which is very important to evaluate cancer relapse susceptibility (Ferri, 2021, Action, 2021). Routine hospital and clinical centre visits are difficult in LMICs and this is an obstacle in improving survival rates (Bispo *et al.*, 2020). Table 1.6 shows the different chemotherapeutic drugs that are used and the mechanism of action involved.

Drug name	Known Mechanism(s) of action	Side effect
Doxorubicin	- Inhibits DNA synthesis and replication via intercalating with DNA base pairs. - Inhibits topoisomerase II that regulates DNA coiling which is required during DNA transcription and repair mechanism.	**- Common**: Nausea, Vomiting, Hair loss mouth and lips sores. **- Less common**: Diarrhoea, Joint pain and shortness of the breath.
Cyclophosphamide	- Alkylating agent. - Activity is triggered by the phosphoramide mustard which binds and crosslinks DNA strands to inhibit DNA replication. - Immunosuppressive drug that targets T cells by reducing interferon gamma and interleukin 12.	**- Common**: hair loss, muscle aches, fatigue, bleeding gums and pain during urination. **- Less common**: loss of hearing, lack of hands sensation and arrythmia.
Vincristine	- Inhibits microtubules formation and chromosome separation during cell division via binding to tubulin.	**- Common**: tingling hand and feet sensation, hair loss, fatigue, joint pain and constipation. **- Less common**: loss of appetite, diarrhoea, mouth sore and dizziness.
Etoposide	- Inhibits topoisomerase II DNA ligation activity. - leads to DNA damage and cell death.	**- Common**: hair loss, constipation, abnormal liver function and arrhythmia. **- Less common**: blurred vision, metallic mouth taste, skin rashes and breathing difficulty.
Cytarabine	- Converts into cytosine arabinoside triphosphate that competes with cytosine within cellular DNA. - Induces DNA damage during cell cycle and DNA synthesis. - Inhibits ribonucleotide reductase leading to inhibition of DNA synthesis.	**- Common**: mouth sores, muscle and joint pain, fatigue, and hands numbness. **- Less common**: Skin rashes, pale skin, heartburn, diarrhoea and dizziness.
Methotrexate	- Inhibits the formation of tetrahydrofolate by targeting dihydrofolate reductase. - Inhibits DNA formation by targeting DNA nucleotides synthesis that uses folate. - Acts as immunosuppressant by targeting T cells via inhibiting aminoimidazole carboxamide ribonucleotide transforlmylase.	**Common**: nausea and vomiting, loss of appetite fatigue, and fever. **Less common**: kidney failure, hepatotoxicity, skin rashes and pancreatitis.
Anthracyclines	- Extracted from Streptomyces species. - Bind DNA and inhibits DNA replications. - Inhibit topoisomerase II. - Generate oxidative stress via reactive oxygen species accumulation by cytochrome P450 reductase.	**- Common**: fever, skin rashes, diarrhoea joint pain and cough. **- Less common**: cardiotoxicity, gastrointestinal bleeding, coma and leukopenia.

Table 1. 6 The different names and molecular function of cytotoxic chemotherapeutic drugs used in BL patients.

1.15.1 Novel BL therapies.

In recent years, significant effort has been put into developing novel therapies that target B cell lymphomas. Increased understanding of the molecular pathways involved in B cell lymphomas have massively helped in detecting some targets that can be used in the designing of effective therapies that also can be used in relapsed cases.

Brutons Tyrosine Kinase (BTK) was found to be involved in the pathogenesis of B cell lymphoma by regulating nuclear factor kappa B (NF-κB) pathway which was found to induce cellular proliferation. Thus, the development of new therapies that target BTK could be a good strategy in treating B cell malignancies. Ibrutinib (BTK inhibitor) was developed to bind the active site of BTK (Cys-481) leading to the inhibition of downstream cascade of B cell receptor to supress cell proliferation signals and induce apoptosis (Davids and Brown, 2014, Shah *et al.*, 2021).

The addition of the α-CD20 monoclonal antibody rituximab as an immunotherapy to the panel of cytotoxic agents in therapeutic regime was reported to increase treatment efficacy with increased survival rate in patients with B cell lymphoma (Pfreundschuh *et al.*, 2006). Rituximab acts by targeting CD20 in B cells and inducing antibody dependent cell mediated cytotoxicity (ADCC) and complement dependent cytotoxicity which causes cell death by apoptosis (Randall, 2016, Shah *et al.*, 2021). It was reported that rituximab had increased overall survival in BL patients and with improved outcome when administered with cyclophosphamide, vincristine, doxorubicin and dexamethasone (Fayad *et al.*, 2007, Wildes *et al.*, 2014).

Increased understanding of how the immune system works and reacts to cancer cells led to the development of chimeric antigen receptor T cell (CARs). Anti-B cell lymphoma CAR T cells are genetically engineered T cells that target CD19 on B cells and initiate cytotoxic effect to kill them and that can be combined as a treatment strategy for B cell malignancies (Feins *et al.*, 2019, Foon *et al.*, 2012).

In SSA, BL accounts for more than 50% of cancer in children diagnosed with cancer. It is worth to consider that BL also accounts for a high percentage among NHL

children that reaches up to 60% worldwide (Bouda *et al.*, 2019b, Frazer *et al.*, 2019, Cunha *et al.*, 2012). Thus, developing more effective low toxicity therapy for BL is important. The treatment regimen for BL requires multiple hospital visit, extended hospitalization and follow-up which are unfortunately costly and expensive and is one of the major obstacles for completing treatment course (Bouda *et al.*, 2019a). In SSA, there is significant shortage of healthcare workers, medical facilities and supplies that are crucial during BL therapy including supportive care.

There are different approaches used in treating BL including radiotherapy. In SSA, there is no accessible radiotherapy centre in more than 20 countries with a presence of a very limited hospital care. This makes BL patient more dependent on other options of treatment. Furthermore, there are very few pathologists who are qualified to evaluate the progression stage of tumours (Gopal *et al.*, 2012).

BL patients can present different responses to BL therapies with some patients presenting with refractory disease or relapsing. Different BL clinical studies which used chemotherapeutic agents reported that although chemotherapeutic agents are effective against BL, there is a risk of developing drug related toxicity and relapse which occurs after remission (Jakobsen *et al.*, 2020, Nkrumah and Perkins, 1976a). Unfortunately, drug resistance can arise some BL patients who received vincristine, cyclophosphamide, methotrexate and dexamethasone (Williams *et al.*, 1983, Cloonan and Williams, 2011, Tabata *et al.*, 2020, Ozuah *et al.*, 2020).

There is an increased need to develop new therapy that is not expensive, that can be easily administered, shows a higher efficiency against BL with safer outcome profile and effective against relapsed and resistant BL cases. New therapies can be used as an adjunctive drug to current BL regimes to help in reducing drug related toxicity seen in BL patients and potentially reducing the course length of chemotherapeutic management.

Drug repurposing is the use of existing drugs in a new clinical setting and has contributed to the development of novel therapies. Clofibrate (CA) or Bezafibrate which is an approved drug used to treat hyperlipidaemia and Medroxyprogesterone acetate (MPA) which is a steroidal sex hormone steroid showed an anti-proliferative

effect on BL cell lines and acute myeloid leukemia (AML) cell lines. BL cell lines were treated with CA and MPA individually and in combination. It was shown that CA alone was not enough to reduce cell growth in primary BL cells and MPA alone was able to have anti-proliferative effect. However, CA and MPA combination showed an increased suppression of cell growth in primary BL cells as represented with low levels of radioactive tritiated thymidine which is used to measure cell replication. Further investigations were taken to understand how CA and MPA acquire anti-proliferative effect against BL cells (Fenton *et al.*, 2003).

Our group participated in a clinical trial in Malawi using BaP (combination of Bezafibrate the Clofibrate alternative and MPA) where 95 children with relapsed and resistant BL were recruited and divided into different groups in which some were given low BaP dose, intermediate and high BaP dose. Administration of BaP began with the first day of conducting the study. BaP was given with other chemotherapy in one cohort of patients. Other patients were given BaP alone for 1 week followed by chemotherapy. Antibiotics were administrated in cases represented with infections. The clinical trial showed that BaP reduced BL disease progression with improved clinical response relatively to increased doses and showed that BaP administration is safe and is effective (Molyneux *et al.*, 2014).

1.16 FMC drug library.

A primary area of research in our laboratory is the development of affordable low toxicity treatments for blood cancers including BL (Jiang *et al.*, 2022, Molyneux *et al.*, 2014). To facilitate this, our group constructed a drug library named (FMC) that contains 100 already approved and licensed drugs that have been used worldwide for many years. The concentration for each drug in the library was adjusted to represent the maximum serum dose (Cmax) achieved when the drug was used clinically. Our group tested and screened different BL cell lines against the FMC drug library, measuring viability at 72 hours using a Celltitre Blue assay. The screening data highlighted zinc acetate as a potent anti-BL activity (Figure 1.22).

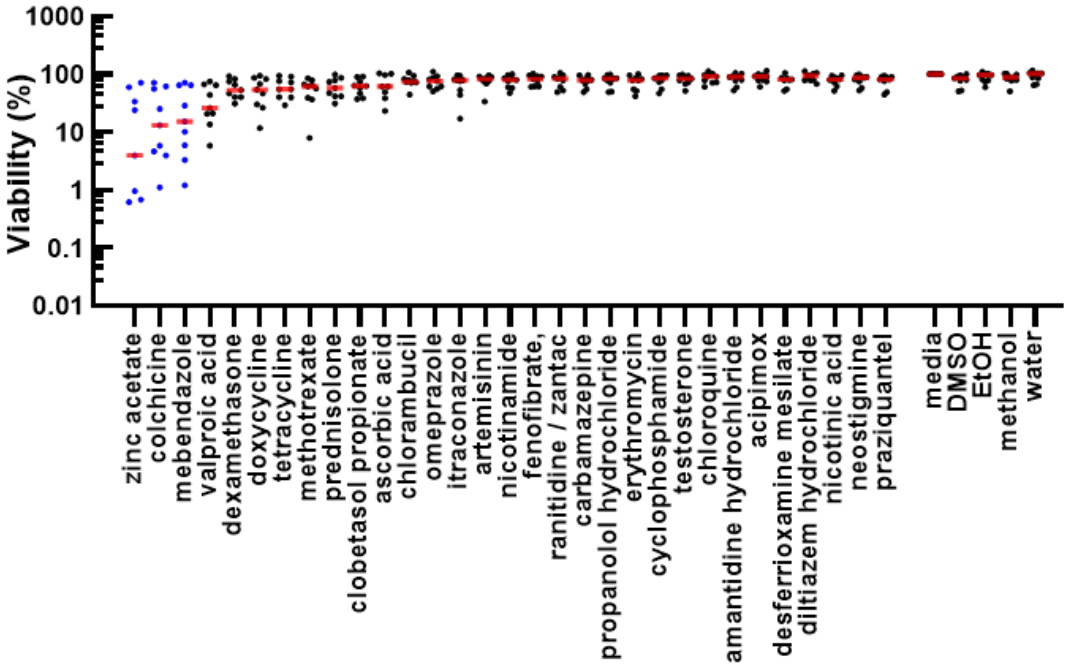

Figure 1. 22 FMC drug library screening data against different BL cell lines. *Different BL cell lines are represented individually in the graph as small dot. Cell lines, viability was screened against FMC drug library agents as presented on the X axis. Zinc acetate showed to be the highest effective drug against all BL cell lines which showed to be sensitive against zinc acetate with decreased viability percentage after 72 hours as presented on the log scale Y axis.*

Further screening studies in our laboratory have demonstrated that BL cells are significantly more sensitive to normal levels of zinc compared to normal B cells with apoptotic cell death of BL cells to be associated with induction of mitochondrial

superoxide (data not shown). A significant proportion of children developing eBL are likely to suffer from malnutrition and zinc deficiency (Fanzo, 2012).

1.17 Zinc.

Zinc is an essential micronutrient. It has functional and structural importance in a significant number of macromolecules and plays a vital role in approximately three hundred enzyme structures with many DNA binding proteins known to be zinc binding (Meunier *et al.*, 2005).

Zinc is important for normal development processes in human body including the skeletal, nervous and immune system. Inadequate zinc levels have been shown to have adverse effects on normal growth status in children and infants during growing stage (Black, 1998, Brion *et al.*, 2020). There are many proteins including transcription factor for instance that require one or more zinc atoms to form their structural motifs and maintain the integrity of functional structure (Cummings and Kovacic, 2009) (Marx *et al.*, 2015, King and Larijani, 2017). Usually in zinc dependent proteins, the zinc atom forms bond with cysteine and histidine amino acids (Figure 1.23). Absence of zinc in zinc dependent proteins accounts for inactivity or malfunctioning. (McCall *et al.*, 2000). Alkaline phosphatase (ALP) for instance, is a zinc dependent enzyme which was deactivated due to zinc deficiency in rats (Cho *et al.*, 2007).

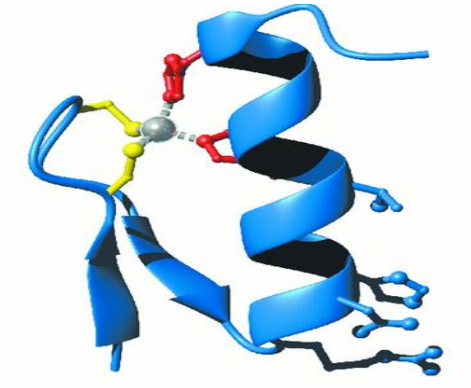

Figure 1. 23 The role of zinc in maintaining zinc finger protein structure. *Zinc finger protein (Zif268) shows the role of zinc (grey) in coordinating two histidine (red) and two cysteine (yellow) structure forming a zinc finger motif (Pabo et al., 2001).*

Zinc sources can be obtained from the diet including fish, lean red meat, chicken, liver, kidney, and cereals. Plant sources of zinc include soy foods, fortified cereals, peas, nuts, dried beans, and seeds. The recommended intake for adult male is 11mg and 8 mg for females. Children in ages between 13 years to 6 months, can have a range of 8mg to 2mg for both genders. Zinc toxicity has been reported after the intake of 4-8g of the mineral (Deshpande *et al.*, 2013).

1.18 Zinc Homeostasis and cellular zinc transporters.

Systemic and cellular zinc homeostasis is important to regulate normal body functioning. The gastrointestinal system, in particular the small intestine mainly, has an important function as the main site of exogenous zinc absorption from the diet. Aqueous form of zinc is more readily absorbed than the solid form including tablet supplementation (Roohani *et al.*, 2013). Continuous consuming of zinc in the diet leads to zinc excretion via faeces and urine, sweat, hair and nails to prevent zinc toxicity. Zinc is rapidly absorbed via the intestine in zinc deficiency to regain normal homeostasis (King, 2011). In adults, the total overall grams of zinc distributed in the body is estimated to be around 3 grams (Jackson, 1989, Sandstead, 1981). Zinc is transported to different tissues via the circulatory system and enters the cell via cellular zinc transporters. Intracellularly, zinc is found generally in very low micromolar concentrations ranging between 10-100 µM or even lower (Hara *et al.*, 2017). Zinc is distributed and stored in cellular compartments including; cell membranes, inside nucleus, endoplasmic reticulum, cytosolic vesicles, mitochondria, bound to zinc binding proteins and metallothionein which functions as cellular zinc pools (Roohani *et al.*, 2013, Kambe *et al.*, 2015, Davis *et al.*, 1998).

Zinc homeostasis, referred to as muffing and buffering, regulates cellular zinc levels by increasing or decreasing zinc binding with proteins and metallothionein and facilitates zinc efflux or influx via zinc transporters to restore normal zinc concentration (Colvin *et al.*, 2010).

Membrane zinc transporter families; SLC39 (ZIP) and SLC30 (ZnT) play a key role in regulating cellular zinc levels with 9 ZnTs and 14 ZIPs proteins (Colvin *et al.*,

2008). ZnT and ZIP work together in a cooperative manner to control cellular zinc concentration. ZnT transporters proteins prevents abnormal increase of cellular zinc concentration by storing zinc in cytosolic vesicles or facilitate cellular zinc excretion (Cousins *et al.*, 2006, Hara *et al.*, 2017). ZnT structure is defined by the presence of transmembrane domains (TMD) with histidine and aspartic acid. ZnT is characterized by NH2 and COOH termini forming zinc binding motifs intracellularly. In contrast, ZIP transporter proteins regulate zinc homeostasis by increasing zinc influx and restoring stored zinc levels. ZIP shares similar ZnT protein structure with transmembrane domains (TMD) and extracellular NH2 and COOH termini domain (Figure 1.24) (Hara *et al.*, 2017, Thingholm *et al.*, 2020).

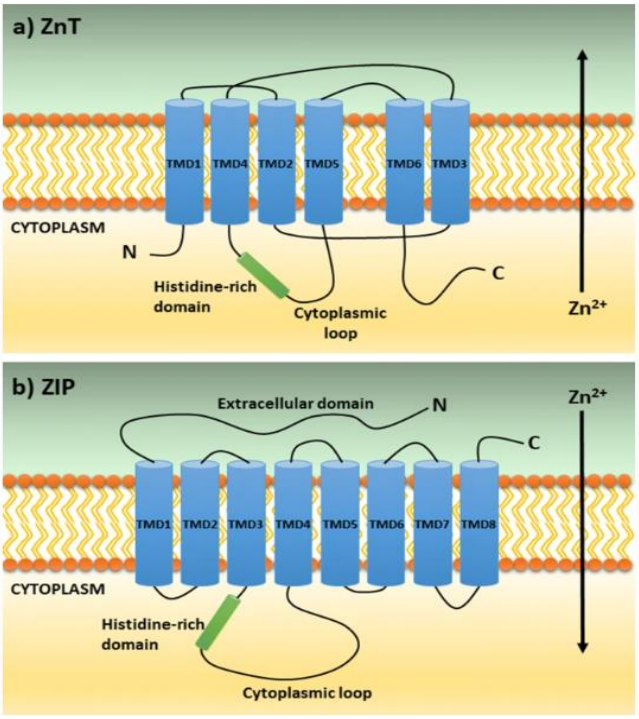

***Figure 1. 24 zinc transporter (ZnT) and (ZIP) structure**. Both transports share similar protein structure and demonstrating the transmembrane domains (TMD) with NH2 and COOH termini and histidine rich domain (Thingholm et al., 2020).*

Whilst zinc is an important metal for the biological system, copper also is another important element for human (Bost *et al.*, 2016). Copper and zinc play an important role in the innate immune integrity. Nutritional deficiency of copper and zinc minerals make the body sensitive to pathogenic infections. It is known that long term high

zinc uptake reduces copper absorption in stomach and cause copper deficiency. Besides competing at absorption sites, excessive zinc uptake induces copper release from metallothionein leading to zinc induced copper deficiency (Tatineni *et al.*, 2020). Thus, it is very important that cells maintain zinc levels with regulated homeostasis process to prevent copper deficiency.

1.19 Importance of zinc for biological system.

Zinc deficiency has been associated with mental disorders such as Alzheimers disease whilst amongst individuals with neck and head cancer, zinc levels were reported to be low (Prasad and Kucuk, 2002, Ho, 2004, Vinkenborg *et al.*, 2009, Ghasemi *et al.*, 2012, Prasad, 2013). It is estimated that about one third of total earth population required increased zinc intake since studies illustrated that zinc levels vary between low to moderate level (Kumari *et al.*, 2015). Zinc acts as an antioxidant. Thus, zinc deficiency increases the risk of reactive oxygen species accumulation and oxidative stress (Dhingra *et al.*, 2009). It is possible for zinc deficiency to deregulate anti-apoptotic genes and some growth factors which facilitate tumorigenesis (Prasad and Kucuk, 2002, Dhingra *et al.*, 2009). Zinc can be used as a therapy strategy to treat macular degeneration which affects the eyes and also to relieve anorexia nervosa symptoms. Zinc was also shown to be effective against rectal cancer and male fertility problems (Reed *et al.*, 2014, Nowak, 2015).

Studies have shown that using zinc supplementation plays a significant role in reducing the adverse effects of diarrhoea incidence (Bolick *et al.*, 2018, Bajait and Thawani, 2011). Diarrhoeal disease is one of the most severe diseases in and is among the top causes leading to childhood death below the age of 5 years (Lazzerini, 2016). In Africa, diarrhoea alone is responsible for over 800,000 children deaths every year (Jiwok *et al.*, 2021). Using zinc supplements for individuals suffering from diarrhoea in Africa was promoted by UNICEF and WHO (Singer and Baer, 2018, Lamberti *et al.*, 2015).

Very low zinc concentrations are able to regulate and control a wide range of cellular mechanism including cell signalling, gene expression, cell proliferation, cell

differentiation, apoptosis, and many other cellular mechanisms which eventually affect tissue and organ of the biological system (Aggett and Comerford, 1995).

Zinc can be found inside the nucleus as it is important for DNA and RNA synthesis (MacDonald, 2000). Proteins like transcription factors or nuclear receptor hormone are found to have zinc finger domain, so presence of zinc is very important for the cell development. Thymidine kinase is an important enzyme which is observed and used as a marker during cell replication in G1 and S phases. In vivo studies were involved in the measurement of low zinc effects and illustrated the significance role of zinc in regulating thymidine kinase level. Thymidine kinase levels were decreased and showed low activity after depleting zinc for 10 days. Similar results were obtained in vitro where fibroblast cell line (C3C) was treated with zinc chelator and showed low Thymidine kinase activity with incomplete cell division and DNA depletion (Prasad and Oberleas, 1974, Chesters *et al.*, 1990).

1.20 The Aims of the study.

As a part of drug redeployment studies, our laboratory previously demonstrated the ability of zinc acetate in killing BL cell lines. This thesis focused on understanding the role and the mechanisms of zinc-induced killing seen in BL cell lines.

The aims of this study were:

1- Investigate the role of zinc in the selective targeting of BL cells and investigate the mechanism of killing by measuring apoptosis events, caspases (3 and 9) activation and evaluating cell cycle patterns.
2- Investigate the impact of zinc against C-MYC at mRNA and protein levels and investigate whether zinc targets Ig locus which is responsible for the deregulation of C-MYC seen in BL cells upon (C-MYC/Ig) translocation.
3- Generate BL cell lines with exogenous expression of C-MYC to rescue BL cells viability when challenged with zinc which would help in understanding the role of C-MYC in maintaining BL cell viability.
4- Inhibit C-MYC proteasomal degradation mechanism by the proteasome inhibitor (bortezomib) to determine whether increased stability of C-MYC protein can rescue BL cells and induce zinc resistance.

CHAPTER TWO
MATERIALS AND METHODS

2 Materials and methods.

All detailed recipes for reagents preparation in this study are provided in appendix A.

2.1 Cell culturing protocols.

2.1.1 Cell lines.

In this study, a panel of lymphoma and leukaemia cell lines were used including BL (NAMALWA, RAJI, Akata, BL 30, BL 31, Glor, SAV and Dante), lymphoblastoid cell lines (LCLs- JT, KJ, LG, AR), acute myeloid leukemia (AML- HL-60) and diffuse large B cell lymphoma (DLBCL- SUDHL4, SUDHL5 and SUDHL6) (Table 2.1).

Cell type	Cell line name	Genetic Mutations/ Translocation	Cell line details	Reference
Burkitt's Lymphoma (BL)	RAJI BL (Endemic)	- t(8:14) *MYC/IgH* -*TP53* (Y234H)	- Male 12 years - EBV+	(Cellosaurus, 2022f, ATCC, 2022c, Gutiérrez *et al.*, 1999, Murai *et al.*, 2005)
	Akata BL (Sporadic)	- t(8:14) *MYC/IgH* - *TP53* (190 frameshift GCCCCT-GCCCT)	- Female 4 years - EBV+	(Cellosaurus, 2022a, Lin *et al.*, 2013, Gutiérrez *et al.*, 1999, Farrell *et al.*, 1991)
	Dante BL (Endemic)	- Unknown	- EBV+	(Cellosaurus, 2022d, Lee *et al.*, 2010, Boyce, 2009)
	NAMALWA BL (Endemic)	- t(8:14) *MYC/IgH* -*TP53* (R248Q)	- Male - EBV+	(ATCC, 2022b, Cellosaurus, 2022e, Gutiérrez *et al.*, 1999, Benjamin *et al.*, 1982, Bhatia *et al.*, 1993)
	Glor BL (Endemic)	- Unknown	- EBV+	(Habeshaw *et al.*, 1999)
	SAV BL (Endemic)	- *TP53* (G244D)	- EBV+	(Cellosaurus, 2020, Kelly *et al.*, 2002, Kelly *et al.*, 2014)
	BL 30 (Sporadic)	- Unknown	- Caucasian Male 19 years - EBV-	(Cellosaurus, 2022b, Philip *et al.*, 1984)

	BL 31 (Sporadic)	- t(8:14) *MYC/IgH* **-**TP53 (V172F)	- Male 14 years - EBV –	(Cellosaurus, 2022c, Philip *et al.*, 1984, Kelly *et al.*, 2014)
Acute myeloid leukaemia (AML)	HL60	- Amplified *C-MYC* gene	- Female 35 years	(ATCC, 2022a, Shima *et al.*, 1989)
Diffuse large B cell lymphoma (DLBCL)	SU-DHL-5	- Negative for t(14;18), *BCL2 /IgH*	- Female 17 years	(ATCC, 2022e, Abbott *et al.*, 2009)
	SU-DHL-6	- t(14;18) *BCL2 /IgH* - *TP53* inactivation (17p13.1) - TP53 (A701G)	- Male 43 years - EBV-	(ATCC, 2022f, Hua *et al.*, 1988, Dharanipragada and Parekh, 2019, de Jong *et al.*, 2019)
	SU-DHL-4	- t(14;18) *BCL2/IgH* -*TP53* (C817T)		(ATCC, 2022d, Abbott *et al.*, 2009, Strauss *et al.*, 2007, de Jong *et al.*, 2019)
Lymphoblastoid (LCL)	KJ LCL	-	- EBV+	-
	JT LCL	-	- EBV+	-
	LG LCL	-	- EBV+	-
	AR LCL	-	- EBV+	-

Table 2. 1 The different cell lines used in this study (BLs, LCLs, AML and DLBCLs). All cell line details were obtained from reported references and databases. *The table shows the charactristics of the cell lines used. B cell lymphoma 2 (BCL2), immunoglubulin heavy chain IgH), Epstein-Barr virus (EBV) and tumour protein p53 (TP53). Amino acids; Tyrosin (Y), Histidine (H), Arginine (R), Glutanime (Q), Glycine (G), Aspartic acid (D), Valine (V), Phenylalanine (F), Alanine (A), Cysteine (C), Threonine (T).*

Cells lines were obtained from the university of Birmingham (school of biosciences and cancer research laboratories). All cell lines were STR profiled and authenticated by using 24 polymorphic STRs by (Northgene, Deeside, UK).

2.1.2 Cell culture nutrient and maintenance.

All cell lines used in this study were cultured in RPMI 1640 medium supplemented with 10% v/v foetal bovine serum (FBS), 1% v/v penicillin (100U/mL) and 1% streptomycin (100U/mL) (all purchased from Gibco, Thermo Fisher Scientific). Cells

were incubated in a humidified incubator at 37˚C and 5% CO_2. Cells were passaged every other day to maintain cell densities between $0.5x10^6$ to no more than $2x10^6$ cells/mL.

2.1.3 Cell storage and recovery from frozen stock.

For long term storage: A total of $5\text{-}10x10^6$ exponentially growing cells were collected and centrifuged at 1500 rpm for 5 minutes in sterile universal tubes. Following centrifugation, supernatant was discarded and the cell pellet resuspended in 1 mL freezing media (90% FBS + 10% DMSO) and transferred to 1 mL cryovials (Greiner). Tubes were transferred to a freezing box (Mr.Frosty) and stored at -80°C. After 24-48 hrs, cryovials were transferred to liquid nitrogen for long term storage.

Cell recovery from frozen stock: frozen stocks of cell were thawed rapidly in a 37°C water bath. Using pasture pipette, cells were transferred from cryovials into sterile 30 ml universal tubes and washed with cold culture medium by adding cold medium (20 mLs) dropwise while swirling gently. Cells were centrifuged at 1500 rpm for 5 minutes and supernatant was discarded. Cell pellet was resuspended in complete medium and cultured in 24 well plate in 1.5-2 ml/well and incubated at 37°C with maintained humidity and 5% CO_2. Following cells recovery, cells were transferred into T25 flask (25 cm^2) (all from Corning) and maintained at 37°C with humidity and 5% CO_2.

2.2 Zinc acetate treatment.

Zinc acetate was purchased from Fisher Scientific (1998872) and prepared in sterile dH_2O at 1M stock. Filter-sterilised stocks were stored at -20°C. Cells were treated with zinc acetate at 50 or 100 µM as described in each specific experiment.

2.3 Flow cytometry protocols.

All flow cytometry experiments were performed using a FACSCalibur machine from BD Bioscience with CellQuest Pro analytical software.

2.4 Cell viability and cell count determination using flow cytometry.

Cell viability and cell counts were determined using flow cytometry. Within each experiment, at the specified time points, 100-200µl cells were collected into 5 mL flow cytometry tubes (Sarsted) and fixed with an equal volume of FACS fix (Appendix A 9.3). 10µl Counting beads (Biolegend, 9.97×10^5 beads/µL) were added and samples analysed by flow cytometry either immediately or stored at 4°C and analysed within 72 hours. Forward and side scatter dot plots were analysed by gating on live cells and beads absolute cell count (cells/mL) was calculated using the following formula:

$$\boldsymbol{Viable\ cell\ count}\ \left(\boldsymbol{cells}/\mu\boldsymbol{L}\right) = \left(\frac{\boldsymbol{number\ of\ beads\ added\ to\ cell\ sample}}{\boldsymbol{volume\ of\ cell\ sample\ (uL)}}\right) \times \left(\frac{\boldsymbol{total\ event\ count\ of\ viable\ cell}}{\boldsymbol{total\ event\ count\ of\ beads}}\right)$$

2.5 Analysis of apoptosis: Annexin V and propidium iodide (PI) staining.

Cells were treated as described in each specific experiment. At the specified time point, 0.5×10^5 - 1×10^5 cells were transferred to FACS tube and washed twice with 2ml cold PBS at 1500 rpm 5 minutes. Annexin V/PI stain was prepared by mixing 100 µL of 1X Binding Buffer (BD pharmingen) + 2 µl of Annexin V FITC (BD bd pharmingen) + 5 µl PI (SIGMA) stain per sample. Cells were incubated with the stain solution for 15 minutes at room temperature (RT)(25°C) in the dark. 250 µl of 1X Binding Buffer was added to each tube and samples analysed by flow cytometry within 1 hour. Annexin V-FITC was analysed in FL-1 and PI in FL-2.

2.5.1 Cell cycle analysis.

For cell cycle analysis, cells were stained with propidium iodide (PI) using Cell Cycle Buffer (Appendix A 9.4). Cells were sampled at the timepoints specified for each experiment in the figure legend and results text. At each specific time point, 200-300 μL of cell sample was transferred into a FACS tube and centrifuged at 1500 rpm for 5 minutes. After discarding the supernatant, 300 μL of PI cell cycle buffer was added and incubated overnight at 5-8 °C in the dark. PI intensity was analysed by flow cytometry using FL-2.

2.6 Protein preparation and analysis.

2.6.1 Cell preparation for total protein extraction.

At the timepoint specified in the text, 0.5-6 x 10^6 cells from treated or non-treated cultures were collected into 1.5 mL eppendorf tubes and centrifuged at 1500 rpm for 5 minutes. Following centrifugation, supernatant was discarded and the cell pellet washed with 1.0 mL PBS before centrifuging again at 1500 rpm for 5 minutes. 100-200 μL of RIPA lysis buffer (Appendix A 9.2.9) supplemented with protease inhibitor cocktail (cOmplete, Mini Protease Inhibitor Cocktail Tablets) (from Roche) was added to the cells and incubated on ice for 1 hour with vortexing every 15 minutes. Protein samples were centrifuged at 14000 rpm for 20 minutes at 4°C and the supernatant transferred into clean tubes before storing at -20 °C.

2.6.2 Protein determination assay.

Protein concentrations in lysates were measured using Protein Assay kit (Bio-rad). Using transparent 96 well plates, 2 μL protein lysate or 2 μL/ well of Bovine Serum Albumin (BSA) protein standards (0, 0.625, 1.25, 2.5, 5 and 10 mg/mL) were added to triplicate wells. Next, 25 μL /well of freshly prepared protein assay reagent (prepared by adding 20 μL of reagent S per 1 mL of reagent A) was added followed by 200 μL of reagent B from protein assay kit. After incubating for 10 minutes at room temperature, absorbance at 690 nm wavelength was measured using plate

reader (Perkin Elmer Victor x3 machine) and Perkin-Elmer software. Protein concentrations of samples were calculated from a standard curve generated from the BSA standards.

2.7 Western blotting assay.

2.7.1 Sample preparation.

Following protein determination, 30 ug total protein was mixed with 4X sodium dodecyl sulphate (SDS) gel loading buffer (Appendix A 9.2.10) and total volume was brought to 20 µL using RIPA lysis buffer. Sample were denatured in a thermal cycler (Applied Biosystem 2720) by incubating at 70 °C for 10 minutes. Samples were centrifuged at 14000rpm briefly to collect all the sample at the bottom of the tube before electrophoresis.

2.7.2 Sodium dodecyl sulphate polyacrylamide gel electrophoresis (SDS-PAGE).

12% polyacrylamide SDS resolving gels were prepared using ProtoGel (acrylamide 12% w/v) (National diagnostics), (0.39 M) trisaminomethane (Tris), 0.1% SDS, 0.1% ammonium persulphate (APS) and 0.04% N,N,NN-Tetramethylethylenediamine (TEMED). Gel mixture was poured into 1.5mm thick casting plates and incubated for 20 minutes at room temperature. Stacking gel was prepared using ProtoGel (5.1%) (from national diagnostics) with dH2O, (0.13 M) tris aminomethane (Tris), 0.1% SDS, 0.1% Ammonium persulphate (APS) and 0.1% N,N,NN-Tetramethylethylenediamine (TEMED). 1.5 mm 10 well combs were inserted into the stacking gel and gels incubated for 20 minutes at room temperature until complete gel polymerization. Gels were placed in Mini Protean 3 gel chamber (Bio-Rad) and filled with 1X running buffer (Appendix A 9.2.1). Following comb removal, 5 µL of BLUeye protein standard ladder (SIGMA) was loaded in the first well and samples loaded into subsequent wells. Gels were electrophoresed at 120 volts for 60 minutes, or until the dye front had reached the bottom of the gel.

2.7.3 Semi-dry protein transfer.

Electrophoresed protein samples were transferred onto prepared sized polyvinylidene difluoride (PVDF) membrane (from Millipore) using semi-dry transfer method. 12 sheets of 3MM filter paper (Whatmann) were cut to the size of the gel. The PVDF membrane was activated in methanol for 20 seconds and washed with dH_2O before soaking in cold 1x Transfer Buffer (Appendix A 9.2.2). 6 filter papers were soaked in cold 1X transfer buffer and placed on the base plate of the Semi-Dry Transfer tank (Bio-rad), followed by the. PVDF membrane gel and the 6 more sheets of 3MM filter paper. Proteins were transferred onto the PVDF membrane at 25 volts for 1 hour.

2.7.4 Immunoblotting and protein visualization.

Following transfer, PVDF membranes were blocked by incubation in 5% skimmed milk powder in Tris buffer saline + Tween (TBS-T, see Appendix A 9.2.5) for 1 hour at room temperature with gentle agitation. Following blocking, membranes were incubated overnight at 4 °C with gentle agitation with primary antibody diluted in 5% skimmed milk in Tris buffer saline with TWEEN 20 (TBS-T) (see Table 2.2 for dilutions).

Primary antibody	Manufacturer	Species	Dilution factor in TBS-T with 5% skimmed milk
Anti β-Actin	Sigma Aldrich (A5441)	Mouse	1:15000
Anti C-MYC - Y69	Abcam (ab32072)	Rabbit	1:1000
Anti-Caspase-3	Cell Signalling Technology (9662)	Rabbit	1:1000
Anti-Caspase-9	Cell Signalling Technology (9504)	Mouse	1:1000
Anti-Ubiquitin	Cell Signalling Technology (P4D1)	Mouse	1:1000

Table 2. 2: Western blot primary antibodies names, species and their dilution factor

Following incubation, membranes were washed with TBS-T with shaking at 70 rpm for 5 min X 3 times. To visualize the protein, secondary fluorescent antibodies were used against on primary antibody species by diluting secondary antibodies in 5% skimmed milk in TBS-T with 0.01% SDS and incubated with gentle agitation for 1 hours at room temperature. All secondary antibodies and their dilution factors are listed in the Table 2.3 below.

secondary antibody	Manufacturer	Species	Dilution factor in TBS-T with 5% skimmed milk and 0.01% SDS
IRDye 800 anti- Rabbit IgG	LI-COR	Goat	1:15000
IRDye 700 anti- mouse IgG	LI-COR	Goat	1:15000

Table 2. 3: Western blot primary antibodies names, species and their dilution factor

Following incubation with secondary antibodies, membranes were washed in TBS-T at 70 rpm for 5 minutes X3 times covered from the light and processed for scanning using LI-COR Odyssey CLx infrared imaging scanner. Protein quantification and analysis was performed using LI-COR Image Studio Light software.

2.8 Quantifying and measuring C-MYC mRNA levels.

2.8.1 Cell preparation for total RNA extraction.

Based on the experimental protocol, 2-5 x 10^6 cells from treated or non-treated cultures were collected into 1.5 mL eppendorf tubes and centrifuged at 1500 rpm for 5 minutes. Following centrifugation, supernatant was discarded and cell pellets

were washed with one mL of PBS and centrifuged again at 1500 for 5 minutes X 2 times. Cell pellets were snap frozen in either a cold methanol bath with dry ice or with liquid nitrogen and stored at – 80 °C.

Total RNA was extracted using the RNeasy RNA extraction kit (Qiagen). As per the kit protocol, cell pellets were resuspended in 350 µL RLT buffer, transferred into Qiashredder tubes and centrifuged to break down DNA into small fragments. 70% ethanol (350 µL) was added to the flowthrough and the mixture was transferred into labelled RNeasy spin columns with collecting tube. Columns were spun at 8000 x g for 15 seconds and flowthrough was discarded. RNA in the column membrane was washed by pipetting 700 µL RW1 buffer onto the column and centrifuging for 15 seconds at 8000 x g. The flowthrough was discarded and 500 µL RPE buffer was added to the column and spun again for 15 seconds at 8000 x g. The flowthrough was discarded and 500 µL of RPE buffer was added to the column and spun for 2 minutes for 8000 x g. The RNeasy column was transferred into new 1.5 mL eppendorf tube and 30 µL RNase free water pipetted onto the column. After a 1 minute incubation, the columns were centrifuged 8000 x g for 1 minute. The concentration the eluted total RNA was measured using IMPLEN Geneflow NanoPhotometer P-Class P330. Total RNA concentration was read as ng/µL.

2.8.2 Converting RNA into complementary DNA (cDNA) using reverse transcriptase.

RNA was converted into cDNA using Superscript III (Invitrogen). Firstly, the following were mixed together in a 0.2ml PCR tube.

Total RNA	dNTP (10 mM)	Hexamer primers (0.4ug/uL)	RNase free dH2O
1 µg	1 µL	0.5 µL	Up to 12 µL

Table 2. 4: Reagents used to synthesise cDNA from RNA (reverse transcription)

Using a thermal cycler (Applied bio system 2720), samples were heated to 65 °C for 5 minutes before 7 µL of the following mix were added.

Reagent	Volume/sample (µL)
5 X first strand buffer (Invitrogen)	4
0.1 M Dithiothreitol (DTT) (Invitrogen)	2
Rnase inhibitor 10000 u (from Bioline)	1

Table 2. 5: Reagents used to synthesise cDNA from RNA (reverse transcription)

Samples were centrifuged quickly to mix the solution completely. Samples were left at room temperature for 2 minutes and then 1 µL of Superscript III reverse transcriptase (Invitrogen) was added and sample was run on thermos cycler as the following:

- 25 °C for 10 minutes
- 42 °C for 90 minutes
- 70 °C for 15 minutes
- 4 °C at the termination

cDNA was stored at -20 °C until required.

2.8.3 Checking the synthesis of cDNA with β-actin PCR.

To check cDNA synthesis process was successful, β-actin PCR was performed. The reaction was performed in 0.2mL PCR tubes (Star Labs) and reagents used are listed in the Table 2.6 below:

Reagent	Volume/sample (µL)
RNAse free dH_20	40.5
cDNA	1
B-actin forward primer (10 µM) **5' GTCACCAACTGGGACGACA 3' (from Sigma)**	1
B-actin reverse primer (10 µM) **5' TGGCCATCTCTTGCTCGAA 3' (from Sigma)**	1
dNTP mix (10 mM)	1
10 X PCR buffer	5
Taq polymerase	0.5

Table 2. 6: Reagents used in the synthesis of β-actin from cDNA

PCR amplification was performed in a thermal cycler using the following cycle conditions:

- 35 cycles of:
    - 92 °C for 1 minute
    - 55 °C for 2 minutes
    - 72 for 1 minute
- 4 °C for storing the sample.

β-actin PCR product was electrophoresed in on 2% agarose gels prepared using 2 g of agarose (Bioline) in 100 mL 1 X Tris borate EDTA (TBE) buffer (Appendix 9.2.11). The mixture was heated in the microwave to completely dissolve the agarose. 5 µL of Ethidium Bromide (EB) was added, mixed properly and the molten agarose solution poured into small gel trays with fixed combs. Once solidified, 12 µL of β-actin DNA PCR product +4 uL 5 X gel loading buffer (from Bioline) was loaded into the wells. Hyperladder I 1kb (from Bioline) was used as a DNA ladder and the gel was electrophoresed at 100 volts in 1 X TBE running buffer for 20-30 minutes. β-actin PCR product (453bp) was visualised under UV light. A strong band indicated successful synthesis of cDNA.

2.8.4 Quantitative real time polymerase chain reaction (qRT-PCR).
2.8.5 Measuring C-MYC mRNA levels via qRT-PCR.

C-MYC mRNA levels were quantified using qRT-PCR on cDNA produced from treated and non-treated cells at the time points specified in the text. Once β-actin was checked, *C-MYC* qRT-PCR was performed using Sensifast SYBR green master mix- Low ROX (Bioline). Reactions were prepared in 0.2ml PCR tubes as described in Table 2.7.

Reagent	Volume/sample (µL)
2 X Sensifast SYBR green (Bioline)	10
***C-MYC* or 18 S *(18SrDNA)* forward primers (10 µM)**	0.4
***C-MYC* or 18 S *(18SrDNA)* reverse primers (10 µM)**	0.4
RNAse free dH_2O	8.2

Table 2. 7 qRT-PCR master mix reagent component

Primers used for this reaction:
C-MYC forward primers: 5' TCAAGAGGTGCCACGTCTCC 3'
C-MYC reverse primers: 5' TCTTGGCAGCAGGATAGTCCTT '3
18 S *(18SrDNA)* forward primers: 5' GCCGCTAGAGGTGAAATTCTT 3'
18 S *(18SrDNA)* reverse primers: 5' CATTCTTGGCAAATGCTTTCG '3

Master Mix was properly mixed by pipetting up and down and 19 µL of master mix was pipetted into 96 well PCR plate (ABA 17500) (from Geneflow). Both *C-MYC* and 18 S (18SrDNA) master mix was pipetted into the labelled plate and 1 µL of cDNA added to each well in triplicate wells. PCR plate was sealed with plastic film and centrifuged at 1500 rpm for 5 minutes. The qRT-PCR was performed using ABI prism 7700 machine (from Applied Biosystem) with ABI 7700 software.

Data analysis was processed by calculating Δ Ct values for each sample by subtracting 18 S ribosomal RNA Ct values from C-MYC Ct values from.

$$\Delta\mathrm{Ct} = \ 18\ \mathrm{S}\ \mathrm{Ct\ value}\ - \ \mathrm{C} - \mathrm{MYC\ Ct\ value}$$

ΔΔCt values were calculated by subtracting ΔCt control samples from each sample.

$$\Delta\Delta\mathrm{Ct} = \text{sample } \Delta\mathrm{Ct} \text{ value} - \text{control } \Delta\mathrm{Ct} \text{ value}$$

And then to calculate the fold change for each sample:

$$\text{fold change} = 2^{-\Delta\Delta\mathrm{Ct}}$$

2.9 Silver staining.

One of the methods used to visualise proteins in SDS-PAGE was silver staining. Silver staining is very sensitive technique in detecting protein and can detect protein at 5 ng concentration. The principle of this method is to deposit silver ions on separated protein present on SDS gel following electrophoresis. Deposited silver ion will later be reduced to form metallic silver which gives a dark pigmentation proportional to bound protein. ProteoSilver™ Silver Stain Kit (SIGMA) was used in this study. The protocol started by electrophoresing 30 µg of total protein lysate in 12% polyacrylamide SDS-PAGE as described earlier. Gels were fixed with fixing solution (dH_2O with 50% ethanol and 10% acetic acid) overnight in cold room at 4 °C. Gels were washed with dH_2O with 30% ethanol for 10 minutes followed by dH_2O wash for 10 minutes. Gels were then incubated in sensitization solution provided by the kit for 10 minutes before washing with dH_2O for 10 minutes. Gels were incubated with silver in equilibration step for 10 minutes and then washed with dH_2O for 1 minute. Silver ion reduction was performed with developer solution provided by the kit for 3-7 minutes until sufficient protein visualization was obtained. 5 ml of ProteoSilver™ stop solution was added to stop the reaction.

2.10 BL transfection with *C-MYC* using Piggyback Transposon System.

In this study, the PiggyBac vector transposon System (Vectorbuilder) was used to transfect and constitutively express *C-MYC* in BL cell lines.

The Piggybac system utilizes a cut and paste method which is defined by the ability of transposase to recognize the cutting sites in plasmid at specific sequence known as inverted terminal repeats (ITRs) to free the sequence of interest (transposon) and insert into the host cell genome. In this study, 2 genes were introduced into BL cell line:

1- *C-MYC* (VB200623-1116ump) showed in Figure 2.1 (VectorBuilder)
2- *EGFP* (VB900088-2218fcw) showed in Figure 2.2 (VectorBuilder) which is used as a transfection control.

Co-transfection with hyPBase (VB160216-10057) was required (coding for the transposase) as shown in Figure 2.3.

The *C-MYC-EGFP* plasmid included antibiotic gene for plasmid selection and the C-MYC gene under the regulation of the constitutively active eukaryotic translation elongation factor 1 α (EF1A) promoter. The *C-MYC* gene was fused with EGFP via small peptide (T2A) that undergoes self-cleavage during translation and the specified region is covered by 5' and 3' ITR sites that are recognized by transposase during gene cutting and pasting process. Thus, cells that express *C-MYC* also express *EGFP*. Full details of vector is provided in appendix B.

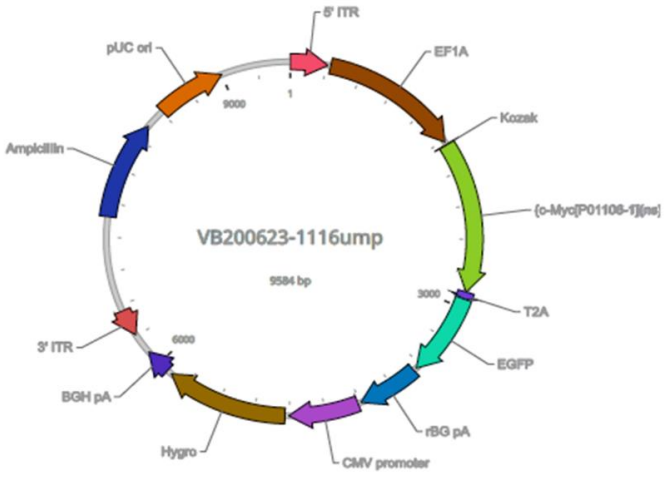

Figure 2. 1 C-MYC-EGFP vector VB200623-1116ump design used to overexpress C-MYC in BL cell lines. *Vector shows 5' and 3' inverted terminal repeats (ITR) site for transposases activity, human eukaryotic translation elongation factor 1 α1 promoter (EF1A), Kozak translation initiation sequence (Kozak), C-MYC gene (c-Myc(P01106-1)), (self-cleaving 2A peptide (T2A), enhanced green fluorescent protein (EGFP), rabbit Polyadenylation signal (rBG pA), human cytomegalovirus immediate early promoter (CMV), Hygromycin resistance (Hygro), polyadenylation signal (BGH pA), Ampicillin resistance (Ampicillin), origin of replication (pUC ori). C-MYC is under the influence of EF1A promoter for continuous expression. EGFP is fused with C-MYC via self cleaved T2A protein.*

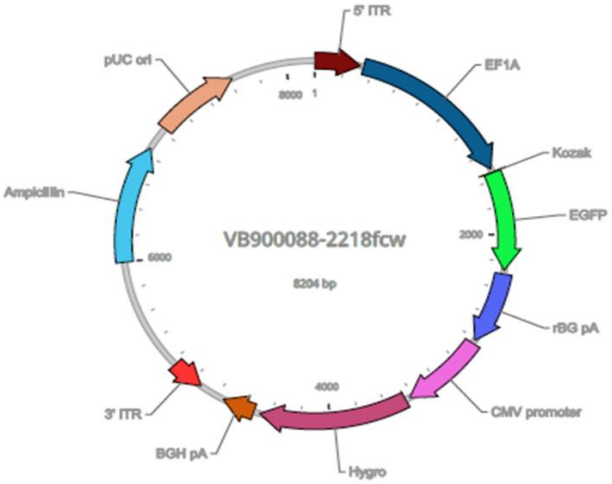

Figure 2.2 EGFP vector VB900088-2218fcw design used to overexpress EGFP in BL cell lines. Vector *shows 5' and 3' inverted terminal repeats (ITR) site for transposases activity, human eukaryotic translation elongation factor 1 α1 promoter (EF1A), Kozak translation initiation sequence (Kozak), enhanced green fluorescent protein (EGFP), rabbit Polyadenylation signal (rBG pA), c, Hygromycin resistance (Hygro), polyadenylation signal (BGH pA), Ampicillin resistance (Ampicillin), origin of replication (pUC ori). EGFP is under the influence of EF1A promoter for continuous expression.*

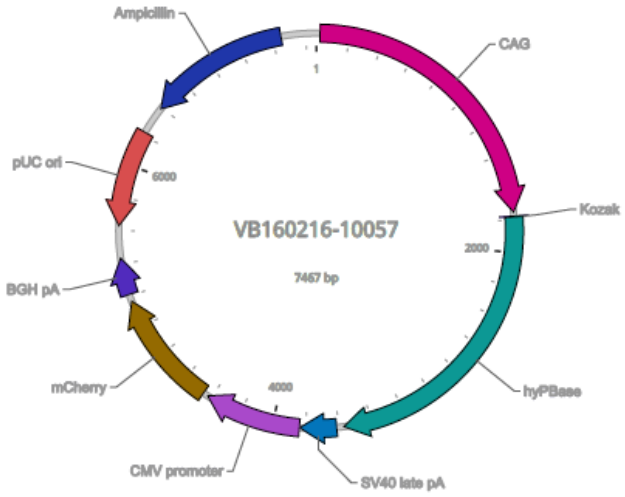

Figure 2.3 hyPBase vector VB160216-10057design used to overexpress transposases in BL cell lines. *hyPBase vector shows piggyBac 5' inverted terminal repeat (CAG), Kozak translation initiation sequence (Kozak), piggyback transposase (hyBase), Simian virus 40 late polyadenylation signal (SV40 late pA), human cytomegalovirus immediate early promoter (CMV), Variant of mRFP1 (mCherry), Polyadenylation signal (BGH pA), origin of replication (pUC ori), Ampicillin resistance (Ampicillin). The mechanism of hyPBase vector activity is initiated by cutting co-transfected vector at ITR sites and pasting into host chromosome*.

Purchased vectors were hosted in VB UltraStable strain. Vectors were grown in LB broth supplemented with Ampicillin (100 µg/mL) overnight shaking at 220 rpm at 30 °C. PureLink™ Expi Endotoxin-Free Maxi Plasmid Purification Kit was (Invitrogen) was used to purify plasmid.

BL cells were prepared for transfection by growing them to exponential phase at $5x10^5$ cells/mL. Cells were collected ($5x10^5$) cells and transferred into 50 ml falcon tubes. Cells were washed with PBS up to 20 mL and centrifuged at 1500 rpm for 5 minutes. Meanwhile, transfection master mix solutions were prepared as follows (Table 2.8).

solution	Required volume - concentration
Ingenio electroporation solution (Mirus)	100 µL / reaction (Including DNA materials)
hyPBase (Transposase)	1 µg/ reaction
C-MYC-EGFP* or *EGFP	1.5 ug/ reaction

Table 2. 8 transfection components and preparation required to transfect BL cell line.

Following centrifugation, supernatant was discarded and pellet was mixed with 100 µL transfection master mix and mixed gently by pipetting up and down. The mix was transferred to transfection cuvettes and electroporated using Nucleofector II. Upon transfection, 500 µL of warm complete media was added and cells were transferred into 6 well plates (Corning) together with 3 mL of complete media / well and incubated at 37 °C for 3 days. During this time, transposase will cut vectors at ITR and paste into the host genome. BL cell lines were then incubated with Hygromycin (100 µg / mL) in complete media (20% FBS).

Transfection efficiencies were evaluated using flow cytometry to measure *EGFP*. Cells that were bright for EGFP (EGFP++) were sorted and enriched by FACS.

CHAPTER THREE

THE CHARACTERISATION OF ZINC ACTIVITY AS AN ANTI-BL

3 The characterisation of zinc activity as an anti-BL.

Whilst intensive cytotoxic chemotherapy and radiation therapy are the mainstay of treatment for BL In HICs, the toxicities and costs associated with these treatments limit their use in LMICs. Outcomes are worsened since many eBL patients in LMICs and SSA often present with more advanced disease due to delays in getting to hospital and obtaining a diagnosis, thus there is an urgent need to develop affordable, low toxicity and effective alternative therapies for BL patients that are suitable for LMICs. Previously in our lab, BL cell lines were screened against a drug repurposing library developed in-house (FMC Library) which comprised of 100 oral, licensed drugs listed in the British National Formulary (BNF). Using a Celltiter Blue viability assay, zinc acetate was identified as possessing anti-BL activity against a panel of BL cell lines including eBL (DANTE, EZEMA, GLOR, NAMALWA and SAV) and sBL (AKATA, BL30 and BL31). Dose response experiments showed that all tested BL cell lines were sensitive to zinc acetate at 100 µM and higher doses with significantly reduced cells viability.

Zinc is an essential mineral that is involved in many different human biological systems including DNA synthesis, cell maturation, immune system integrity, hemostasis, oxidative stress and development (Yan *et al.*, 2008). Zinc is an essential cofactor in more than 300 proteins as a key component of zinc finger like domains which are involved in structural and functional integrity (Cheng and Chen, 2021).

The essential role of zinc is highlighted by the fact that zinc deficiency has been linked with various disorders including hepatic failure, immune dysfunction, growth retardation and diarrhoea (Tuerk and Fazel, 2009, Wong *et al.*, 2012). Also, it was found that 65% individuals with head and nick cancer had zinc deficiency and zinc was found to be very low in prostate cancer samples suggesting the potential link between zinc deficiency and disease progression (Prasad *et al.*, 2009, Jarrard, 2005). The clinical benefit of zinc was seen among children in SSA where zinc supplementation helped in reducing diarrhoeal events caused by Rotavirus and *Escherichia coli* as a consequences of poor sanitation system and limited access to

hygienic water for consumption (Pande *et al.*, 2008, Jamison, 2006). The World Health Organisation (WHO) recommends 20 mg of zinc orally in diarrhoea management which has been shown to be effective in reducing diarrhoeal severity and duration in acute cases (Yeshaw *et al.*, 2020, Dhingra *et al.*, 2020, Walker *et al.*, 2007). The estimation of zinc deficiency among worldwide population is about 17.3%. In SSA, a high phytate diet means that ~30% of the population are estimated to be zinc deficient (Wessells and Brown, 2012, Bailey *et al.*, 2015, Belay *et al.*, 2021, Agedew *et al.*, 2022).

The aims of this section of work were to characterise the anti-BL activity of zinc. The effect of zinc acetate against different BL cell lines including eBL and sBL was characterized at different time points and zinc concentrations. The response of BL cell lines was compared to a panel of non-BL lines including diffuse large B cell lymphoma (DLBCL) cell lines which are a germinal center B cell tumour similar to BL, and acute myeloid leukemia (AML) which represents a non-B cell tumour to investigate whether zinc is primarily targeting BL cells. Lymphoblastoid cell lines (LCLs), which are immortalized EBV-infected B cells, were also used as normal controls to focus on the role of zinc against control B cells. Cell viability was assessed using flow cytometry analysis and cellular morphology were investigated via Jenner-Giemsa stain to image damaged cell.

In order to characterize the mode of cell death induced by zinc in BL cells, markers of apoptosis were tested. Apoptosis was assessed using staining with annexin V and flow cytometry. Additionally, western blot analysis was performed to measure caspase 3 and 9 protein levels which are crucial during intrinsic apoptosis pathway in zinc treated BL cells. Furthermore, both BL and non-BL cell lines were stained with propidium iodide to investigate cell cycle via flow cytometry to investigate whether zinc can induce cell cycle arrest in treated cells. All these tests will help in further characterizing zinc acetate effects in BL and non-BL cell lines.

3.1 Screening of FMC drug library against BL cell lines.

In our lab we have established the FMC drug library containing already approved drugs at concentrations, that when used in in vitro, screens reflect the maximum concentration achieved in human serum when used for their primary indication. Drug screening using FMC drug library was applied against a panel of eBL (DANTE, EZEMA, GLOR, NAMALWA and SAV) and sBL (AKATA, BL30, BL31) cell lines. The viability of BL cells after 72 hours treatment was measured using the CellTiter blue assay. Figure 3.1 shows data from the FMC screen redacted to show the top 31 hits (greatest reduction in average viability across all BL lines tested) (the complete FMC drug list is in appendix C). Each treatment including solvent controls (DMSO, EtOH, methanol and water) were normalised to non-treatment controls (media). In this analysis zinc acetate was the best hit and selected for further investigation.

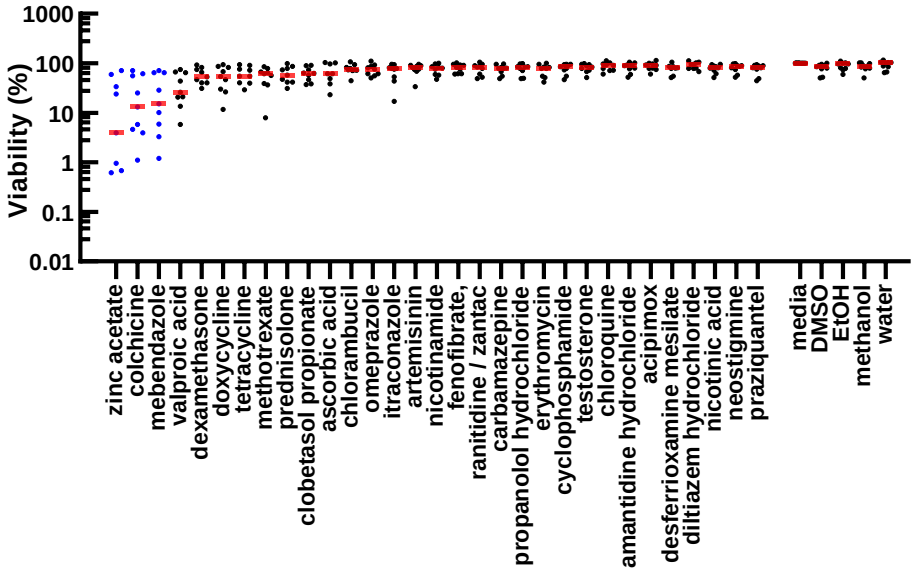

Figure 3. 1 FMC drug library screening against BL cell lines*. AKATA, BL30, BL31, DANTE, EZEMA, GLOR, NAMALWA and SAV BL cell lines were seeded at 5x10^5 cells/mL and treated with FMC drug library for 72 hours. Drug stocks are designed to be at the maximum dose achieved in serum when used for their primary indication and when diluted (1:1000) into the assay. Cell titer blue assay was performed to measure the viability of BL cell lines. X axis show the top 31 hits (greatest reduction in average viability across all BL lines tested) and solvent controls. Y axis represents a log scale of relative viability to untreated controls (media). The data in this figure was generated by other members in the group before the beginning of this project.*

3.2 Determining the zinc acetate dose response of a panel of BL cell lines.

Having identified the potential anti-BL activity of zinc, the same panel of eBL (DANTE, EZEMA, GLOR, NAMALWA and SAV) and sBL (AKATA, BL30, BL31) cell lines were exposed to a range of zinc acetate concentrations to determine the dose response of the cell lines, again using the celltiter blue assay after 72 hours. As shown in Figure 3.2, the individual BL cell lines demonstrated similar dose responses when challenged with zinc acetate with the majority of lines being relatively unaffected below 100 µM zinc acetate and demonstrating greater than 90% loss of viability within the range of 100-250 µM zinc acetate.

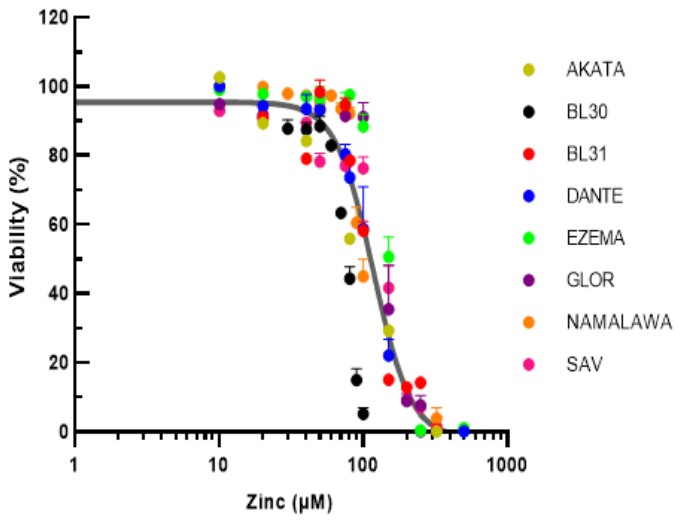

Figure 3. 2 Zinc acetate dose reponse in BL cell lines*. BL cell lines were seeded at 5x10^5 cells/mL and treated with increasing doses of zinc acetate for 72 hours. Celltiter blue assay was performed to measure cell viability. X axis represents zinc acetate concentration and Y axis shows viability percentage. The data in this figure was generated by other members in the group before the beginning my project.*

To further characterise the effects of zinc acetate on sBL cells lines (AKATA, BL30) and eBL (DANTE, GLOR and SAV) cells were treated with 50 and 100 µM zinc acetate to assess their viability and cell counts at 24 and 48 hours using flow cytometry. Figure 3.3 shows representative forward and side scatter plots using individual viable cell gates for each cell line that were set using the corresponding plots for 0 µM zinc acetate.

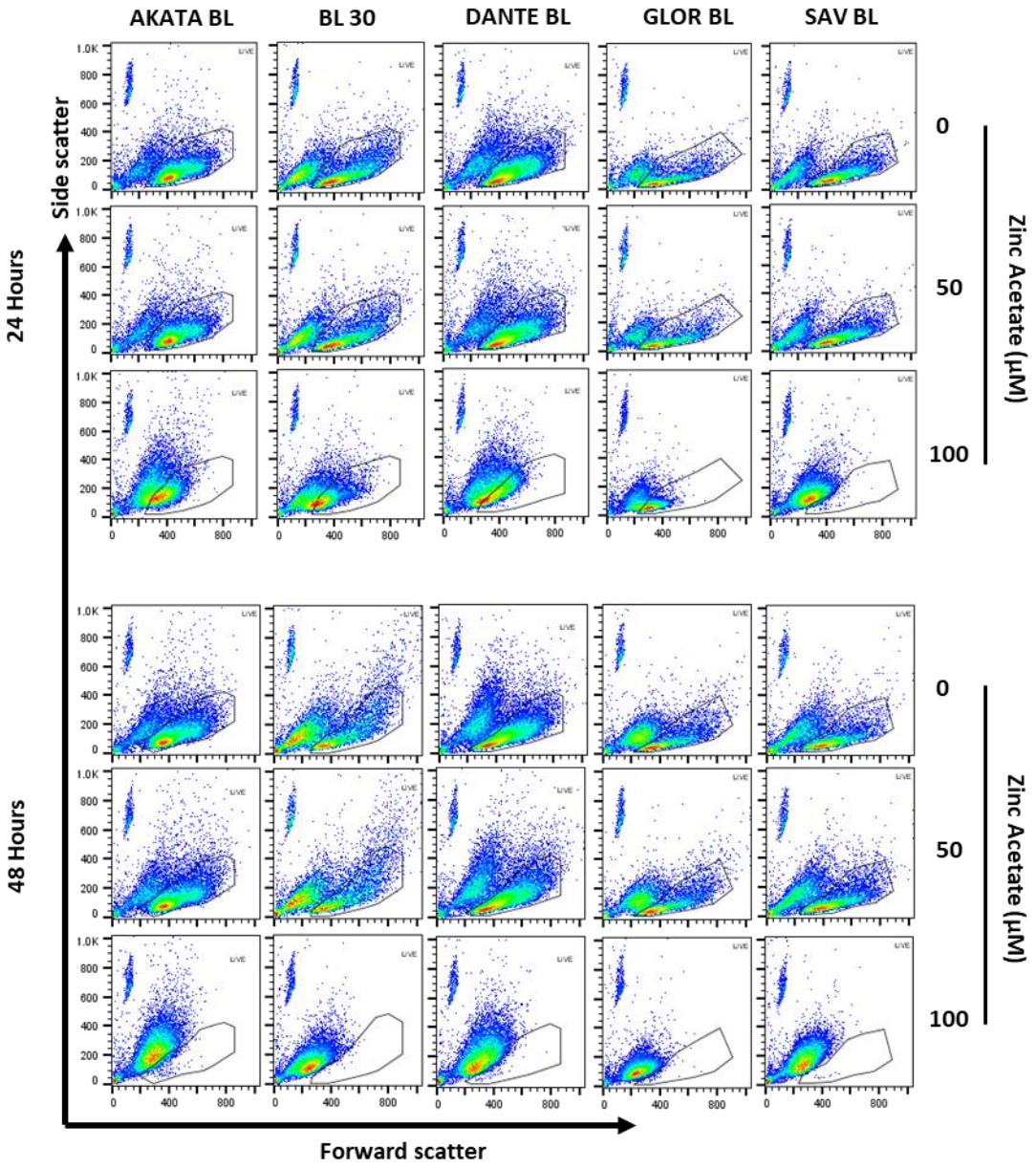

Figure 3. 3 Flow cytometry analysis of zinc acetate effect of on BL cell lines viability after 24 hours (top panel) and 48 hours (bottom panel). *BL cell lines (AKATA BL, BL 30, DANTE BL, GLOR BL and SAV BL) were seeded at 5x10^5 cells/mL and treated with 0, 50 and 100 µM zinc acetate for 24 and 48 hours. Cell viability and cell count were measured using Flow cytometry assay with counting beads.*

The plots show events inside and outside of these gates and include counting beads which appear as a distinct cloud in the upper left of the plots. As shown, 50 µM zinc acetate showed little effect on BL cells at 24 hours and only minor shifts in cell viability at 48 hours. In contrast, 100 uM zinc acetate induced loss in viability at 24

hours and total or near complete loss of viability at 48 hours in all tested BL cell lines. Figure 3.4 shows meaned data from N=3 experiments performed as in Figure 3.3.

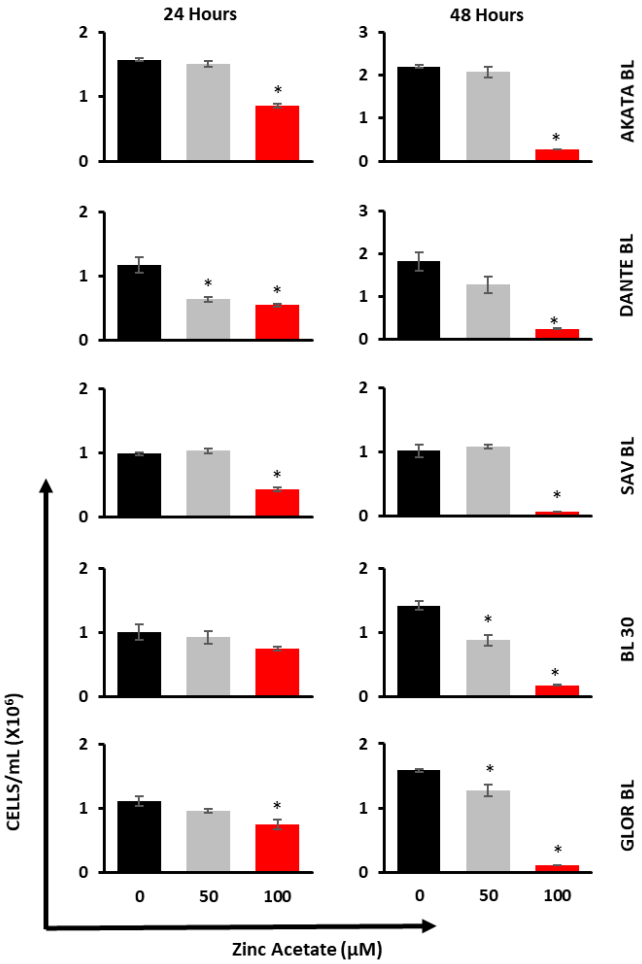

Figure 3. 4 Effect of zinc acetate on BL cell lines viability after 24 and 48 hours*. BL cell lines (AKATA BL, BL 30, DANTE BL, GLOR BL and SAV BL) were seeded at 5x10^5 cells/mL and treated with 0, 50 and 100 µM zinc acetate for 24 and 48 hours. Data are the mean from N=3 experiments measured using flow cytometry as shown in figure 3.3. Analysis was performed using one-way ANOVA.* P<0.05.*

The data confirm that there was near complete loss of cell viability in all BL cell lines tested when treated with 100 µM zinc acetate for 48 hours and that a diminished viability was detected after 24 hours. After 24 hours only the eBL cells DANTE showed statistically reduced viability in response to 50 µM zinc acetate. After 48 hours, BL 30 and GLOR BL showed a statistically difference in viability between cells exposed to 0 or 50 µM zinc acetate. To investigate morphological changes in

zinc acetate treated BL cell lines, cytopspin preparations of treated cells were stained with Jenner-Giemsa (JG) (Figure 3.5). The (top panel) shows representative images for each cell line at 24 hours and (bottom panel) at 48 hours. The images demonstrate the marked decrease in viable cell numbers at both 24 and 48 hours in all the treated cell lines when exposed to 100 µM zinc acetate at both 24 and 48 hours. The figures also illustrate the non-viable morphologies of the cells that remained in these cultures. In contrast, the morphologies and density of the cells treated with 50 µM zinc acetate at either 24 or 48 hours were similar to those of untreated control cells.

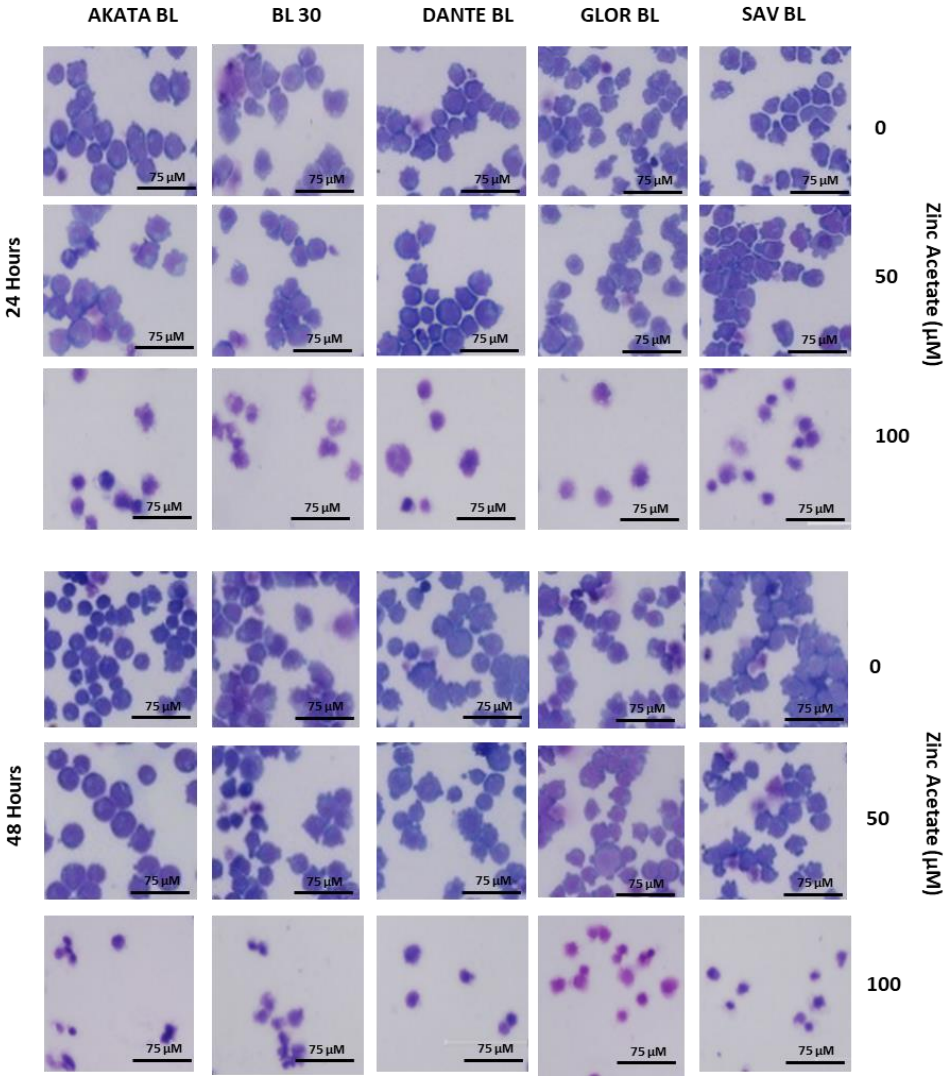

Figure 3. 5 Effect of zinc acetate on BL cell lines viability morphology after 24 and 48 hours*. sBL (AKATA BL and BL 30) and eBL (DANTE BL, GLOR BL and SAV) cell lines were seeded at 5x10^5 cells/mL and treated with 0, 50 and 100 µM zinc acetate for 24 and 48 hours. Cytospin slides were prepared and stained with Jenner-Giemsa stain. Images are represented with 75 µM bar scale.*

3.3 Zinc acetate has no/limited activity against diffuse large B cell lymphoma (DLBCL) acute myeloid leukemia (AML), or and lymphoblastoid cell lines (LCLs).

The above data showed BL cells are killed by 48 hours exposure to 100 µM zinc acetate. To investigate the potential selectivity, or not, of BL cell sensitivity to zinc, a panel of non-BL cell line were also investigated. Lymphoblastoid cell lines (LCLs) are immortalised B cells generated in the laboratory by infecting normal peripheral B cells with Epstein - Barr virus (EBV) causing B cells to proliferate continuously (Padmanabhan, 2014). LCLs are commonly used to represent a model of proliferating karyotypically normal B cells. Four LCLs cell lines JT, LG, KJ and AR LCL together with cell lines representing diffuse large B cell lymphoma (DLBCL; SU-DHL-4, SU-DHL5 and SU-DHL-6) and acute myeloid leukaemia (AML; HL 60) were treated used to assess their response to 50 and 100 µM zinc acetate. Exponentially grown cells were seeded at $5x10^5$ cells/mL and exposed to zinc acetate 50 and 100 µM for 24, 48 and 72 hours.

Flow cytometry dot plots were generated for each non-BL cell line at 24, 48 and 72 hours. Analysis at 24 and 48 hours revealed no significant loss of cell viability 24 or 48 hours when exposed to 50 or 100 µM zinc acetate. Representative forward and side scatter dot plots generated using flow cytometry after 72 hours treatment with zinc acetate data for 72 hours exposure is shown in Figure 3.6. As shown in the figure, neither 50 nor 100 µM zinc acetate caused significant loss of cell viability in LCLs, DLBCL or AML cells after 72 hours.

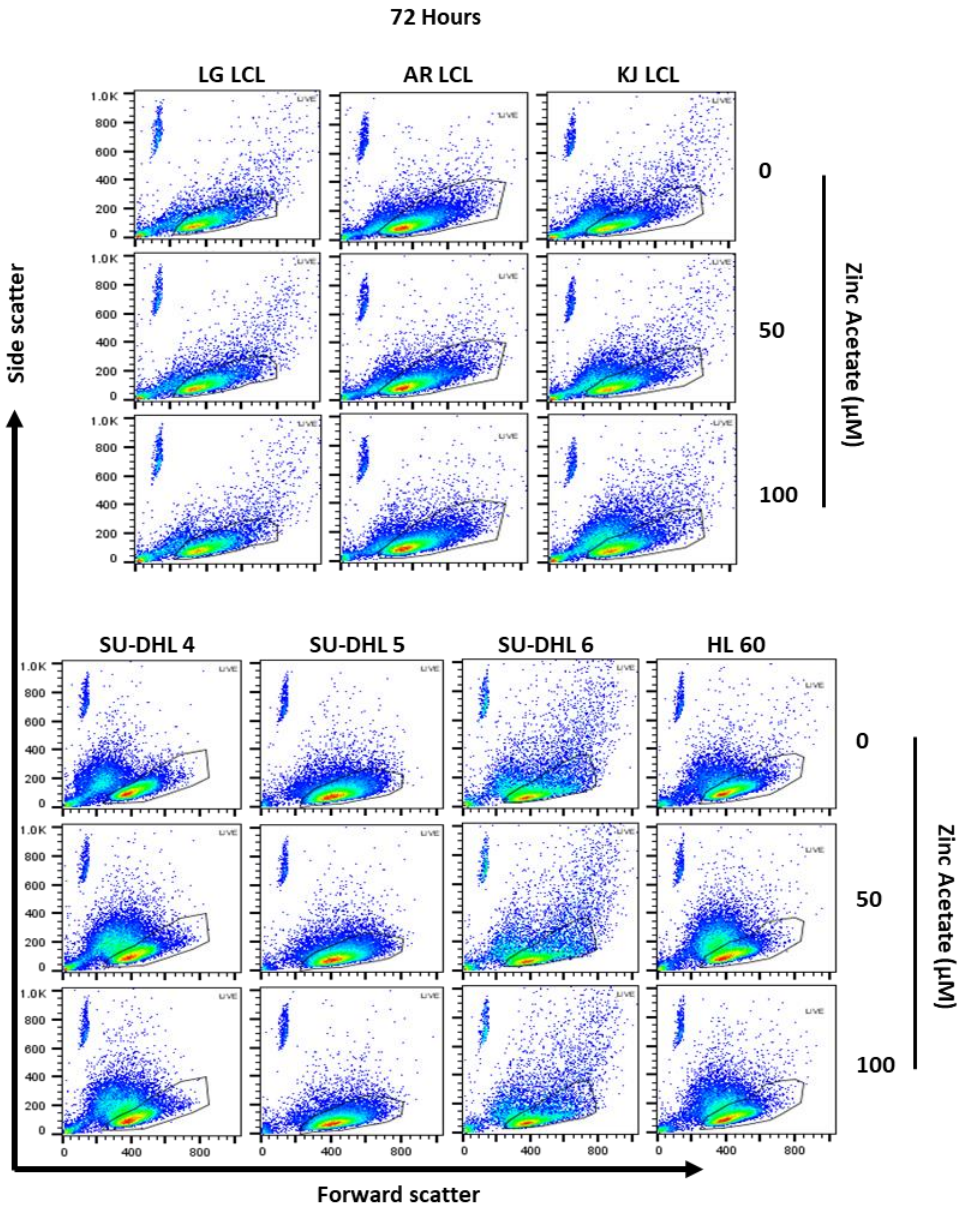

Figure 3. 6 Effect of zinc acetate on non-BL cell lines viability after 72 hours*. Non-BL cell lines (LG LCL, AR LCL, KJ LCL, SU-DHL 4, SU-DHL 5, SU-DHL 6 and HL 60) were seeded at 5x105 cells/mL and treated with 0, 50 and 100 µM zinc acetate for 72 hours. Cell viability and cell count were acquired using Flow cytometry assay with counting beads. Dot plots show side scattered on Y axis and forward scattered on X axis.*

Data for N=3 experiments for each cell line were meaned and compared to untreated control as shown in Figure 3.7. Neither 50 nor 100 µM zinc acetate caused noticeable loss of cell viability of LCL and DLBCL cell lines after 72 hours of treatment. HL 60 showed a minor significant reduction in cell viability with both 50 and 100 µM.

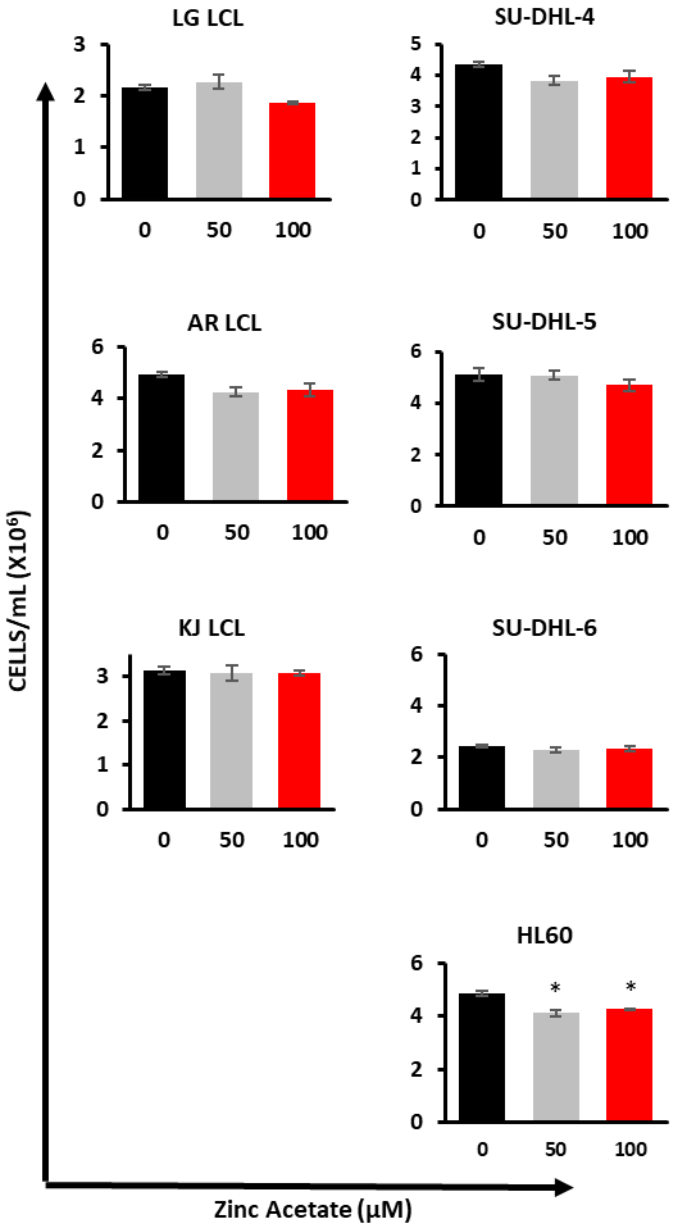

Figure 3. 7 Effect of zinc acetate on non-BL cell lines viability. *Non-BL cell lines (LG LCL, AR LCL, KJ LCL, SU-DHL 4, SU-DHL 5, SU-DHL 6 and HL60) were seeded at 5x10^5 cells/mL and treated with 0, 50 and 100 µM zinc acetate for 72 hours. Data are the mean from N=3 experiments measured using flow cytometry as shown in figure 3.6. Analysis was performed using one-way ANOVA.* P<0.05.*

Jenner-Giemsa stained images at 72 hours are shown in Figure 3.8. These images show no morphological changes in non-BL cells with 50 and 100 µM zinc acetate at 72 hours.

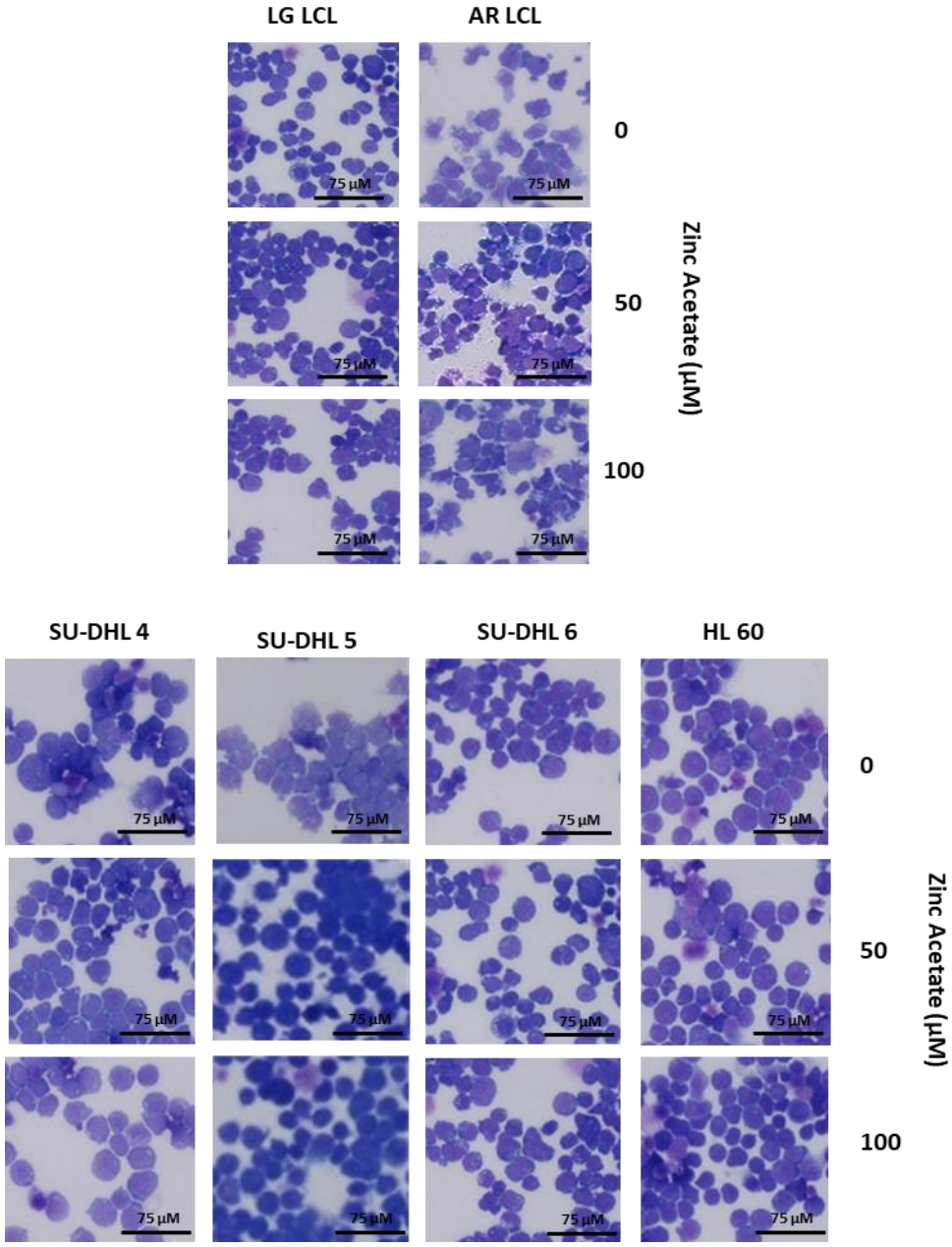

Figure 3. 8 Effect of zinc acetate treatment on non- BL cell lines morphology after 72 hours. *Non-BL cell lines (JT LCL, LG LCL, AR LCL, SU-DHL-4, SU-DHL-5, SU-DHL-6 and HL 60) were seeded at 5x10^5 cells/mL and treated with 0, 50 and 100 µM zinc acetate for 24 hours. Cytospin slides were prepared and stained with Jenner-Giemsa stain.*

Hereto, the results demonstrate that 100 µM zinc acetate targets sBL (AKATA, and BL 30) and eBL (DANTE, GLOR and SAV) cell lines selectively and reduces their viability after 24 hours and near complete loss of viability was seen after 48 hours. On the other hand, non- BL cell lines LCLs (JT, AR, KJ and LG), DLBCL (SU-DHL-4, SU-DHL-5 and SU-DHL-6) and AML (HL 60) were not reflecting the same viability response to zinc acetate treatment seen in BL cell lines over the time.

Cumulative viability data for both of BL and non-BL group of cells from all previous experiments are represented in Figure 3.9. Total cell count (viability) over the time is represented in the figure where it illustrates that BL cells were sensitive and were killed with zinc acetate treatment at 100 µM more than 50 µM as seen with the halted cell proliferation pattern over 24 and 48 hours, while non-BL cells generally are remained viable and grow over the extended time points for up to 72 hours.

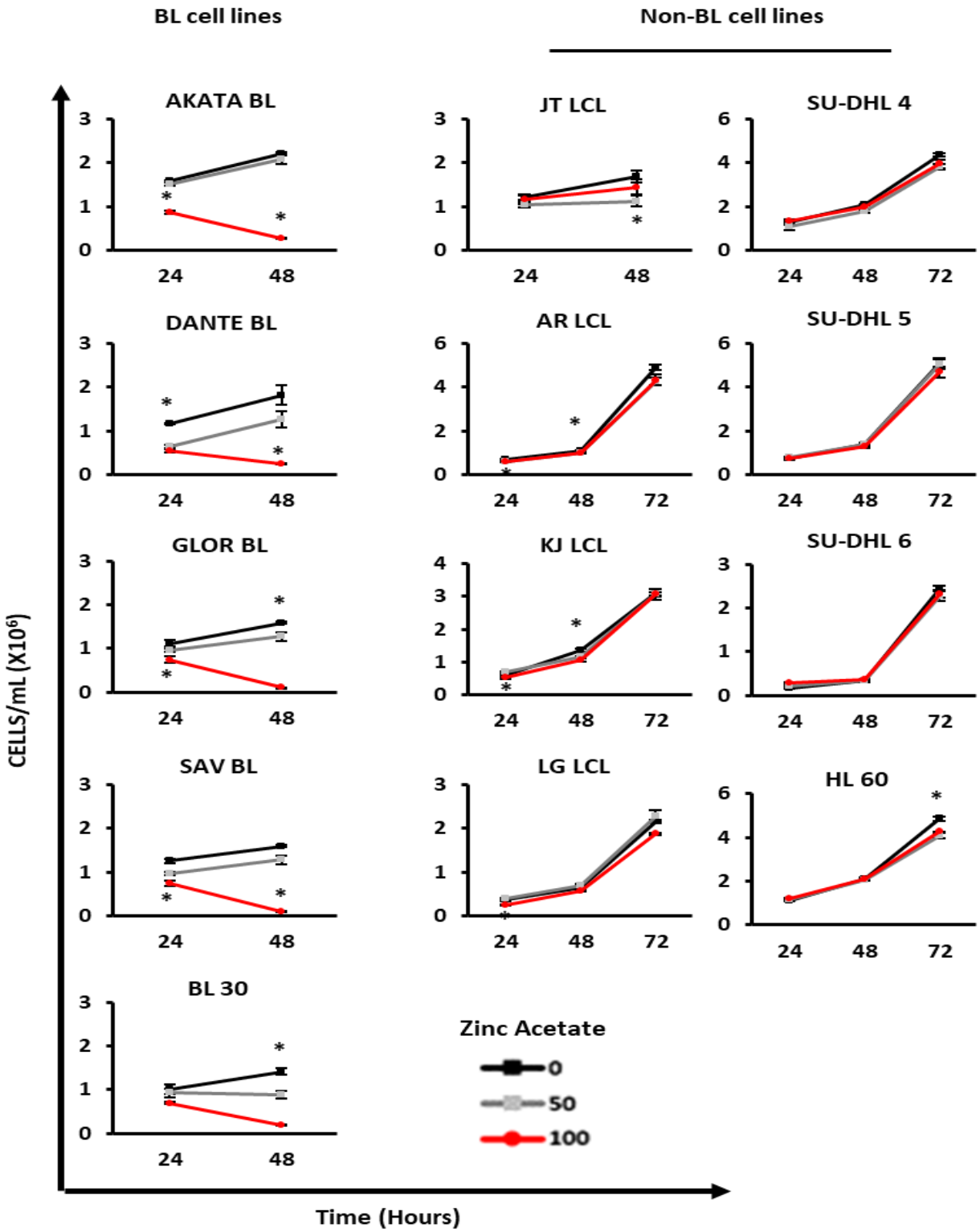

Figure 3. 9 Cumulative proliferation pattern of BL and non-BL cell line in a response to zinc acetate treatment*. sBL (Akata BLand BL 30), eBL (SAV BL, DANTE BL and GLOR) and non-BL cell lines (JT LCL, AR LCL, KJ LCL and LG LCL, SU-DHL-4, SU-DHL-5, SU-DHL-6, and HL 60) were seeded at 5x10^5 cells/mL and treated with 0, 50 and 100 µM zinc acetate for 24,48 and 72 hours. Data are the mean from N=3 experiments of each cell line. Analysis was performed using one way ANOVA *p<0.05.*

3.4 Zinc acetate increases Apoptosis in BL cell lines.

Combined annexin V and propidium iodide (PI) staining was used to investigate the possible role of apoptosis in the differential response of BL and non-BL cell lines to 50 and 100 µM zinc acetate. In viable cells, phosphatidylserine is located on the inner surface of cell membrane and during apoptosis it is exposed to the outer surface. Phosphatidylserine can be detected using flow cytometry when the cells are stained with Annexin V conjugated with fluorescent APC which has affinity to bind phosphatidylserine. Alongside Annexin V, propidium iodide is used to stain cellular DNA in dead but not live cells.

Thus, increased apoptosis events correlate with increased Annexin V signals and PI signals. eBL: DANTE and GLOR BL, sBL: BL 31, AKATA and BL 30 with non-BL cell lines; AR LCL, SU-DHL-4 and HL 60 were tested. All cells were grown exponentially then seeded at $5x10^5$ cells/mL and treated with 50 and 100 µM zinc acetate for 24 hours. Figure 3.10 shows the representative flow cytometry dot plot generated for each cell line.

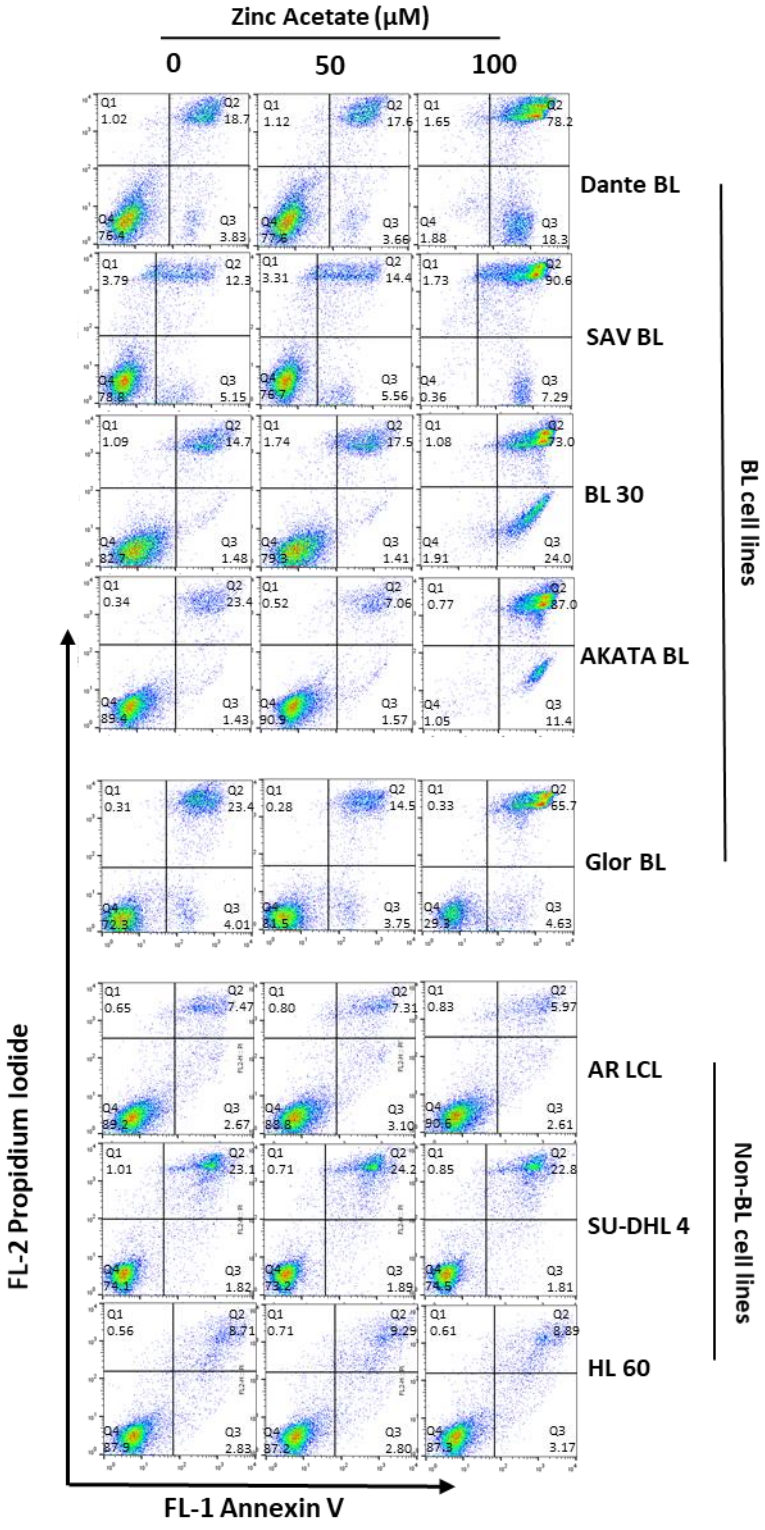

Figure 3. 10 Annexin V and PI flow cytometry dot plots for BL and non-BL cell lines treated with zinc acetate for 24 hours. *BL cell lines (DANTE BL, BL 30, AKATA, GLOR BL and BL 31) and non-BL cell lines (AR LCL, SU-DHL-4 and HL 60) were treated with zinc acetate 0, 50 and 100 µM. After 24 hours of incubation, cells were stained with propidium iodide and annexin V. Flow cytometry dot plots represent propidium iodide signal intensity on Y axis and Annexin V signal intensity on X axis.*

As shown in Figure 3.10, lower left quadrant of the dot plot shows the live cells events for each cell line which defines cells that are not undergoing apoptosis. Lower right quadrant defines an early stage of apoptosis where cells are exposing phosphatidylserine into outer membrane and becoming annexin V+. Upper right quadrant represents cells which are undergoing later stage of apoptosis as cells are represented with annexin V+ and become leaky allowing PI to enter the cells and stain DNA as described in the materials and methods in chapter 2.

In BL cells (eBL:DANTE BL, SAV BL and sBL: BL 30 and AKATA), data showed that 100 µM zinc acetate induced apoptosis as seen in the noticeable event shift from lower left to lower right suggesting an increase in annexin V staining. Moreover, upper right quadrant showed an increase in late apoptosis events. No activation of apoptosis was observed with 50 µM. eBL GLOR cells treated with 100 µM showed no increased sign of early apoptosis as represented in lower right quadrant, however, it showed a late apoptosis event with loss of viable cell events as seen in the upper right quadrant when compared to control. Similar to other BL cell lines tested, 50 µM showed no major changes when compared to the control. In a comparison, annexin V and PI stain levels in cells treated with 50 and 100 µM remained nearly the same as the control the non-BL group (AR LCL, SU-DHL-4 and HL 60)

Figure 3.11 shows meaned annexin V data for N=3 experiments as in Figure 3.10. 100 µM zinc acetate significantly increased annexin V in all BL cell lines tested after 24 hours while non-BL cells showed no difference in annexin V staining compared to control cells. There were no significant differences seen with 50 µM zinc acetate dose in either BL or non-BL cell lines after 24 hours.

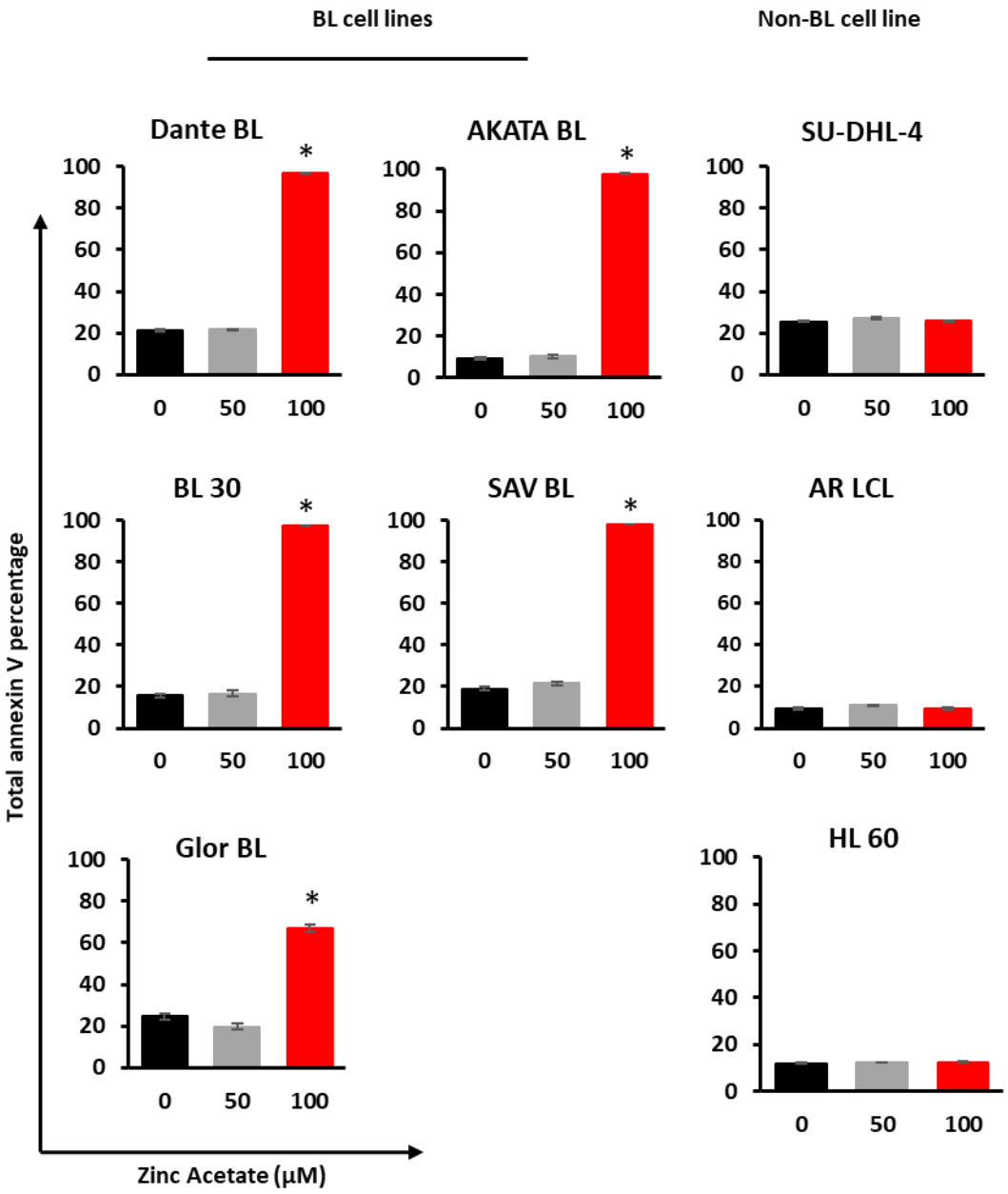

Figure 3. 11 Apoptosis evaluation in BL and non-BL cell lines treated with zinc acetate for 24 hours. *BL cell lines (DANTE BL, BL 30, AKATA, GLOR BL and BL 31) and non-BL cell lines (AR LCL, SU-DHL-4 and HL 60) were treated with 0, 50 and 100 µM zinc acetate. After 24 hours, cells were stained with propidium iodide and annexin V. Data represent meaned analysis of total annexin V staging (upper and lower right quadrant) from N=3 experiments using flow cytometry dot plots as shown in figure 3.10. Data analysis was performed using one-Way ANOVA. *P<0.05.*

3.5 Activation of caspases in BL cell lines as a response to zinc acetate.

The above data showed that BL cells demonstrated increased levels of apoptosis in response to 100uM zinc acetate after 24 hours. Caspases are key mediators in apoptosis, especially executioner caspases such as caspase 3 and 9 which activate downstream signalling cascades once cleaved and activated. Therefore, caspase 3 and 9 activation were assessed in BL cell lines (eBL: DANTE, SAV BL and sBL: BL 30) and non-BL cell (JT LCL) when exposed to zinc acetate for 6 hours. Western blotting assay was performed to measure the inactive (uncleaved) form of caspase 3 and 9 protein levels.

Figure 3.12 shows representative caspase 3 western blot images and meaned densitometry data from N=3 experiments normalised with β-actin and compared to control untreated cells for three BL cell lines (sBL: BL 30, and SAV and eBL: DANTE) and one non-BL LCL (JT LCL) after 6 hours.

As illustrated in the figure, all tested BL cell lines had reduced levels of uncleaved caspase 3 protein compared to control which is significant with 100 µM zinc acetate treatment. Western blot images show 2 bands captured by the antibody used in all tested cells which is used to detect the full length of caspase 3. Only the lower band (33 kDa) was sensitive to 100 µM zinc acetate whilst the top one was more stable. This upper band may be due to non-specific binding of the antibody or alternatively, may be caspase 3 which has been post-translationally modified. Phosphorylation of caspase 3 at Ser150 by p38-MAPK is believed to adjust protein threshold to prevent apoptosis (Thomas *et al.*, 2018). This finding was not seen with 50 µM as caspase 3 levels remained similar to the control in BL cell lines. In contrast, the non-BL cell lines JT LCL showed no changes to caspase 3 protein levels with 50 or 100 µM zinc acetate after 6 hours.

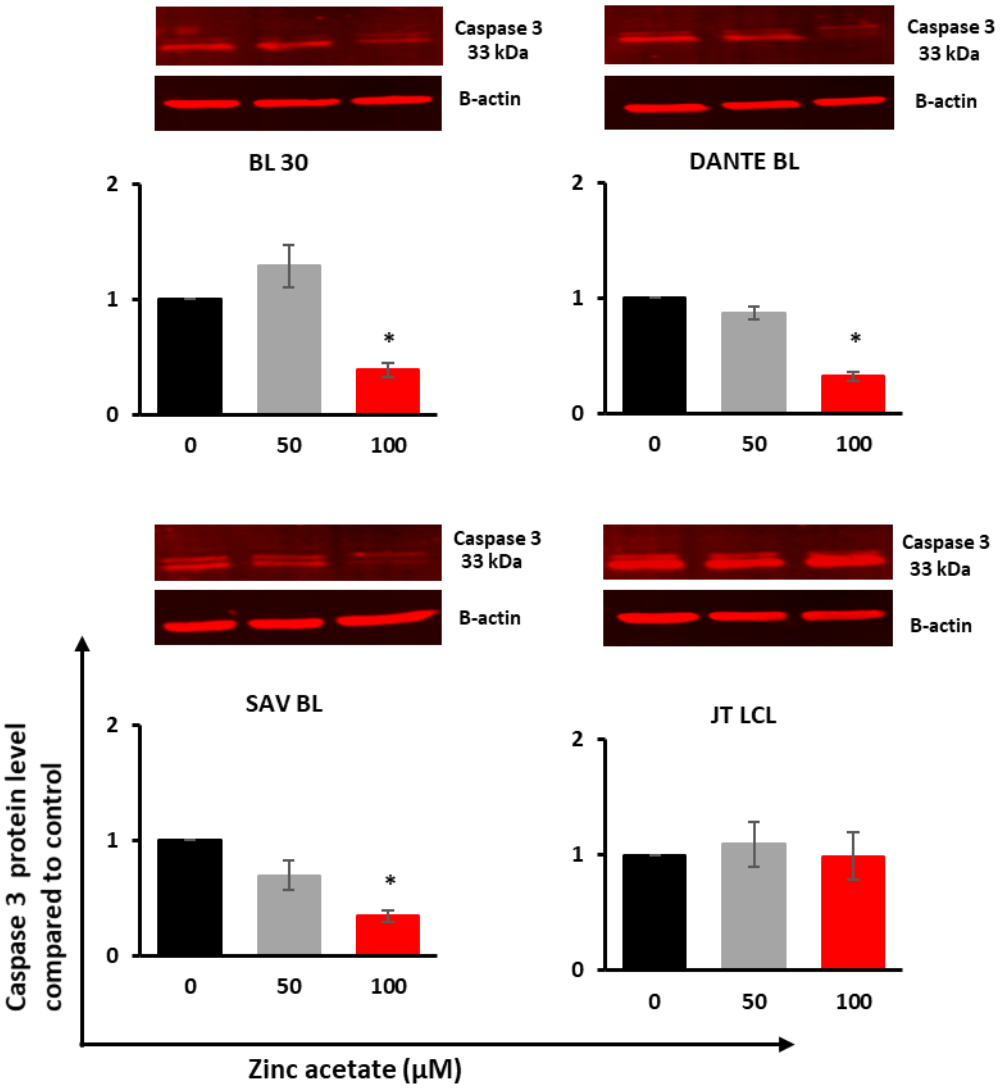

Figure 3. 12 Caspase 3 protein levels in zinc acetate treated BL and non-BL cell lines after 6 hours*. BL cell lines (DANTE, BL30, SAV), LCL cell line (JT LCL) were treated with 0, 50 and 100 µM zinc acetate for 6 hours. Western blot images are represented for each cell lines. Both images are represented in red colour since both primary anti caspase 3 and anti β-actin were generated in mouse and secondary fluorescence antibodies are anti mouse (Red 700). Primary Caspase 3 protein levels were normalised to β-actin and compared to control. Data analysis was performed using one way ANOVA. * P<0.05.*

Investigation of caspase 9 protein levels by western blotting is shown in Figure 3.13. Meaned protein levels of N=3 experiments of cells treated with 50 and 100 µM zinc acetate are represented after being normalised with β-actin and compared to control. Significant reduction in caspase 9 protein level was observed with 100 µM zinc acetate in BL cell lines (sBL: BL 30 and eBL: SAV and Dante) while 50 µM showed no significant changes as compared to control. No caspase 9 changes were observed in JT LCL for either zinc doses.

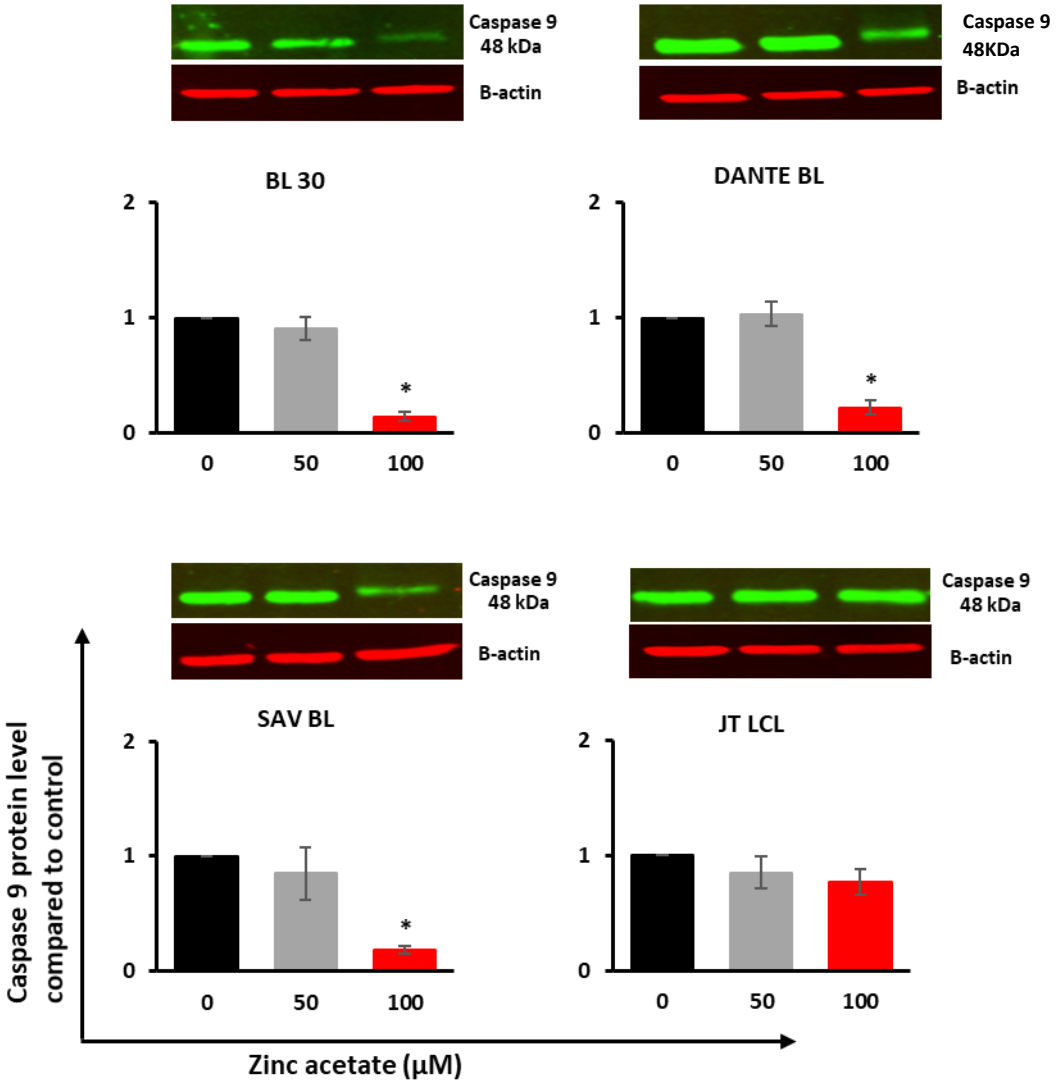

Figure 3. 13 Caspase 9 protein levels in zinc acetate treated BL and non-BL cell lines after 6 hours*. BL cell lines (DANTE, BL30, SAV), LCL cell line (JT LCL) were treated with 0, 50 and 100 µM zinc acetate for 6 hours. Western blot images are represented for each cell lines. Caspase 9 protein levels were normalised to β-actin and compared to control. Data analysis was performed using one way ANOVA. * P<0.05.*

3.6 Cell cycle analysis in BL and non-BL cell line and their response to zinc acetate.

The previous analysis showed that zinc acetate initiates apoptotic cell killing in BL cell lines. Cell cycle analysis was also performed on zinc acetate treated cells.

Exponentially grown BL cell lines (eBL: DANTE, GLOR and SAV) and (sBL: AKATA and BL 30) and non-BL cell lines; AR LCL, SU-DHL-4 and HL 60 were seeded at $5x10^5$ and treated with 0, 50 and 100 µM zinc acetate. After 24 hours, cells were permeabilised, stained with propidium iodide and analysed by flow cytometry. Representative histograms of cell cycle phases are shown in Figure 3.14 A Meaned data for N=3 of all BL cell lines tested and non-BL cells are represented in stacked bar charts in Figure 3.14 B. The data show that after 24 hours of treating BL cells with 100 µM zinc acetate, no arrest was seen in cell cycle. However, the majority of BL cells line tested had significant increases in sub-G0 events which corresponds with apoptosis derived DNA fragments. These were not observed in control and 50 zinc acetate treated cultures. None of the non-BL cell lines displayed significant differences in cell cycle phases when compared to controls at either 50 or 100 µM zinc acetate.

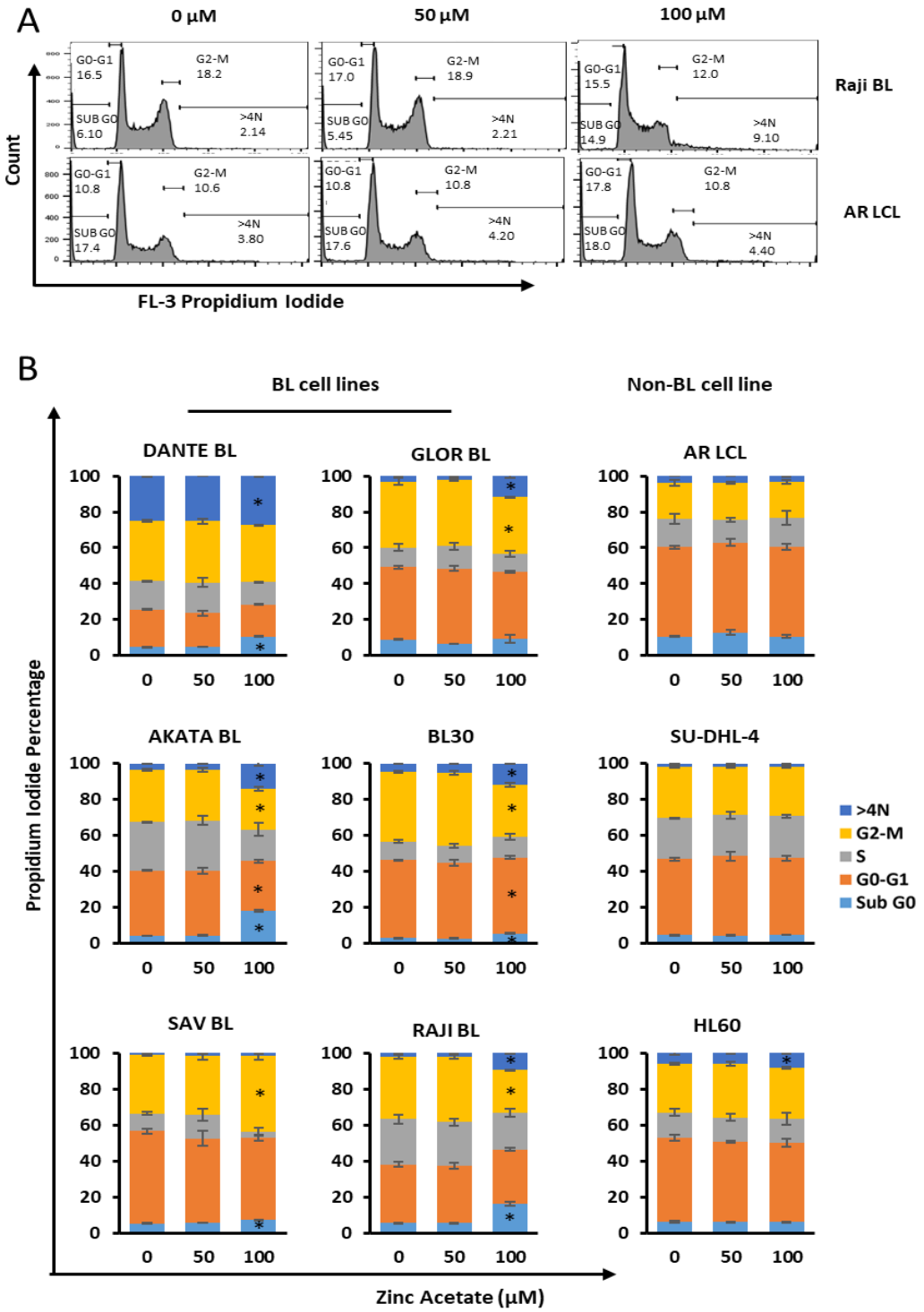

Figure 3. 14 Cell cycle phase evaluation and measurement in BL and Non-BL cell lines treated with zinc acetate for 24 hours*. BL cell lines (DANTE BL, SAV BL, NAMALWA BL, GLOR BL and RAJI BL) and Non-BL cell lines (HL 60, AR LCL and SU-DHL-4) were seeded at 5x10^5 cells/mL and treated with 0, 50 and 100 µM zinc acetate. After 24 hours of incubation, cells were permeabilized and DNA was stained with Propidium Iodide (PI). (A): flow cytometry histogram for a representative BL cell line (RAJI) and non-BL (AR LCL). X axis represents PI stain that indicates cell cycle phases and Y axis represent the count. (B): Meaned data of N=3 experiment represents phase PI peaks analysis of BL and non-BL cell lines demonstrate the percentage of each cell cycle phase (Y) axis and zinc acetate concentration on X axis. Analysis was performed using one-way ANOVA. P<0.05.*

3.7 Discussion and summary.

The need to develop an alternative, safe, effective and affordable BL therapy in LMIC is due to the challenges of treating BL which needs significant resources to help in managing the outcomes and side effects of intensive chemotherapy. Due to financial limitations, these resources are not always easily available, thereby limiting treatment options and reducing response rates. In addition to newly diagnosed BL, some BL patients present with a tumour that is drug resistant and others will relapse. For these patients, survival rates are reduced to ~ 20% (Woessmann *et al.*, 2020). Radiotherapy and surgical intervention to debulk the tumor is another procedure that also form a challenge in treating advanced cases of the disease.

Prior to the start of this project, our group had demonstrated that the repurposed drug combination of bezafibrate and medroxyprogesterone acetate (BaP) had potent in vitro anti-BL activity (Fenton *et al.*, 2003). This was translated into improved outcomes in a phase 2 clinical trial in relapsed/refractory BL in Malawi (Molyneux *et al.*, 2014). These data demonstrated that repurposed drugs can improve outcomes in LMICs. Thus, further work was done to identify additional repurposed drugs that had anti-BL activity. A panel of BL cell lines were screened against a custom in-house library of repurposed drugs (FMC library) and viability assessed using the Cell Titre Blue Assay. These experiments identified that the mineral supplement zinc acetate had potent anti-BL activity. Dose titration experiments showed that zinc at 100 µM was able to significantly reduce the cell viability of eBL; DANTE, EZEMA, GLOR, NAMALWA and SAV and sBL; AKATA, BL30, BL31 in 72 hrs. The effect of zinc was characterised in the context of time and dose in greater depth against BL cell lines. The responses of BL cell lines were compared to a panel of non-BL cell lines including DLBCLs, AML and LCLs which represent “normal” B cells. Flow cytometry using counting beads were used to obtain cell counts and showed that BL cell lines were acutely sensitive to 100 µM zinc acetate. BL cell numbers decreased by nearly 80% after 48 hrs among sBL; AKATA, BL30 and eBL; DANTE, GLOR and SAV, whereas 50 µM zinc had no significant effect on cell viability. In all of the non-BL cell lines tested, including LCL; JT, AR, KJ and LG and non-BL tumour cell line DLBCL; SU-DHL-4, SU-DHL-5 and

SU-DHL-6 and AML; HL60, cell numbers increased over 72 hours equally in the presence or absence of zinc demonstrating that zinc had no effect on these cells. Combined, these data suggest a BL-specific action of zinc. Interestingly, Sirinian *et al* demonstrated that 100 µM zinc sulfate was able reduce C-MYC protein levels in the eBL RAJI cell line even after 24 hours which was not seen in the tested HL 60 cell line as the study showed. In addition, different leukemic cell lines (JURKAT and K562) were tested and showed no zinc-related apoptotic effects (Sirinian et al., 2003). Different study showed that thin films coated with zinc oxide (ZnO) was able to induce cell death after 24 hours among RAJI cell line with no significant effect observed in tested peripheral blood mononuclear cells (PBMCs). Furthermore, ZnO was found to induce the generation of reactive oxygen species in RAJI cells which also downregulate inhibitor of apoptosis proteins (IAPs) levels and modulating phosphorylated form of P53 to facilitate apoptosis in BL cells (Moon *et al.*, 2016).

A previous study described that 60 -100 µM zinc acetate activated the executioner caspase 3 via intrinsic pathways in RAMOS BL cells with no apoptotic response found with lower concentrations. Caspase 3 activation led to the cleavage of poly-ADP ribose polymerase (PARP) which is a hallmark in apoptosis event. In the same study, adding the caspase inhibitor zVAD-fmk prevented apoptosis indicating an essential role for apoptosis in zinc-mediated killing of RAMOS cells (Schrantz *et al.*, 2001b). This was confirmed in the present study. Using Annexin V and propidium iodide staining and flow cytometry, all the BL cell lines tested (DANTE, SAV, GLOR, AKATA and BL30) showed an increased annexin V signals with 100 µM dose of zinc with no significant increase seen at 50 µM. Neither 50 nor 100 µM zinc doses induced significant annexin V staining on non-BL cell lines. Apoptosis is either activated via the intrinsic or extrinsic pathway. Western blot analysis of caspase 9 and the executioner caspase 3 showed that 100 µM zinc is triggering apoptosis in different BL subtypes including eBL (DANTE and SAV) and sBL (BL30) cell lines which is not seen on the non-BL LCL (JT). These findings indicate that zinc is initiating apoptosis in BL cells via the intrinsic pathway in a mechanism involving mitochondrial stress and cytochrome C release leading to activate procaspase 9 and procaspase 3. Measuring of cytochrome C release from the mitochondria would

further confirm the ability of zinc to induce apoptosis via intrinsic pathway in BL cell lines as the killing mechanism.

Cell cycle analysis demonstrated that zinc does not induce cell cycle arrest in BL cells. However, an increase in the sub-G1 peak was observed which further support the presence of apoptosis.

In conclusion, characterization of zinc treatment against BL showed that zinc is able to kill all tested BL cell lines tested at 100 µM after 48 hrs via induction of apoptosis involving caspase 3 and 9 activation with no cell cycle arrest. These effects were not observed among the other non-BL cells lines and controls LCLs treated with either 50 or 100 µM dose. The data suggest the potential of zinc as an adjunctive therapy in BL. Zinc has been used in management of several different diseases. Studies have shown that adding zinc in treating malaria can reduce febrile episodes (Shankar *et al.*, 2000). Whilst in leprosy, giving 400 mg of zinc twice a day was found to help in managing skin nodules and erythema reduction which is also found to be useful in patients with cutaneous leishmaniasis in a dose of 10 mg/kg (El-Shafei *et al.*, 1988, Sharquie *et al.*, 2001). Up to 600 mg dose of zinc was given daily to patients with Wilson's disease aimed to excrete excessive stored copper and helped in managing disease symptoms (Rossaro *et al.*, 1990). Moreover, zinc was also found to be effective in managing rheumatoid arthritis, diabetes type 1 and 2, leg ulcers, atopic eczema, macular degeneration and others more (Haase *et al.*, 2008). The effect of zinc against BL cells was studied by using different form of zinc including nanoparticles materials. It was indicated via WST-1 assay that zinc oxide (ZnO) nanoparticles triggered a significant toxic effect against the eBL DAUDI cell line than normal B cells after 24 hours of incubation (Carofiglio *et al.*, 2021). Indeed, zinc nanoparticles were studied in several studies against different types of cancers including blood cancers and showed an increased efficiency in targeting and killing cancer cells in multiple pathways and also helped in increase the potency of photodynamic therapy (Akhtar *et al.*, 2012, Luengas *et al.*, 2015, Yi *et al.*, 2020, Firdous, 2018, Li *et al.*, 2023). ZnO nanoparticles investigation were tested using multiple cancer cells of different origins including; hepatocellular carcinoma (HepG2) and lung carcinoma (A549) and showed an increased loss of cell viability

compared to primary hepatocytes cells. It was reported that ZnO induced DNA fragmentation and affect apoptotic proteins including; P53, BAX and BCL-2 (Akhtar *et al.*, 2012).

The data in this chapter identified that zinc was killing BL cells selectively and that involved the induction of apoptosis whereas non-BL cell lines were not sensitive. A remarkable feature of the killing of BL cell lines observed with zinc was that the dose responses were very similar between all the BL cells tested indicating a similar mechanism of action or target. A key defining feature of BL is translocation of *C-MYC* to one of the Ig genes located on chromosomes 14, 2 or 22 resulting in dysregulated constitutive expression of C-MYC. Whilst some of the other cancer cell lines overexpress *C-MYC*, it is not due to this particular translocation. Thus, it was postulated that zinc may be killing BL cells by targeting *C-MYC* gene or protein. This was investigated in the next chapter.

CHAPTER FOUR

IMPACT OF ZINC ACETATE TREATMENT ON EXPRESSION OF *C-MYC* IN BL CELL LINES

4 Impact of zinc acetate treatment on expression of *C-MYC* in BL cell lines.

C-MYC deregulation is very common in many human cancers. The oncogenic effect of C-MYC protein was found to be linked to more than 60% of human cancers including; breast cancer, colorectal carcinoma, esophageal cancer, ovarian cancer and lymphoma (Duffy *et al.*, 2021). In BL, *C-MYC* is translocated to either the immunoglobulin heavy chain *IgH* (14q32), light chain kappa *IgK* (2p12) or lambda *IgL* (22q11) loci. This translocation occurs in GC B cell during B cell development where an extensive gene editing process is involved carried out by the DNA editing enzyme activation induced cytidine deaminase (AID). AID is essential for somatic hypermutation and class switch recombination during B cell development (Stavnezer, 2011). Off-site activity of AID has been shown to cause *C-MYC* translocation to the Ig locus bringing expression of *C-MYC* under the control of Ig intron and 3' enhancer elements resulting in constitutive expression of C-*MYC* (Hu et al., 2007, Schmitz et al., 2014, Poole et al., 2018).

In BL, the different *C-MYC* breakpoint can occurs within exon 1 (class I), head-to-head break points (class II) or involve the far distant breakpoint (class III) with *MYC/IgH* t(8;14) to be the common translocation (Nguyen et al., 2017, Boxer and Dang, 2001). Despite the important role of *C-MYC* in many cancers, no clinically available drugs have been developed that can target *C-MYC*. Zinc (100 µM) was previously reported to target C-MYC protein in the RAJI BL cell line causing protein reduction but not in LCL cells which were used as a control for B cell (Sirinian *et al.*, 2003). This study also looked at HL60 cells which have an amplified *C-MYC* (Birnie, 1988). Whilst a short-term decrease in C-MYC protein was observed in HL 60 cells, this was not sustained beyond 8 hours (Sirinian *et al.*, 2003). Since *C-MYC* is important and plays an essential role in driving the proliferation and pathogenesis of BL cells, the effect of zinc against C-MYC mRNA and protein will be investigated and assessed in this chapter.

There are multiple possibilities in how zinc may regulate *C-MYC* including at the transcriptional level by regulation of the promotor or the enhancers, or by regulating protein degradation. To address whether the Ig enhancer regions are targeted by zinc, we looked at another translocation involving the *IgH* locus, notably the

BCL2/IgH t(14;18) (q32;q21) translocation. The BCL-2 protein family regulates apoptosis by inducing or suppressing cell death. It is crucial for BCL-2 protein to be tightly regulated to prevent potential cancer development (Czabotar et al., 2014). Given its role in preventing cell death, irregular *BCL2* overexpression is common in neuroblastoma, breast cancer, lung and squamous cell carcinoma (Um, 2016). *BCL2* gene is located on chromosome 18 and its translocation to *IgH* is a common mutation reported in follicular lymphoma (FL) and DLBCL leading to *BCL2* overexpression (Salam *et al.*, 2020). In *BCL2/IgH* t(14;18), *BCL2* overexpression is initiated from both promoters P1 and P2 which usually have low to no activity. However the close proximity to the Ig enhancer elements resulting from the translocation induces high levels of expression (Figure 4.1) (Duan *et al.*, 2007).

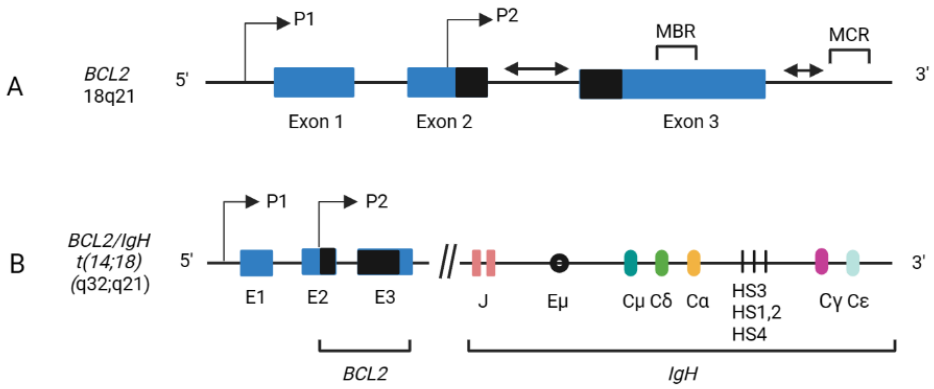

Figure 4. 1 The architecture of BCL2/IgH t(14;18) (q32;q21) translocation. *(A) BCL2 gene structure shows the three exons of BCL2, P1 and P2 promoter, major breakpoint (MBR), minor cluster region (MCR), coding parts of the gene (black). (B) shows the BCL2/IgH t(14;18) (q32;q21) translocation where BCL2 overexpression is hijacked by IgH HS enhancer elements. Figure was generated using BioRender platform (www.BioRender.com).*

This translocation pattern shows a similar pattern to the *C-MYC* translocation t(8;14)(q24;q32) found in BL where *IgH* enhancers deregulate *C-MYC* expression (Kirkin *et al.*, 2004, Xiang *et al.*, 2011). The DLBCL cell line (SU-DHL-4) is characterized by *BCL-2/IgH* translocation and thus can be used to investigate whether zinc is targeting Ig enhancer elements to affects *BCL2* expression and relate these findings with the effect of zinc against *C-MYC* in BL cell lines.

4.1 Evaluation of basal C-MYC protein levels in BL and non-BL cell lines.

In 2003, Sirinian *et al* reported that C-MYC protein levels were reduced in response to zinc sulphate in RAJI BL cells when measured by western blotting (Sirinian *et al.*, 2003). We therefore wished to investigate whether the action of zinc acetate in BL cells involves decreasing C-MYC expression. In order to test this, basal C-MYC protein levels were determined in multiple BL (eBL: NAMALWA BL, RAJI BL, GLOR BL, SAV BL and sBL: AKATA, BL 30, BL 31), LCL (AR LCL and KJ LCL), AML (HL 60) and DLBCL (SU-DHL-4, SU-DHL-5 and SU-DHL-6) cell lines using western blotting.

As shown in Figure 4.2 A and B, C-MYC protein was present as three commonly occurring bands variably expressed across all cell lines with molecular masses of 66 kDa, 62 kDa and 55 kDa. Although not investigated here these differences are most likely related to different post translational modification of C-MYC (Sears, 2004).

Figure 4.2 A and B show representative western and total basal C-MYC protein levels for N=3 experiments meaned and represented as a stack bar graphs with the corresponding protein band sizes. C-MYC protein levels were calculated using densitometry and represented as relative expression in comparison to the housekeeping gene protein β-actin. Not all samples could be run on the same gel therefore HL 60 as a representative non-BL cell line and eBL: NAMALWA as a representative BL cell line were included in all gels to aid comparison of the data. The analysis showed that C-MYC protein levels were variable between BL cell lines but were significantly lower in all non-BL cell line tested, an observation consistent with the translocation driven constitutive expression of C-MYC in BL. The 62 kDa C-MYC band was the most strongly represented amongst BL and non-BL cells.

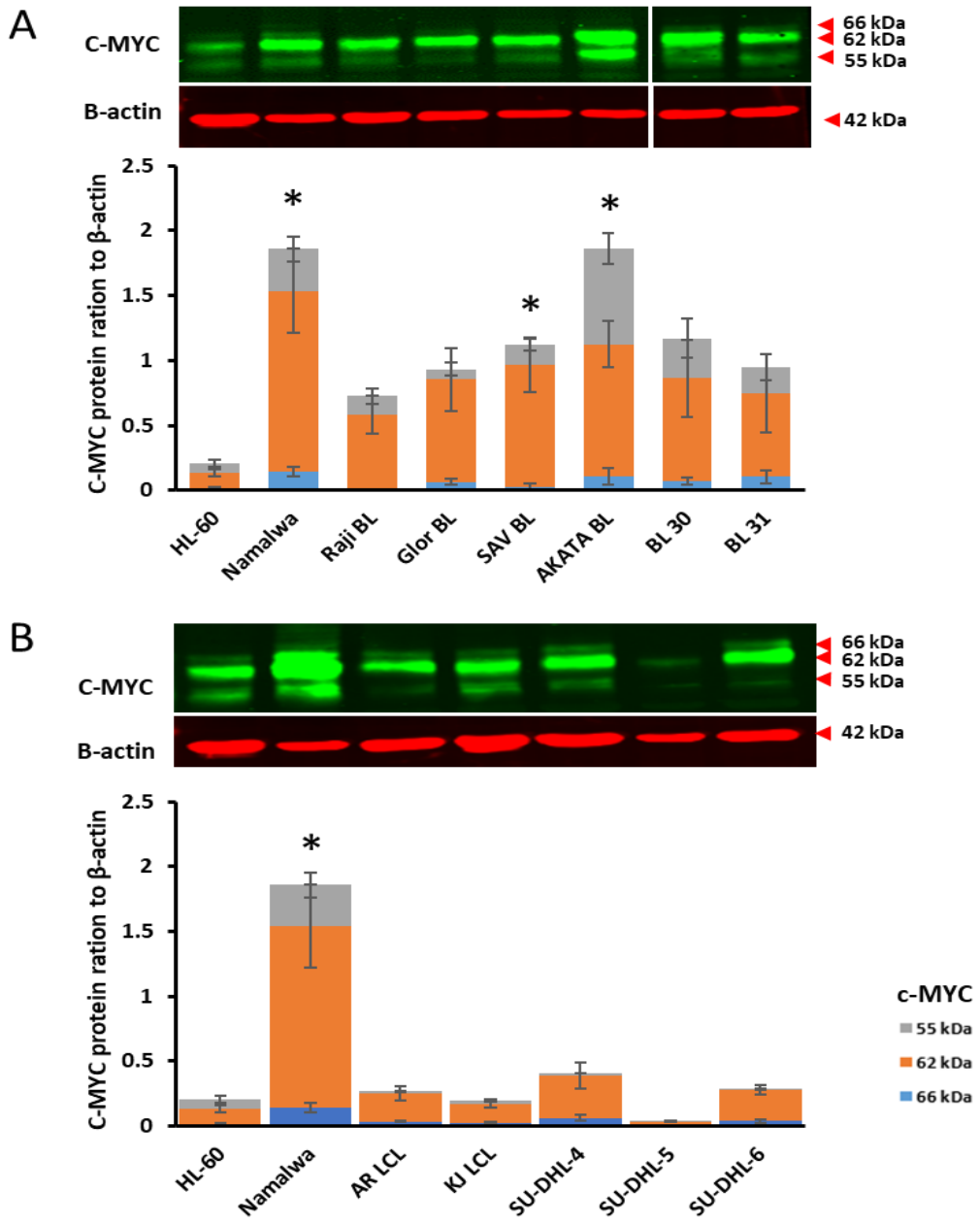

Figure 4. 2 Basal C-MYC protein levels in BL and Non-BL cell lines. *BL cell lines (eBL: NAMALWA BL, RAJI BL, GLOR BL, SAV BL, and sBL: AKATA BL, BL 30, BL 31) and Non-BL cell lines (HL 60, AR LCL, KJ LCL, SU-DHL-4, SU-DHL-5 and SU-DHL-6) were provided by cancer research centre and school of biosciences- university of Birmingham and were STR profiled. Cells were run with electrophoreses assay as detailed in materials and methods. 30 µg protein of each sample were loaded to the gels. (**A**) Western blot immunoblotting images for C-MYC and β-actin with corresponding stack bar chart represents the different C-MYC protein sizes as total protein levels among all BL cell lines and AML (HL 60). (**B**) Western blot immunoblotting images for C-MYC and β-actin with corresponding stack bar chart represents the different C-MYC protein sizes as total protein levels among all non-BL cell lines (AML, LCLs and DLBCL) and NAMALWA BL. Data analysis was performed using one way ANOVA. SAV BL analysis was performed using unpaired T-test. *P<0.05.*

4.2 C-MYC protein levels are selectively regulated by zinc acetate in BL cell lines.

It was investigated whether the loss of cell viability in all BL cell lines when exposed to 100 μM zinc acetate is associated with downregulation of C-MYC protein levels. Since only one BL cell line was tested in Sirinian *et al* study and since they used a different zinc salt, we wished to investigate the effect of zinc acetate on C-MYC levels on a larger panel of BL and non-BL cell lines (Sirinian *et al.*, 2003).

C-MYC protein levels was investigated in BL cell lines (eBL: NAMALWA, SAV, GLOR and sBL: BL 30, BL 31,) and LCLs (AR and KJ) treated with 0, 50 and 100 μM zinc acetate for 1, 2 and 6 hours using western blotting as referred in Figure 4.3 (A and C). As shown, 100 μM zinc acetate noticeably and selectively reduced C-MYC protein in all BL cell lines after 6 hours, but not in LCLs. Although there is an increase in C-MYC signal seen with 50 μM zinc in eBL NAMALWA and sBL BL30 after 6 hours, other repeats showed no differences.

Since zinc-mediated death of BL cells occurs later than 6 hours, we also looked at C-MYC protein at 24 hours for the same panel of cell lines treated with 0, 50 and 100 μM zinc acetate in a separate experiment. Figure 4.3 (B and D) shows representative BL and non-BL western blot images respectively at 24 hours. As can be seen the western images for untreated cells at 24 hours appear different to those from the cells harvested at 6 hours. The reason for this is unclear but due to supply issues with the C-MYC antibody, a different batch of antibody was used and may explain the difference. Nonetheless, C-MYC bands were detected at the same molecular weights. Importantly, a complete loss of all C-MYC bands was seen after 24 hours in BL cells treated with 100 μM zinc acetate but not the LCLs. The complete loss of all bands by 24 hours in 100 μM zinc acetate treated BL cells suggests that quantifying total C-MYC may be more informative than focusing on the distribution between the bands. Indeed, quantifying loss of signal in one of the bands cannot distinguish between loss of protein per se or movement of protein from one post transcriptionally altered state to another.

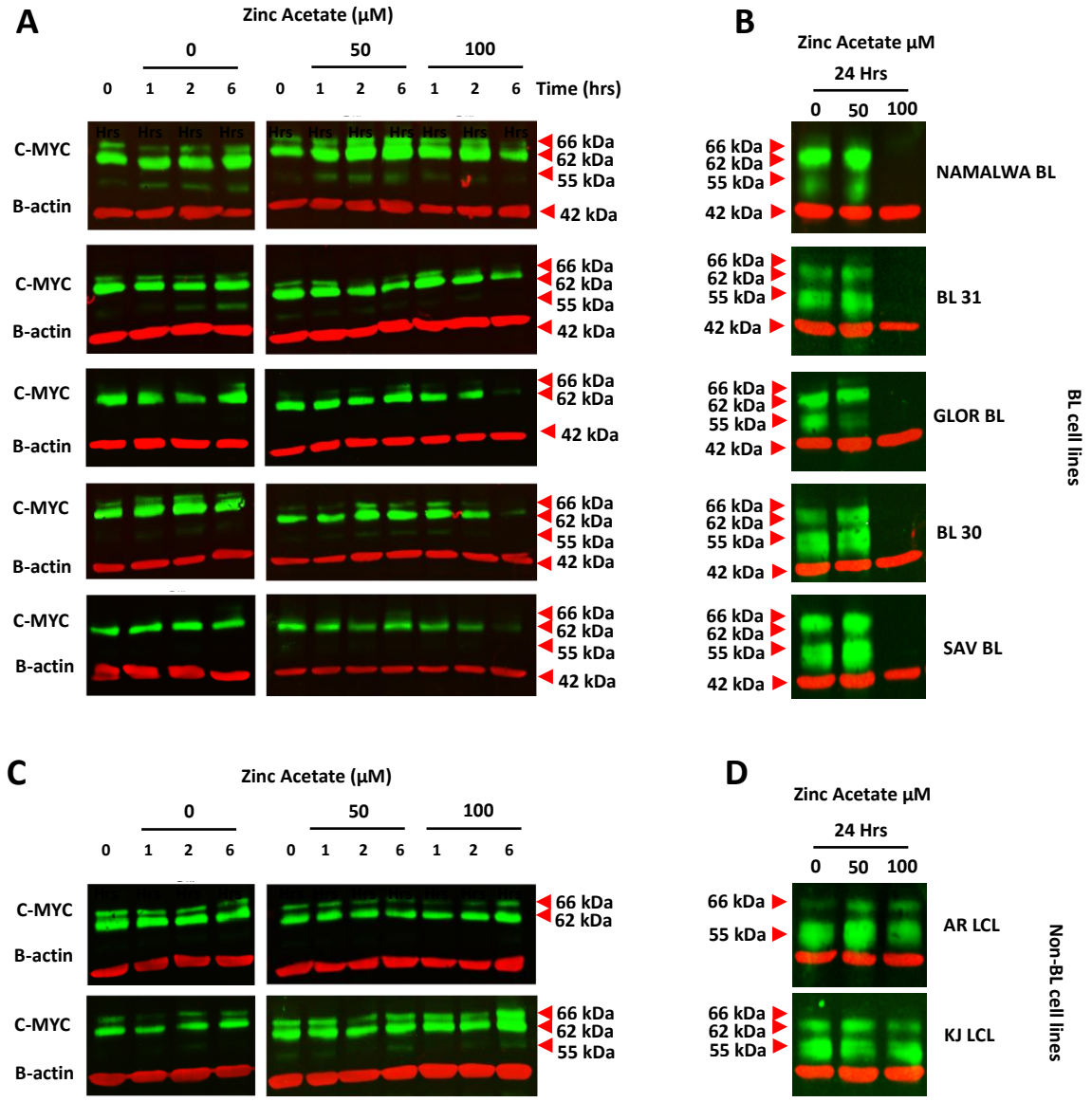

Figure 4. 3 The effect of zinc acetate on C-MYC protein levels in BL and non-BL cell lines*. Different BL cell lines (sBL: BL 31, BL 30, and eBL: SAV BL, NAMALWA BL and GLOR BL) (A and B) and non-BL (AR LCL and KJ LCL) (C and D) were seeded at 5x10^5 cells/mL and treated with 0, 50 and 100 µM zinc acetate 1, 2,6 (A) and 24 hours (B). 30 µg of total protein was electrophoresed and C-MYC and β-actin protein levels assessed by western blot as shown from N=3 experiments.*

Total C-MYC protein levels were measured and densitometry values were normalised with β-actin and meaned from N=3 experiments. The data in Figure 4.4 shows that in each of the BL cell lines tested there is a 50% or greater loss of total C-MYC protein by 6 hours in response to 100 µM zinc and a complete loss of

detectable C-MYC by 24 hours. In contrast, there was sustained C-MYC expression when the same cells were treated with 50 µM zinc acetate. The loss of C-MYC expression in response to 100 µM zinc acetate was not recapitulated in either KJ or AR LCLs.

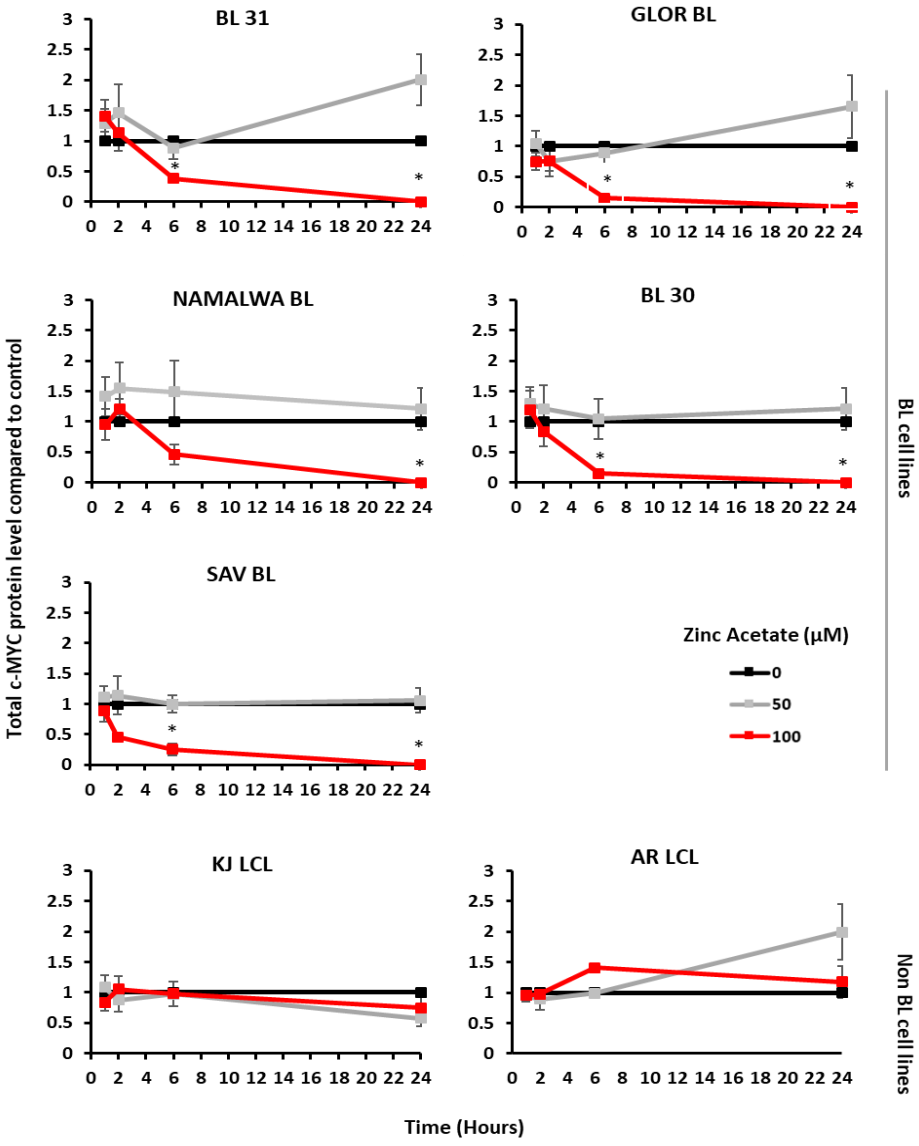

Figure 4. 4 Measuring C-MYC protein levels in zinc acetate treated BL and non-BL cell lines. *Different BL cell lines (sBL: BL 31, BL 30, and eBL: SAV BL, NAMALWA BL, GLOR BL) and LCLs (AR LCL and KJ LCL). Total C-MYC values from Figure 3.16 were normalised to β-actin and compared to the control at the same time point normalised value of total C-MYC and treated with. Data analysis was performed using two-way ANOVA. * P<0.05.*

Besides LCLs, we also measured the impact of zinc acetate on C-MYC expression in DLBCL (SU-DHL-4, SU-DHL-5 and SU-DHL-6) and AML (HL 60) cell lines. Cells were treated with 0, 50 and 100 µM zinc acetate for 6 and 24 hours. Samples were collected and analysed using western blotting. As presented in Figure 4.5, 6 and 24 hours total C-MYC protein levels were meaned from N=3 experiment are represented for each cell line with its representative western blotting images. The data show that like LCL cells but in contrast to BL cells, C-MYC was not reduced in DLBCL and AML cell lines after 6 or 24 hours with any of zinc acetate doses when compared to its control at the same time.

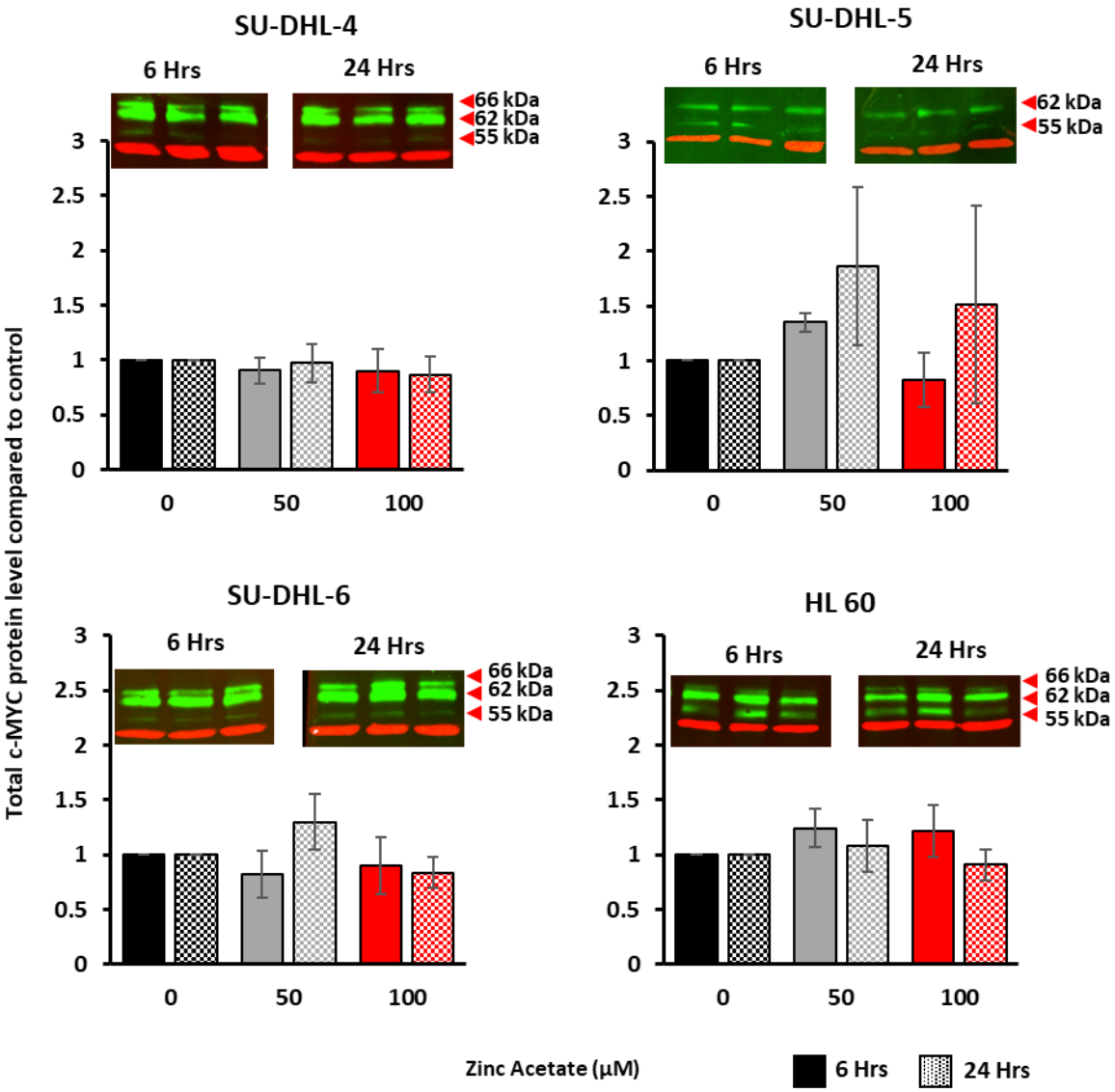

Figure 4. 5 C-MYC protein level in zinc acetate treated non-BL cell lines DLBCLs (SU-DHL-4, SU-DHL-5 and SU-DHL-6) and AML (HL 60) after 6 and 24 hours*. Different Non-BL cell lines (SU-DHL-4, SU-DHL-5, SU-DHL-6 and HL 60) were seeded at 5x106 cells/mL and treated with 0, 50 and 100 µM zinc at for 6 and 24 hours. Western blotting was performed and total C-MYC was compared to control. Data analysis was performed using one way ANOVA. * P<0.05.*

4.3 The modulation of C-MYC gene expression in BL cell lines as a response to zinc acetate.

Having observed the significant and selective reduction of C-MYC protein in BL in response to 100 µM zinc acetate, it was useful to understand the mechanism of zinc in reducing C-MYC protein levels by investigating whether zinc interferes with *C-MYC* expression at the transcriptional level. Figure 4.6 shows *C-MYC* qrt-PCR analysis for BL and non-BL LCL cell lines when treated with 0, 50 and 100 µM zinc acetate for 6 hours. Mean *C-MYC* mRNA levels from N=4 experiments as a fold change compared to 0 µM zinc acetate for each cell line was measured. In BL cell lines, *C-MYC* mRNA was reduced in response to zinc acetate after 6 hours in sBL: BL 30, BL31 and eBL: GLOR, SAV, NAMALWA BL. This reduction was significant in all BL cell lines with 100 µM while 50 µM zinc acetate showed no significant effects. These findings correlate with the loss of C-MYC protein in the same cells after 6 hours with 100 µM zinc acetate. mRNA data for non-BL cells (KJ, JT and AR LCL) showed no reduction in *C-MYC* mRNA which again correlates with sustained C-MYC protein expression in these cell lines.

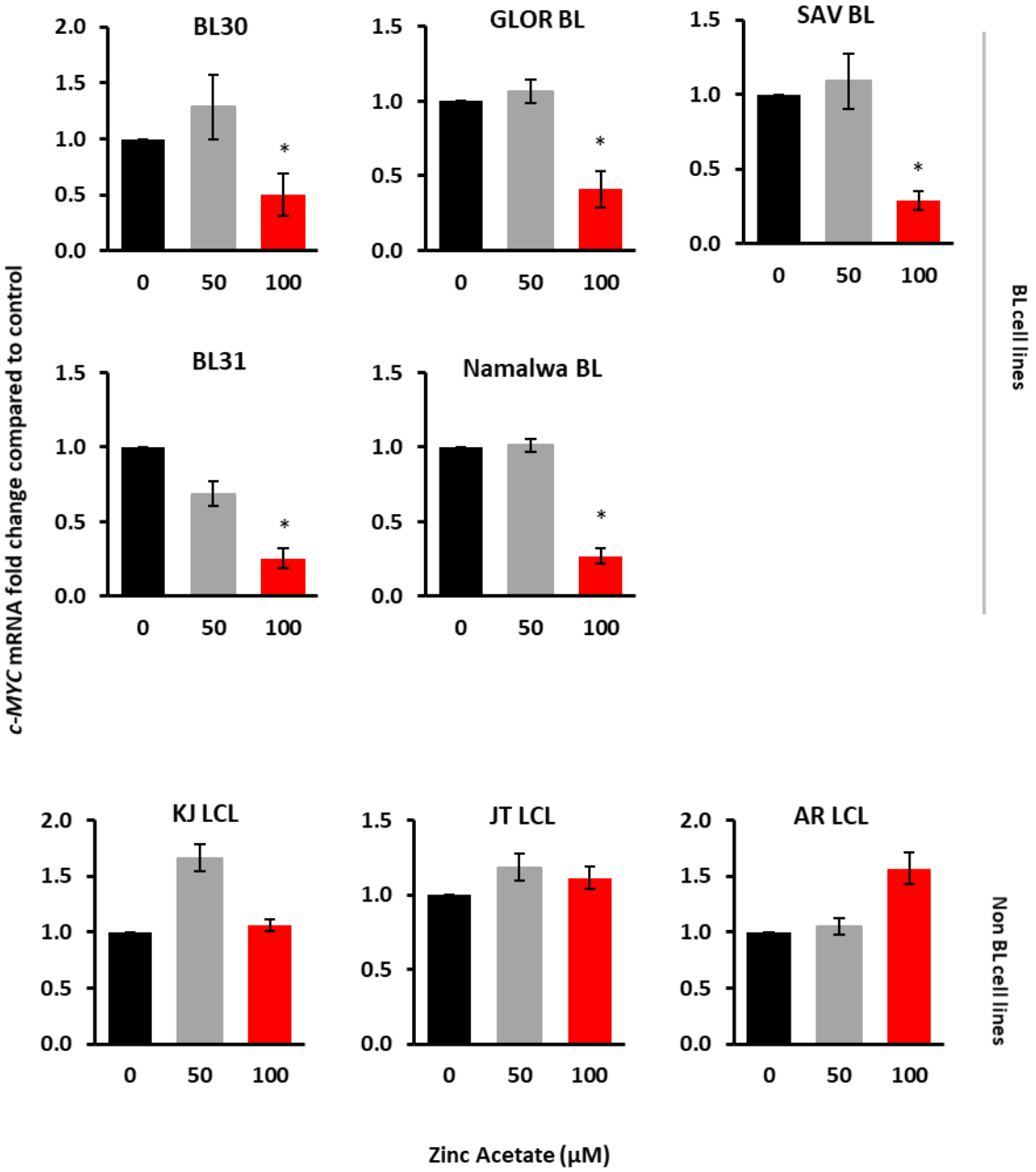

Figure 4. 6 C-MYC mRNA levels in BL and non-BL cell after 6 hours treatment with zinc acetate*. BL cell lines (eBL: SAV, GLOR and NAMALWA and sBL: BL 30, BL 31), LCL cell line (AR LCL, KJ LCL and JT LCL) were seeded at 5x10^5 cells/mL and treated with 0, 50 and 100 µM zinc acetate for 6 hours. Total RNA was extracted and cDNA synthesized as mentioned in material and methods. Data represent C-MYC mRNA fold changes levels compared to control untreated sample. Data analysis was performed using one- way ANOVA. BL 30 data analysis was performed using unpaired T-test.P<0.05.*

4.4 Does zinc acetate also regulate other genes translocated to Ig gene in non-BL cancer cell lines?

One rationale for the regulation of *C-MYC* by zinc acetate in BL but not the other cell lines is that zinc acetate targets transcription of the translocated *C-MYC* in BL via the Ig enhancer. In BL, the translocated *C-MYC* allele is regulated via Ig enhancer elements; intronic element (Eμ) or 3' regulatory (HS1-2, HS3 and HS4) which upregulate *C-MYC* expression. Given that C-MYC mRNA was decreased preferentially in BL cells in response to zinc, It was hypothesized that zinc may regulate *C-MYC* expression by affecting the Ig gene enhancer regions. To study this hypothesis, the DLBCL cell line SU-DHL-4 was used which has translocation of *BCL2* gene to the IgH locus t(14;18) which makes *BCL2* under the control of enhancer elements activity (Bertram et al., 2021).

SU-DHL-4 and SU-DHL-5 (which does not have t(14;18)) were seeded at $5x10^5$ cells/mL and treated with 50 and 100 μM zinc acetate for 6 and 24 hours. Figure 4.7 shows representative BCL-2 western blot images and meaned densitometry data analysis of N=3 experiments. The data demonstrate that BCL-2 protein levels in SU-DHL-4 and SU-DHL-5 were unchanged with either 50 or 100 μM zinc acetate after 6 and 24 hours.

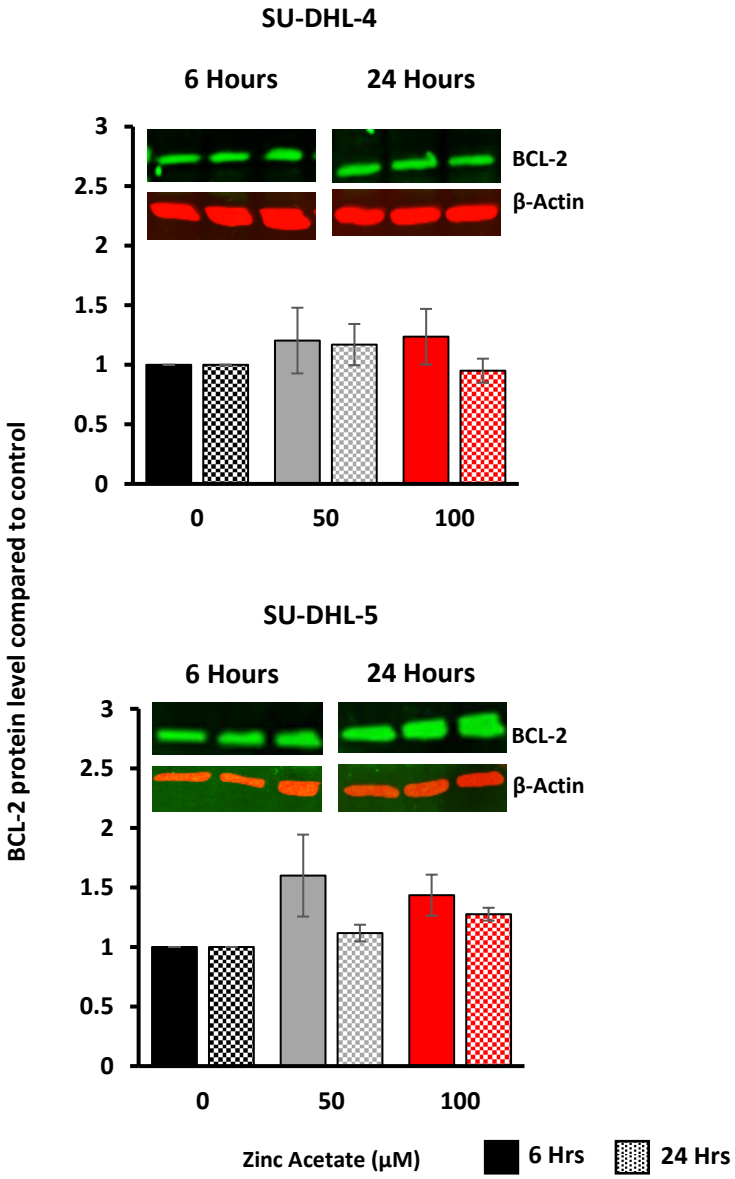

Figure 4. 7 BCL-2 protein level in zinc acetate treated non-BL cell lines DLBCLs (SU-DHL-4 and SU-DHL-5) after 6 and 24 hours. *DLBCL cell lines (SU-DHL-4 and SU-DHL-5) were seeded at 5x10^5 cells/mL and treated with 0, 50 and 100 μM zinc at for 6 and 24 hours. Western blotting was performed to measure BCL-2 and housekeeping β-actin. Data analysis was performed using one way ANOVA. * P<0.05.*

4.5 Discussion and summary.

Given the importance of *C-MYC* as a master regulator of hundreds of genes involved in metabolism, cell cycle and proliferation, it is not surprising that *C-MYC* deregulation is a common genetic feature observed in more than 60% including breast cancer, colorectal carcinoma, esophageal cancer, ovarian cancer and lymphoma (Duffy et al., 2021). In BL, the C-MYC translocation to *IgH* (14q32) or *IgK* (2p12) or lambda *IgL* (22q11) is the hallmark genetic mutation found in all BLs. Despite the involvement of C-MYC in so many cancers, no therapies are clinically available that directly target *C-MYC*.

In 2003, Sirinian et al demonstrated that zinc reduced C-MYC protein levels in the BL cell lines RAJI (Sirinian *et al.*, 2003). Thus, given the very selective activity of zinc against BL cell and the similar dose responses observed, we postulated that zinc targets *C-MYC* in BL cells. Before testing the effect of zinc, baseline C-MYC protein levels were established. As expected, western blotting for C-MYC demonstrated that BL cell lines (eBL: RAJI, GLOR, SAV, and sBL: AKATA, BL 30, BL 31) possessed higher levels of C-MYC protein compared to LCLs (AR and KJ) which were used as B cell controls. Although DLBCL (SU-DHL-4, SU- DHL-5 and SU-DHL-6) arise similarly from GC B cells, C-MYC protein levels were shown to be higher in the BL cell lines. In addition, the AML cell line HL60 is characterized by *C-MYC* gene amplification but still had lower levels when compared to BL cell lines.

The effect of zinc treatment on *C-MYC* was then tested in BL cell lines (eBL: NAMALWA, SAV, GLOR, and sBL: BL 30, BL 31) and compared to non-BL cells; LCL (AR and KJ), DLBCL (SU-DHL-4, SU-DHL-5 and SU-DHL-6) and AML (HL 60). C-MYC protein levels in BL cell lines were decreased significantly with 100 µM zinc within 6 hrs. Protein reduction was seen firstly in the highest molecular weight band (66 kDa). C-MYC phosphorylation at S62 causes protein activation and stabilization while phosphorylation at both of S62 and T58 are the key regulator in C-MYC degradation to initiate protein ubiquitination (Cao *et al.*, 2011). Data from antibody websites and the molecular weight indicates that the 66 kDa band (represents the S62 and T58 biphosphorylated form of C-MYC. Extended exposure to zinc treatment for 24 hours showed complete protein loss with no effects seen with 50

µM as shown by western blot analysis. No changes in C-MYC protein levels were observed in all of the non-BL cell lines tested. These findings strongly correlate with the cell viability data in chapter 3 where 100 µM zinc induced killing of BL cell lines, but not the non-BL cell lines tested. This is in agreement with the published data of Sirinian et al (Sirinian *et al.*, 2003).

Zinc-mediated decreases in C-MYC protein can occur at either the transcriptional or the post-transcriptional levels. In order to determine whether zinc modulates *C-MYC* at the transcriptional level, qRT-PCR was performed on BL and non-BL cell lines treated with zinc. qRT-PCR showed that within 6 hours, 100 µM zinc significantly decreased C-MYC mRNA levels in tested BL cell lines (eBL; SAV, NAMALWA, GLOR and sBL; BL 30 and BL 31) with no changes seen in non-BL LCL (AR, KJ and JT). Given the half-life of C-MYC mRNA (30-60 mins), and C-MYC protein (20-30 mins), decreases in mRNA will result in rapid decreases in the protein (Gregory and Hann, 2000, Lemm *et al.*, 2002).

C-MYC breakpoints in BL cells are divided into 3 different types: class I where breakpoint is located within *C-MYC* first exon, class II or head-to-head translocation with 5' end of *C-MYC* gene is localized to the 5' end of *Ig* and class III with distant *C-MYC* breakpoint (Nguyen *et al.*, 2017). Upon translocation, intronic and distant 3' enhancer elements of Ig gene are responsible for inducing *C-MYC* constitutive overexpression in BL cells.

In a similar scenario, follicular lymphoma cells and some of DLBCL cells possess a *BCL2/ IgH* translocation of t(14;18) (q32;q21) putting the expression of the apoptosis regulator gene *BCL2* under the control of constitutive *IgH* enhancer elements activity. The DLBCL SU-DHL-4 cell line is characterized by the presence of *BCL2/IgH* translocation (Xiang *et al.*, 2011, Kasprzyk *et al.*, 2021, Salam *et al.*, 2020). *BCL2* breakpoints fall majorly within major breakpoint region (MBR) and less commonly within minor cluster region (MCR). This makes this line a reasonable comparator model of translocations involving the *IgH* locus. Thus, the effect of zinc on BCL-2 protein levels was tested in SU-DHL-4 cells and compared with the other DLBCL cell line SU-DHL-5 which has no *BCL2/IgH* translocation. Western blot analysis showed that neither 50 nor 100 µM doses of zinc induced BCL-2 protein

reduction in either DLBCL cell lines after 6 and 24 hrs. These data would suggest that zinc is not reducing *C-MYC* expression by working directly on the *IgH* enhancer elements. In translating this finding to BL cells, this finding suggests that zinc is targeting *C-MYC* in BL in a different mechanism.

It is worth noting that whilst all the BL cell lines and SU-DHL-4 have translocation involving the Ig enhancer regions, the exact breakpoint and translocation site is not known in all the BL cell lines. Future work would sequence the breakpoint regions and identify exactly which transcription factor binding sites are conserved or different between the cell lines. It is known that the transcription factors Yin-Yang 1 (YY1) and nuclear factor kappa B (NF-κB) are key regulators of Ig enhancer activity (Kanda et al., 2000, Gordon et al., 2003). Thus, further experiments would aim to look at the activity of these and whether zinc affects their activity.

Given that zinc reduced C-MYC protein and mRNA levels and this directly correlated with cell death, there may be a link to the Ig enhancer regions. We next attempted to rescue the BL cells by overexpressing *C-MYC* from the EF1A promotor using stable transfections. These experiments would give further insight as to how zinc is switching off *C-MYC* in the BL cells.

CHAPTER FIVE

OVEREXPRESSION OF C-MYC IN BL CELL LINES

5 Overexpression of *C-MYC* in BL cell lines

Previous experiments observed the role of zinc in reducing deregulated C-MYC protein and mRNA levels in BL cell lines which correlated with reduced cell viability. This suggests that *C-MYC* is an important regulator in maintaining BL cell proliferation and viability. In order to determine the role of *C-MYC* downregulation in BL cell death, we aimed to overexpress *C-MYC* stably from an independent promoter. Cellular *C-MYC* overexpression experiments have been conducted in several studies to understand the different cellular pathways of *C-MYC*. Responses were dependent on cell type and levels of *C-MYC* overexpression. Ectopic expression of *C-MYC* increased the rate of cell proliferation in mesenchymal stromal cells (Melnik *et al.*, 2019). In contrast, the human fibrosarcoma cell line (HT1080), human colon carcinoma and lymphoblastoid (LCL) cells were shown to be sensitive to increased levels of *C-MYC* expression and presented with increased rate of apoptosis (You *et al.*, 2002a, Cutrona *et al.*, 1995, Donzelli *et al.*, 1999). Thus, controlled *C-MYC* expression is crucial for preventing irregular protein activity in the cells. To understand the process of *C-MYC* in protecting BL cell lines against zinc, it was hypothesized in this thesis that restoring C-MYC protein levels via ectopic *C-MYC* gene expression would protect BL cells and overcome zinc mediated killing of BL cells.

In this chapter, stable transfection of *C-MYC* in eBL cell lines; NAMALWA and RAJI was performed using the transposon-transposase PiggyBac system which involves the cutting and inserting of exogenous *C-MYC* to random TTAA sites in the host genome. The human elongation factor 1 α (EF1A) promoter was used to maintain constitutive co-expression of *C-MYC* and *EGFP,* the latter helps in confirming successful transfection and gene expression. EF1A promoter activity is regulated via several proteins as referred by their binding sites including; activator protein 1 (AP-1), Nuclear factor kappa B (NF-kB), signal transducers and activator of transcription (Stat), GATA-binding factor (GATA) and specificity protein 1 (Sp1) (Wakabayashi-Ito and Nagata, 1994, Wang *et al.*, 2017). Using similar techniques described in the previous chapters, the effect of zinc at 50 and 100 µM on cell viability and on C-MYC levels was investigated on stably transfected C-MYC BL cell lines.

5.1 The transfection of BL cells with *C-MYC* PiggyBac transposon victor

The previous observations have shown that 100µM zinc acetate reduces BL cell viability in association with down regulating C-MYC RNA and protein levels. To attempt to understand the link between loss of C-MYC and cell killing, exogenous C-MYC overexpression in BL was used to determine whether higher levels of C-MYC can render the cells more tolerant to zinc acetate. Although different BL cell lines were transfected, only eBL: NAMALWA and RAJI were able to survive and grow following the transfection while other BL cells died and could not survive.

As shown in Figure 5.1, VB200623-1116ump vector was used to transfect different BL cell lines aimed to overexpress *C-MYC* (transfection details are provided in materials and methods). The plasmid design includes 5' and 3' ITR sites that are recognized by transposase during gene cutting and pasting process. *C-MYC* gene which is fused with EGFP via small peptide (T2A) that undergoes a self-cleavage during translation. Expression was controlled by eukaryotic translation elongation factor 1 α (EF1A) which is continuously activated. In parallel, BL cells were transfected with EGFP plasmid as a transfection control set of cells.

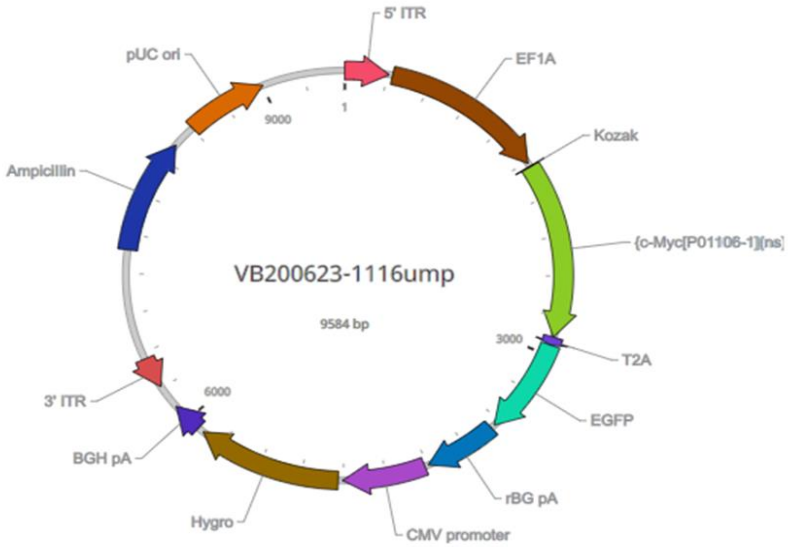

Figure 5. 1 Structure of VB200623-1116ump vector*. C-MYC (c-Myc) expression is controlled via constitutive human elongation factor 1 α (EF1A) promoter and fused with enhanced green fluorescent protein (EGFP) by self-cleaved peptide (T2A). Two ITR transposase cutting sites 5' and 3' which determine plasmid insertion sites into host chromosomes. (5' ITR) piggyBac 5' inverted terminal repeat, (Kozak) Kozak translation initiation sequence, (T2A) Self-cleaving 2A peptide, (rBG pA) Rabbit beta globin polyadenylation signal, (CMV Promoter) Human cytomegalovirus immediate early enhancer/promoter, (Hygro) Hygromycin resistance gene, (BGH pA) Bovine growth hormone polyadenylation signal, (3' ITR) piggyBac 3' inverted terminal repeat, (Ampicillin) Ampicillin resistance gene, (pUC ori) pUC origin of replication.*

Flow cytometry was used to measure EGFP signals from WT, EGFP (transfection control cells) and C-MYC cells as a measure of the efficacy of transfection (Figure 5.2).

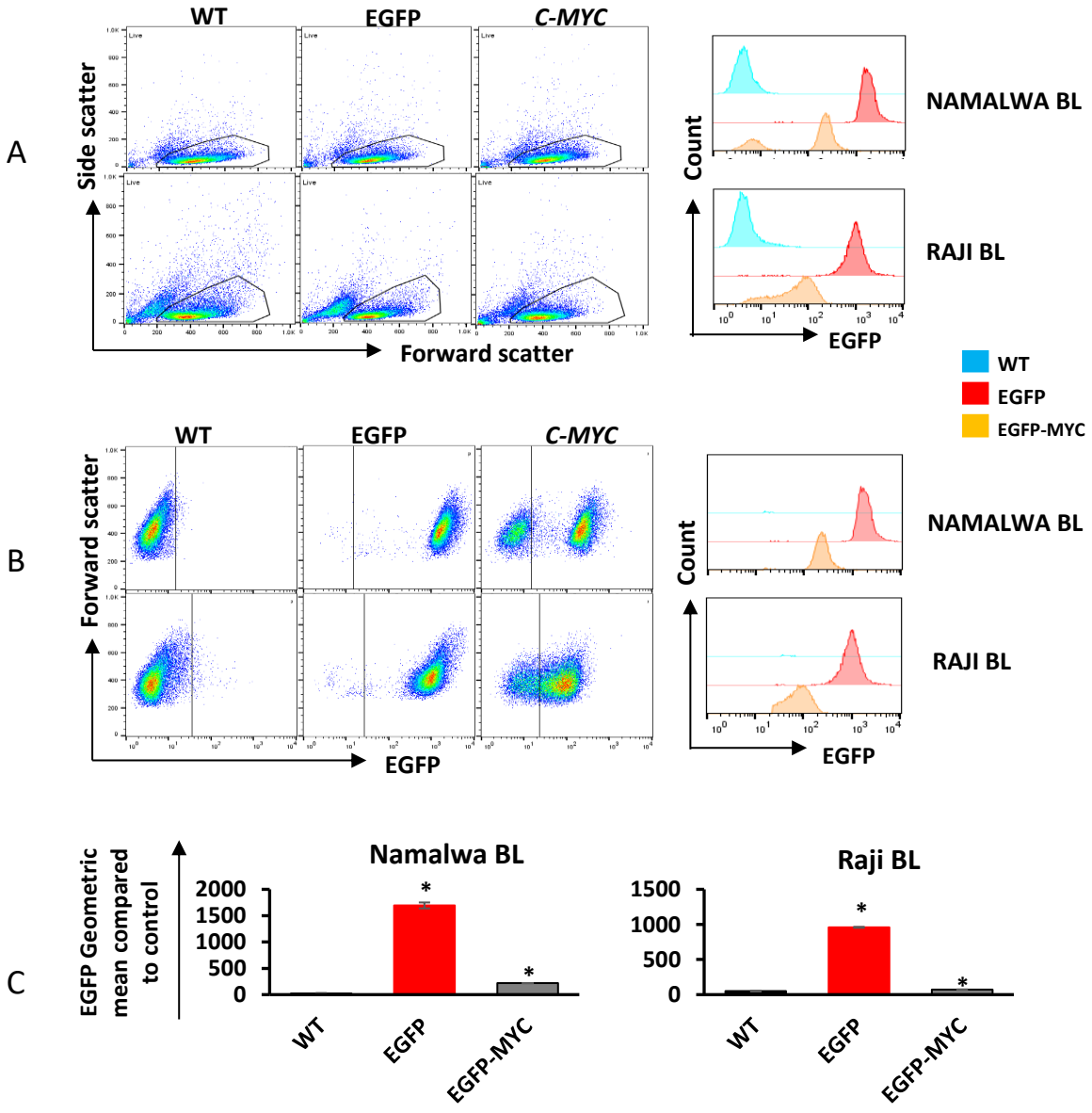

Figure 5. 2 Measuring EGFP signals in WT, EGFP and C-MYC transfected BL cell line*. eBL cell lines (RAJI and NAMALWA BL) were transfected with EGFP and C-MYC plasmids. EGFP signals were measured from exponentially growing cells using flow cytometry. (A) Side and forward scatter dot plot for NAMALWA (top) and RAJI (bottom) BL with EGFP histogram corresponding to viable gate. (B) NAMALWA (top) and RAJI (bottom) BL flow cytometry dot plot representing live gate forward scatter against EGFP+ with corresponding histogram. (C) EGFP geometric mean analysis for NAMALWA and RAJI BL cells. Analysis was performed using one way ANOVA. * P<0.05.*

As seen in the Figure 5.2 A, the live cells of both eBL: NAMALWA and RAJI BL cells showed positive EGFP signals as represented by the representative EGFP histogram for both C-MYC and EGFP cells compared to WT. Figure 5.2 B shows dot plots of forward scatter against EGFP for the live cell gate as shown in Figure 5.2 A. As shown in Figure 5.2 B & C EGFP cells had stronger EGFP expression compared to C-MYC cells. Furthermore C-MYC eBL: NAMALWA cultures contained a distinct sub-population of EGFP weak/negative cells and *C-MYC* eBL: RAJI cells also had a less bright EGFP positive population that appears as part of the same cloud in the dot plots and a shoulder in the histogram. Figure 5.2 (C) shows meaned EGFP signal levels from N=3 experiments.

5.2 BL cell lines growth kinetic profile as a response to *C-MYC* overexpression.

In order to investigate the effects of exogenous *C-MYC* expression on BL cell growth eBL: RAJI and NAMALWA BL (WT, *EGFP* and *C-MYC*) were seeded at $5x10^5$ cells/mL and counted at days 2, 4 and 6 using flow cytometry. Figure 5.3 shows the cumulative cell count for eBL: RAJI and NAMALWA BL (WT, EGFP and C-MYC) for N=3 experiments.

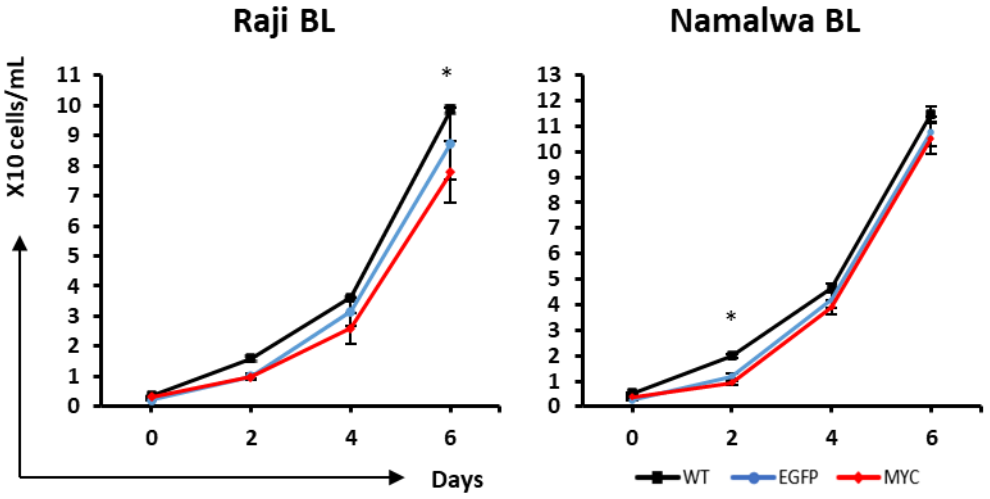

Figure 5. 3 Growth kinetics of eBL: NAMALWA and RAJI WT, EGFP and C-MYC overexpressing cells lines*. WT, EGFP and C-MYC overexpression eBL cell lines NAMALWA and RAJI were seeded at $5x10^5$ cells/mL. Cell count was measured using flow cytometry on days 2, 4, and 6. Data analysed using two way ANOVA. * P<0.05.*

As shown in Figure 5.3 transfection of BL cells and expression of either EGFP or C-MYC had little impact on the growth rate of the cells. Statistical analysis showed that in RAJI BL, *C-MYC* cells grew slightly slower when compared to WT whilst in eBL: NAMALWA BL, a difference was seen at day 2 when compared to WT for the same set of cells.

5.3 Measuring C-MYC protein levels in *C-MYC* overexpressed BL cell lines.

Having confirmed by *EGFP* expression that both eBL: NAMALWA and RAJI BL cell lines had been stably transfected, their level of *C-MYC* expression was compared to WT type cells. Total protein was extracted from exponentially growing NAMALWA and RAJI BL (WT, EGFP and C-MYC) As shown in Figure 5.4, both WT and transfected NAMALWA and RAJI BL showed the different C-MYC bands previously observed. Noticeably, *C-MYC* cells also showed a faint upper C-MYC band that is most likely related to uncleaved C-MYC that remains fused with EGFP. Meaned densitometry analysis for of N=4 experiments for total C-MYC signals were calculated as a ratio to β-actin as referred for each sample. Data in Figure 5.4 shows that unexpectedly there was no statistical difference in total C-MYC protein levels in *C-MYC* transfected cells compared to either EGFP or WT NAMALWA and RAJI BL cells.

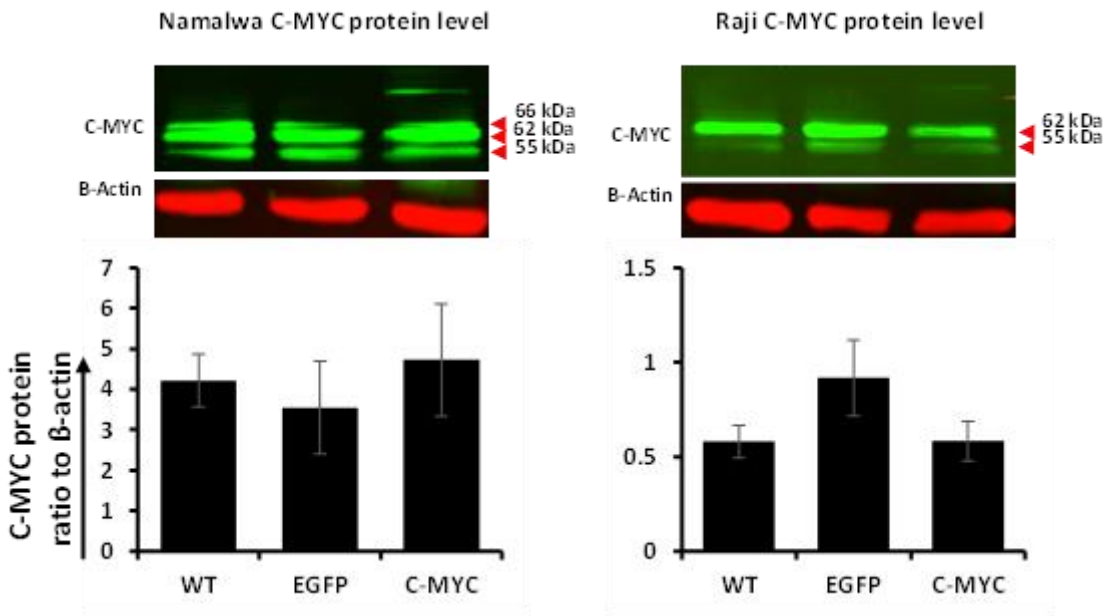

Figure 5. 4 Western blotting for total C-MYC protein levels in WT, EGFP and C-MYC transfected BL cells eBL: NAMALWA and RAJI*. Both eBL: NAMALWA and RAJI BL cells (WT, EGFP and C-MYC transfected cells) were grown exponentially at 0.5x10^6 cells/mL. Total protein extraction and 30 µg of protein loaded into SDS-PAGE electrophoresis. Total C-MYC calculated as a ratio to β-actin. Bar charts represent data analysis as referred in western blot images. Data analysis was performed using one way ANOVA.*

5.4 Assessing zinc acetate sensitivity of transfected BL cell lines.

Despite that no difference was seen in basal C-MYC protein levels in WT and *C-MYC* transfected BL cell lines, the effect of zinc acetate against *C-MYC* transfected BL cells was tested. eBL: NAMALWA and RAJI BL cells were seeded at 5x10^5 cells/mL and treated with 0 and 100 µM zinc acetate for 6 and 24 hours. After 6 hours, total protein was extracted and analysed by western blotting. Data are represented in Figure 5.5 which illustrates representative western blot images for both of eBL: NAMALWA and RAJI WT, *EGFP* and *C-MYC* cells and meaned densitometry data from N=3 experiments. Figure 5.5 shows that as expected 100µM zinc acetate reduced overall C-MYC protein after 6 hours in both eBL: NAMALWA and RAJI BL WT and *EGFP* cells. In contrast, exposure of eBL: NAMALWA or RAJI *C-MYC* cells to 100µM zinc acetate for 6 hours did not lower overall *C-MYC* expression. This observation suggests that although in unchallenged conditions there was no overexpression of *C-MYC* in eBL: NAMALWA and RAJI *C-MYC* cells,

that *C-MYC* expression from the transfected plasmid was occurring and became evident at 6 hours exposure to 100 µM hours when endogenous *C-MYC* expression was lowered. This has further implications for interpreting the unchallenged *C-MYC* expression data and may indicate that BL cells regulate *C-MYC* expression in complex ways.

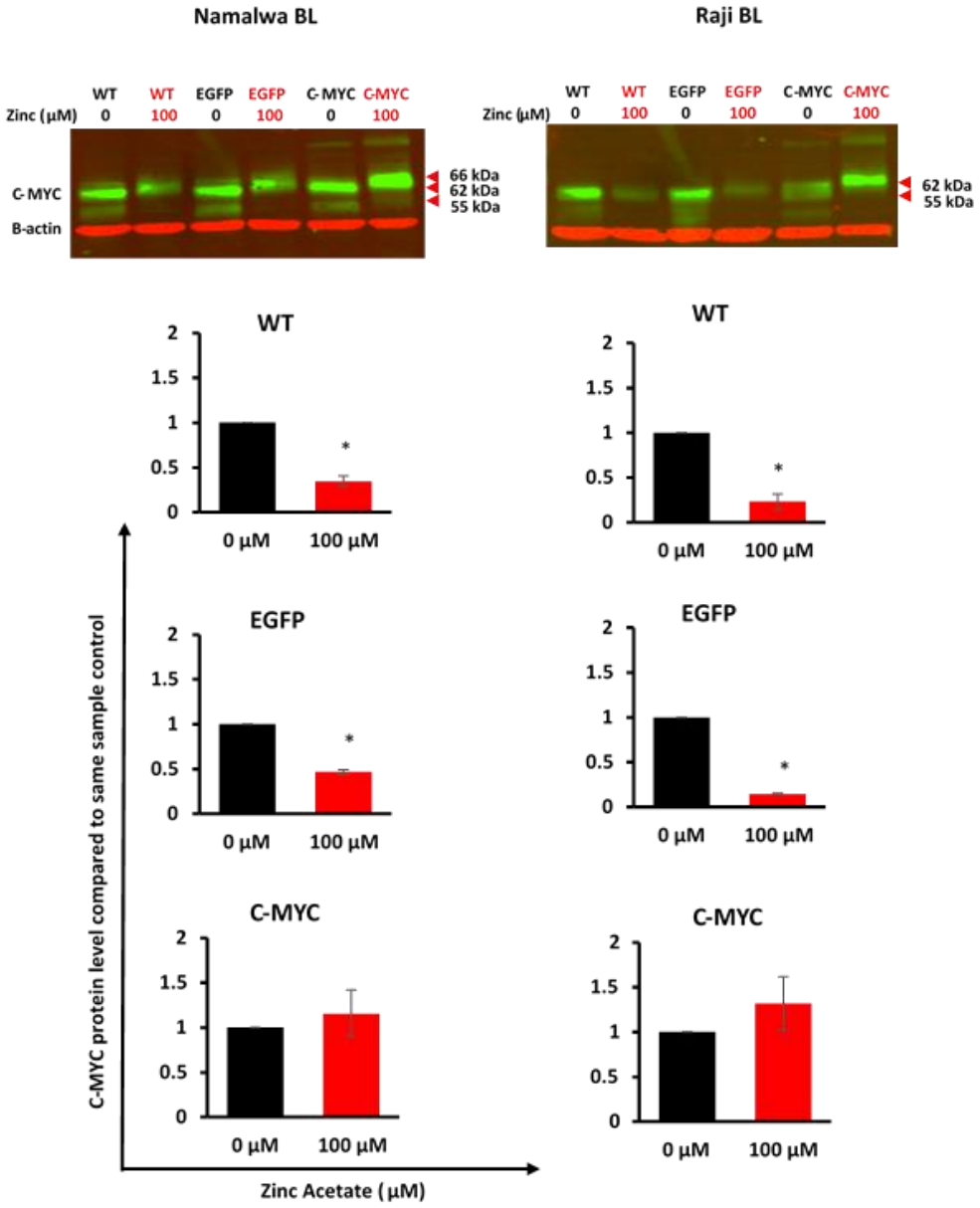

Figure 5. 5 Measurement of C-MYC protein in C-MYC transfected BL cell line eBL: NAMALWA and RAJI BL after 6 hours of treating with zinc acetate. *eBL: NAMALWA and RAJI BL cell lines (WT, EGFP and C-MYC) were seeded at 5x10^{5}cells/mL. Cells were treated with 0 and 100 µM zinc acetate for 6 hours. Western blot images represent C-MYC protein levels in (WT, EGFP and C-MYC) eBL: NAMALWA and RAJI BL cell lines with corresponding control cells. Data analysis showed total C-MYC protein levels in zinc acetate treated BL cell line compared to same cell control. Data analysis was performed using one way ANOVA. * P<0.05.*

We next investigated *C-MYC* expression by transfectants after 24 hours exposure to zinc acetate. Figure 5.6 shows representative western blots and meaned densitometry data from N=3 experiments. As expected, both WT and *EGFP* transfection control cells showed a significant reduction at C-MYC protein levels after 24 hours following zinc acetate treatment at 100 µM. However, importantly at 24 hours eBL: NAMALWA and RAJI C-MYC cells also showed dramatic loss of C-MYC protein indicating that exogenous expressed *C-MYC* was also sensitive to prolonged exposure to 100µM zinc acetate.

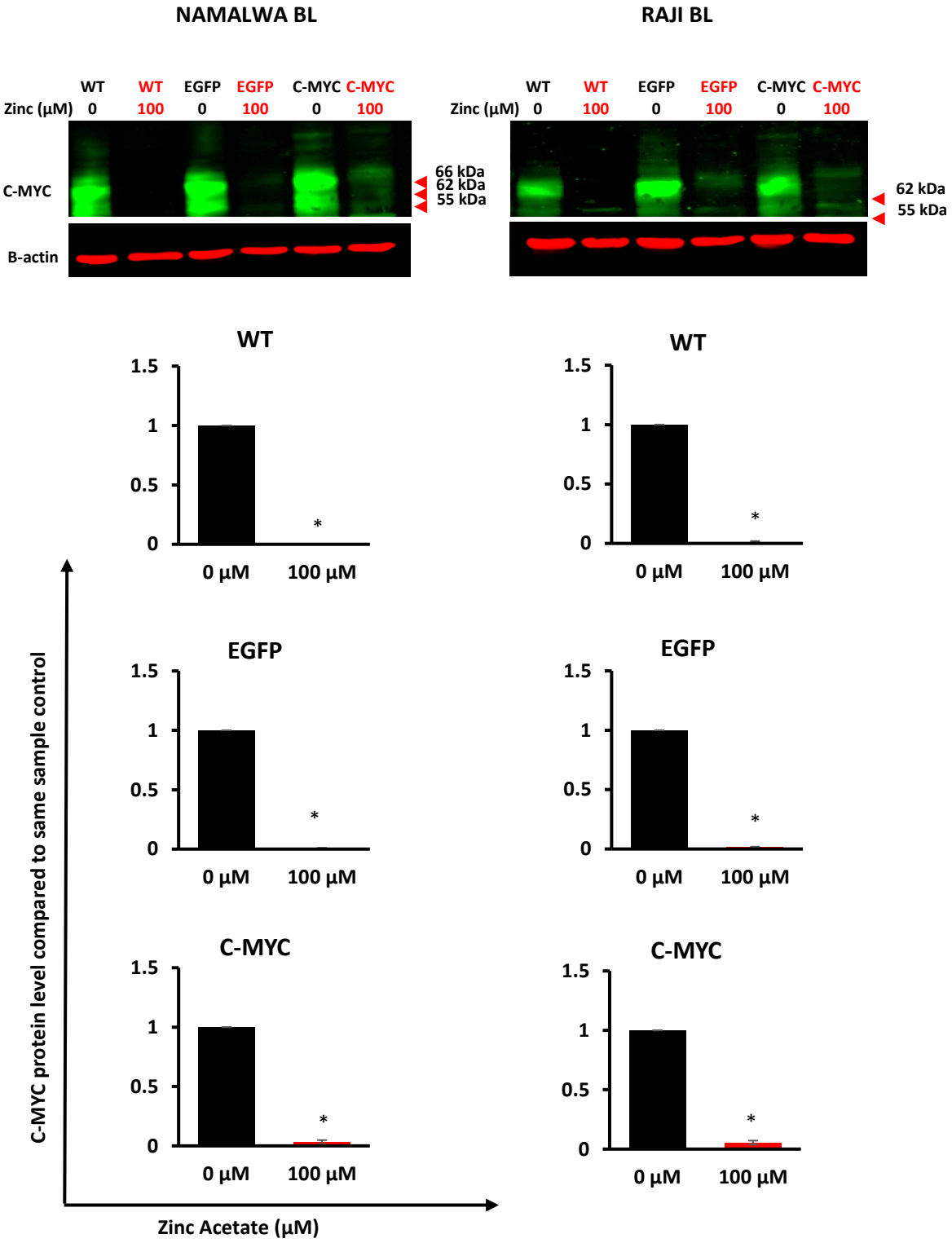

Figure 5. 6 24 hours measurement of C-MYC protein in C-MYC transfected eBL cell line NAMALWA and RAJI BL after 24 hours of treating with zinc acetate*. eBL: NAMALWA and RAJI BL cell lines (WT, EGFP and C-MYC) were grown exponentially and seeded at 5x10^{5}cells/mL. Cells were treated with 0 and 100 µM zinc acetate for 6 hours. Western blot images represent C-MYC protein levels in (WT, EGFP and C-MYC) eBL: NAMALWA and RAJI BL cell lines with corresponding control cells. Data analysis showed total C-MYC protein levels in zinc acetate treated BL cell line compared to same cell control. Data analysis was performed using one way ANOVA. * P<0.05.*

5.5 Impact of exogenous *C-MYC* overexpression on the cell viability response of BL cell lines to zinc acetate.

Thus, zinc acetate caused C-MYC protein reduction in the cells BL cell line after 24 hours. This pattern was not only seen in WT BL cells lines, but this was also seen in both BL cell lines which were transfected with *C-MYC*. To link that with cell viability, WT, *EGFP* and *C-MYC* transfected BL cells were tested against zinc acetate to evaluate their viability for different time points by flow cytometry assay.

Exponentially growing eBL: NAMALWA and RAJI BL (WT, *EGFP* and *C-MYC*) cells were seeded at $5x10^5$ cells/mL and treated with 0 and 100 µM zinc acetate for 24, 48 and 72 hours to investigate whether overexpressing *C-MYC* in BL cells can encounter zinc effect against BL cell viability and rescue the cells. At each time point, cells were collected and cell numbers determined using flow cytometry. Analysis of N=3 experiments are shown in Figure 5.7.

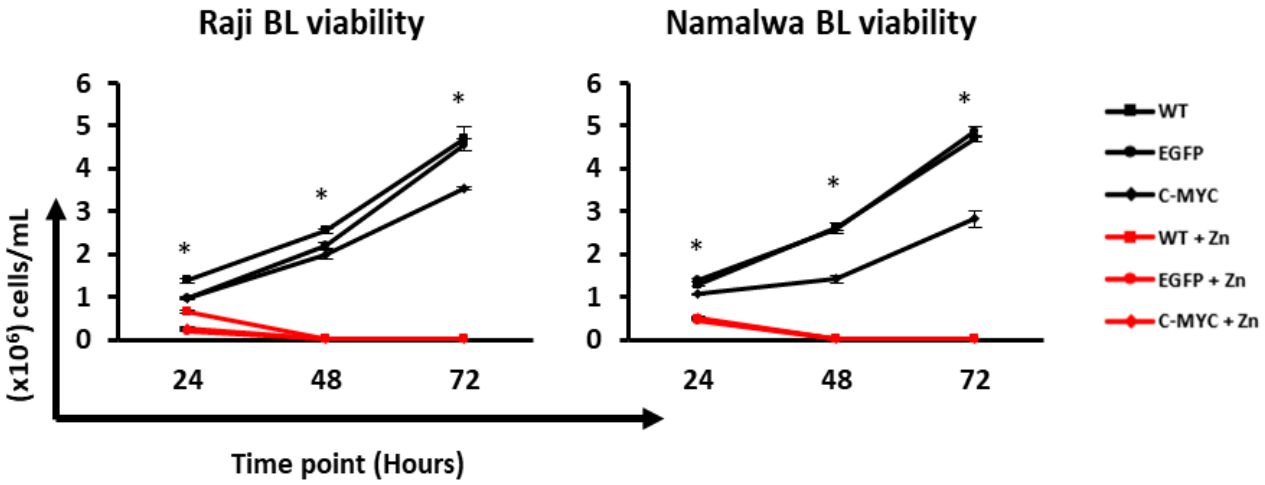

Figure 5. 7 eBL NAMALWA and RAJI BL (WT, EGFP and C-MYC) cells viability as a response to zinc acetate*. WT, EGFP and C-MYC overexpression eBL cell lines (NAMALWA and RAJI) were seeded at $5x10^5$ cells/mL and treated with zinc acetate with 0 and 100 µM for 24, 48 and 72 hours. Viability was measured using flow cytometry. Analysis represents cumulative cell count at 24, 48 and 72 hours. Data analysed using two way ANOVA. * P<0.05.*

The analysis shows that BL cells viability was reduced in eBL: NAMALWA and RAJI BL including WT, *EGFP* and *C-MYC* as a response to zinc acetate at 100 µM. Significant reduction in cell viability was seen after 24 hours of zinc acetate

treatment with near total loss of cell viability at 72 hours. This pattern was not only seen in WT cell lines but also occurred in *C-MYC* and *EGFP* transfection control cell lines. Therefore, no rescue of the cells was seen in exogenous *C-MYC* overexpression eBL: NAMALWA and RAJI BL cell lines.

5.6 Discussion and summary.

In this thesis, it was shown that 100 µM zinc acetate reduced the viability of BL cell lines via activation of apoptosis and reduced C-MYC protein and mRNA levels. In this chapter, it was hypothesized that if zinc reduces C-MYC protein levels by regulating transcription then overexpressing *C-MYC* from an independent promoter in BL cell lines might protect the BL cells against zinc mediated killing. The PiggyBac transposon-transposase system was used to stably transfect multiple sBL and eBL cell lines with exogenous *C-MYC* that is linked with reporter *EGFP* via the self-cleavage peptide T2A. The constitutive promoter EF1A was used to ensure constitutive *C-MYC* expression in transfected cells.

There are several promoters that can be used in research to express genes of interest in transfected cells including; Simian virus 40 (SV40) and Rous sarcoma virus (RSV) and Cytomegalovirus promoter (CMV) which is one of the commonly used promoters. Although CMV is known to induce efficient gene expression, the promoter activity is likely to be repressed due to DNA methylation process. Using constitutively active promoter of mammalian origin like EF1A can produce a stronger gene expression that is more resistant to promoter silencing (Wang *et al.*, 2017). In eukaryotic cells, the EF1A enzyme which facilitates the transferring of aminoacyl tRNA to ribosomes was found to be abundantly expressed in all types of mammalian cells (Kim *et al.*, 1990, Ejiri and biochemistry, 2002). The EF1A promoter possesses binding sites for regulatory proteins including; TATA box, CAAT box, NF-kB, Ap1 and Sp1 (Wang *et al.*, 2017, Ferreira *et al.*, 2011, Wakabayashi-Ito and Nagata, 1994). Thus, in transfected cells, *C-MYC* expression should be driven from both the EF1A promoter in addition to the endogenous promoter. The *C-MYC* promoter is activated via signal transducing pathways and involves APC, (wnt/β-catenin) and TCF proteins. Similar to the EF1A promoter, Ig enhancer elements have been

shown to contain NF-kB binding site motifs. Octamer transcription factor (OCT-1 and OCT-2), YY1, E47 and E12 were also found to bind Ig enhancer region that regulate Ig transcription process (Sepulveda *et al.*, 2004, Eckhardt, 1992).

In this chapter, transfection was successfully achieved in NAMALWA and RAJI eBL cell lines as represented by flow cytometry analysis for EGFP after transfection and selection with hygromycin. Interestingly, it was noted that *C-MYC* transfected BL cell lines had variable *EGFP* expression with cells with either high and low EGFP signals. Importantly, the *EGFP* expression should correlates with *C-MYC* expression since they are co-expressed, thus it would be fair to assume that there were also high and low levels of *C-MYC*. Thus, we would predict that the transfected cells would be expressing *C-MYC* from both the endogenous promoters (WT and translocated) and also from the plasmid EF1A promoter.

Previous studies have shown that ectopic constitutive expression of *C-MYC* has different cellular impacts where it can increase proliferation rate or increase apoptosis events and proliferation arrest depending upon the cell types used (Sears, 2004, De Alboran *et al.*, 2001, Felsher *et al.*, 2000). The ability to obtain a successful *C-MYC* transfection in only 2 BL cell lines could be due to increased sensitivity of the other BL cells or the inability to tolerate increased high *C-MYC* expression which possibly induced cell death (Mitchell et al., 2000). These data would further support that different cell types and cell lines have different thresholds for *C-MYC* overexpression. Different cell lines responses were mentioned upon *C-MYC* overexpression and transfection in rat and mouse quiescent fibroblasts, Chinese hamster ovary (CHO-K1) and human small cell Lung cancer cells (SCLC) (De Alboran *et al.*, 2001, Palmieri *et al.*, 1983, Ifandi and Al-Rubeai, 2003, Johnson *et al.*, 1986). As discussed earlier, *C-MYC* is involved in multiple cellular pathways including; cellular proliferation, apoptosis and differentiation. It was reported that mesenchymal cells transfected with *C-MYC* had 2.5 fold increase of their proliferation rate compared to the control group. In addition, the effect of *C-MYC* overexpressing in mesenchymal cells induced cellular differentiation delay as measured via Alizarin Red S stain (Melnik et al., 2019). Dental pulp stem cells (DPSCs) transfected with *C-MYC* were shown to have increased rates of apoptosis when compared to the control cells which was suggested to be related to increased

caspase 3 activity (Dissanayaka *et al.*, 2017). In LCLs, ectopic expression of *C-MYC* increased apoptosis rate in transfected cells. Apoptosis rate was measured via flow cytometry analysis of PI stained cells and was found to be sensitive to fetal calf serum concentration (Cutrona *et al.*, 1995). Additionally, Human fetal lung (WI38) fibroblast cells transfected with *C-MYC* showed high apoptosis rates that presented with the inhibition of cell cycle modulator P21 protein (Mitchell and El-Deiry, 1999).

In our experiments, WT and transfected eBL cell lines were analyzed for growth kinetic for 6 days using flow cytometry analysis. These data showed that all cells were growing and proliferating over the time at approximately the same rate and there was no major difference between WT, *EGFP* or *C-MYC* transfectants cells. Although successful transfection was achieved with both the *EGFP* control plasmid and the *EGFP-C-MYC* plasmid as defined by EGFP expression, western blot showed that total C-MYC protein levels were not significantly different in *C-MYC* transfected cell lines as compared to the WT and *EGFP* control cells. This would imply that there is an upper threshold or limit of *C-MYC* overexpression in BL cells.

Published data also indicate that the C-MYC protein threshold may vary between different cell types. *C-MYC*-driven tumor cells of transgenic mice and UBR5 ubiquitin ligase depleted cultured Hela cells showed to regulate C-MYC protein levels to a point that cannot be exceeded or subceeded to the oncogenic levels otherwise cells will be programmed to undergo proliferation arrest and apoptosis (Qiao *et al.*, 2019, Shachaf *et al.*, 2008, Ambrosio *et al.*, 2019, Murphy *et al.*, 2008, Lin *et al.*, 2012). This was supported in a different study where RAJI BL western blot images showed no increase in the protein levels upon transfection with *C-MYC* under CMV promoter activity. The BL CA46 cell line also showed no differences in C-MYC protein levels upon transfection with *C-MYC that is also under* CMV *promoter activity and* suggest that there is an upper limit of C-MYC protein levels that cells can tolerate (Bahram *et al.*, 2000, Gregory and Hann, 2000).

The mechanisms by which *C-MYC* transfected cells may regulate exogenous *C-MYC* overexpression is not very clear, but it is suggested to be via downregulating expression of the WT endogenous *C-MYC*, increased mRNA degradation of either exogenous or endogenous *C-MYC* mRNA to balance transcripts pool and post

translational modification to target either endogenous or exogenous protein.

In zinc treatment experiments, both *C-MYC* transfected eBL NAMALWA and RAJI cell lines demonstrated some rescue of C-MYC protein levels after treatment with 100 µM zinc for 6 hrs compared to WT and *EGFP* transfection control cells. However, by 24 hours, almost all the C-MYC protein was gone in all the cell lines, both WT, *EGFP* and *C-MYC* transfected indicating that zinc is targeting C-MYC protein. Similarly to WT and *EGFP* control cells, flow cytometry analysis showed that transfected eBL cell lines; NAMALWA and RAJI showed to lose their viability after 24-48 and 72 hrs and suggesting the inability of *C-MYC* transfection to rescue the cells against zinc.

Both transfected eBL cell lines showed high and low *C-MYC* expression levels as represented by EGFP signals. Neither of these populations were able to rescue BL viability following zinc treatment and it is not shown whether C-MYC protein reduction after 24 hrs is related to low or high EGFP population of transfected cells. It could be that exogenous *C-MYC* gene transcripts are undergoing mRNA degradation, or the exogenous protein is being affected by post translational modification, ubiquitination and T2A cleavage. From the presented data, it is not possible to determine whether the C-MYC protein observed in the *EGFP-C-MYC* positive transfected cells is all coming from the EF1A promoter, and the endogenous promoter has been silenced, or whether both promoters have moderated expression levels. A targeted qRT-PCR using primers specific to the transfected transcript would answer this. Further work could also use an epitope tagged exogenous *C-MYC* that can be distinguished from the endogenous form by selective antibodies and would thus allow us to determine which protein is being moderated to give a tolerable maximal *C-MYC* expression.

Since attempts to overexpress *C-MYC* did not rescue the BL cells from zinc-mediated killing, in the following chapter, another approach for rescuing BL cells was used. Bortezomib, the proteasome inhibitor was used to inhibit C-MYC protein proteasomal degradation and rescue the WT and *EGFP*, *C-MYC* transfected BL cells.

CHAPTER SIX

DOES PROTEOSOME INHIBITION PROTECT AGAINST ZINC ACETATE INDUCED C-MYC DEGRADATION IN BL CELL LINES?

6 Does proteosome inhibition protect against zinc acetate induced C-MYC degradation in BL cell lines?

Proteins are regulated at multiple levels by several mechanisms to maintain them at functional levels. Rates of transcription, translation and degradation are crucial cellular processes that control protein levels. Inactive or misfolded proteins undergo degradation which is also an important mechanism in regulating transcription factors that have a higher tendency to rapid degradation mechanism (Cooper, 2000, Majumder and Baumeister, 2020).

The proteasome and ubiquitin system (UPS) is an ATP dependent proteolysis system that plays a major role in protein degradation. The UPS initiates protein degradation by recruiting ubiquitin molecules that bind to targeted proteins and function as signaling mediators for the proteasome 26S complex that is composed of 2 components, the 20S (core) and the 19S subunits to form the cylinder shape (Marshall and Vierstra, 2019, Schweitzer *et al.*, 2016). Colon and breast cancer cells were shown to have increased proteasome activity. The 26S proteasome was proposed to be an interesting target in several cancer therapy studies where inhibiting proteasomal activity in multiple myeloma and mantel cell lymphoma induced increased reactive oxygen species production and higher P53 activation leading to cellular apoptosis (Soave *et al.*, 2017, Ding *et al.*, 2009, Pandit and Gartel, 2011).

Bortezomib, a clinically approved proteasome inhibitor binds reversibly to the proteasomes 20S core causing proteasome 26S inactivity and protein accumulation. In multiple myeloma, the NF-kB inhibitor (IκB) is insufficiently active giving rise to deregulated NF-kB activity that drives cell proliferation. Bortezomib was found to prevent the degradation of IκB leading to suppression of the NF-kB pathway and inhibition of cell proliferation. Additionally, proteasome inhibition induced apoptosis via c-Jun N-terminal protein kinase (JNK) pathway and caspase 3 activation (Fennell *et al.*, 2008, Nunes and Annunziata, 2017, Hideshima *et al.*, 2011).

In this thesis previously, data demonstrated that overexpression of *C-MYC* in eBL cell lines NAMALWA and RAJI could not prevent zinc-induced C-MYC protein

reduction and no cell rescue was achieved. Thus, in this chapter, the ability of bortezomib (BTZ) to inhibit proteasome 26S activity was used to try and prevent C-MYC protein proteasomal degradation. It was hypothesized that inhibition of the proteasome, rescue of C-MYC expression would rescue BL cells against zinc-induced apoptosis. The eBL cell lines NAMALWA and RAJI were used for these experiments as were the *EGFP* and *C-MYC* stably transfected lines.

6.1 Bortezomib (BTZ), treatment leads to accumulation of poly-ubiquitinylated proteins in BL cell lines

It is well established the C-MYC protein has a short half-life of nearly 20 minutes and this is in part mediated by proteasomal degradation (Gregory and Hann, 2000). The drug Bortezomib (BTZ) inhibits proteasome activity, thus we hypothesised that using (BTZ) may prevent C-MYC degradation and stabilize C-MYC protein levels in zinc acetate treated BL cells. Firstly, both eBL: NAMALWA and RAJI BL cell lines were treated with Bortezomib alone at 6, 7, 8, 9 and 10 nM for 6 and 24 hours. Total protein was extracted and run using electrophoresis. Figure 6.1 shows silver staining images (left panel) and western blotting for ubiquitin (right panel).

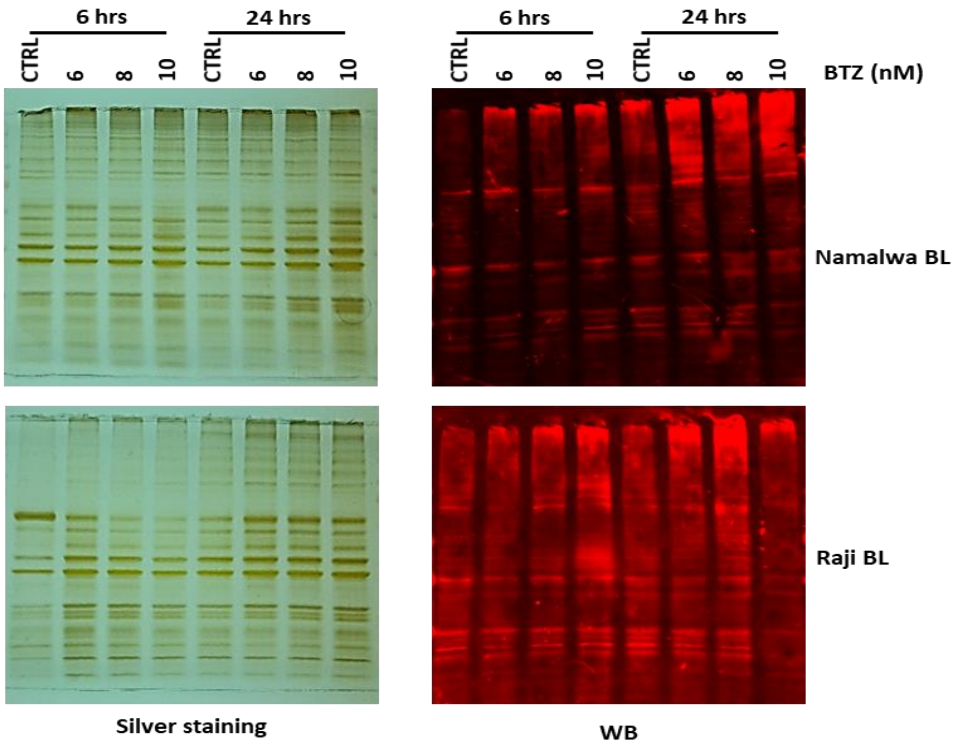

Figure 6. 1 Visualizing total protein levels as a response to Bortezomib in eBL: NAMALWA and RAJI BL cells*. eBL: NAMALWA and RAJI BL cells were seeded at 5x105 cells/mL and treated with BTZ 6, 7, 8, 9 and 10 nM for 6 and 24 hours. Western blotting for ubiquitin and silver staining images are indicated with corresponding bortezomib (BTZ) doses.*

As seen in the figure, both overall protein levels in the cell lines as revealed using silver staining, were not dramatically altered in either BL cell line. Increased levels of higher molecular weight bands were seen in ubiquitin western blots of eBL: NAMALWA BL cells after 24 hours exposure to all concentrations of BTZ. This is consistent with successful proteasome inhibition and the accumulation of poly-ubiquitinated proteins. In RAJI cells there was increased presence of higher molecular weight ubiquitinated protein at 6 hrs in response to 10 nM BTZ and at 24 hrs in response to 6 and 8 nM BTZ.

6.2 The impact of BTZ on BL cell lines in the presence and absence of zinc acetate.

eBL; NAMALWA and RAJI BL cell lines were treated with BTZ at 6, 7, 8, 9 and 10 nM for 6 and 24 hours with and without 100 µM zinc acetate. Cell viability was measured at each time point using flow cytometry.

As shown in Figure 6.2, 6.3 and Figure 6.4, no significant changes in viability were observed after 6 hours in either tested cell lines when treated with BTZ alone or with 100 µM zinc acetate. At 24 hours, BTZ alone did not markedly alter cell viability in eBL: NAMALWA BL cells. In contrast eBL: RAJI cells appeared to show a dose dependent loss of cell viability when treated with BTZ. As expected, there was significant loss of viability in both cells line in response to 100 µM zinc acetate which was not altered in the presence of BTZ at the concentrations used.

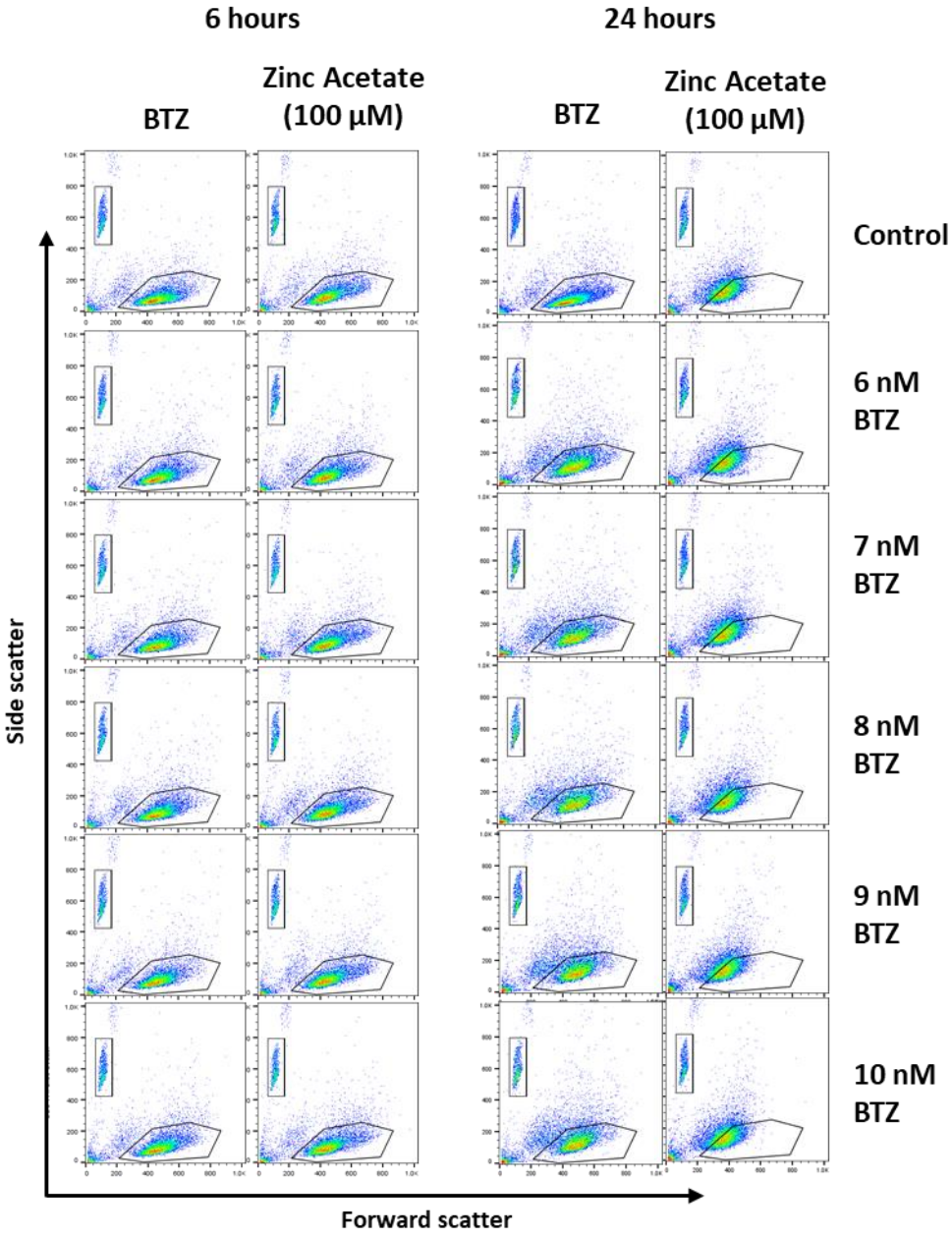

Figure 6. 2 eBL: NAMALWA BL forward and side scatter flow cytometry dot plot treated with BTZ and zinc acetate for 6 and 24 hours. *eBL: NAMALWA BL cell line were grown exponentially and seeded at 5x10^5 cells/mL and treated with 6, 7, 8, 9 and 10 nM BTZ with and without 100 µM zinc acetate. Each time point is presented with only BTZ doses (left column) and BTZ with 100 µM zinc acetate (right column).*

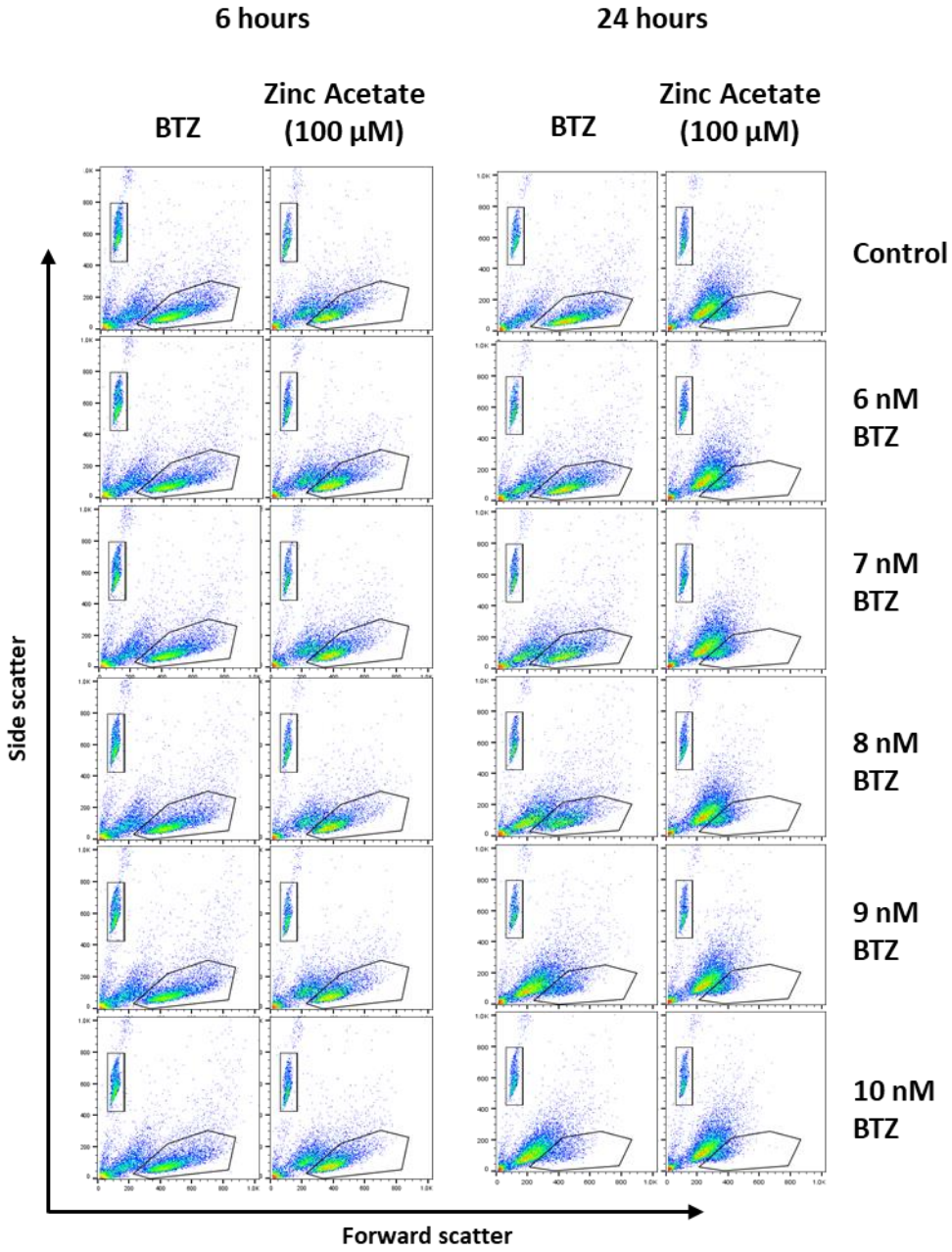

Figure 6. 3 eBL: RAJI BL forward and side scatter flow cytometry dot plot treated with BTZ and zinc acetate for 6 and 24 hours*. eBL: RAJI BL cell line were grown exponentially and seeded at 5x105 cells/mL and treated with 6, 7, 8, 9 and 10 nM BTZ with and without 100 µM zinc acetate. Each time point is presented with only BTZ doses (left column) and BTZ with 100 µM zinc acetate (right column).*

Meaned data for numbers of viable cells /ml for N=3 experiments is shown in Figure 6.4 The viability of both cell lines at 6 hours was unchanged with increasing BTZ concentrations either in the absence or presence of 100 µM zinc acetate. At 24 hours both cell lines demonstrated a dose dependent decrease in cell number in response to BTZ. Combining the data from Figures 6.2, 6.3 and 6.4 would suggest that this dose response in NAMALWA cells constitutes a cytostatic response without major loss of cell viability. Cytostatic cell responses to proteosome inhibitors have been described by others (Suk et al., 2022). In contrast RAJI cells appear to demonstrate a dose dependent loss of cell viability in response to increasing BTZ. As seen in Figures 6.2 and 6.3 no concentrations of BTX enhanced killing by 100 µM zinc acetate.

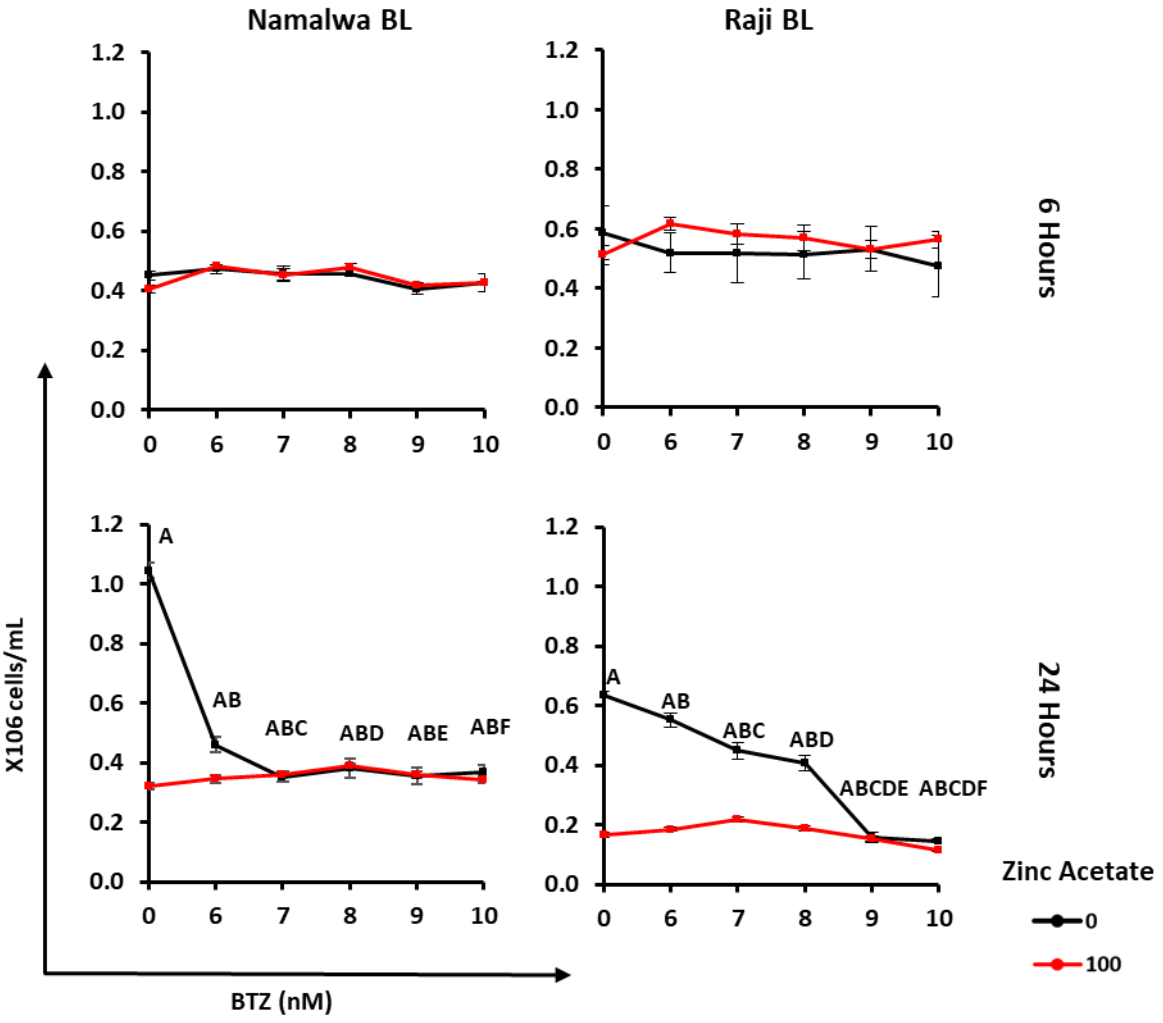

Figure 6. 4 eBL: NAMALWA and RAJI BL cell viability treated with BTZ with and without zinc acetate after 6 and 24 hours*. eBL: NAMALWA and RAJI BL cells were grown exponentially and seeded at 5x10^5 cells/mL and treated with 6, 7, 8, 9 and 10 nM BTZ with and without 100 µM zinc acetate for 6 and 24 hours. Each letter represents BTZ dose in nM (A=0 - B=6 – C=7 – D=8 – E=9 – F=10). Letters represent statistical significance among annotated BTZ doses. Data analysis was performed using one way ANOVA. * P<0.05.*

6.3 Does BTZ prevent C-MYC degradation in zinc acetate treated BL cells?

In order to investigate the impact of BTZ on C-MYC protein levels in BL cell lines, eBL: NAMALWA and RAJI BL cells were seeded and treated with 6, 8 and 10 nM BTZ with and without 100 µM zinc acetate for 6 and 24 hours. Total protein was extracted at each time point and western blotting for C-MYC performed.

Figure 6.5 shows representative C-MYC westerns for eBL: NAMALWA and RAJI BL cells and meaned densitometry data for N=3 experiments at 6 and 24 hours. In the case of eBL: NAMALWA cells, C-MYC levels were significantly elevated at 6 hours in a dose dependent fashion in response to BTZ treatment alone. At 24 hours, C-MYC levels became normalised with no significant changes in BTZ treated cells compared to controls. As seen before, eBL: NAMALWA C-MYC protein levels were decreased by 6 hrs upon exposure to 100 µM zinc acetate and were undetectable by 24 hours in the absence of BTZ. At both 6 and 12 hrs there was a trend towards BTZ treated cells exposed to 100 µM zinc having slightly higher C-MYC levels than cells treated with 100 µM zinc alone. Thus, in eBL: NAMALWA cells BTZ had some protective activity against diminished C-MYC levels in response to zinc but the effect was small, especially at 24 hours.

The result with eBL: RAJI cells was different as in Figure 6.5 B. In eBL: RAJI BL cells, 6 hours treatment with BTZ appeared not to significantly elevate C-MYC in the absence of 100 µM zinc acetate and did not show evidence of countering loss of C-MYC at 6 hrs in response to µM zinc acetate. At 24 hours, C-MYC was undetectable in all BTZ treated cells exposed to µM zinc acetate. Interestingly 24 hrs exposure to 10 nM BTZ appeared to also ablate C-MYC expression in RAJI cells.

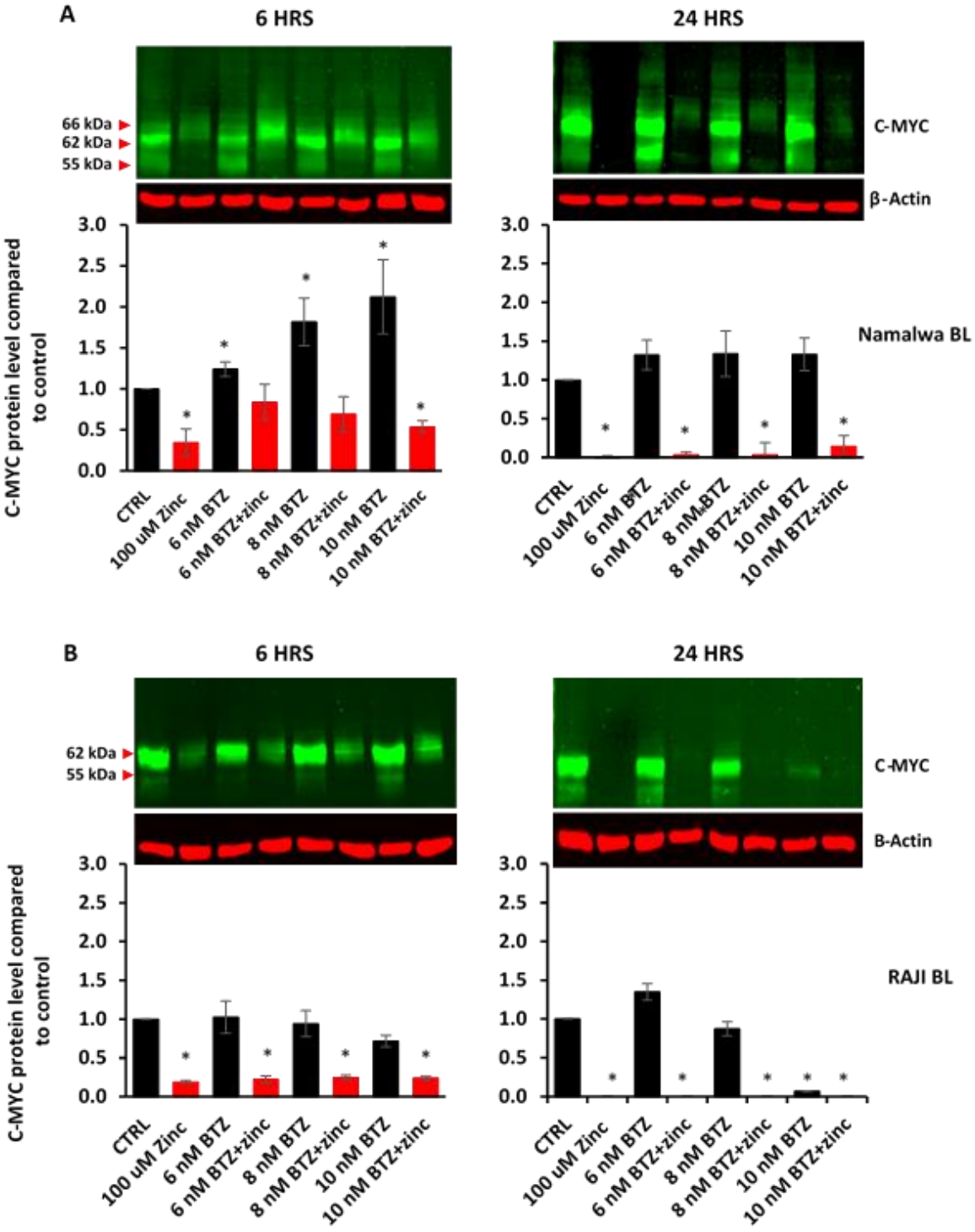

Figure 6. 5 C-MYC protein levels in BTZ treated eBL cell NAMALWA and RAJI with and without 100 µM zinc acetate after 6 and 24 hours. *eBL: NAMALWA and RAJI BL cell lines were seeded at 5x10^5 cells/mL and treated with 6, 8 and 10 nM BTZ with and without 100 µM zinc acetate for 6 and 24 hours. (A) eBL: NAMALWA BL 6 and 24 hours western blot images with analysed data. (B) eBL: RAJI BL 6 and 24 hours western blot images with analysed data. Data analysis for N=3 experiments was performed using unpaired T-test. * P<0.05.*

6.4 Evaluation of cell viability and C-MYC protein levels as a response to BTZ and zinc acetate in BL cells with exogenous *C-MYC* expression

eBL; NAMALWA and RAJI BL transfected with *C-MYC* were tested for further investigations to the role of BTZ in preventing C-MYC reduction and rescuing BL cells against zinc acetate. eBL: NAMALWA and RAJI BL WT, *EGFP* and *C-MYC* cells were treated with 6, 8 and 10 nM BTZ with and without zinc acetate 100 µM for 24 hours. Samples were run using flow cytometry and representative flow cytometry dot plots and meaned data analysis from N=3 experiments for eBL: NAMALWA BL are showed in Figure 6.6.

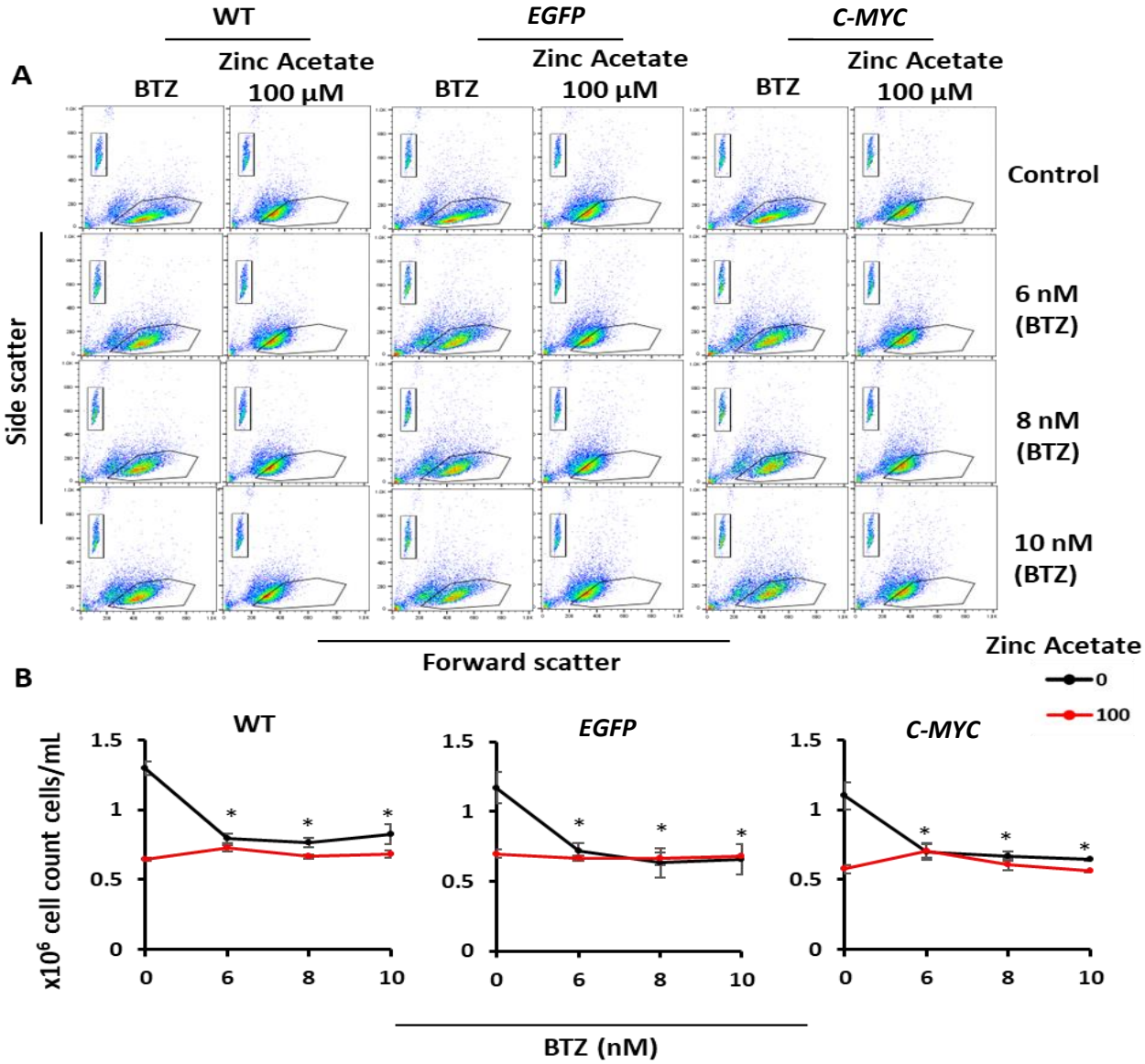

Figure 6. 6 eBL: NAMALWA BL (WT, EGFP and C-MYC) cells viability as a response to BTZ alone or with and without zinc acetate after 24 hours*. Cells were seeded at 5x10^5 cells/mL and treated with 6, 8, and 10 nM BTZ with and without 100 µM zinc acetate for 24 hours. (A) Representative forward and side scatter dot plots for different set of cells. (B) Cell viability meaned data for each set of cells. Analysis was performed using one way ANOVA. * P<0.05.*

Flow cytometry dot plots showed BTZ to cause a small shift in viable cells of all sets compared to control with a clear shift in zinc acetate treated cells. Data analysis of the dot plots showed that C-MYC transfected cells also had the cytostatic effect of BTZ in a dose dependant pattern reducing cell viability significantly compared to control with no recovery seen following adding zinc acetate. eBL: RAJI BL cells (WT, EGF and C-MYC) also were tested with BTZ in a similar way for 24 hours as showed in Figure 6.7.

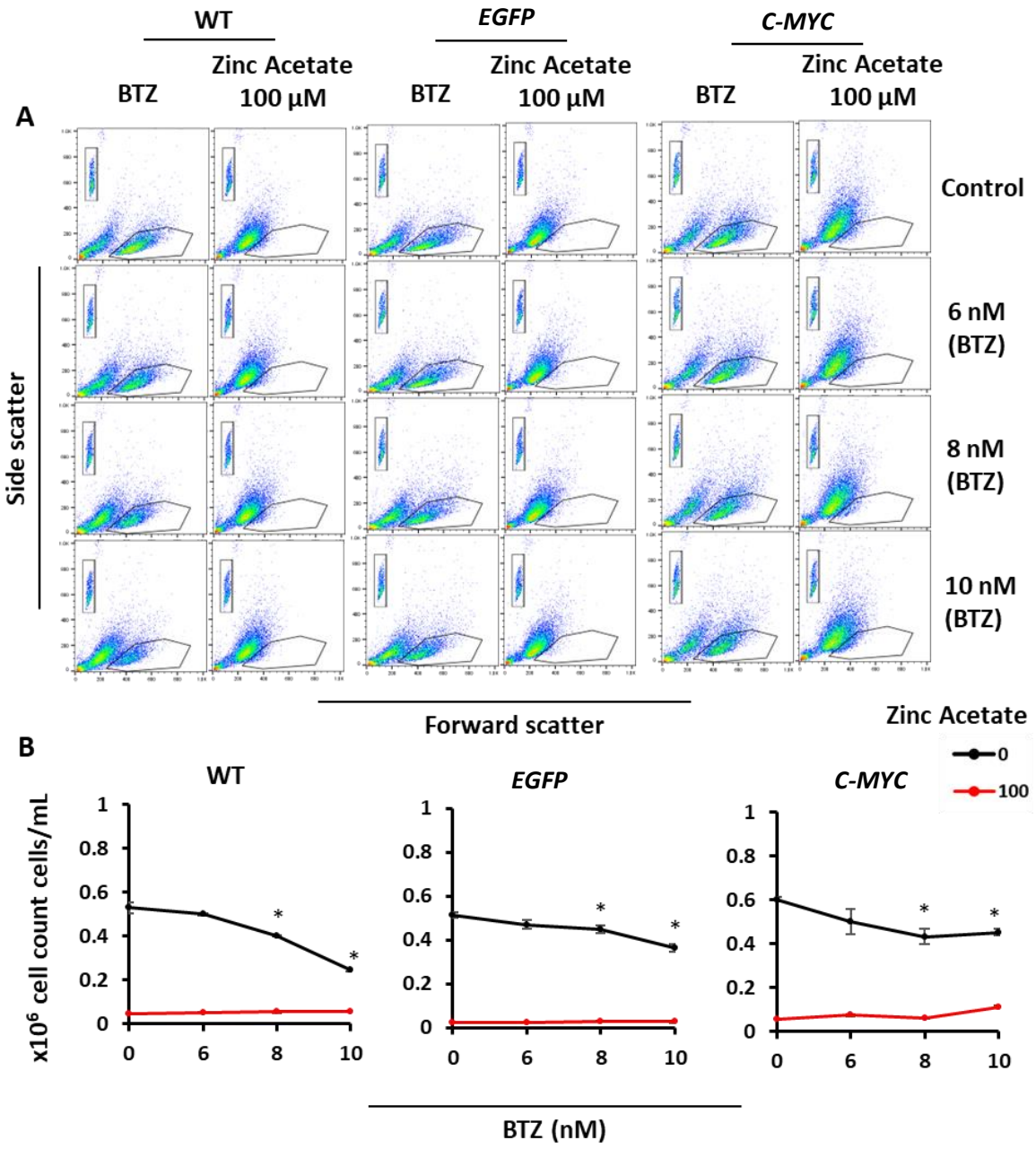

Figure 6. 7 ***eBL: RAJI BL (WT, EGFP and C-MYC) cells viability as a response to BTZ alone or with and without zinc acetate after 24 hours***. *Cells were seeded at 5x10^5 cells/mL and treated with 6, 8, and 10 nM BTZ with and without 100 µM zinc acetate for 24 hours. (A) Representative forward and side scatter dot plots for different set of cells. (B) Cell viability meaned data for each set of cells.* Data analysis for N=3 experiments was *performed using one way ANOVA. * P<0.05.*

As show in the figure, eBL: RAJI WT, *EGFP* and *C-MYC* transfected cells were sensitive to increased doses of BTZ alone when compared to control with no rescued cells following zinc acetate. Data analysis represents meaned data for N=3 experiments.

Total protein was extracted after 24 hours of treatment from eBL: NAMALWA and RAJI BL *C-MYC* cells and run on electrophoresis. Figure 6.8 showed representative western blot images for C-MYC protein for both cell lines with meaned analysis for N=3 experiments. Analysis showed that C-MYC protein was not increased with BTZ doses after 24 hours. However, no protein rescue and significant loss of the protein levels were noticed with 100 µM zinc acetate.

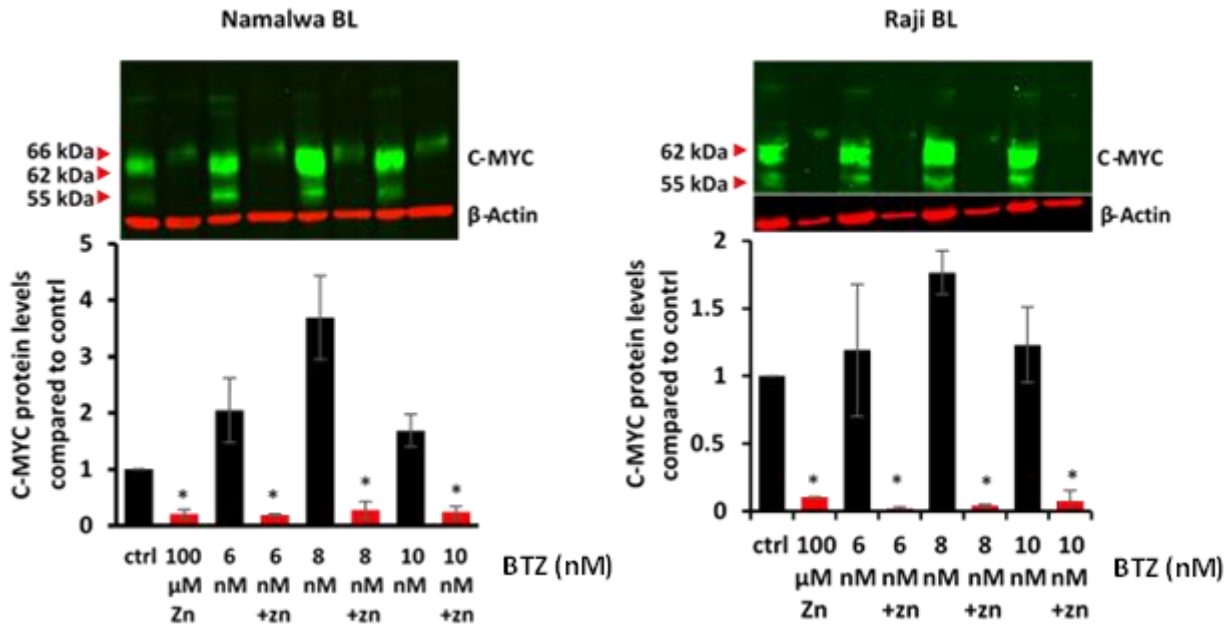

Figure 6. 8 C-MYC protein levels in C-MYC transfected eBL: NAMALWA and RAJI BL treated with BTZ with and without zinc acetate after 24 hours*. C-MYC cells from eBL: NAMALWA and RAJI BL were treated with 6, 8 and 10 nM BTZ with and without zinc acetate for 24 hours and run with western blot to measure C-MYC protein levels. Data analysis was performed using unpaired T-test. * P<0.05.*

6.5 Discussion and summary.

Since 2003, BTZ has been used to treat multiple myeloma patients clinically as the first proteasome inhibitor. The ability of BTZ to inhibit 26S proteasomal protein degradation showed to be effective against multiple myeloma cells where increased accumulation of cell cycle inhibitors proteins, misfolded proteins were correlating with increased apoptosis rate and mitochondrial depolarization process (Robak and Robak, 2019). C-MYC protein is known to be regulated by 26S proteasomal degradation (Gregory *et al.*, 2000).

As demonstrated in this thesis, zinc treatment resulted in decreased C-MYC protein in BL cell lines. Since BL is a C-MYC dependent, it was hypothesized that preventing C-MYC degradation in BL cells might be able to rescue cell viability against zinc treatment. Overexpression of *C-MYC* in BL cell lines by stable transfection showed no cell rescue. In this chapter, an alternative method of stabilizing C-MYC protein was approached. Bortezomib was used to inhibit proteasome activity to prevent C-MYC protein degradation.

Different bortezomib doses were used (6,8 and 10 nM) against eBL NAMALWA and RAJI cell lines to visualize the accumulation of proteins ubiquitination by western blot and silver staining methods. Since BL cells are sensitive to bortezomib, the specified mentioned doses of bortezomib used in this section of the study were to find a suitable bortezomib concentration that inhibit proteasome activity against C-MYC protein and prevent its degradation with minimal cytotoxic effect which would be beneficial to understand C-MYC protein responses. Different studies used higher bortezomib concentrations that range from 16 nM up to 2 µM. Approximately, doses of 5, 8, 10 and 12 nM were also used in different studies to understand the role of bortezomib against BL cells (Zhang *et al.*, 2016, Suk *et al.*, 2015, Zou *et al.*, 2007).

In this chapter, increasing doses of bortezomib resulted in increasing proteins accumulation inside the cells as shown by silver staining, reflecting the inhibition of 26S proteasome activity.

After 24 hrs treatment with BTZ, the NAMALWA eBL cell line showed accumulation

of ubiquitinated proteins which increased with escalating BTZ doses.

Analysis of viability showed that NAMALWA and RAJI cell lines treated with 6, 7, 8, 9 and 10 nM bortezomib demonstrated a dose dependent decrease in cell number after 24 hrs of treatment. Adding 100 µM zinc to bortezomib treated eBL cells showed no cell rescue as represented by flow cytometry analysis. No major changes were seen after 6 hrs of treating the cells with either bortezomib or zinc and bortezomib combination.

In a different study, different doses of bortezomib (4,8,12,16 nM) were found to reduce DAUDI BL cell line viability after 24 hrs when measured by CCK-8 assay (Zhang et al., 2016). It was reported that bortezomib induced apoptosis in eBL cell line RAJI in a mechanism involves the activation of NF-kB and p53 proteins (Yang *et al.*, 2009). In observing C-MYC protein stabilization as a response to bortezomib, western blot analysis was performed on both BL cell line treated with bortezomib with and without zinc. 6 hrs samples showed C-MYC protein was protected against 100 µM zinc in the presence of bortezomib. A slight increased C-MYC protein protection was seen with increased doses of bortezomib (6, 8 and 10 nM). However, this protection was lost after 24 hrs in eBL Raji cell line which was presented with a significant C-MYC protein loss where eBL NAMALWA cell line showed to have a little protected C-MYC protein. Bortezomib alone showed to increase C-MYC total protein levels in both eBL cell lines after 6 hrs with no major changes seen at 24 hrs. However, eBL RAJI cell line showed a significant protein drop after 24 hrs with 10 nM bortezomib alone.

In previous study, C-MYC protein was reported to be targeted by bortezomib (10 nM) significantly after 12 hours (Suk *et al.*, 2015). On the other hands, the heterogenous ribonucleoprotein-K (hnRNP-K) protein is found inside the nucleus which is recruited for DNA repair mechanism, chromatin remodelling and works as a telomere regulator (Inoue *et al.*, 2007). It was found that hnRNP-K is involved in cancer progression and can target *C-MYC* at transcriptional and translational levels (Baber *et al.*, 1999, Notari *et al.*, 2006). Low levels of SUMOylated hnRnP-K protein are relative to low C-MYC protein levels. Interestingly, 10 nM bortezomib was reported to decrease hnRNP-K SUMOylation thus inducing C-MYC degradation in

the BL cell line DAUDI which is also presented with low proliferation rate after 24 hours. DAUDI BL cell line transfected with *C-MYC* - luciferase reporter plasmid and treated with (1,5 and 10 nM) bortezomib showed a declined luciferase and hnRnP-K proteins levels suggesting that bortezomib is targeting *C-MYC* transcription via hnRnP-K downregulation after 12 hours of treatment (Suk *et al.*, 2015). *C-MYC* is targeted via Stat3 protein. In a different cell line type, 10-50 nM bortezomib doses were found to target Stat3 activity and reduced C-MYC protein expression eventually after 48 hours in chondrosarcoma cell line SW1353 in a dose and time dependent pattern (Bao *et al.*, 2017).

eBL NAMALWA and RAJI cell lines transfected with *C-MYC and EGFP* were also treated with similar bortezomib doses with and without zinc. No differences were obtained from *C-MYC* transfected cell compared to WT cell lines where cell viability count showed to be sensitive to either bortezomib alone or with combination with zinc. Similar findings also were seen at C-MYC protein levels where no rescue of the protein was obtained after 24 hrs which is again suggest the role of bortezomib an activating apoptosis in BL cells (Bota *et al.*, 2013, Poulaki *et al.*, 2007, Coquelle *et al.*, 2006). It was hypothesized that treating BL cells with bortezomib could rescue C-MYC protein levels but it showed to induced apoptosis. In this thesis it was shown that zinc induces apoptosis in tested BL cell lines, thus in this chapter, adding zinc to bortezomib treated BL cell line could further increase apoptosis events which is reflected by low viable cells count after 24 hrs.

CHAPTER SEVEN

DISCUSSION AND FUTURE WORK

7 Discussion.

BL is a NHL malignancy that is developed in the germinal centre stage of B cell development (Mukhtar *et al.*, 2017). In SSA, BL is associated with EBV and malaria infections. In BL, the translocated *C-MYC* is deregulated which drives the uncontrolled cell proliferation. The treatment course for BL involves intensive chemotherapy drugs which requires an intensive and supportive medical care system with high ability to diagnose the disease at early stage. Many of these resources are limited in SSA and LMIC (Gopal and Gross, 2018).

Although using chemotherapy regimens and protocols in treating BL are effective, there are still some concerns about the increased rate of relapsed cases and drug resistance among patients who had cancer remission. Clinical studies have demonstrated that patients who completed a limited treatment course are showing relapse signs up to 50% while intensive chemotherapeutic and supportive care bring relapse rate down to 7% during observation period after completing treatment course (Nkrumah and Perkins, 1976b, Ziegler, 1977, Intermesoli *et al.*, 2013). BL is uncommon in the United Kingdom with 5 years survival rate to be around 55%. As compared to the United kingdom, the survival rate in SSA is lower and reported to be around 30% (Ozuah *et al.*, 2020, UK, 2022).

In this study, the main goal was to develop alternative an anti-BL therapy that is affordable and exert a very low toxicity to overcome the side effects seen with traditional strategies of treatment. Before the beginning of this study, drug repurposing studies were performed using different BL cell lines screened against FMC drug library. Among all candidate drugs, zinc acetate, a commonly used mineral supplement was found to be effective against BL cells viability with a good safety profile. It was reported that 17% of world population is zinc deficient with African population to be the most zinc deficient (Belay *et al.*, 2021).

Zinc deficiency is suggested to be linked to the increased morbidity and mortality rate among children due to malnutrition in Africa. Clinical studies reported that in Nigeria, over 60% of woman and children are suffering from zinc deficiency. Quite similarly, clinical study conducted in Tanzania showed that 67% of 153 participated

children are zinc deficient (Young *et al.*, 2014, Veenemans *et al.*, 2012, Gupta *et al.*, 2020).

A series of experiments were conducted in this study as shown in chapter 3 to 6 to characterise the anti-BL activity of zinc. Detailed analysis of BL cell viability was conducted and identified a steep dose response with 50 µM not killing BL cells whereas all BL cell lines died in response to 100 µM zinc. These findings were found in both of sBL: AKATA, BL 30 and BL 31 and eBL: RAJI, NAMALWA, DANTE, SAV and GLOR. Additionally, zinc acetate demonstrated selective killing of BL cells when compared to non-BL cell lines tested in this study including AML: HL 60), DLBCL: SU-DHL-4, SU-DHL-5 and SU-DHL-6 and LCL: LG, KJ and AR.

This study showed that zinc had no impact on cell cycle among any cell lines used. Zinc impact was seen in annexin V, caspase 3 and 9 activation in BL cell lines as a response to 100 µM zinc acetate only. Zinc has demonstrated to regulate apoptosis events in different cancer cells (Truong-Tran *et al.*, 2001, Franklin and Costello, 2009). As compared to findings observed in this study, Schrantz et al (2001) in their study tested zinc against the BL cell line RAMOS and found that zinc chloride induced apoptosis and caspase 3 activation as measured by western blotting at doses ranged from 60-100 µM with no effect seen at doses lower that 60 µM which is interestingly agreed to the dose range used in this thesis (100 µM) (Schrantz *et al.*, 2001a). This mechanism is suggested to be linked to the ability of zinc to induces higher levels of mitochondrial superoxide production thus decreases mitochondrial membrane potential and rapidly increases apoptosis due to PARP cleavage. Also, the activation of caspase 9 seen in this thesis is linked to the intrinsic pathway of apoptosis where mitochondrial membrane potential is targeted to release cytochrome C which is important in the cascade of caspase 3 activation (Allan and Clarke, 2007).

A key defining feature of all BL is the constitutive expression of *C-MYC* due to translocation to one of the Ig loci which brings the C-MYC gene under the control of the Ig enhancer. *C-MYC* is normally tightly regulated as the gene undergoes expression, translation and eventually proteasomal degradation with protein half life of 20-30 minutes (Gregory and Hann, 2000). Considering C-MYC protein as a

driving force for BL cell proliferation, one of the questions was if there is any link between zinc induced killing in BL and *C-MYC*.

Sirinian *et al* (2003) in their study reported that another form of zinc, zinc sulphate, was decreasing C-MYC protein levels in BL cell line (RAJI) after 6 hours of treatment with 100 µM zinc sulphate (Sirinian *et al.*, 2003). This agreed with what was observed in this study among all BL cell lines tested. *C-MYC* amplification is defined by the increased levels of gene transcripts due to increased number of gene. The AML HL 60 cell line is characterised by *C-MYC* amplification and was reported to show decreased levels of C-MYC protein as a response to 100 µM zinc sulphate in the early time point with protein levels recovering back to normal levels after 24 hours (Sirinian *et al.*, 2003).

Similarly, no C-MYC protein reduction was seen in LCLs lines nor DLBCL cells tested in this thesis. The rapid C-MYC protein sensitivity seen previously in the BL cell lines after 6 hours is linked to the ability of zinc acetate to reduce mRNA levels which is translated by reduced translation and protein levels especially when considering the short half life of the protein. This C-MYC reduction was thought to be linked to the ability of zinc acetate to regulate the Ig enhancer elements (HS1-2, HS3 and HS4) that control the translocated *C-MYC* allele in BL cells. Thus, the DLBCL cell line SU-DHL-4 which has a *BCL2/IgH* t(14;18) translocation was used and tested. In *BCL2/IgH* translocation, *BCL2* is translocated to a proximity to *IgH* enhancer elements which makes it under the control of Ig enhancer elements hyperactivity. This model can be used as a representative model of *C-MYC/IgH* translocation in BL. No BCL-2 protein reduction was observed suggesting that zinc acetate did not target the enhancer element. It is worth noting this could be due to breakpoint differences.

As explained previously, *C-MYC* is tightly regulated inside the cell which begins by gene expression, translation and degradation. The 26S proteasome machinery is an important mechanism that is involved in C-MYC degradation and maintaining C-MYC protein levels at levels of tolerance. The FDA approved Bortezomib is a drug that works by inhibiting 26S proteasome and leading to proteins accumulation. BL cell lines are sensitive to bortezomib. Thus, it was difficult and challenging in this

study to identify the suitable dose that inhibits proteasome without killing the cells. In this thesis findings, the lowest dose of bortezomib used 6 nM was sufficient to induce cell death in both tested BL cell lines eBL: NAMALWA and RAJI after 24 hours in a dose dependent pattern with very slight rescue of C-MYC protein seen in eBL: NAMALWA cells in the presence of zinc. Bortezomib was reported to prevent proteasome 26S induced C-MYC degradation in RAMOS BL cell line when treated with BL mitochondrial superoxide inducer BZ-234 drug after 6 hours (Sundberg *et al.*, 2006).

Tellingly, in our study we found that bortezomib is not efficient for extended zinc acetate exposure as both cell lines had lost the protein after 24 hours with no rescue seen in their viability as well. In a different study, Suk *et al* (2015) reported C-MYC protein reduction after 12 hours in DAUDI BL cell line as a response to 10 nM bortezomib alone (Suk *et al.*, 2015). This mechanism is related to the activity of bortezomib to downregulate the Heterogeneous nuclear ribonucleoprotein K (hnRNP K) leading to C-MYC protein reduction (Suk *et al.*, 2015). Bortezomib was found to induce apoptosis and proliferation repression in BL cell lines due to caspase 3 activation pathway which kills BL cells in C-MYC independent pattern (Bota *et al.*, 2013, Poulaki *et al.*, 2007, Coquelle *et al.*, 2006).

In BL, the tumour suppressor (*TP53*) gene product (P53) is a DNA binding protein that is involved in cell cycle suppression, DNA repair mechanism and apoptosis. Irregular P53 functioning and mutation is linked to many cancers including: (head and neck, ovarian, colorectal and almost in 5% of leukaemia cases) (Olivier *et al.*, 2010). In BL, *TP53* is commonly mutated with up to 40% in primary BL cells and 70% among BL cell lines (Klumb *et al.*, 2001). Almost all BL cell lines used in this study were reported in different studies to have missense *TP53* mutations rendering different amino acid substitution that affect protein functioning. Clinically, *TP53* mutations are highly associated with aggressive refractory or relapsed BL cases. Almost, all relapsed BL patients possess *TP53* mutations or gene deficient (Reutter *et al.*, 2021). In the context of this study, P53 is a zinc dependent protein that requires zinc to maintain the functional folding and structure of the protein. Thus, insufficient zinc levels may lead to protein dysfunction (Loh, 2010, Ha *et al.*, 2022). Observations seen with all BL cell lines tested in this study and zinc suggest that

zinc may also target P53 in BL cells. Different studies reported zinc can refold misfolded P53 to its WT confirmational structure (Kogan and Carpizo, 2018, Farrell *et al.*, 1991, Sachdeva *et al.*, 2009). This study suggests that adding zinc to BL cells may activate mutant P53 which leads to apoptosis. This pathway is interesting, and this thesis is proposing to study this pathway in the future to understand the mechanism involved. This can be performed using the available antibody Pab 240 which recognizes the mutant misfolded form of P53 via immunoprecipitation assay. Interestingly, Puca *et al* (2011) had transfected the human non-small cell lung carcinoma cell line (H1299) with mutant misfolded P53 expressing vector and found that 100 µM of zinc chloride was able to restore P53 folding after 24 hours as reported via immunoprecipitation and western blotting (Puca *et al.*, 2011). Zinc chloride also increased drug sensitivity in tested cells. This finding can be related with what was reported in this thesis. Investigating the role of P53 activation in BL is highly recommended for future work. Different studies investigated the role of P53 in regulating *C-MYC* expression in a process involves recruiting histone deacetylases to *C-MYC* promoter region (Hoffman *et al.*, 2002, Ho *et al.*, 2005). Both in vivo and in vitro studies showed the role of P53 in supressing *C-MYC* transcription as reported by Ho *et al.*, 2005 where activation of P53 in human acute myeloid leukaemia cells via γ-irradiation result in *C-MYC* suppression with no expression in p53-null cells. Moreover, it was shown that the tumour suppressor miR-145 can regulate *C-MYC* expression as a response to P53 activation in breast and colon cancer cells through Akt pathway (Sachdeva *et al.*, 2009). This study proposes the study of this pathway by suggesting that zinc is reactivating P53 in BL cells which later increase the miR-145 expression as a direct target which later supress *C-MYC* expression.

In this thesis, overexpression of *C-MYC* was used to prevent and rescue BL cell viability in response to zinc. Different BL cell lines were stably transfected with *C-MYC* plasmid that is controlled by the constitutively active promoter EF1A. Whilst BL cells are difficult to transfect, flow cytometry data indicated that transfection was successfully achieved in both eBL: NAMALWA and RAJI BL cell lines as represented by EGFP signals. Due to tight regulation of *C-MYC* inside the cells, *C-MYC* expression as represented by the EGFP signals is variable among the two BL

cell lines suggesting that there is an upper limit of the protein where cells are tolerating to avoid cell death linked with elevated C-MYC levels (Thompson, 1998, Nilsson and Cleveland, 2003). No C-MYC rescue and no BL cell viability was achieved as a response to zinc treatment after 24 hours. There is no clear mechanism in describing that reduction of C-MYC when considering its complex regulation pathways involved. However, the suggested mechanism is that exogenous *C-MYC* is sensitive to the continuous zinc acetate exposure causing protein degradation. It is recommended to investigate the role of overexpressing *C-MYC* in BL at earlier time points between 6 and 12 hours which can show if there is any protein resistance seen as a response to zinc.

Zinc is an important micronutrient as discussed earlier. Zinc is already implicated in medical uses including reducing diarrhoeal series among children, reducing malarial febrile episodes, managing skin nodule in leprosy, Wilson's disease and furthermore cases. (Shankar *et al.*, 2000, El-Shafei *et al.*, 1988, Sharquie *et al.*, 2001). The recommended daily dose of zinc is 11 mg and 8 mg for male and female respectively with normal serum level of 70 - 180 µgm/100mL (Deshpande *et al.*, 2013, Arora *et al.*, 2002). Zinc is important for normal growth and importantly in boosting and developing the immune system which help in fighting cancer cells (Prasad, 2008). In combining findings from this study, zinc may be a promising anti BL therapy where it also can be given adjunctively to current BL therapy protocol and management. Collectively, this thesis recommends using zinc in the protocol of treating BL cases especially in SSA and in LMIC where alternative therapy is required to overcome the difficulties in providing traditional BL therapy.

8 Future Work.

To further understand how zinc is effective against BL cells, it is recommended to test zinc effect against normal B cells. Although in this study, in vitro culturing and proliferation of B cells (purified from peripheral blood mononuclear cell) was successfully achieved, it is useful in the future to test zinc against GC B cells models

which can be obtained from tonsils which represent a better model than peripheral blood B cells.

In vivo zinc studies are also recommended for future studies. This can be performed by using a model that resembles *C-MYC* translocation in BL. The available mouse model (Eμ-*Myc* transgenic mice) which possess *C-MYC/IgH* t(8;14) translocation is a good representative model of *C-MYC* driven B cell lymphomagenesis where deregulated *C-MYC* expression is controlled by the Ig enhancer element (Eμ).

Although using cell lines is useful in scientific research, zinc can be tested in vitro against primary BL cells obtained from BL patients which help in further understanding of how primary BL cells respond to zinc. Moreover, primary BL cells can be implanted in an immunodeficient mouse to generate patient-derived xenograft mouse model (PDX) which help in understanding the mechanism and the effects of zinc in BL progression thoroughly (Zhang *et al.*, 2017, Forde *et al.*, 2021).

Zinc transporter is another important aspect to be investigated in future studies for BL cells. An important question that needs addressing is whether there is a difference in the zinc uptake by BL cells compared to other tumour cells. To test this, a cellular fluorescent zinc probe was used. Preliminary data indicated that zinc acetate was highly accumulated in the tested eBL: NAMALWA cell line with no signs of zinc acetate accumulation in the other tested non-BL cell line SU-DHL-4 (N=1). In this experiment, both eBL: NAMALWA BL and DLBCL: SU-DHL-4 cell lines were treated with zinc acetate at 50 and 100 μM with and without zinc chelator (provided with assay kit) 30 minutes and 2 hours. To measure cellular zinc acetate levels, cells were probed at each time point with GFP zinc probes and analysed by flow cytometry. Cytospin slides were also made to visualize zinc acetate under the fluorescent microscope. Figure 7.1 shows the 30 minutes and 2 hours fluorescent microscopic images for both eBL: NAMALWA BL and DLBCL: SU-DHL-4 cell lines which include the positive control and zinc acetate treated sample with and without zinc chelator. There were clear differences in GFP signals in the microscopic images for eBL: NAMALWA BL cells treated with zinc acetate especially at 100 μM when compared to DLBCL: SU-DHL-4 which showed minimal fluorescence. Further flow cytometry analysis to measure GFP signals are showed in Figure 7.2. eBL:

NAMALWA BL showed an increased GFP signal with 100 µM zinc acetate after 30 minutes where DLBCL: SU-DHL-4 cells showed no changes. Fluorescence was shown to be time dependent in eBL: NAMALWA BL cell lines where higher GFP signals were measured after 2 hours. Still, DLBCL: SU-DHL-4 showed no changes to the untreated control even after 2 hours. Thus, suggesting that BL cell lines accumulate zinc intracellularly in a higher level than non BL cells. Further investigations are needed to study the role of zinc transporters in BL cell lines as one of the approaches to understand zinc sensitivity in BL cell lines.

Considering data generated in this study beside the general understating of zinc pharmacodynamics and pharmacokinetic with zinc deficiency studies, there is no significant point that stands as an obstacle for starting to give zinc to BL patients or to be a part of designing a clinical trial to study disease progression especially in relapsed and resistance cases. Given the fact of how zinc deficiency is common, findings from this thesis can be clinically translated into BL patients by giving high zinc doses and measuring serum zinc levels with continuous evaluation of cancer symptom and progression. Clinical trial of zinc is already in progress in Africa which was designed, planned, initiated and led by members from the lab with all hopes to find positive outcomes that can be translated into actual clinical use for BL patients.

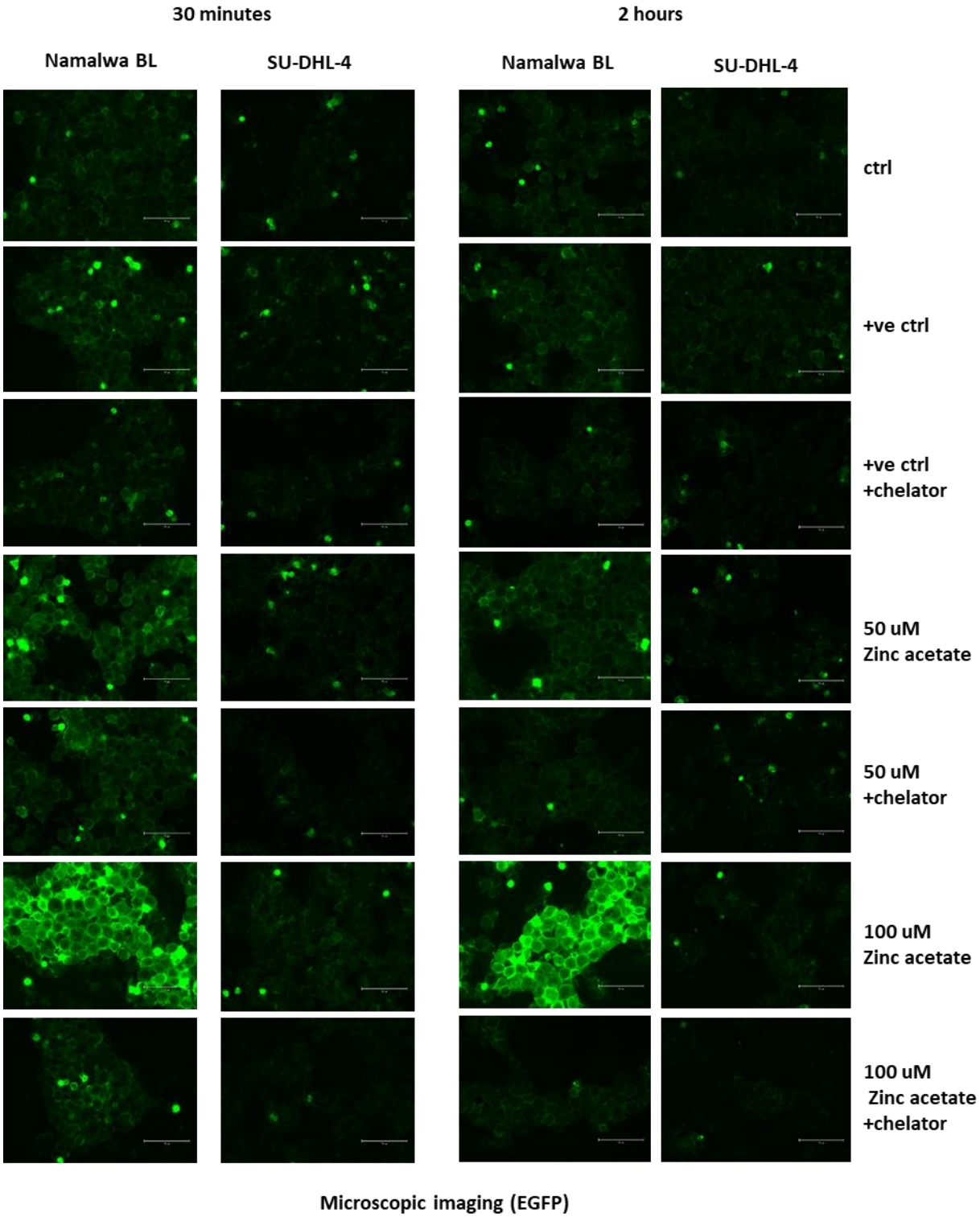

Figure 7. 1 Visualizing zinc acetate in NAMALWA BL and SU-DHL-4 after 30 minutes and 2 hours of treatment. *Both NAMALWA BL and SU-DHL-4 were treated with zinc acetate at 50 and 100 µM with control sample preparation with and without zinc chelator. Samples were probed with zinc probes at the time point with cytosine slides preparation. Images were taken using fluorescent microscopy.*

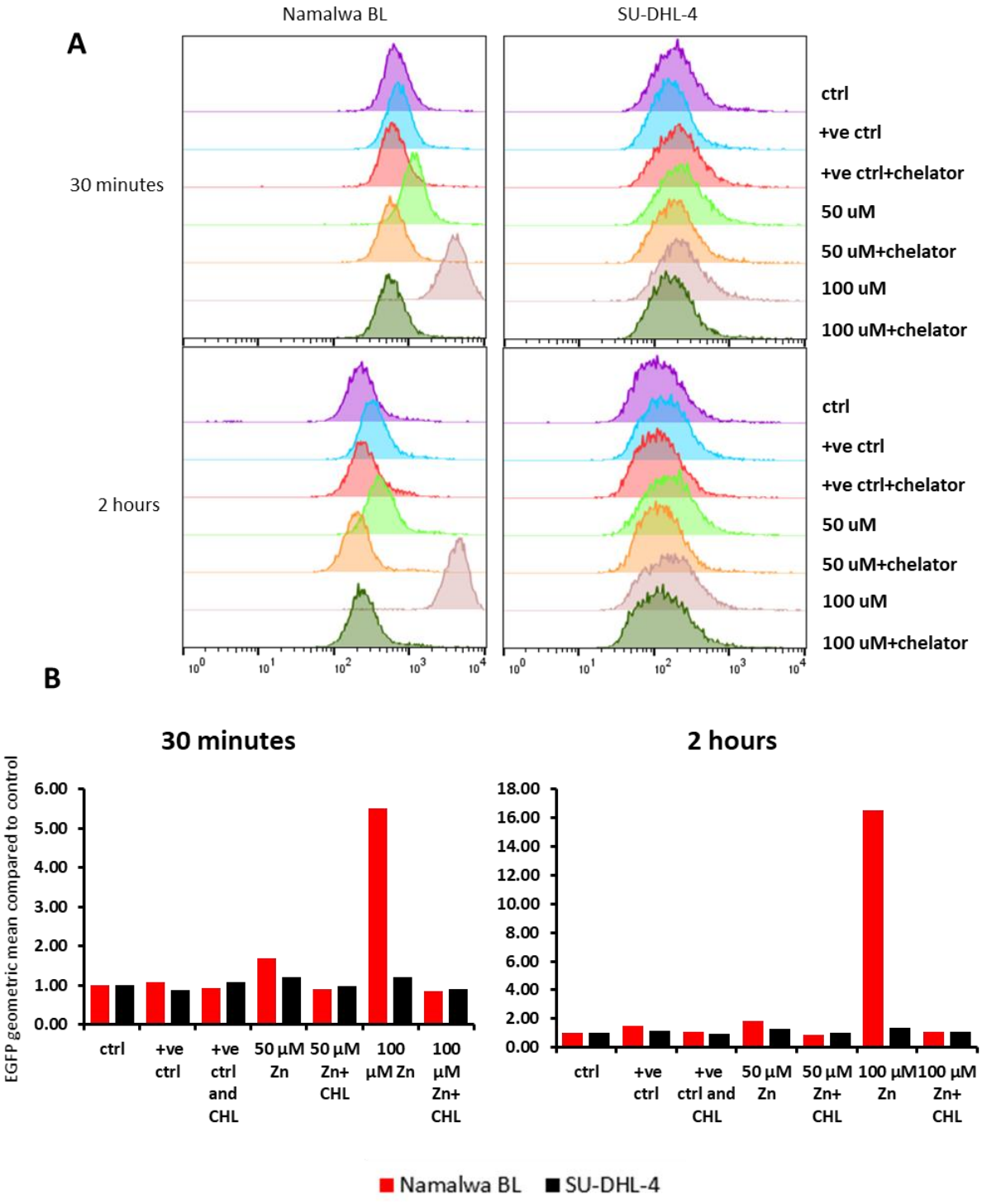

Figure 7. 2 Measuring cellular zinc acetate level in NAMALWA BL and SU-DHL-4 cell lines after 30 minutes and 2 hours. *(A) EGFP signal intensity represent by histograms for each treated sample in NAMALWA BL and SU-DHL-4 cell line. (B) EGFP geometric mean analysis compared to the control for each treated samples in NAMALWA BL and SU-DHL-4 at 30 minutes and 2 hours (N=1).*

9 Reference list.

(HMRN), H. M. R. N. 2022. *Survival statistics: Burkitt lymphoma - Overall relative survival* [Online]. Available: https://hmrn.org/statistics/survival [Accessed 24/06/2022.

ABARRATEGI, A., MIAN, S. A., PASSARO, D., ROUAULT-PIERRE, K., GREY, W. & BONNET, D. 2018. Modeling the human bone marrow niche in mice: From host bone marrow engraftment to bioengineering approaches. *Journal of Experimental Medicine,* 215**,** 729-743.

ABATE, F., AMBROSIO, M. R., MUNDO, L., LAGINESTRA, M. A., FULIGNI, F., ROSSI, M., ZAIRIS, S., GAZANEO, S., DE FALCO, G. & LAZZI, S. J. P. P. 2015. Distinct viral and mutational spectrum of endemic Burkitt lymphoma. 11**,** e1005158.

ABBASI, M. R. 2022. Mantle Cell Lymphoma. *Medscape*.

ABBOTT, D. R., ABBOTT, R. T., JENSON, S. D., FILLMORE, G. C., ELENITOBA-JOHNSON, K. S. & LIM, M. S. J. J. O. H. 2009. Apoptosis of t (14; 18)-positive lymphoma cells by a Bcl-2 interacting small molecule. 2**,** 113-119.

ACTION, L. 2021. Follow-up for lymphoma.

ADıYAMAN, S. C., ALACACıOĞLU, İ., DANYELI, A. E., TÜRKYıLMAZ, D., SEVINDIK, Ö. G., DEMIRKAN, F., PIŞKIN, Ö., ÖZCAN, M. A., ÜNDAR, B. & ÖZKAL, S. J. T. J. O. H. 2019. Prognostic Factors in Elderly Patients with Diffuse Large B-Cell Lymphoma and Their Treatment Results. 36**,** 81.

AGEDEW, E., TSEGAYE, B., BANTE, A., ZERIHUN, E., AKLILU, A., GIRMA, M., KEREBIH, H., WALE, M. Z. & YIRSAW, M. T. J. P. O. 2022. Zinc deficiency and associated factors among pregnant women's attending antenatal clinics in public health facilities of Konso Zone, Southern Ethiopia. 17**,** e0270971.

AGGARWAL, P. & LIMAIEM, F. 2019. Reed Sternberg Cells.

AGGETT, P. J. & COMERFORD, J. G. 1995. Zinc and human health. *Nutrition Reviews,* 53**,** S16.

AKHTAR, M. J., AHAMED, M., KUMAR, S., KHAN, M. M., AHMAD, J. & ALROKAYAN, S. A. J. I. J. O. N. 2012. Zinc oxide nanoparticles selectively induce apoptosis in human cancer cells through reactive oxygen species. 845-857.

ALBERTS, B. 2017. *Molecular biology of the cell*, Garland science.

ALDERUCCIO, J. P., OLSZEWSKI, A. J., EVENS, A. M., COLLINS, G. P., DANILOV, A. V., BOWER, M., JAGADEESH, D., ZHU, C., SPERLING, A. & KIM, S.-H. 2021. HIV-associated Burkitt lymphoma: outcomes from a US-UK collaborative analysis. *Blood advances,* 5**,** 2852-2862.

ALLAN, L. A. & CLARKE, P. R. J. M. C. 2007. Phosphorylation of caspase-9 by CDK1/cyclin B1 protects mitotic cells against apoptosis. 26**,** 301-310.

AMATI, B. & LAND, H. 1994. Myc—Max—Mad: a transcription factor network controlling cell cycle progression, differentiation and death. *Current opinion in genetics & development,* 4**,** 102-108.

AMATO, T., ABATE, F., PICCALUGA, P., IACONO, M., FALLERINI, C., RENIERI, A., DE FALCO, G., AMBROSIO, M. R., MOURMOURAS, V. & OGWANG, M. J. A. J. O. C. P. 2016. Clonality analysis of immunoglobulin gene rearrangement by next-generation sequencing in endemic Burkitt lymphoma suggests antigen drive activation of BCR as opposed to sporadic Burkitt lymphoma. 145**,** 116-127.

AMBROSIO, M. R., LAZZI, S., BELLO, G. L., SANTI, R., DEL PORRO, L., DE SANTI, M. M., GUAZZO, R., MUNDO, L., RIGACCI, L. & KOVALCHUCK, S. J. H. 2019. MYC protein expression scoring and its impact on the prognosis of aggressive B-cell lymphoma patients. 104**,** e25.

AMBROSIO, M. R., NAVARI, M., DI LISIO, L., LEON, E. A., ONNIS, A., GAZANEO, S., MUNDO, L., ULIVIERI, C., GOMEZ, G. & LAZZI, S. 2014. The Epstein Barr-encoded BART-6-3p microRNA

affects regulation of cell growth and immuno response in Burkitt lymphoma. *Infectious agents and cancer,* 9**,** 1-12.
ANTHONY, B. A. & LINK, D. C. 2014. Regulation of hematopoietic stem cells by bone marrow stromal cells. *Trends in immunology,* 35**,** 32-37.
ARORA, P., DHILLON, K., RAJAN, S., SAYAL, S. & DAS, A. J. M. J. A. F. I. 2002. Serum zinc levels in cutaneous disorders. 58**,** 304-306.
ARRUGA, F., GIZDIC, B., SERRA, S., VAISITTI, T., CIARDULLO, C., COSCIA, M., LAURENTI, L., D'ARENA, G., JAKSIC, O. & INGHIRAMI, G. J. L. 2014. Functional impact of NOTCH1 mutations in chronic lymphocytic leukemia. 28**,** 1060-1070.
ATCC. 2022a. *HL-60* [Online]. Available: https://www.atcc.org/products/ccl-240.
ATCC 2022b. NAMALWA.
ATCC. 2022c. *Raji BL* [Online]. Available: https://www.atcc.org/products/ccl-86.
ATCC. 2022d. *SU-DHL-4* [Online]. Available: https://www.atcc.org/products/crl-2957.
ATCC. 2022e. *SU-DHL-5* [Online]. Available: https://www.atcc.org/products/crl-2958.
ATCC. 2022f. *SU-DHL-6* [Online]. Available: https://www.atcc.org/products/crl-2959.
BABER, J. L., LIBUTTI, D., LEVENS, D. & TJANDRA, N. J. J. O. M. B. 1999. High precision solution structure of the C-terminal KH domain of heterogeneous nuclear ribonucleoprotein K, a c-myc transcription factor. 289**,** 949-962.
BAHRAM, F., VON DER LEHR, N., CETINKAYA, C. & LARSSON, L.-G. J. B., THE JOURNAL OF THE AMERICAN SOCIETY OF HEMATOLOGY 2000. c-Myc hot spot mutations in lymphomas result in inefficient ubiquitination and decreased proteasome-mediated turnover. 95**,** 2104-2110.
BAILEY, R. L., WEST JR, K. P., BLACK, R. E. J. A. O. N. & METABOLISM 2015. The epidemiology of global micronutrient deficiencies. 66**,** 22-33.
BAJAIT, C. & THAWANI, V. 2011. Role of zinc in pediatric diarrhea. *Indian journal of pharmacology,* 43**,** 232.
BAKR, A., HEY, J., SIGISMONDO, G., LIU, C.-S., SADIK, A., GOYAL, A., CROSS, A., IYER, R. L., MÜLLER, P. & TRAUERNICHT, M. J. N. A. R. 2021. ID3 promotes homologous recombination via non-transcriptional and transcriptional mechanisms and its loss confers sensitivity to PARP inhibition. 49**,** 11666-11689.
BAKSHI, R. K., COX, M. A. & ZAJAC, A. J. 2014. Cytotoxic T Lymphocytes. *Encyclopedia of Medical Immunology: Autoimmune Diseases***,** 332-342.
BAO, X., REN, T., HUANG, Y., REN, C., YANG, K., ZHANG, H. & GUO, W. J. I. J. O. O. 2017. Bortezomib induces apoptosis and suppresses cell growth and metastasis by inactivation of Stat3 signaling in chondrosarcoma. 50**,** 477-486.
BARISTA, I., ROMAGUERA, J. E. & CABANILLAS, F. 2001. Mantle-cell lymphoma. *The lancet oncology,* 2**,** 141-148.
BARRETO, V. M. & MAGOR, B. G. 2011. Activation-induced cytidine deaminase structure and functions: a species comparative view. *Developmental & Comparative Immunology,* 35**,** 991-1007.
BELAY, A., GASHU, D., JOY, E. J., LARK, R. M., CHAGUMAIRA, C., LIKOSWE, B. H., ZERFU, D., ANDER, E. L., YOUNG, S. D. & BAILEY, E. H. J. S. R. 2021. Zinc deficiency is highly prevalent and spatially dependent over short distances in Ethiopia. 11**,** 1-13.
BELLO-FERNANDEZ, C., PACKHAM, G. & CLEVELAND, J. L. 1993. The ornithine decarboxylase gene is a transcriptional target of c-Myc. *Proceedings of the National Academy of Sciences,* 90**,** 7804-7808.
BENDE, R. J., SMIT, L. A. & VAN NOESEL, C. J. 2007. Molecular pathways in follicular lymphoma. *Leukemia,* 21**,** 18-29.
BENJAMIN, D., MAGRATH, I., MAGUIRE, R., JANUS, C., TODD, H. & PARSONS, R. J. T. J. O. I. 1982. Immunoglobulin secretion by cell lines derived from African and American undifferentiated lymphomas of Burkitt's and non-Burkitt's type. 129**,** 1336-1342.

BERNITZ, J. M., DANIEL, M., FSTKCHYAN, Y. S. & MOORE, K. 2017. Granulocyte-colony stimulating factor mobilizes dormant hematopoietic stem cells without proliferation in mice. *Blood*, blood-2016-11-752923.

BHATIA, K., GOLDSCHMIDTS, W., GUTIERREZ, M., GAIDANO, G., DALLA-FAVERA, R. & MAGRATH, I. J. T. F. J. 1993. Hemi-or homozygosity: a requirement for some but not other p53 mutant proteins to accumulate and exert a pathogenetic effect. 7**,** 951-956.

BIRLUTIU, V., BIRLUTIU, R.-M., ZAHARIE, I. S. & SANDU, M. 2020. Burkitt lymphoma associated with human immunodeficiency virus infection and pulmonary tuberculosis: a case report. *Medicine,* 99.

BIRNIE, G. J. T. B. J. O. C. S. 1988. The HL60 cell line: a model system for studying human myeloid cell differentiation. 9**,** 41.

BISHOP, P. C., RAO, V. K. & WILSON, W. H. 2000. Burkitt's lymphoma: molecular pathogenesis and treatment. *Cancer investigation,* 18**,** 574-583.

BISPO, J. A. B., PINHEIRO, P. S. & KOBETZ, E. K. 2020. Epidemiology and Etiology of Leukemia and Lymphoma. *Cold Spring Harbor Perspectives in Medicine,* 10**,** a034819.

BLACK, M. M. 1998. Zinc deficiency and child development. *The American journal of clinical nutrition,* 68**,** 464S-469S.

BOLICK, D., MEDEIROS, P., LEDWABA, S., LIMA, A., NATARO, J., BARRY, E. & GUERRANT, R. 2018. The Critical Role of Zinc in a New Murine Model of Enterotoxigenic E. coli (ETEC) Diarrhea. *Infection and immunity***,** IAI. 00183-18.

BOST, M., HOUDART, S., OBERLI, M., KALONJI, E., HUNEAU, J.-F. & MARGARITIS, I. 2016. Dietary copper and human health: Current evidence and unresolved issues. *Journal of Trace Elements in Medicine and Biology,* 35**,** 107-115.

BOTA, D. A., ALEXANDRU, D., KEIR, S. T., BIGNER, D., VREDENBURGH, J. & FRIEDMAN, H. S. J. J. O. N. 2013. Proteasome inhibition with bortezomib induces cell death in GBM stem-like cells and temozolomide-resistant glioma cell lines, but stimulates GBM stem-like cells' VEGF production and angiogenesis. 119**,** 1415-1423.

BOUDA, G. C., TRAORÉ, F., COUITCHERE, L., RAQUIN, M.-A., GUEDENON, K. M., PONDY, A., MOREIRA, C., RAKOTOMAHEFA, M., HARIF, M. & PATTE, C. 2019a. Advanced Burkitt lymphoma in sub-Saharan Africa pediatric units: results of the third prospective multicenter study of the Groupe Franco-Africain d'Oncologie Pediatrique. *Journal of global oncology,* 5**,** 1-9.

BOUDA, G. C., TRAORÉ, F., COUITCHERE, L., RAQUIN, M.-A., GUEDENON, K. M., PONDY, A., MOREIRA, C., RAKOTOMAHEFA, M., HARIF, M. & PATTE, C. J. J. O. G. O. 2019b. Advanced Burkitt lymphoma in sub-Saharan Africa pediatric units: results of the third prospective multicenter study of the Groupe Franco-Africain d'Oncologie Pediatrique. 5**,** 1-9.

BOUSKA, A., BI, C., LONE, W., ZHANG, W., KEDWAII, A., HEAVICAN, T., LACHEL, C. M., YU, J., FERRO, R. & ELDORGHAMY, N. 2017. Adult high-grade B-cell lymphoma with Burkitt lymphoma signature: genomic features and potential therapeutic targets. *Blood, The Journal of the American Society of Hematology,* 130**,** 1819-1831.

BOXER, L. M. & DANG, C. V. J. O. 2001. Translocations involving c-myc and c-myc function. 20**,** 5595-5610.

BOYCE, A. J. 2009. *Epstein-Barr virus genome loss from Endemic Burkitt lymphoma and its effect on cell phenotype.* University of Birmingham.

BRETONES, G., DELGADO, M. D. & LEÓN, J. 2015. Myc and cell cycle control. *Biochimica et Biophysica Acta (BBA)-Gene Regulatory Mechanisms,* 1849**,** 506-516.

BRION, L. P., HEYNE, R., STEVEN BROWN, L., LAIR, C. S., EDWARDS, A., BURCHFIELD, P. J. & CARAIG, M. 2020. Zinc deficiency limiting head growth to discharge in extremely low gestational age infants with insufficient linear growth: a cohort study. *Journal of Perinatology,* 40**,** 1694-1704.

BRUZEAU, C., COOK-MOREAU, J., PINAUD, E. & LE NOIR, S. J. F. I. I. 2022. Contribution of Immunoglobulin Enhancers to B Cell Nuclear Organization. 13.

BUDZKO, L., JACKOWIAK, P. & FIGLEROWICZ, M. 2013. Activation-induced cytidine deaminase (AID): single activity–pleiotrophic effect. *BioTechnologia. Journal of Biotechnology Computational Biology and Bionanotechnology,* 94.

BUDZKO, L., JACKOWIAK, P., KAMEL, K., SARZYNSKA, J., BUJNICKI, J. M. & FIGLEROWICZ, M. 2017. Mutations in human AID differentially affect its ability to deaminate cytidine and 5-methylcytidine in ssDNA substrates in vitro. *Scientific reports,* 7**,** 3873.

BURKHARDT, B., MICHGEHL, U., ROHDE, J., ERDMANN, T., BERNING, P., REUTTER, K., ROHDE, M., BORKHARDT, A., BURMEISTER, T. & DAVE, S. J. N. C. 2022. Clinical relevance of molecular characteristics in Burkitt lymphoma differs according to age. 13**,** 1-12.

CANCER-RESEARCH-UK. 2022. *Burkitt lymphoma* [Online]. Available: https://www.cancerresearchuk.org/about-cancer/non-hodgkin-lymphoma/types/burkitt-lymphoma#:~:text=Each%20year%20around%20210%20people,but%20it%20is%20more%20unusual. [Accessed 26/06/2022 2022].

CANO, R. L. E. & LOPERA, H. D. E. 2013. Introduction to T and B lymphocytes. *Autoimmunity: From Bench to Bedside [Internet].* El Rosario University Press.

CAO, Z., FAN-MINOGUE, H., BELLOVIN, D. I., YEVTODIYENKO, A., ARZENO, J., YANG, Q., GAMBHIR, S. S. & FELSHER, D. W. J. C. R. 2011. MYC phosphorylation, activation, and tumorigenic potential in hepatocellular carcinoma are regulated by HMG-CoA reductase. 71**,** 2286-2297.

CAROFIGLIO, M., LAURENTI, M., VIGHETTO, V., RACCA, L., BARUI, S., GARINO, N., GERBALDO, R., LAVIANO, F. & CAUDA, V. J. N. 2021. Iron-doped ZnO nanoparticles as multifunctional nanoplatforms for theranostics. 11**,** 2628.

CARTLIDGE, R. C. 2015. *The Epstein-Barr virus BCL-2 homologues: interactions with cellular BCL-2 proteins and their role in apoptosis.* University of Birmingham.

CASALI, P., PAL, Z., XU, Z. & ZAN, H. 2006. DNA repair in antibody somatic hypermutation. *Trends in immunology,* 27**,** 313-321.

CASELLAS, R., NUSSENZWEIG, A., WUERFFEL, R., PELANDA, R., REICHLIN, A., SUH, H., QIN, X. F., BESMER, E., KENTER, A. & RAJEWSKY, K. 1998. Ku80 is required for immunoglobulin isotype switching. *The EMBO Journal,* 17**,** 2404-2411.

CASIMIRO, M. C., CROSARIOL, M., LORO, E., LI, Z., PESTELL, R. G. J. G. & CANCER 2012. Cyclins and cell cycle control in cancer and disease. 3**,** 649-657.

CELLOSAURUS 2020. Sav-BL (CVCL_7210).

CELLOSAURUS 2022a. Akata (CVCL_0148).

CELLOSAURUS. 2022b. *BL-30 (CVCL_C142)* [Online]. Available: https://web.expasy.org/cellosaurus/CVCL_C142.

CELLOSAURUS. 2022c. *BL-31 (CVCL_C143)* [Online]. Available: https://web.expasy.org/cellosaurus/CVCL_C143.

CELLOSAURUS 2022d. Dante (CVCL_7186).

CELLOSAURUS. 2022e. *Namalwa (CVCL_0067)* [Online]. Available: https://web.expasy.org/cellosaurus/CVCL_0067.

CELLOSAURUS 2022f. Raji (CVCL_0511).

CHANARIN, I. 1989. *Laboratory haematology: an account of laboratory techniques*, Churchill Livingstone.

CHANU, S. I. & SARKAR, S. 2014. Cell & Development Biology.

CHEN, X. & JENSEN, P. E. 2008. The role of B lymphocytes as antigen-presenting cells. *Archivum immunologiae et therapiae experimentalis,* 56**,** 77.

CHENG, Y. & CHEN, H. J. N. 2021. Aberrance of zinc metalloenzymes-induced human diseases and its potential mechanisms. 13**,** 4456.

CHESNOKOVA, L. S. & HUTT-FLETCHER, L. M. 2014. Epstein-Barr virus infection mechanisms. *Chinese journal of cancer,* 33**,** 545.
CHESTERS, J. K., PETRIE, L. & TRAVIS, A. J. 1990. A requirement for Zn2+ for the induction of thymidine kinase but not ornithine decarboxylase in 3T3 cells stimulated from quiescence. *Biochemical journal,* 272**,** 525-527.
CHIAL, H. 2008. Proto-oncogenes to oncogenes to cancer. *Nature education,* 1**,** 33.
CHO, Y.-E., LOMEDA, R.-A. R., RYU, S.-H., SOHN, H.-Y., SHIN, H.-I., BEATTIE, J. H. & KWUN, I.-S. 2007. Zinc deficiency negatively affects alkaline phosphatase and the concentration of Ca, Mg and P in rats. *Nutrition research and practice,* 1**,** 113-119.
CHUANG, S. S., HUANG, W. T., HSIEH, P. P., JUNG, Y. C., YE, H., DU, M. Q., LU, C. L., CHO, C. Y., HSIAO, S. C. & HSU, Y. H. J. H. 2008. Sporadic paediatric and adult Burkitt lymphomas share similar phenotypic and genotypic features. 52**,** 427-435.
CLOONAN, S. M. & WILLIAMS, D. C. J. I. J. O. C. 2011. The antidepressants maprotiline and fluoxetine induce Type II autophagic cell death in drug-resistant Burkitt's lymphoma. 128**,** 1712-1723.
COLVIN, R. A., BUSH, A. I., VOLITAKIS, I., FONTAINE, C. P., THOMAS, D., KIKUCHI, K. & HOLMES, W. R. 2008. Insights into Zn2+ homeostasis in neurons from experimental and modeling studies. *American Journal of Physiology-Cell Physiology,* 294**,** C726-C742.
COLVIN, R. A., HOLMES, W. R., FONTAINE, C. P. & MARET, W. 2010. Cytosolic zinc buffering and muffling: their role in intracellular zinc homeostasis. *Metallomics,* 2**,** 306-317.
CONACCI-SORRELL, M., MCFERRIN, L. & EISENMAN, R. N. 2014. An overview of MYC and its interactome. *Cold Spring Harbor perspectives in medicine,* 4**,** a014357.
CONTICELLO, S. G. 2008. The AID/APOBEC family of nucleic acid mutators. *Genome biology,* 9**,** 229.
COOPER, G. M. 2000. The Cell 2nd edition. Sinauer Associates Inc.
COQUELLE, A., MOUHAMAD, S., PEQUIGNOT, M., BRAUN, T., CARVALHO, G., VIVET, S., METIVIER, D., CASTEDO, M., KROEMER, G. J. C. D. & DIFFERENTIATION 2006. Cell cycle-dependent cytotoxic and cytostatic effects of bortezomib on colon carcinoma cells. 13**,** 873-875.
CORREIA, C., SCHNEIDER, P. A., DAI, H., DOGAN, A., MAURER, M. J., CHURCH, A. K., NOVAK, A. J., FELDMAN, A. L., WU, X. & DING, H. J. B., THE JOURNAL OF THE AMERICAN SOCIETY OF HEMATOLOGY 2015. BCL2 mutations are associated with increased risk of transformation and shortened survival in follicular lymphoma. 125**,** 658-667.
COSTA, L. J., XAVIER, A. C., WAHLQUIST, A. E. & HILL, E. G. 2013. Trends in survival of patients with Burkitt lymphoma/leukemia in the USA: an analysis of 3691 cases. *Blood, The Journal of the American Society of Hematology,* 121**,** 4861-4866.
COUSINS, R. J., LIUZZI, J. P. & LICHTEN, L. A. 2006. Mammalian zinc transport, trafficking, and signals. *Journal of Biological Chemistry,* 281**,** 24085-24089.
CRANE, G. M., JEFFERY, E. & MORRISON, S. J. 2017. Adult haematopoietic stem cell niches. *Nature Reviews Immunology,* 17**,** 573-590.
CROMBIE, J. & LACASCE, A. 2021. The treatment of Burkitt lymphoma in adults. *Blood,* 137**,** 743-750.
CUMMINGS, J. E. & KOVACIC, J. P. 2009. The ubiquitous role of zinc in health and disease. *Journal of veterinary emergency and critical care,* 19**,** 215-240.
CUNHA, K. C. C. M. S., OLIVEIRA, M. C. L. A., GOMES, A. C. S., CASTRO, L. P. F. D. & VIANA, M. B. J. R. B. D. H. E. H. 2012. Clinical course and prognostic factors of children with Burkitt's lymphoma in a developing country: the experience of a single centre in Brazil. 34**,** 361-366.
CUTRONA, G., ULIVI, M., FAIS, F., RONCELLA, S. & FERRARINI, M. J. T. J. O. E. M. 1995. Transfection of the c-myc oncogene into normal Epstein-Barr virus-harboring B cells results in new phenotypic and functional features resembling those of Burkitt lymphoma cells and normal centroblasts. 181**,** 699-711.

CYTOLOGY, C. *Burkitt lymphoma - CELL - Atlas of Haematological Cytology* [Online]. Available: http://www.leukemia-cell.org/atlas/index.php?pg=images--mature-b-cell-neoplasms--burkitt-lymphoma#4 [Accessed 6-1 2018].

DANG, C. V. 1999. c-Myc target genes involved in cell growth, apoptosis, and metabolism. *Molecular and cellular biology,* 19**,** 1-11.

DANG, CHI V. 2012. MYC on the Path to Cancer. *Cell,* 149**,** 22-35.

DAVIDS, M. S. & BROWN, J. R. 2014. Ibrutinib: a first in class covalent inhibitor of Bruton's tyrosine kinase. *Future oncology,* 10**,** 957-967.

DAVIS, S. R., MCMAHON, R. J. & COUSINS, R. J. 1998. Metallothionein knockout and transgenic mice exhibit altered intestinal processing of zinc with uniform zinc-dependent zinc transporter-1 expression. *The Journal of nutrition,* 128**,** 825-831.

DE ALBORAN, I. M., O'HAGAN, R. C., GÄRTNER, F., MALYNN, B., DAVIDSON, L., RICKERT, R., RAJEWSKY, K., DEPINHO, R. A. & ALT, F. W. J. I. 2001. Analysis of C-MYC function in normal cells via conditional gene-targeted mutation. 14**,** 45-55.

DE CONINCK, W., GOVAERTS, D., BILA, M., VANSTEENKISTE, G., UYTTEBROECK, A., TOUSSEYN, T. & POLITIS, C. J. C. C. R. 2021. Burkitt lymphoma in children causing an osteolytic lesion in the mandible: A case report. 9**,** 938-943.

DE JONG, M. R. W., LANGENDONK, M., REITSMA, B., HERBERS, P., NIJLAND, M., HULS, G., VAN DEN BERG, A., AMMATUNA, E., VISSER, L. & VAN MEERTEN, T. J. C. 2019. WEE1 inhibition enhances anti-apoptotic dependency as a result of premature mitotic entry and DNA damage. 11**,** 1743.

DECKER, J. M. *B Cell Development* [Online]. Available: http://microvet.arizona.edu/Courses/MIC419/Tutorials/Bcelldevelopment.html [Accessed 22/12 2017].

DESHPANDE, J. D., JOSHI, M. M. & GIRI, P. A. 2013. Zinc: The trace element of major importance in human nutrition and health. *Int J Med Sci Public Health,* 2**,** 1-6.

DHARANIPRAGADA, P. & PAREKH, N. J. P. C. M. 2019. Genome-wide characterization of copy number variations in diffuse large B-cell lymphoma with implications in targeted therapy. 2**,** 246-258.

DHINGRA, U., HIREMATH, G., MENON, V. P., DHINGRA, P., SARKAR, A. & SAZAWAL, S. 2009. Zinc deficiency: descriptive epidemiology and morbidity among preschool children in peri-urban population in Delhi, India. *Journal of health, population, and nutrition,* 27**,** 632.

DHINGRA, U., KISENGE, R., SUDFELD, C. R., DHINGRA, P., SOMJI, S., DUTTA, A., BAKARI, M., DEB, S., DEVI, P. & LIU, E. J. N. E. J. O. M. 2020. Lower-dose zinc for childhood diarrhea—A randomized, multicenter trial. 383**,** 1231-1241.

DI NOIA, J. M. & NEUBERGER, M. S. 2007. Molecular mechanisms of antibody somatic hypermutation. *Annu. Rev. Biochem.,* 76**,** 1-22.

DING, W.-X., NI, H.-M., GAO, W., CHEN, X., KANG, J. H., STOLZ, D. B., LIU, J. & YIN, X.-M. J. M. C. T. 2009. Oncogenic transformation confers a selective susceptibility to the combined suppression of the proteasome and autophagy. 8**,** 2036-2045.

DISSANAYAKA, W., ZHU, X. & ZHANG, C. J. I. J. S. C. R. T. 2017. Effects of Overexpression of C-Myc and Bcl-2 on Viability, Apoptosis and Differentiation of Dental Pulp Stem Cells. 3**,** 046.

DONZELLI, M., BERNARDI, R., NEGRI, C., PROSPERI, E., PADOVAN, L., LAVIALLE, C., BRISON, O. & SCOVASSI, A. I. J. O. 1999. Apoptosis-prone phenotype of human colon carcinoma cells with a high level amplification of the c-myc gene. 18**,** 439-448.

DORSHKIND, K. & RAWLINGS, D. J. 2018. B-Cell development. *Hematology (Seventh Edition).* Elsevier.

DOZZO, M., CAROBOLANTE, F., DONISI, P. M., SCATTOLIN, A., MAINO, E., SANCETTA, R., VIERO, P. & BASSAN, R. 2017. Burkitt lymphoma in adolescents and young adults: management challenges. *Adolescent health, medicine and therapeutics,* 8**,** 11.

DOZZO, M., CAROBOLANTE, F., DONISI, P. M., SCATTOLIN, A., MAINO, E., SANCETTA, R., VIERO, P., BASSAN, R. J. A. H., MEDICINE & THERAPEUTICS 2016. Burkitt lymphoma in adolescents and young adults: management challenges. 11-29.

DRAPER, J. E., SROCZYNSKA, P., TSOULAKI, O., LEONG, H. S., FADLULLAH, M. Z., MILLER, C., KOUSKOFF, V. & LACAUD, G. 2016. RUNX1B expression is highly heterogeneous and distinguishes megakaryocytic and erythroid lineage fate in adult mouse hematopoiesis. *PLoS genetics,* 12**,** e1005814.

DUAN, H., HECKMAN, C. A. & BOXER, L. M. J. O. 2007. The immunoglobulin heavy-chain gene 3' enhancers deregulate bcl-2 promoter usage in t (14; 18) lymphoma cells. 26**,** 2635-2641.

DUFFY, M. J., O'GRADY, S., TANG, M. & CROWN, J. J. C. T. R. 2021. MYC as a target for cancer treatment. 94**,** 102154.

DUGAN, J. P., COLEMAN, C. B. & HAVERKOS, B. 2019. Opportunities to target the life cycle of Epstein-Barr virus (EBV) in EBV-associated lymphoproliferative disorders. *Frontiers in oncology,* 9**,** 127.

DUNLEAVY, K. 2018. Approach to the diagnosis and treatment of adult Burkitt's lymphoma. *Journal of Oncology Practice,* 14**,** 665-671.

DUNLEAVY, K., LITTLE, R. F. & WILSON, W. H. 2016. Update on Burkitt lymphoma. *Hematology/Oncology Clinics,* 30**,** 1333-1343.

EBERHARDY, S. R. & FARNHAM, P. J. 2001. c-Myc mediates activation of the cad promoter via a post-RNA polymerase II recruitment mechanism. *Journal of Biological Chemistry,* 276**,** 48562-48571.

ECKHARDT, L. A. J. T. F. J. 1992. Immunoglobulin gene expression only in the right cells at the right time. 6**,** 2553-2560.

EDRY, E., AZULAY-DEBBY, H. & MELAMED, D. 2008. TOLL-like receptor ligands stimulate aberrant class switch recombination in early B cell precursors. *International immunology,* 20**,** 1575-1585.

EICHENAUER, D. A. & ENGERT, A. J. H., THE AMERICAN SOCIETY OF HEMATOLOGY EDUCATION PROGRAM BOOK 2017. Nodular lymphocyte-predominant Hodgkin lymphoma: a unique disease deserving unique management. 2017**,** 324-328.

EJIRI, S.-I. J. B., BIOTECHNOLOGY, & BIOCHEMISTRY 2002. Moonlighting functions of polypeptide elongation factor 1: from actin bundling to zinc finger protein R1-associated nuclear localization. 66**,** 1-21.

EL-SHAFEI, M., KAMAL, A., SOLIMAN, H., EL SHAYEB, F., BAQUI, A., FARAGALLA, S. & SABRY, M. J. T. J. O. T. E. P. H. A. 1988. Effect of oral zinc supplementation on the cell mediated immunity in lepromatous leprosy. 63**,** 311-336.

FALKO FEND, L. Q.-M. 2018. *Hematopathology*

FANZO, J. 2012. The nutrition challenge in sub-Saharan Africa. United Nations Development Programme, Regional Bureau for Africa.

FARAMARZ NAEIM, P. N. R., SOPHIE X. SONG, WAYNE W. GRODY 2013. 39 - Burkitt Lymphoma. *Atlas of Hematopathology***,** 465-471.

FARRELL, P. J., ALLAN, G. J., SHANAHAN, F., VOUSDEN, K. & CROOK, T. 1991. p53 is frequently mutated in Burkitt's lymphoma cell lines. *The EMBO journal,* 10**,** 2879-2887.

FAYAD, L., THOMAS, D. & ROMAGUERA, J. 2007. Update of the MD Anderson Cancer Center experience with hyper-CVAD and rituximab for the treatment of mantle cell and Burkitt-type lymphomas. *Clinical Lymphoma and Myeloma,* 8**,** S57-S62.

FEAR, D. J. 2013. Mechanisms regulating the targeting and activity of activation induced cytidine deaminase. *Current opinion in immunology,* 25**,** 619-628.

FEINS, S., KONG, W., WILLIAMS, E. F., MILONE, M. C. & FRAIETTA, J. A. 2019. An introduction to chimeric antigen receptor (CAR) T-cell immunotherapy for human cancer. *American journal of hematology,* 94**,** S3-S9.

FELDMAN, A. L., PITTALUGA, S. & JAFFE, E. S. 2006. Classification and histopathology of the lymphomas. *The lymphomas.* Elsevier Inc.

FELSHER, D. W., ZETTERBERG, A., ZHU, J., TLSTY, T. & BISHOP, J. M. J. P. O. T. N. A. O. S. 2000. Overexpression of MYC causes p53-dependent G2 arrest of normal fibroblasts. 97**,** 10544-10548.

FENNELL, D., CHACKO, A. & MUTTI, L. J. O. 2008. BCL-2 family regulation by the 20S proteasome inhibitor bortezomib. 27**,** 1189-1197.

FENTON, S., LUONG, Q., SARAFEIM, A., MUSTARD, K., POUND, J., DESMOND, J., GORDON, J., DRAYSON, M. & BUNCE, C. 2003. Fibrates and medroxyprogesterone acetate induce apoptosis of primary Burkitt's lymphoma cells and cell lines: potential for applying old drugs to a new disease. *Leukemia,* 17**,** 568-575.

FERREIRA, J. P., PEACOCK, R. W., LAWHORN, I. E., WANG, C. L. J. S. & BIOLOGY, S. 2011. Modulating ectopic gene expression levels by using retroviral vectors equipped with synthetic promoters. 5**,** 131-138.

FERRERI, A. J. & ZUCCA, E. 2007. Marginal-zone lymphoma. *Critical reviews in oncology/hematology,* 63**,** 245-256.

FERRI, F. F. 2021. *Ferri's Clinical Advisor 2022, E-Book*, Elsevier Health Sciences.

FERRY, J. A. 2006. Burkitt's lymphoma: clinicopathologic features and differential diagnosis. *The Oncologist,* 11**,** 375-383.

FIRDOUS, S. J. L. P. L. 2018. Development and imaging of zinc oxide nanorods as a photosensitizer for the diagnosis and treatment of cancer using lasers1. 15**,** 095604.

FITZSIMMONS, L., CARTLIDGE, R., CHANG, C., SEJIC, N., GALBRAITH, L. C., SURAWEERA, C. D., CROOM-CARTER, D., DEWSON, G., TIERNEY, R. J., BELL, A. I. J. C. D. & DIFFERENTIATION 2020. EBV BCL-2 homologue BHRF1 drives chemoresistance and lymphomagenesis by inhibiting multiple cellular pro-apoptotic proteins. 27**,** 1554-1568.

FLAHERTY, D. 2014. *Immunology for Pharmacy-E-Book*, Elsevier Health Sciences.

FOON, K. A., TAKESHITA, K. & ZINZANI, P. L. 2012. Novel therapies for aggressive B-cell lymphoma. *Advances in hematology,* 2012.

FORDE, S., MATTHEWS, J. D., JAHANGIRI, L., LEE, L. C., PROKOPH, N., MALCOLM, T. I., GIGER, O. T., BELL, N., BLAIR, H. & O'MARCAIGH, A. J. B. J. O. H. 2021. Paediatric Burkitt lymphoma patient-derived xenografts capture disease characteristics over time and are a model for therapy. 192**,** 354-365.

FRANKLIN, R. B. & COSTELLO, L. C. 2009. The important role of the apoptotic effects of zinc in the development of cancers. *Journal of cellular biochemistry,* 106**,** 750-757.

FRAPPIER, L. J. V. 2012. Contributions of Epstein–Barr nuclear antigen 1 (EBNA1) to cell immortalization and survival. 4**,** 1537-1547.

FRAZER, J. K., LI, K. J., GALARDY, P. J., PERKINS, S. L., AUPERIN, A., ANDERSON, J. R., PINKERTON, R., BUXTON, A., GROSS, T. G. & MICHON, J. J. B. J. O. H. 2019. Excellent outcomes in children and adolescents with CNS+ Burkitt lymphoma or other mature B-NHL using only intrathecal and systemic chemoimmunotherapy: results from FAB/LMB96 and COG ANHL01P1. 185**,** 374.

GABORIAUD, C., THIELENS, N. M., GREGORY, L. A., ROSSI, V., FONTECILLA-CAMPS, J. C. & ARLAUD, G. J. 2004. Structure and activation of the C1 complex of complement: unraveling the puzzle. *Trends in immunology,* 25**,** 368-373.

GALANIS, A. & LEVIS, M. 2015. Inhibition of c-Kit by tyrosine kinase inhibitors. *Haematologica,* 100**,** e77-e79.

GEQUELIN, L. C. F., RIEDIGER, I. N., NAKATANI, S. M., BIONDO, A. W. & BONFIM, C. M. 2011. Epstein-Barr virus: general factors, virus-related diseases and measurement of viral load after transplant. *Revista brasileira de hematologia e hemoterapia,* 33**,** 383-388.

GERMINI, D., TSFASMAN, T., KLIBI, M., EL-AMINE, R., PICHUGIN, A., IAROVAIA, O., BILHOU-NABERA, C., SUBRA, F., SAADA, Y. B. & SUKHANOVA, A. 2017. HIV Tat induces a prolonged MYC relocalization next to IGH in circulating B-cells. *Leukemia,* 31**,** 2515.

GHASEMI, A., ZAHEDIASL, S., HOSSEINI-ESFAHANI, F. & AZIZI, F. 2012. Reference values for serum zinc concentration and prevalence of zinc deficiency in adult Iranian subjects. *Biological trace element research,* 149**,** 307-314.

GOGIA, A., DAS, C. K., KUMAR, L., SHARMA, A., TIWARI, A., SHARMA, M. & MALLICK, S. J. S. A. J. O. C. 2018. Diffuse large B-cell lymphoma: an institutional analysis. 7**,** 200-202.

GOLSTEIN, P. & GRIFFITHS, G. M. 2018. An early history of T cell-mediated cytotoxicity. *Nature Reviews Immunology,* 18**,** 527-535.

GOOD-JACOBSON, K. L. 2014. Regulation of germinal center, B-cell memory, and plasma cell formation by histone modifiers. *Frontiers in immunology,* 5.

GOODSELL, D. S. 1999. The molecular perspective: the ras oncogene. *The oncologist,* 4**,** 263-264.

GOPAL, S. & GROSS, T. G. 2018. How I treat Burkitt lymphoma in children, adolescents, and young adults in sub-Saharan Africa. *Blood,* 132**,** 254-263.

GOPAL, S., WOOD, W. A., LEE, S. J., SHEA, T. C., NARESH, K. N., KAZEMBE, P. N., CASPER, C., HESSELING, P. B. & MITSUYASU, R. T. J. B., THE JOURNAL OF THE AMERICAN SOCIETY OF HEMATOLOGY 2012. Meeting the challenge of hematologic malignancies in sub-Saharan Africa. 119**,** 5078-5087.

GORDON, S. J., SALEQUE, S. & BIRSHTEIN, B. K. J. T. J. O. I. 2003. Yin Yang 1 is a lipopolysaccharide-inducible activator of the murine 3' Igh enhancer, hs3. 170**,** 5549-5557.

GRAHAM, B. S. & LYNCH, D. T. 2021. Burkitt Lymphoma. *StatPearls [Internet].* StatPearls Publishing.

GREGORY, C. D. & MILNER, A. E. J. I. J. O. C. 1994. Regulation of cell survival in burkitt lymphoma: implications from studies of apoptosis following cold-shock treatment. 57**,** 419-426.

GREGORY, M. A. & HANN, S. R. 2000. c-Myc proteolysis by the ubiquitin-proteasome pathway: stabilization of c-Myc in Burkitt's lymphoma cells. *Molecular and cellular biology,* 20**,** 2423-2435.

GREGORY, M. A., HANN, S. R. J. M. & BIOLOGY, C. 2000. c-Myc proteolysis by the ubiquitin-proteasome pathway: stabilization of c-Myc in Burkitt's lymphoma cells. 20**,** 2423-2435.

GROGG, K., MILLER, R. & DOGAN, A. 2007. HIV infection and lymphoma. *Journal of Clinical Pathology,* 60**,** 1365-1372.

GRÖMMINGER, S., MAUTNER, J. & BORNKAMM, G. W. J. B. J. O. H. 2012. Burkitt lymphoma: the role of Epstein-Barr virus revisited. 156**,** 719-729.

GUPTA, S., BRAZIER, A., LOWE, N. J. J. O. H. N. & DIETETICS 2020. Zinc deficiency in low-and middle-income countries: prevalence and approaches for mitigation. 33**,** 624-643.

GUPTA, S., HOWARD, S. C., HUNGER, S. P., ANTILLON, F. G., METZGER, M. L., ISRAELS, T., HARIF, M. & RODRIGUEZ-GALINDO, C. 2015. Treating childhood cancer in low-and middle-income countries. *Cancer. Washington DC: The World Bank Group***,** 121-46.

GUTIÉRREZ, M. I., CHERNEY, B., HUSSAIN, A., MOSTOWSKI, H., TOSATO, G., MAGRATH, I. & BHATIA, K. J. C. R. 1999. Bax is frequently compromised in Burkitt's lymphomas with irreversible resistance to Fas-induced apoptosis. 59**,** 696-703.

HA, J.-H., PRELA, O., CARPIZO, D. R. & LOH, S. N. J. F. I. M. B. 2022. p53 and Zinc: A Malleable Relationship. 9.

HAASE, H., OVERBECK, S. & RINK, L. J. E. G. 2008. Zinc supplementation for the treatment or prevention of disease: current status and future perspectives. 43**,** 394-408.

HABESHAW, G., YAO, Q., BELL, A., MORTON, D. & RICKINSON, A. 1999. Epstein-Barr virus nuclear antigen 1 sequences in endemic and sporadic Burkitt's lymphoma reflect virus strains prevalent in different geographic areas. *Journal of virology,* 73**,** 965-975.

HÄMMERL, L., COLOMBET, M., ROCHFORD, R., OGWANG, D. M. & PARKIN, D. M. 2019. The burden of Burkitt lymphoma in Africa. *Infectious agents and cancer,* 14**,** 1-6.

HAPGOOD, G. & SAVAGE, K. J. J. B., THE JOURNAL OF THE AMERICAN SOCIETY OF HEMATOLOGY 2015. The biology and management of systemic anaplastic large cell lymphoma. 126**,** 17-25.
HARA, T., TAKEDA, T.-A., TAKAGISHI, T., FUKUE, K., KAMBE, T. & FUKADA, T. 2017. Physiological roles of zinc transporters: molecular and genetic importance in zinc homeostasis. *The Journal of Physiological Sciences,* 67**,** 283-301.
HASSE, B., HANNAN, M., KELLER, P. M., MAURER, F. P., SOMMERSTEIN, R., MERTZ, D., WAGNER, D., FERNÁNDEZ-HIDALGO, N., NOMURA, J. & MANFRIN, V. 2020. International society of cardiovascular infectious diseases guidelines for the diagnosis, treatment and prevention of disseminated Mycobacterium chimaera infection following cardiac surgery with cardiopulmonary bypass. *Journal of Hospital Infection,* 104**,** 214-235.
HIDESHIMA, T., RICHARDSON, P. G. & ANDERSON, K. C. J. M. C. T. 2011. Mechanism of action of proteasome inhibitors and deacetylase inhibitors and the biological basis of synergy in multiple myeloma. 10**,** 2034-2042.
HO, E. 2004. Zinc deficiency, DNA damage and cancer risk. *The Journal of nutritional biochemistry,* 15**,** 572-578.
HO, J. S., MA, W., MAO, D. Y. & BENCHIMOL, S. 2005. p53-Dependent transcriptional repression of c-myc is required for G1 cell cycle arrest. *Molecular and cellular biology,* 25**,** 7423-7431.
HOFFBRAND, A. V. & MOSS, P. A. 2015. *Hoffbrand's essential haematology*, John Wiley & Sons.
HOFFMAN, R., BENZ, E. J., SILBERSTEIN, L. E., HESLOP, H., WEITZ, J. & ANASTASI, J. 2017. *Hematology: Basic Principles and Practice E-Book*, Elsevier Health Sciences.
HOFFMAN, W. H., BIADE, S., ZILFOU, J. T., CHEN, J. & MURPHY, M. J. J. O. B. C. 2002. Transcriptional repression of the anti-apoptoticsurvivin gene by wild type p53. 277**,** 3247-3257.
HONJO, T., KINOSHITA, K. & MURAMATSU, M. 2002. Molecular mechanism of class switch recombination: linkage with somatic hypermutation. *Annual review of immunology,* 20**,** 165-196.
HU, H., KANDA, K., ZHANG, L. & BOXER, L. J. L. 2007. Activation of the c-myc p1 promoter in Burkitt's lymphoma by the hs3 immunoglobulin heavy-chain gene enhancer. 21**,** 747-753.
HUA, C., ZORN, S., JENSEN, J., COUPLAND, R., KO, H. S., WRIGHT, J. & BAKHSHI, A. J. O. R. 1988. Consequences of the t (14; 18) chromosomal translocation in follicular lymphoma: deregulated expression of a chimeric and mutated BCL-2 gene. 2**,** 263-275.
HUANG, H., LIU, Z.-L., ZENG, H., ZHANG, S.-H., HUANG, C.-S., XU, H.-Y., WU, Y., ZENG, S.-T., XIONG, F. & YANG, W.-P. J. C. M. J. 2015. Clinicopathological study of sporadic Burkitt lymphoma in children. 128**,** 510-514.
HUGLI, T. E. 1986. Biochemistry and biology of anaphylatoxins. *Complement,* 3**,** 111-127.
HUI-YUEN, J., MCALLISTER, S., KOGANTI, S., HILL, E. & BHADURI-MCINTOSH, S. 2011. Establishment of Epstein-Barr virus growth-transformed lymphoblastoid cell lines. *JoVE (Journal of Visualized Experiments)***,** e3321.
HUNT, K. E. & REICHARD, K. K. 2008. Diffuse large B-cell lymphoma. *Archives of pathology & laboratory medicine,* 132**,** 118-124.
HWANG, J. K., ALT, F. W. & YEAP, L.-S. 2015. Related mechanisms of antibody somatic hypermutation and class switch recombination. *Microbiology spectrum,* 3.
IFANDI, V. & AL-RUBEAI, M. J. C. 2003. Stable transfection of CHO cells with the c-myc gene results in increased proliferation rates, reduces serum dependency, and induces anchorage independence. 41**,** 1-10.
INOUE, A., SAWATA, S. Y., TAIRA, K. & WADHWA, R. J. P. O. T. N. A. O. S. 2007. Loss-of-function screening by randomized intracellular antibodies: identification of hnRNP-K as a potential target for metastasis. 104**,** 8983-8988.
INTERMESOLI, T., RAMBALDI, A., ROSSI, G., DELAINI, F., ROMANI, C., POGLIANI, E. M., PAGANI, C., ANGELUCCI, E., TERRUZZI, E. & LEVIS, A. J. H. 2013. High cure rates in Burkitt lymphoma

and leukemia: a Northern Italy Leukemia Group study of the German short intensive rituximab-chemotherapy program. 98**,** 1718.
IQBAL, J., SANGER, W. G., HORSMAN, D. E., ROSENWALD, A., PICKERING, D. L., DAVE, B., DAVE, S., XIAO, L., CAO, K. & ZHU, Q. 2004. BCL2 translocation defines a unique tumor subset within the germinal center B-cell-like diffuse large B-cell lymphoma. *The American journal of pathology,* 165**,** 159-166.
IVANOVS, A., RYBTSOV, S., NG, E. S., STANLEY, E. G., ELEFANTY, A. G. & MEDVINSKY, A. 2017. Human haematopoietic stem cell development: from the embryo to the dish. *Development,* 144**,** 2323-2337.
IWASATO, T., SHIMIZU, A., HONJO, T. & YAMAGISHI, H. 1990. Circular DNA is excised by immunoglobulin class switch recombination. *Cell,* 62**,** 143-149.
JACKSON, M. 1989. Physiology of zinc: general aspects. *Zinc in human biology.* Springer.
JAKOBSEN, L. H., ELLIN, F., SMELAND, K. B., WÄSTERLID, T., CHRISTENSEN, J. H., JØRGENSEN, J. M., JOSEFSSON, P. L., ØVLISEN, A. K., HOLTE, H. & BLAKER, Y. N. J. B. J. O. H. 2020. Minimal relapse risk and early normalization of survival for patients with Burkitt lymphoma treated with intensive immunochemotherapy: an international study of 264 real-world patients. 189**,** 661-671.
JAMISON, D. T. 2006. Disease and mortality in sub-Saharan Africa.
JANEWAY, C. A., TRAVERS, P., WALPORT, M. & SHLOMCHIK, M. J. 2005. Immunobiology: the immune system in health and disease.
JANEWAY JR, C. A., TRAVERS, P., WALPORT, M. & SHLOMCHIK, M. J. 2001. B-cell activation by armed helper T cells.
JARCZAK, J., KOŚCIUCZUK, E. M., LISOWSKI, P., STRZAŁKOWSKA, N., JÓŹWIK, A., HORBAŃCZUK, J., KRZYŻEWSKI, J., ZWIERZCHOWSKI, L. & BAGNICKA, E. 2013. Defensins: natural component of human innate immunity. *Human immunology,* 74**,** 1069-1079.
JARRARD, D. F. J. A. O. O. 2005. Does zinc supplementation increase the risk of prostate cancer? 123**,** 102-103.
JAY, J., BRAY, B., QI, Y., IGBINIGIE, E., WU, H., LI, J. & REN, G. 2018. IgG antibody 3D structures and dynamics. *Antibodies,* 7**,** 18.
JEONG, W.-J., RO, E. J. & CHOI, K.-Y. 2018. Interaction between Wnt/β-catenin and RAS-ERK pathways and an anti-cancer strategy via degradations of β-catenin and RAS by targeting the Wnt/β-catenin pathway. *NPJ Precision oncology,* 2**,** 1-10.
JIANG, Y., SOUTHAM, A. D., TROVA, S., BEKE, F., ALHAZMI, B., FRANCIS, T., RADOTRA, A., DI MAIO, A., DRAYSON, M. T. & BUNCE, C. M. 2022. Valproic acid disables the Nrf2 anti-oxidant response in acute myeloid leukaemia cells enhancing reactive oxygen species-mediated killing. *British journal of cancer,* 126**,** 275-286.
JIWOK, J. C., ADEBOWALE, A. S., WILSON, I., KANCHERLA, V. & UMEOKONKWO, C. D. 2021. Patterns of diarrhoeal disease among under-five children in Plateau State, Nigeria, 2013–2017. *BMC Public Health,* 21**,** 1-9.
JOHN, L. B. & WARD, A. C. 2011. The Ikaros gene family: transcriptional regulators of hematopoiesis and immunity. *Molecular immunology,* 48**,** 1272-1278.
JOHNSON, B. E., BATTEY, J., LINNOILA, I., BECKER, K. L., MAKUCH, R. W., SNIDER, R. H., CARNEY, D. N. & MINNA, J. D. J. T. J. O. C. I. 1986. Changes in the phenotype of human small cell lung cancer cell lines after transfection and expression of the c-myc proto-oncogene. 78**,** 525-532.
JULIEN, E., EL OMAR, R. & TAVIAN, M. 2016. Origin of the hematopoietic system in the human embryo. *FEBS letters,* 590**,** 3987-4001.
KALE, J., OSTERLUND, E. J., ANDREWS, D. W. J. C. D. & DIFFERENTIATION 2018. BCL-2 family proteins: changing partners in the dance towards death. 25**,** 65-80.

KAMBE, T., TSUJI, T., HASHIMOTO, A. & ITSUMURA, N. 2015. The physiological, biochemical, and molecular roles of zinc transporters in zinc homeostasis and metabolism. *Physiological reviews,* 95**,** 749-784.

KANDA, K., HU, H.-M., ZHANG, L., GRANDCHAMPS, J. & BOXER, L. M. J. J. O. B. C. 2000. NF-κB activity is required for the deregulation of c-myc expression by the immunoglobulin heavy chain enhancer. 275**,** 32338-32346.

KAO, E. Y., MUKKAMALLA, S. K. R. & LYNCH, D. T. 2018. ALK negative anaplastic large cell lymphoma.

KASPRZYK, M. E., ŁOSIEWSKI, W., PODRALSKA, M., KAZIMIERSKA, M., SURA, W. & DZIKIEWICZ-KRAWCZYK, A. J. E. J. O. P. 2021. 7-[[(4-methyl-2-pyridinyl) amino](2-pyridinyl) methyl]-8-quinolinol (compound 30666) inhibits enhancer activity and reduces B-cell lymphoma growth–A question of specificity. 910**,** 174505.

KELEMEN, K., BRAZIEL, R. M., GATTER, K., BAKKE, T. C., OLSON, S. & FAN, G. 2010. Immunophenotypic variations of Burkitt lymphoma. *American journal of clinical pathology,* 134**,** 127-138.

KELLY, G., BELL, A. & RICKINSON, A. J. N. M. 2002. Epstein–Barr virus–associated Burkitt lymphomagenesis selects for downregulation of the nuclear antigen EBNA2. 8**,** 1098-1104.

KELLY, G. L., GRABOW, S., GLASER, S. P., FITZSIMMONS, L., AUBREY, B. J., OKAMOTO, T., VALENTE, L. J., ROBATI, M., TAI, L., FAIRLIE, W. D. J. G. & DEVELOPMENT 2014. Targeting of MCL-1 kills MYC-driven mouse and human lymphomas even when they bear mutations in p53. 28**,** 58-70.

KELLY, G. L., LONG, H. M., STYLIANOU, J., THOMAS, W. A., LEESE, A., BELL, A. I., BORNKAMM, G. W., MAUTNER, J., RICKINSON, A. B. & ROWE, M. J. P. P. 2009. An Epstein-Barr virus anti-apoptotic protein constitutively expressed in transformed cells and implicated in burkitt lymphomagenesis: the Wp/BHRF1 link. 5**,** e1000341.

KELLY, G. L., STYLIANOU, J., RASAIYAAH, J., WEI, W., THOMAS, W., CROOM-CARTER, D., KOHLER, C., SPANG, R., WOODMAN, C. & KELLAM, P. J. J. O. V. 2013. Different patterns of Epstein-Barr virus latency in endemic Burkitt lymphoma (BL) lead to distinct variants within the BL-associated gene expression signature. 87**,** 2882-2894.

KENNEDY, G., KOMANO, J. & SUGDEN, B. J. P. O. T. N. A. O. S. 2003. Epstein-Barr virus provides a survival factor to Burkitt's lymphomas. 100**,** 14269-14274.

KENNEY, S. C. & MERTZ, J. E. Regulation of the latent-lytic switch in Epstein–Barr virus. Seminars in cancer biology, 2014. Elsevier, 60-68.

KETZER, F., ABDELRASOUL, H., VOGEL, M., MARIENFELD, R., MÜSCHEN, M., JUMAA, H., WIRTH, T. & USHMOROV, A. J. O. 2022. CCND3 is indispensable for the maintenance of B-cell acute lymphoblastic leukemia. 11**,** 1-12.

KHARAZMI, J., MOSHFEGH, C. & BRODY, T. 2012. Identification of cis-Regulatory Elements in the dmyc Gene of Drosophila Melanogaster. *Gene regulation and systems biology,* 6**,** GRSB. S8044.

KIM, D. W., UETSUKI, T., KAZIRO, Y., YAMAGUCHI, N. & SUGANO, S. J. G. 1990. Use of the human elongation factor 1α promoter as a versatile and efficient expression system. 91**,** 217-223.

KING, J. C. 2011. Zinc: an essential but elusive nutrient–. *The American journal of clinical nutrition,* 94**,** 679S-684S.

KING, J. J. & LARIJANI, M. 2017. A novel Regulator of Activation-induced Cytidine Deaminase/APOBeCs in immunity and Cancer: Schrödinger's CATalytic Pocket. *Frontiers in Immunology,* 8.

KIRKIN, V., JOOS, S. & ZÖRNIG, M. J. B. E. B. A.-M. C. R. 2004. The role of Bcl-2 family members in tumorigenesis. 1644**,** 229-249.

KLANOVA, M., KAZANTSEV, D., POKORNA, E., ZIKMUND, T., KAROLOVA, J., BEHOUNEK, M., RENESOVA, N., SOVILJ, D., KELEMEN, C. D. & HELMAN, K. J. M. C. T. 2022. Anti-apoptotic

MCL1 protein represents critical survival molecule for most Burkitt lymphomas and BCL2-negative diffuse large B-cell lymphomas. 21**,** 89-99.
KLEIN, L., KYEWSKI, B., ALLEN, P. M. & HOGQUIST, K. A. 2014. Positive and negative selection of the T cell repertoire: what thymocytes see (and don't see). *Nature Reviews Immunology,* 14**,** 377.
KLINKEN, S. P. 2002. Red blood cells. *The international journal of biochemistry & cell biology,* 34**,** 1513-1518.
KLUMB, C. E. N. P., RESENDE, L. M. M. D., TAJARA, E. H., BERTELLI, E. C. P., RUMJANEK, V. M. & MAIA, R. C. 2001. p53 gene analysis in childhood B non-Hodgkin's lymphoma. *Sao Paulo Medical Journal,* 119**,** 212-215.
KOGAN, S. & CARPIZO, D. R. 2018. Zinc metallochaperones as mutant p53 reactivators: a new paradigm in cancer therapeutics. *Cancers,* 10**,** 166.
KOMATSU, N., KAWASE-KOGA, Y., MORI, Y., KAMIKUBO, Y., KUROKAWA, M. & TAKATO, T. 2013. Human immunodeficiency virus-associated Burkitt lymphoma in a Japanese patient with early submandibular swelling: a case report. *BMC Research Notes,* 6**,** 1-5.
KONKAY, K., PAUL, T. R., UPPIN, S. G., RAO, D. R. J. I. J. O. M. & ONCOLOGY, P. 2016. Hodgkin lymphoma: A clinicopathological and immunophenotypic study. 37**,** 59-65.
KUMARI, D., NAIR, N. & BEDWAL, R. S. 2015. Dietary Zinc Deficiency and Testicular Apoptosis. *Handbook of Fertility.* Elsevier.
KUROSAKI, T., KOMETANI, K. & ISE, W. 2015. Memory B cells. *Nature Reviews Immunology,* 15**,** 149.
KVANSAKUL, M., WEI, A. H., FLETCHER, J. I., WILLIS, S. N., CHEN, L., ROBERTS, A. W., HUANG, D. C. & COLMAN, P. M. J. P. P. 2010. Structural basis for apoptosis inhibition by Epstein-Barr virus BHRF1. 6**,** e1001236.
LAI, A. Y. & KONDO, M. 2006. Asymmetrical lymphoid and myeloid lineage commitment in multipotent hematopoietic progenitors. *The Journal of experimental medicine,* 203**,** 1867-1873.
LAI, A. Y. & KONDO, M. T and B lymphocyte differentiation from hematopoietic stem cell. Seminars in immunology, 2008. Elsevier, 207-212.
LAMBERTI, L. M., WALKER, C. L. F., TANEJA, S., MAZUMDER, S. & BLACK, R. E. 2015. Adherence to zinc supplementation guidelines for the treatment of diarrhea among children under–five in Uttar Pradesh, India. *Journal of global health,* 5.
LASSMANN, H., NIEDOBITEK, G., ALOISI, F., MIDDELDORP, J. M. & BRAIN, N. E. W. G. J. 2011. Epstein–Barr virus in the multiple sclerosis brain: a controversial issue—report on a focused workshop held in the Centre for Brain Research of the Medical University of Vienna, Austria. 134**,** 2772-2786.
LAZZERINI, M. 2016. Oral zinc provision in acute diarrhea. *Current opinion in clinical nutrition and metabolic care,* 19**,** 239-243.
LEE, S., SYED, N., TAYLOR, J., SMITH, P., GRIFFIN, B., BAENS, M., BAI, M., BOURANTAS, K., STEBBING, J. & NARESH, K. J. B. J. O. C. 2010. DUSP16 is an epigenetically regulated determinant of JNK signalling in Burkitt's lymphoma. 103**,** 265-274.
LEFFLER, E. M., BAND, G., BUSBY, G. B., KIVINEN, K., LE, Q. S., CLARKE, G. M., BOJANG, K. A., CONWAY, D. J., JALLOW, M. & SISAY-JOOF, F. 2017. Resistance to malaria through structural variation of red blood cell invasion receptors. *Science,* 356**,** eaam6393.
LEMM, I., ROSS, J. J. M. & BIOLOGY, C. 2002. Regulation of c-myc mRNA decay by translational pausing in a coding region instability determinant. 22**,** 3959-3969.
LEVENS, D. J. J. O. T. N. C. I. M. 2008. How the c-myc promoter works and why it sometimes does not. 2008**,** 41-43.
LI, S., YOUNG, K. H. & MEDEIROS, L. J. 2018. Diffuse large B-cell lymphoma. *Pathology,* 50**,** 74-87.

LI, Y., CHOI, P. S., CASEY, S. C., DILL, D. L. & FELSHER, D. W. 2014. MYC through miR-17-92 suppresses specific target genes to maintain survival, autonomous proliferation, and a neoplastic state. *Cancer cell,* 26**,** 262-272.

LI, Y., SUN, X.-X., QIAN, D. Z. & DAI, M.-S. 2020. Molecular crosstalk between MYC and HIF in cancer. *Frontiers in Cell and Developmental Biology***,** 1319.

LI, Z., YIN, X., LYU, C., WANG, T., WANG, W., ZHANG, J., WANG, J., WANG, Z., HAN, C., ZHANG, R. J. B. & PHARMACOTHERAPY 2023. Zinc oxide nanoparticles induce toxicity in diffuse large B-cell lymphoma cell line U2932 via activating PINK1/Parkin-mediated mitophagy. 164**,** 114988.

LIN, C. Y., LOVÉN, J., RAHL, P. B., PARANAL, R. M., BURGE, C. B., BRADNER, J. E., LEE, T. I. & YOUNG, R. A. J. C. 2012. Transcriptional amplification in tumor cells with elevated c-Myc. 151**,** 56-67.

LIN, Z., WANG, X., STRONG, M. J., CONCHA, M., BADDOO, M., XU, G., BARIBAULT, C., FEWELL, C., HULME, W. & HEDGES, D. J. J. O. V. 2013. Whole-genome sequencing of the Akata and Mutu Epstein-Barr virus strains. 87**,** 1172-1182.

LINCH, D. C. 2012. Burkitt lymphoma in adults. *British journal of haematology,* 156**,** 693-703.

LOH, S. N. J. M. 2010. The missing zinc: p53 misfolding and cancer. 2**,** 442-449.

LOMBARDO, K. A., COFFEY, D. G., MORALES, A. J., CARLSON, C. S., TOWLERTON, A. M., GERDTS, S. E., NKRUMAH, F. K., NEEQUAYE, J., BIGGAR, R. J. & OREM, J. J. B. A. 2017. High-throughput sequencing of the B-cell receptor in African Burkitt lymphoma reveals clues to pathogenesis. 1**,** 535-544.

LOVE, C., SUN, Z., JIMA, D., LI, G., ZHANG, J., MILES, R., RICHARDS, K. L., DUNPHY, C. H., CHOI, W. W. & SRIVASTAVA, G. J. N. G. 2012a. The genetic landscape of mutations in Burkitt lymphoma. 44**,** 1321-1325.

LOVE, C. L., JIMA, D., SUN, Z., MILES, R. R., DUNPHY, C. H., CHOI, W. W., AU, W. Y., SRIVASTAVA, G., LUGAR, P. & RIZZIERI, D. A. 2012b. ID3 Is a Novel Tumor Suppressor Gene in Burkitt Lymphom. *Blood,* 120**,** 898.

LUENGAS, S. L. P., MARIN, G. H., RIVERA, L., TARDITTI, A., ROQUE, G. & MANSILLA, E. 2015. Zinc oxide nanoparticles and photodynamic therapy for the treatment of B-chronic lymphocytic leukemia. *Leukemias-Updates and New Insights.* IntechOpen.

LUMSDEN, J. M., MCCARTY, T., PETINIOT, L. K., SHEN, R., BARLOW, C., WYNN, T. A., MORSE, H. C., GEARHART, P. J., WYNSHAW-BORIS, A. & MAX, E. E. 2004. Immunoglobulin class switch recombination is impaired in Atm-deficient mice. *Journal of Experimental Medicine,* 200**,** 1111-1121.

MABUCHI, S., HIJIOKA, F., WATANABE, T., YANAGI, Y., OKUNO, Y., MASUD, H. A. A., SATO, Y., MURATA, T. & KIMURA, H. J. C. 2021. Role of epstein–barr virus c promoter deletion in diffuse large b cell lymphoma. 13**,** 561.

MACDONALD, R. S. 2000. The role of zinc in growth and cell proliferation. *The Journal of nutrition,* 130**,** 1500S-1508S.

MAGRATH, I. 2009. Lessons from clinical trials in African Burkitt lymphoma. *Current Opinion in Oncology,* 21**,** 462-468.

MAGRATH, I. 2012. Epidemiology: clues to the pathogenesis of Burkitt lymphoma. *British journal of haematology,* 156**,** 744-756.

MAJUMDER, P. & BAUMEISTER, W. J. B. C. 2020. Proteasomes: unfoldase-assisted protein degradation machines. 401**,** 183-199.

MALYNN, B. A., DE ALBORAN, I. M., O'HAGAN, R. C., BRONSON, R., DAVIDSON, L., DEPINHO, R. A. & ALT, F. W. 2000. N-myc can functionally replace c-myc in murine development, cellular growth, and differentiation. *Genes & development,* 14**,** 1390-1399.

MANIS, J. P., TIAN, M. & ALT, F. W. 2002. Mechanism and control of class-switch recombination. *Trends in immunology,* 23**,** 31-39.

MARSHALL, R. S. & VIERSTRA, R. D. J. F. I. M. B. 2019. Dynamic regulation of the 26S proteasome: from synthesis to degradation. 6**,** 40.
MÅRTENSSON, I.-L., ALMQVIST, N., GRIMSHOLM, O. & BERNARDI, A. I. 2010. The pre-B cell receptor checkpoint. *FEBS letters,* 584**,** 2572-2579.
MARX, A., GALILEE, M. & ALIAN, A. 2015. Zinc enhancement of cytidine deaminase activity highlights a potential allosteric role of loop-3 in regulating APOBEC3 enzymes. *Scientific reports,* 5.
MATON, D., HOPKINS, J., MCLAUGHLIN, C. W., JOHNSON, S., WARNER, M., LAHART, D., WRIGHT, J. & DEEP, V. K. 1997. Human Biology and Health. Englewood Cliffs, New Jersey, US. *Prentice Hall. ISBN 0-13-981176-1. OCLC,* 32308337**,** 1993.
MATSUOKA, Y., NAKATSUKA, R., SUMIDE, K., KAWAMURA, H., TAKAHASHI, M., FUJIOKA, T., UEMURA, Y., ASANO, H., SASAKI, Y. & INOUE, M. 2015. Prospectively isolated human bone marrow cell-derived MSCs support primitive human CD34-negative hematopoietic stem cells. *Stem Cells,* 33**,** 1554-1565.
MAUL, R. W. & GEARHART, P. J. 2010. AID and somatic hypermutation. *Advances in immunology.* Elsevier.
MAVERAKIS, E., KIM, K., SHIMODA, M., GERSHWIN, M. E., PATEL, F., WILKEN, R., RAYCHAUDHURI, S., RUHAAK, L. R. & LEBRILLA, C. B. 2015. Glycans in the immune system and The Altered Glycan Theory of Autoimmunity: a critical review. *Journal of autoimmunity,* 57**,** 1-13.
MAWSON, A. R. & MAJUMDAR, S. 2017. Malaria, Epstein-Barr virus infection, and the Pathogenesis of Burkitt's Lymphoma. *International journal of cancer*.
MBULAITEYE, S. M. 2013. Burkitt Lymphoma: beyond discoveries. *Infectious agents and cancer,* 8**,** 35.
MCCALL, K. A., HUANG, C.-C. & FIERKE, C. A. 2000. Function and mechanism of zinc metalloenzymes. *The Journal of nutrition,* 130**,** 1437S-1446S.
MCDONALD, D. R. & LEVY, O. 2019. Innate immunity. *Clinical Immunology (Fifth Edition).* Elsevier.
MEDEIROS, L. & GREINER, T. J. C. 1995. Hodgkin's disease. 75**,** 357-369.
MELNIK, S., WERTH, N., BOEUF, S., HAHN, E.-M., GOTTERBARM, T., ANTON, M., RICHTER, W. J. S. C. R. & THERAPY 2019. Impact of c-MYC expression on proliferation, differentiation, and risk of neoplastic transformation of human mesenchymal stromal cells. 10**,** 1-18.
MESIN, L., ERSCHING, J. & VICTORA, G. D. 2016. Germinal center B cell dynamics. *Immunity,* 45**,** 471-482.
METCHNIKOFF, E. 1905. *Immunity in infective diseases*, University Press.
MEUNIER, N., O'CONNOR, J., MAIANI, G., CASHMAN, K., SECKER, D., FERRY, M., ROUSSEL, A. & COUDRAY, C. 2005. Importance of zinc in the elderly: the ZENITH study. *European journal of clinical nutrition,* 59**,** S1-S4.
MILLER, D. M., THOMAS, S. D., ISLAM, A., MUENCH, D. & SEDORIS, K. 2012. c-Myc and cancer metabolism. AACR.
MILNER, A., GRAND, R., WATERS, C. & GREGORY, C. J. O. 1993. Apoptosis in Burkitt lymphoma cells is driven by c-myc. 8**,** 3385-3391.
MIRANDA, M. & JOHNSON, D. 2007. Signal transduction pathways that contribute to myeloid differentiation. *Leukemia,* 21**,** 1363-1377.
MITCHELL, K. O. & EL-DEIRY, W. S. 1999. Overexpression of c-Myc inhibits p21WAF1/CIP1 expression and induces S-phase entry in 12-O-tetradecanoylphorbol-13-acetate (TPA)-sensitive human cancer cells.
MITCHELL, K. O., RICCI, M. S., MIYASHITA, T., DICKER, D. T., JIN, Z., REED, J. C. & EL-DEIRY, W. S. J. C. R. 2000. Bax is a transcriptional target and mediator of c-myc-induced apoptosis. 60**,** 6318-6325.
MIYAI, T., TAKANO, J., ENDO, T. A., KAWAKAMI, E., AGATA, Y., MOTOMURA, Y., KUBO, M., KASHIMA, Y., SUZUKI, Y. & KAWAMOTO, H. 2018. Three-step transcriptional priming that

drives the commitment of multipotent progenitors toward B cells. *Genes & development,* 32**,** 112-126.
MOLYNEUX, E., MERRICK, B., KHANIM, F. L., BANDA, K., DUNN, J. A., IQBAL, G., BUNCE, C. M. & DRAYSON, M. T. 2014. Bezafibrate and medroxyprogesterone acetate in resistant and relapsed endemic B urkitt lymphoma in M alawi; an open-label, single-arm, phase 2 study (ISRCTN34303497). *British journal of haematology,* 164**,** 888-890.
MOLYNEUX, E. M., ROCHFORD, R., GRIFFIN, B., NEWTON, R., JACKSON, G., MENON, G., HARRISON, C. J., ISRAELS, T. & BAILEY, S. 2012. Burkitt's lymphoma. *The Lancet,* 379**,** 1234-1244.
MOON, S.-H., CHOI, W. J., CHOI, S.-W., KIM, E. H., KIM, J., LEE, J.-O. & KIM, S. H. J. T. R. 2016. Anti-cancer activity of ZnO chips by sustained zinc ion release. 3**,** 430-438.
MORRISON, S. J. & SPRADLING, A. C. 2008. Stem cells and niches: mechanisms that promote stem cell maintenance throughout life. *Cell,* 132**,** 598-611.
MUKHTAR, F., BOFFETTA, P., RISCH, H. A., PARK, J. Y., BUBU, O. M., WOMACK, L., TRAN, T. V., ZGIBOR, J. C. & LUU, H. N. 2017. Survival predictors of Burkitt's lymphoma in children, adults and elderly in the United States during 2000–2013. *International journal of cancer,* 140**,** 1494-1502.
MURAI, Y., HAYASHI, S., TAKAHASHI, H., TSUNEYAMA, K., TAKANO, Y. J. P.-R. & PRACTICE 2005. Correlation between DNA alterations and p53 and p16 protein expression in cancer cell lines. 201**,** 109-115.
MURATA, T., SUGIMOTO, A., INAGAKI, T., YANAGI, Y., WATANABE, T., SATO, Y. & KIMURA, H. J. V. 2021. Molecular basis of epstein–barr virus latency establishment and lytic reactivation. 13**,** 2344.
MURPHY, D. J., JUNTTILA, M. R., POUYET, L., KARNEZIS, A., SHCHORS, K., BUI, D. A., BROWN-SWIGART, L., JOHNSON, L. & EVAN, G. I. J. C. C. 2008. Distinct thresholds govern Myc's biological output in vivo. 14**,** 447-457.
MURPHY, K. & WEAVER, C. 2016. *Janeway's immunobiology*, Garland Science.
MWANDA, O. 2004. Clinical characteristics of Burkitt's lymphoma seen in Kenyan patients. *East African medical journal***,** S78-89.
MWANDA, O., ROCHFORD, R., MOORMANN, A. M., MACNEIL, A., WHALEN, C. & WILSON, M. 2004. Burkitt's lymphoma in Kenya: geographical, age, gender and ethnic distribution. *East African medical journal***,** S68-77.
NESBIT, C. E., GROVE, L. E., YIN, X. & PROCHOWNIK, E. V. 1998. Differential apoptotic behaviors of c-myc, N-myc, and L-myc oncoproteins. *Cell Growth and Differentiation-Publication American Association for Cancer Research,* 9**,** 731-742.
NEUBERGER, M. S., DI NOIA, J. M., BEALE, R. C., WILLIAMS, G. T., YANG, Z. & RADA, C. 2005a. Somatic hypermutation at A· T pairs: polymerase error versus dUTP incorporation. *Nature Reviews Immunology,* 5**,** 171-178.
NEUBERGER, M. S., DI NOIA, J. M., BEALE, R. C., WILLIAMS, G. T., YANG, Z. & RADA, C. 2005b. Somatic hypermutation at A· T pairs: polymerase error versus dUTP incorporation. *Nature Reviews Immunology,* 5**,** 171.
NEWMAN, A. M., ZAKA, M., ZHOU, P., BLAIN, A. E., ERHORN, A., BARNARD, A., CROSSLAND, R. E., WILKINSON, S., ENSHAEI, A. & DE ZORDI, J. J. L. 2022. Genomic abnormalities of TP53 define distinct risk groups of paediatric B-cell non-Hodgkin lymphoma. 36**,** 781-789.
NGUYEN-KHAC, F., BOUZY, S., ROOS-WEIL, D., BRAVETTI, C., MAILLON, A., DIOP, M. B., DOUALLE, C., DROIN, N., BERNARD, O. A. & CHAPIRO, E. J. H. 2021. Acquisition of TCF3 and CCND3 Mutations and Transformation to Burkitt Lymphoma in a Case of B-Cell Prolymphocytic Leukemia. 5.
NGUYEN, L., PAPENHAUSEN, P. & SHAO, H. J. G. 2017. The role of c-MYC in B-cell lymphomas: diagnostic and molecular aspects. 8**,** 116.

NHS, G. 2022. *Full Blood Count (FBC)* [Online]. Available: https://www.gloshospitals.nhs.uk/our-services/services-we-offer/pathology/tests-and-investigations/full-blood-count-fbc/ [Accessed 14/06/2022 2022].
NIEHRS, C. & ACEBRON, S. P. 2012. Mitotic and mitogenic Wnt signalling. *The EMBO journal,* 31**,** 2705-2713.
NILSSON, J. A. & CLEVELAND, J. L. 2003. Myc pathways provoking cell suicide and cancer. *Oncogene,* 22**,** 9007-9021.
NKRUMAH, F. & PERKINS, I. J. C. 1976a. Burkitt's lymphoma. A clinical study of 110 patients. 37**,** 671-676.
NKRUMAH, F. & PERKINS, I. J. I. J. O. C. 1976b. Relapse in Burkitt's lymphoma. 17**,** 455-460.
NKUMAMA, I. N., O'MEARA, W. P. & OSIER, F. H. 2017. Changes in malaria epidemiology in Africa and new challenges for elimination. *Trends in parasitology,* 33**,** 128-140.
NOSSAL, G. J. 2003. The double helix and immunology. *Nature,* 421**,** 440-444.
NOTARI, M., NEVIANI, P., SANTHANAM, R., BLASER, B. W., CHANG, J.-S., GALIETTA, A., WILLIS, A. E., ROY, D. C., CALIGIURI, M. A. & MARCUCCI, G. J. B. 2006. A MAPK/HNRPK pathway controls BCR/ABL oncogenic potential by regulating MYC mRNA translation. 107**,** 2507-2516.
NOWAK, G. 2015. Zinc, future mono/adjunctive therapy for depression: mechanisms of antidepressant action. *Pharmacological Reports,* 67**,** 659-662.
NUNES, A. T. & ANNUNZIATA, C. M. Proteasome inhibitors: structure and function. Seminars in oncology, 2017. Elsevier, 377-380.
ODEGARD, V. H. & SCHATZ, D. G. 2006. Targeting of somatic hypermutation. *Nature reviews Immunology,* 6**,** 573.
ODUMADE, O. A., HOGQUIST, K. A. & BALFOUR JR, H. H. 2011. Progress and problems in understanding and managing primary Epstein-Barr virus infections. *Clinical microbiology reviews,* 24**,** 193-209.
OGUONU, T., EMODI, I. & KAINE, W. J. A. O. T. P. 2002. Epidemiology of Burkitt's lymphoma in Enugu, Nigeria. 22**,** 369-374.
OLIVE, V., JIANG, I. & HE, L. 2010. mir-17-92, a cluster of miRNAs in the midst of the cancer network. *The international journal of biochemistry & cell biology,* 42**,** 1348-1354.
OLIVIER, M., HOLLSTEIN, M. & HAINAUT, P. J. C. S. H. P. I. B. 2010. TP53 mutations in human cancers: origins, consequences, and clinical use. 2**,** a001008.
OLIVOTTO, I. A., LINK, E., PHILLIPS, C., WHELAN, T. J., BRYANT, G., KUNKLER, I. H., WESTENBERG, A. H., PUROHIT, K., AHERN, V. & GRAHAM, P. H. 2020. International comparison of cosmetic outcomes of breast conserving surgery and radiation therapy for women with ductal carcinoma in situ of the breast. *Radiotherapy and Oncology,* 142**,** 180-185.
OREM, J., MBIDDE, E. K., LAMBERT, B., DE SANJOSE, S. & WEIDERPASS, E. 2007. Burkitt\'s lymphoma in Africa, a review of the epidemiology and etiology. *African health sciences,* 7.
ORGANIZATION, W. H., CONTROL, C. F. D. & PREVENTION 2014. Blood donor counselling: implementation guidelines.
OTTO, T. & SICINSKI, P. J. N. R. C. 2017. Cell cycle proteins as promising targets in cancer therapy. 17**,** 93-115.
OZUAH, N. W., LUBEGA, J., ALLEN, C. E. & EL-MALLAWANY, N. K. 2020. Five decades of low intensity and low survival: adapting intensified regimens to cure pediatric Burkitt lymphoma in Africa. *Blood Advances,* 4**,** 4007-4019.
PADMANABHAN, S. 2014. *Handbook of pharmacogenomics and stratified medicine*, Academic Press.
PALMIERI, S., KAHN, P. & GRAF, T. J. T. E. J. 1983. Quail embryo fibroblasts transformed by four v-myc-containing virus isolates show enhanced proliferation but are non tumorigenic. 2**,** 2385-2389.

PANDE, S., KEYZER, M. A., AROUNA, A. & SONNEVELD, B. G. J. I. J. O. H. G. 2008. Addressing diarrhea prevalence in the West African Middle Belt: social and geographic dimensions in a case study for Benin. 7**,** 1-17.

PANDIT, B. & GARTEL, A. L. J. T. A. J. O. P. 2011. Proteasome inhibitors induce p53-independent apoptosis in human cancer cells. 178**,** 355-360.

PANNONE, G., ZAMPARESE, R., PACE, M., PEDICILLO, M. C., CAGIANO, S., SOMMA, P., ERRICO, M. E., DONOFRIO, V., FRANCO, R. & DE CHIARA, A. 2014. The role of EBV in the pathogenesis of Burkitt's Lymphoma: an Italian hospital based survey. *Infectious agents and cancer,* 9**,** 34.

PATTON, D. T., PLUMB, A. W. & ABRAHAM, N. 2014. The survival and differentiation of Pro-B and Pre-B cells in the bone marrow is dependent on IL-7Rα Tyr449. *The Journal of Immunology***,** 1302925.

PFREUNDSCHUH, M., TRÜMPER, L., ÖSTERBORG, A., PETTENGELL, R., TRNENY, M., IMRIE, K., MA, D., GILL, D., WALEWSKI, J. & ZINZANI, P.-L. 2006. CHOP-like chemotherapy plus rituximab versus CHOP-like chemotherapy alone in young patients with good-prognosis diffuse large-B-cell lymphoma: a randomised controlled trial by the MabThera International Trial (MInT) Group. *The lancet oncology,* 7**,** 379-391.

PHILIP, I., PHILIP, T., FAVROT, M., VULLLAUME, M., FONTANIERE, B., CHAMARD, D. & LENOIR, G. M. J. J. O. T. N. C. I. 1984. Establishment of lymphomatous cell lines from bone marrow samples from patients with Burkitt's lymphoma. 73**,** 835-840.

PHILIP, T. 1985. Burkitt's lymphoma in Europe. *IARC scientific publications***,** 107-118.

POOLE, C. J., ZHENG, W., LEE, H., YOUNG, D., LODH, A., CHADLI, A. & VAN RIGGELEN, J. J. C. 2018. Targeting the MYC oncogene in Burkitt lymphoma through HSP90 inhibition. 10**,** 448.

POULAKI, V., MITSIADES, C. S., KOTOULA, V., NEGRI, J., MCMILLIN, D., MILLER, J. W., MITSIADES, N. J. I. O. & SCIENCE, V. 2007. The proteasome inhibitor bortezomib induces apoptosis in human retinoblastoma cell lines in vitro. 48**,** 4706-4719.

PRASAD, A. S. 2013. Discovery of human zinc deficiency: its impact on human health and disease. *Advances in Nutrition: An International Review Journal,* 4**,** 176-190.

PRASAD, A. S., BECK, F. W., SNELL, D. C., KUCUK, O. J. N. & CANCER 2009. Zinc in cancer prevention. 61**,** 879-887.

PRASAD, A. S. & KUCUK, O. 2002. Zinc in cancer prevention. *Cancer and metastasis Reviews,* 21**,** 291-295.

PRASAD, A. S. & OBERLEAS, D. 1974. Thymidine kinase activity and incorporation of thymidine into DNA in zinc-deficient tissue. *The Journal of laboratory and clinical medicine,* 83**,** 634-639.

PRASAD, A. S. J. M. M. 2008. Zinc in human health: effect of zinc on immune cells. 14**,** 353-357.

PREUDHOMME, C., DERVITE, I., WATTEL, E., VANRUMBEKE, M., FLACTIF, M., LAI, J. L., HECQUET, B., COPPIN, M. C., NELKEN, B. & GOSSELIN, B. J. J. O. C. O. 1995. Clinical significance of p53 mutations in newly diagnosed Burkitt's lymphoma and acute lymphoblastic leukemia: a report of 48 cases. 13**,** 812-820.

PRICE, A. M. & LUFTIG, M. A. J. P. P. 2015. To be or not IIb: a multi-step process for Epstein-Barr virus latency establishment and consequences for B cell tumorigenesis. 11**,** e1004656.

PUCA, R., NARDINOCCHI, L., PORRU, M., SIMON, A. J., RECHAVI, G., LEONETTI, C., GIVOL, D. & D'ORAZI, G. J. C. C. 2011. Restoring p53 active conformation by zinc increases the response of mutant p53 tumor cells to anticancer drugs. 10**,** 1679-1689.

QIAO, X., LIU, Y., PRADA, M. L., GUPTA, A., JAISWAL, A., SHARMA, M., HAIKALA, H., TALVINEN, K., YETUKURI, L. & PYLVÄNÄINEN, J. W. J. B. 2019. Control of MYC-dependent apoptotic threshold by a co-amplified ubiquitin E3 ligase UBR5. 515247.

RADA, C., DI NOIA, J. M. & NEUBERGER, M. S. 2004. Mismatch recognition and uracil excision provide complementary paths to both Ig switching and the A/T-focused phase of somatic mutation. *Molecular cell,* 16**,** 163-171.

RADA, C. & MILSTEIN, C. 2001. The intrinsic hypermutability of antibody heavy and light chain genes decays exponentially. *The EMBO journal,* 20**,** 4570-4576.
RAMIRO, A. R. & BARRETO, V. M. 2015. Activation-induced cytidine deaminase and active cytidine demethylation. *Trends in biochemical sciences,* 40**,** 172-181.
RANDALL, K. L. 2016. Rituximab in autoimmune diseases. *Australian prescriber,* 39**,** 131.
RAWAT, J., BHADAURIA, H., SINGH, A. & VIRMANI, J. Review of leukocyte classification techniques for microscopic blood images. 2015 2nd International Conference on Computing for Sustainable Global Development (INDIACom), 2015. IEEE, 1948-1954.
REED, S., QIN, X., RAN-RESSLER, R., BRENNA, J. T., GLAHN, R. P. & TAKO, E. 2014. Dietary zinc deficiency affects blood linoleic acid: Dihomo-γ-linolenic acid (LA: DGLA) ratio; a sensitive physiological marker of zinc status in vivo (Gallus gallus). *Nutrients,* 6**,** 1164-1180.
REUTTER, K., SANDMANN, S., ROHDE, J., MÜLLER, S., WÖSTE, M., KHANAM, T., MICHGEHL, U., KLAPPER, W., WÖßMANN, W. & SEGGEWIß, J. J. L. 2021. Reconstructing clonal evolution in relapsed and non-relapsed Burkitt lymphoma. 35**,** 639-643.
REZK, S. A. & WEISS, L. M. 2007. Epstein-Barr virus–associated lymphoproliferative disorders. *Human pathology,* 38**,** 1293-1304.
RICHTER, J., M, S. & S, H. 2012. Recurrent mutation of the ID3 gene in Burkitt lymphoma identified by integrated genome, exome and transcriptome sequencing %J Nature genetics. 44**,** 1316-1320.
ROBAK, P. & ROBAK, T. J. D. I. R. 2019. Bortezomib for the treatment of hematologic malignancies: 15 years later. 19**,** 73-92.
ROCHFORD, R. 2016. Epstein-Barr virus infection of infants: implications of early age of infection on viral control and risk for Burkitt lymphoma. *Boletín Médico Del Hospital Infantil de México (English Edition),* 73**,** 41-46.
RODRIGUEZ-ABREU, D., BORDONI, A. & ZUCCA, E. 2007. Epidemiology of hematological malignancies. *Annals of oncology,* 18**,** i3-i8.
ROHDE, M., BONN, B. R., ZIMMERMANN, M., LANGE, J., MÖRICKE, A., KLAPPER, W., OSCHLIES, I., SZCZEPANOWSKI, M., NAGEL, I. & SCHRAPPE, M. 2017. Relevance of ID3-TCF3-CCND3 pathway mutations in pediatric aggressive B-cell lymphoma treated according to the non-Hodgkin Lymphoma Berlin-Frankfurt-Münster protocols. *Haematologica,* 102**,** 1091.
ROOHANI, N., HURRELL, R., KELISHADI, R. & SCHULIN, R. 2013. Zinc and its importance for human health: An integrative review. *Journal of research in medical sciences: the official journal of Isfahan University of Medical Sciences,* 18**,** 144.
ROSCHGER, C., CABRELE, C. J. C. C. & SIGNALING 2017. The Id-protein family in developmental and cancer-associated pathways. 15**,** 1-26.
ROSSARO, L., STURNIOLO, G. C., GIACON, G., MONTINO, M. C., LECIS, P. E., SCHADE, R. R., CORAZZA, G. R., TREVISAN, C. & NACCARATO, R. J. A. J. O. G. 1990. Zinc therapy in Wilson's disease: observations in five patients. 85.
ROTH, L. G., WANG, K., MACDONALD, T., MATHEW, S., TAM, Y., CRONIN, M. T., PALMER, G., LUCENA-SILVA, N., PEDROSA, F. & PEDROSA, M. J. B. 2012. Novel Genomic Alterations in MCL1 and ARID1A Identified in Pediatric Burkitt Lymphoma Using Targeted High-Throughput Sequencing. 120**,** 899.
S, S. 2019. Crystal Structures and Nuclear Magnetic Resonance Studies of the Apo Form of the c_MYC:MAX bHLHZip Complex Reveal a Helical Basic Region in the Absence of DNA. *Biochemistry,* 58**,** 3144-3154.
SACHDEVA, M., ZHU, S., WU, F., WU, H., WALIA, V., KUMAR, S., ELBLE, R., WATABE, K. & MO, Y.-Y. 2009. p53 represses c-Myc through induction of the tumor suppressor miR-145. *Proceedings of the National Academy of Sciences,* 106**,** 3207-3212.
SAHA, A. & ROBERTSON, E. S. 2019. Mechanisms of B-cell oncogenesis induced by Epstein-Barr virus. *Journal of Virology,* 93**,** e00238-19.

SALAM, D. S. D. A., THIT, E. E., TEOH, S. H., TAN, S. Y., PEH, S. C. & CHEAH, S.-C. J. J. O. C. 2020. C-MYC, BCL2 and BCL6 translocation in B-cell Non-Hodgkin Lymphoma cases. 11**,** 190.

SALGHETTI, S. E., KIM, S. Y. & TANSEY, W. P. 1999. Destruction of Myc by ubiquitin-mediated proteolysis: cancer-associated and transforming mutations stabilize Myc. *The EMBO journal,* 18**,** 717-726.

SALL, F. B., SHMAKOVA, A., KARPUKHINA, A., TSFASMAN, T., LOMOV, N., CANOY, R. J., BOUTBOUL, D., OKSENHENDLER, E., TOURE, A. O. & LIPINSKI, M. J. J. O. M. V. 2023. Epstein− Barr virus reactivation induces MYC-IGH spatial proximity and t (8; 14) in B cells. 95**,** e28633.

SAMMAK, S., HAMDANI, N., GORREC, F., ALLEN, M. D., FREUND, S. M., BYCROFT, M. & ZINZALLA, G. 2019. Crystal Structures and Nuclear Magnetic Resonance Studies of the Apo Form of the c-MYC: MAX bHLHZip Complex Reveal a Helical Basic Region in the Absence of DNA. *Biochemistry,* 58**,** 3144-3154.

SANDSTEAD, H. H. 1981. Zinc in human nutrition. *Disorders of mineral metabolism.* Elsevier.

SAPKOTA, S. & SHAIKH, H. 2020. Non-Hodgkin Lymphoma.

SAULS, R. S., MCCAUSLAND, C. & TAYLOR, B. N. 2018. Histology, T-Cell Lymphocyte.

SCHMITZ, R., CERIBELLI, M., PITTALUGA, S., WRIGHT, G. & STAUDT, L. M. 2014. Oncogenic mechanisms in Burkitt lymphoma. *Cold Spring Harbor perspectives in medicine,* 4**,** a014282.

SCHMITZ, R., YOUNG, R. M., CERIBELLI, M., JHAVAR, S., XIAO, W., ZHANG, M., WRIGHT, G., SHAFFER, A. L., HODSON, D. J. & BURAS, E. J. N. 2012. Burkitt lymphoma pathogenesis and therapeutic targets from structural and functional genomics. 490**,** 116-120.

SCHNITZER, B. 2012. *In:* HSI, E. D. (ed.) *Hematopathology (Second Edition).*

SCHRANTZ, N., AUFFREDOU, M., BOURGEADE, M., BESNAULT, L., LECA, G. & VAZQUEZ, A. 2001a. Zinc-mediated regulation of caspases activity: dose-dependent inhibition or activation of caspase-3 in the human Burkitt lymphoma B cells (Ramos). *Cell Death & Differentiation,* 8**,** 152-161.

SCHRANTZ, N., AUFFREDOU, M., BOURGEADE, M., BESNAULT, L., LECA, G., VAZQUEZ, A. J. C. D. & DIFFERENTIATION 2001b. Zinc-mediated regulation of caspases activity: dose-dependent inhibition or activation of caspase-3 in the human Burkitt lymphoma B cells (Ramos). 8**,** 152-161.

SCHROEDER JR, H. W. & CAVACINI, L. 2010. Structure and function of immunoglobulins. *Journal of Allergy and Clinical Immunology,* 125**,** S41-S52.

SCHWEITZER, A., AUFDERHEIDE, A., RUDACK, T., BECK, F., PFEIFER, G., PLITZKO, J. M., SAKATA, E., SCHULTEN, K., FÖRSTER, F. & BAUMEISTER, W. J. P. O. T. N. A. O. S. 2016. Structure of the human 26S proteasome at a resolution of 3.9 Å. 113**,** 7816-7821.

SEARS, R. C. 2004. The life cycle of C-myc: from synthesis to degradation. *Cell cycle,* 3**,** 1131-1135.

SENBANJO, I. J. I. J. O. N. 2009. Tumor lysis and acute renal failure in Burkitt's lymphoma: A review on pathophysiology and management. 19**,** 83.

SEPULVEDA, M. A., EMELYANOV, A. V. & BIRSHTEIN, B. K. J. T. J. O. I. 2004. NF-κB and Oct-2 synergize to activate the human 3′ Igh hs4 enhancer in B cells. 172**,** 1054-1064.

SHABIR, S., GIRDLESTONE, J., BRIGGS, D., KAUL, B., SMITH, H., DAGA, S., CHAND, S., JHAM, S., NAVARRETE, C. & HARPER, L. 2015. Transitional B lymphocytes are associated with protection from kidney allograft rejection: a prospective study. *American Journal of Transplantation,* 15**,** 1384-1391.

SHACHAF, C. M., GENTLES, A. J., ELCHURI, S., SAHOO, D., SOEN, Y., SHARPE, O., PEREZ, O. D., CHANG, M., MITCHEL, D. & ROBINSON, W. H. J. C. R. 2008. Genomic and proteomic analysis reveals a threshold level of MYC required for tumor maintenance. 68**,** 5132-5142.

SHAH, H., STEPHENS, D., SEYMOUR, J. & MADDOCKS, K. 2021. Incorporating Novel Targeted and Immunotherapeutic Agents in the Treatment of B-Cell Lymphomas. *American Society of Clinical Oncology Educational Book,* 41**,** 310-327.

SHAHAF, G., ZISMAN-ROZEN, S., BENHAMOU, D., MELAMED, D. & MEHR, R. 2016. B cell development in the bone marrow is regulated by homeostatic feedback exerted by mature B cells. *Frontiers in immunology,* 7**,** 77.

SHAIKH, A. & BHARTIYA, D. 2012. Pluripotent stem cells in bone marrow and cord blood. *Blood Cell-An Overview of Studies in Hematology***,** 69-88.

SHAMOON, R. P., ALI, M. D. & SHABILA, N. P. J. P. O. 2018. Overview and outcome of Hodgkin's Lymphoma: Experience of a single developing country's oncology centre. 13**,** e0195629.

SHANKAR, A. H., GENTON, B., BAISOR, M., PAINO, J., TAMJA, S., ADIGUMA, T., WU, L., RARE, L., BANNON, D., TIELSCH, J. M. J. T. A. J. O. T. M. & HYGIENE 2000. The influence of zinc supplementation on morbidity due to Plasmodium falciparum: a randomized trial in preschool children in Papua New Guinea. 62**,** 663-669.

SHAPIRA, J. & PEYLAN-RAMU, N. 1998. Burkitt's lymphoma. *Oral oncology,* 34**,** 15-23.

SHARQUIE, K., NAJIM, R., FARJOU, I., AL-TIMIMI, D. J. C. & DERMATOLOGY, E. 2001. Oral zinc sulphate in the treatment of acute cutaneous leishmaniasis. 26**,** 21-26.

SHECHTER, O., SAUSEN, D. G., GALLO, E. S., DAHARI, H. & BORENSTEIN, R. J. I. J. O. M. S. 2022. Epstein–Barr Virus (EBV) Epithelial Associated Malignancies: Exploring Pathologies and Current Treatments. 23**,** 14389.

SHEN, W.-C. & LOUIE, S. G. 2014. *Immunology for pharmacy students*, Routledge.

SHIMA, H., NAKAYASU, M., AONUMA, S., SUGIMURA, T. & NAGAO, M. J. P. O. T. N. A. O. S. 1989. Loss of the MYC gene amplified in human HL-60 cells after treatment with inhibitors of poly (ADP-ribose) polymerase or with dimethyl sulfoxide. 86**,** 7442-7445.

SHIMABUKURO-VORNHAGEN, A., HAVERKAMP, H., ENGERT, A., BALLEISEN, L., MAJUNKE, P., HEIL, G., EICH, H. T., STEIN, H., DIEHL, V. & JOSTING, A. J. J. C. O. 2005. Lymphocyte-rich classical Hodgkin's lymphoma: clinical presentation and treatment outcome in 100 patients treated within German Hodgkin's Study Group trials. 23**,** 5739-45.

SIEGAL, F. P., KADOWAKI, N., SHODELL, M., FITZGERALD-BOCARSLY, P. A., SHAH, K., HO, S., ANTONENKO, S. & LIU, Y.-J. 1999. The nature of the principal type 1 interferon-producing cells in human blood. *Science,* 284**,** 1835-1837.

SIMPSON, L. J. & SALE, J. E. 2003. Rev1 is essential for DNA damage tolerance and non-templated immunoglobulin gene mutation in a vertebrate cell line. *The EMBO journal,* 22**,** 1654-1664.

SINGER, M. & BAER, H. 2018. *Critical medical anthropology*, Routledge.

SINGH, R., SOMAN-FAULKNER, K. & SUGUMAR, K. 2019. Embryology, Hematopoiesis.

SIRINIAN, M., PISEGNA, S., PAROLI, M., MILITI, S., TESTA, U. & PESCHLE, C. 2003. Zinc modulates c-Myc/Mad1 balance in human leukemia cells. *Leukemia,* 17**,** 272.

SMATTI, M. K., AL-SADEQ, D. W., ALI, N. H., PINTUS, G., ABOU-SALEH, H. & NASRALLAH, G. K. 2018. Epstein–Barr virus epidemiology, serology, and genetic variability of LMP-1 oncogene among healthy population: an update. *Frontiers in oncology,* 8**,** 211.

SOAVE, C. L., GUERIN, T., LIU, J., DOU, Q. P. J. C. & REVIEWS, M. 2017. Targeting the ubiquitin-proteasome system for cancer treatment: discovering novel inhibitors from nature and drug repurposing. 36**,** 717-736.

SOCHOCKA, M. & BŁACH-OLSZEWSKA, Z. 2005. Mechanisms of innate immunity. *Postepy higieny i medycyny doswiadczalnej (Online),* 59**,** 250-258.

SPENCER, C. A. & GROUDINE, M. J. A. I. C. R. 1991. Control of c-myc regulation in normal and neoplastic cells. 56**,** 1-48.

SPERANDIO, B., FISCHER, N. & SANSONETTI, P. J. Mucosal physical and chemical innate barriers: Lessons from microbial evasion strategies. Seminars in immunology, 2015. Elsevier, 111-118.

SRIVASTAVA, P. & PANDEY, A. 2015. Role of immunostimulants in immune responses of fish and shellfish. *Biochemical and Cellular Archives,* 15**,** 47-73.

STAVNEZER, J. J. T. I. I. 2011. Complex regulation and function of activation-induced cytidine deaminase. 32**,** 194-201.
STEFAN, C., BRAY, F., FERLAY, J., LIU, B. & PARKIN, D. M. 2017. Cancer of childhood in sub-Saharan Africa. *ecancermedicalscience,* 11.
STRAUSS, S. J., HIGGINBOTTOM, K., JÜLIGER, S., MAHARAJ, L., ALLEN, P., SCHENKEIN, D., LISTER, T. A. & JOEL, S. P. J. C. R. 2007. The proteasome inhibitor bortezomib acts independently of p53 and induces cell death via apoptosis and mitotic catastrophe in B-cell lymphoma cell lines. 67**,** 2783-2790.
SUK, F.-M., LIN, S.-Y., LIN, R.-J., HSINE, Y.-H., LIAO, Y.-J., FANG, S.-U. & LIANG, Y.-C. 2015. Bortezomib inhibits Burkitt's lymphoma cell proliferation by downregulating sumoylated hnRNP K and c-Myc expression. *Oncotarget,* 6**,** 25988.
SUNDBERG, T. B., NEY, G. M., SUBRAMANIAN, C., OPIPARI JR, A. W. & GLICK, G. D. 2006. The immunomodulatory benzodiazepine Bz-423 inhibits B-cell proliferation by targeting c-myc protein for rapid and specific degradation. *Cancer research,* 66**,** 1775-1782.
SWERDLOW, S. H., CAMPO, E., PILERI, S. A., HARRIS, N. L., STEIN, H., SIEBERT, R., ADVANI, R., GHIELMINI, M., SALLES, G. A. & ZELENETZ, A. D. J. B., THE JOURNAL OF THE AMERICAN SOCIETY OF HEMATOLOGY 2016. The 2016 revision of the World Health Organization classification of lymphoid neoplasms. 127**,** 2375-2390.
TABATA, M., TSUBAKI, M., TAKEDA, T., TATEISHI, K., TSURUSHIMA, K., IMANO, M., SATOU, T., ISHIZAKA, T., NISHIDA, S. J. B. C. M. & THERAPIES 2020. Dasatinib reverses drug resistance by downregulating MDR1 and Survivin in Burkitt lymphoma cells. 20**,** 1-9.
TANSEY, W. P. 2014. Mammalian MYC proteins and cancer. *New Journal of Science,* 2014.
TATINENI, V., AN, J. Y., LEFFEW, M. R. & MAHESH, S. A. 2020. Anemia from A to zinc: hypocupremia in the setting of gastric bypass and zinc excess. *Clinical Case Reports,* 8**,** 745-750.
TAVIAN, M. & PEAULT, B. 2003. Embryonic development of the human hematopoietic system. *International Journal of Developmental Biology,* 49**,** 243-250.
TERME, J.-M., CALVIGNAC, S., DUC DODON, M., GAZZOLO, L. & JORDAN, A. 2009. E box motifs as mediators of proviral latency of human retroviruses. *Retrovirology,* 6**,** 1-5.
THIDA, A. M. & TUN, A. M. 2021. Lymphocyte Depleted Hodgkin Lymphoma. *StatPearls [Internet].* StatPearls Publishing.
THINGHOLM, T., RÖNNSTRAND, L. & ROSENBERG, P. 2020. Why and how to investigate the role of protein phosphorylation in ZIP and ZnT zinc transporter activity and regulation. *Cellular and Molecular Life Sciences,* 77**,** 3085-3102.
THOMAS, D. A., O'BRIEN, S., FADERL, S., MANNING, J. T., ROMAGUERA, J., FAYAD, L., HAGEMEISTER, F., MEDEIROS, J., CORTES, J. & KANTARJIAN, H. 2011. Burkitt lymphoma and atypical Burkitt or Burkitt-like lymphoma: should these be treated as different diseases? *Current hematologic malignancy reports,* 6**,** 58-66.
THOMAS, L. R. & TANSEY, W. P. 2011. Proteolytic control of the oncoprotein transcription factor Myc. *Advances in cancer research.* Elsevier.
THOMAS, M. E., GRINSHPON, R., SWARTZ, P. & CLARK, A. C. J. J. O. B. C. 2018. Modifications to a common phosphorylation network provide individualized control in caspases. 293**,** 5447-5461.
THOMPSON, E. B. 1998. The many roles of c-Myc in apoptosis. *Annual review of physiology,* 60**,** 575.
THORLEY-LAWSON, D., DEITSCH, K. W., DUCA, K. A. & TORGBOR, C. 2016. The Link between Plasmodium falciparum Malaria and Endemic Burkitt's Lymphoma—New Insight into a 50-Year-Old Enigma. *PLoS pathogens,* 12**,** e1005331.
TOBÓN, G. J., IZQUIERDO, J. H. & CAÑAS, C. A. 2013. B Lymphocytes: development, tolerance, and their role in autoimmunity—focus on systemic lupus erythematosus. *Autoimmune diseases,* 2013.

TRUONG-TRAN, A. Q., CARTER, J., RUFFIN, R. E. & ZALEWSKI, P. D. 2001. The role of zinc in caspase activation and apoptotic cell death. *Zinc Biochemistry, Physiology, and Homeostasis***,** 129-144.

TSUJI, T., KATSURANO, M., IBARAGI, S., SHIMA, K., SASAKI, A. & HU, G.-F. 2007. Ornithine decarboxylase antizyme upregulates DNA-dependent protein kinase and enhances the nonhomologous end-joining repair of DNA double-strand breaks in human oral cancer cells. *Biochemistry,* 46**,** 8920-8932.

TUERK, M. J. & FAZEL, N. J. C. O. I. G. 2009. Zinc deficiency. 25**,** 136-143.

TW MAK, M. S., BD JETT 2014. Chapter 5 - B Cell Development, Activation and Effector Functions. *Primer to the Immune Response (Second Edition).* Boston: Academic Cell.

UK, C. R. 2022. *Non-Hodgkin lymphoma-Survival* [Online]. Available: https://www.cancerresearchuk.org/about-cancer/non-hodgkin-lymphoma/survival#:~:text=Burkitt%20lymphoma%20is%20a%20less,or%20more%20after%20their%20diagnosis.

VAN RIGGELEN, J., MÜLLER, J., OTTO, T., BEUGER, V., YETIL, A., CHOI, P. S., KOSAN, C., MÖRÖY, T., FELSHER, D. W. & EILERS, M. 2010. The interaction between Myc and Miz1 is required to antagonize TGFβ-dependent autocrine signaling during lymphoma formation and maintenance. *Genes & development,* 24**,** 1281-1294.

VEENEMANS, J., SCHOUTEN, L. R., OTTENHOF, M. J., MANK, T. G., UGES, D. R., MBUGI, E. V., DEMIR, A. Y., KRAAIJENHAGEN, R. J., SAVELKOUL, H. F. & VERHOEF, H. 2012. Effect of preventive supplementation with zinc and other micronutrients on non-malarial morbidity in Tanzanian pre-school children: a randomized trial.

VERDU-BOU, M., TAPIA, G., HERNANDEZ-RODRIGUEZ, A. & NAVARRO, J.-T. 2021. Clinical and Therapeutic Implications of Epstein–Barr Virus in HIV-Related Lymphomas. *Cancers,* 13**,** 5534.

VINKENBORG, J. L., NICOLSON, T. J., BELLOMO, E. A., KOAY, M. S., RUTTER, G. A. & MERKX, M. 2009. Genetically encoded FRET sensors to monitor intracellular Zn2+ homeostasis. *Nature methods,* 6**,** 737-740.

VOYNOW, J. A. & RUBIN, B. K. 2009. Mucins, mucus, and sputum. *Chest,* 135**,** 505-512.

WAKABAYASHI-ITO, N. & NAGATA, S. J. J. O. B. C. 1994. Characterization of the regulatory elements in the promoter of the human elongation factor-1 alpha gene. 269**,** 29831-29837.

WALKER, C. F., ABOUBAKER, S., VAN DE WEERDT, R. & BLACK, R. E. J. E. A. M. J. 2007. Zinc for diarrhoea managment in sub-Saharan Africa: a review. 84**,** 441-449.

WANG, G., WANG, F., HUANG, Q., LI, Y., LIU, Y. & WANG, Y. 2015. Understanding transcription factor regulation by integrating gene expression and dnase i hypersensitive sites. *BioMed research international,* 2015.

WANG, H., GUO, M., WEI, H., CHEN, Y. J. J. O. H. & ONCOLOGY 2021. Targeting MCL-1 in cancer: current status and perspectives. 14**,** 1-18.

WANG, X., XU, Z., TIAN, Z., ZHANG, X., XU, D., LI, Q., ZHANG, J., WANG, T. J. J. O. C. & MEDICINE, M. 2017. The EF-1α promoter maintains high-level transgene expression from episomal vectors in transfected CHO-K1 cells. 21**,** 3044-3054.

WANG, Z., STRASSER, A., KELLY, G. L. J. C. D. & DIFFERENTIATION 2022. Should mutant TP53 be targeted for cancer therapy? 29**,** 911-920.

WAPNER, J. 2014. *The Philadelphia chromosome: a genetic mystery, a lethal cancer, and the improbable invention of a lifesaving treatment*, The Experiment.

WESSELLS, K. R. & BROWN, K. H. J. P. O. 2012. Estimating the global prevalence of zinc deficiency: results based on zinc availability in national food supplies and the prevalence of stunting. 7**,** e50568.

WILDES, T. M., FARRINGTON, L., YEUNG, C., HARRINGTON, A. M., FOYIL, K. V., LIU, J., KREISEL, F., BARTLETT, N. L. & FENSKE, T. S. 2014. Rituximab is associated with improved survival in

Burkitt lymphoma: a retrospective analysis from two US academic medical centers. *Therapeutic Advances in Hematology,* 5**,** 3-12.
WILLIAMS, C., FOLAMI, A., SERIKI, O. J. E. J. O. C. & ONCOLOGY, C. 1983. Patterns of treatment failure in Burkitt's lymphoma. 19**,** 741-746.
WOESSMANN, W., ZIMMERMANN, M., MEINHARDT, A., MÜLLER, S., HAUCH, H., KNÖRR, F., OSCHLIES, I., KLAPPER, W., NIGGLI, F. & KABICKOVA, E. J. B. 2020. Progressive or relapsed Burkitt lymphoma or leukemia in children and adolescents after BFM-type first-line therapy. 135**,** 1124-1132.
WONG, C. P., HO, E. J. M. N. & RESEARCH, F. 2012. Zinc and its role in age-related inflammation and immune dysfunction. 56**,** 77-87.
WOOD, E. 2004. Cellular and molecular immunology: Abbas AK, and Lichtman, AH. *Biochemistry and Molecular Biology Education,* 32**,** 65-66.
WU, R.-C., WANG, T.-L., SHIH, I.-M. J. C. B. & THERAPY 2014. The emerging roles of ARID1A in tumor suppression. 15**,** 655-664.
WYŻEWSKI, Z., MIELCARSKA, M. B., GREGORCZYK-ZBOROCH, K. P. & MYSZKA, A. J. I. J. O. M. S. 2022. Virus-mediated inhibition of apoptosis in the context of EBV-associated diseases: Molecular mechanisms and therapeutic perspectives. 23**,** 7265.
XIANG, H., NOONAN, E. J., WANG, J., DUAN, H., MA, L., MICHIE, S. & BOXER, L. M. J. L. 2011. The immunoglobulin heavy chain gene 3′ enhancers induce Bcl2 deregulation and lymphomagenesis in murine B cells. 25**,** 1484-1493.
XIE, Y., PITTALUGA, S. & JAFFE, E. S. The histological classification of diffuse large B-cell lymphomas. Seminars in hematology, 2015. Elsevier, 57-66.
XU, Z., IWATSUKI, K., OYAMA, N., OHTSUKA, M., SATOH, M., KIKUCHI, S., AKIBA, H. & KANEKO, F. J. B. J. O. C. 2001. The latency pattern of Epstein–Barr virus infection and viral IL-10 expression in cutaneous natural killer/T-cell lymphomas. 84**,** 920-925.
YAMAZAKI, T., LIU, L., CONLON, E. G. & MANLEY, J. L. J. R. B. 2020. Burkitt lymphoma-related TCF3 mutations alter TCF3 alternative splicing by disrupting hnRNPH1 binding. 17**,** 1383-1390.
YAN, M., SONG, Y., WONG, C. P., HARDIN, K. & HO, E. J. T. J. O. N. 2008. Zinc deficiency alters DNA damage response genes in normal human prostate epithelial cells. 138**,** 667-673.
YANG, J., LIU, Z., ZENG, B., HU, G. & GAN, R. J. C. L. 2020. Epstein–Barr virus-associated gastric cancer: A distinct subtype. 495**,** 191-199.
YANG, X.-G., LI, X.-L., CHEN, Y.-J., XIE, Z.-X., PENG, M.-Y., HUANG, X.-C. & HUANG, R.-X. J. Z. S. Y. X. Y. X. Z. Z. 2009. Apoptosis of Burkitt's lymphoma Raji cell line induced by bortezomib. 17**,** 592-596.
YESHAW, Y., WORKU, M. G., TESSEMA, Z. T., TESHALE, A. B. & TESEMA, G. A. J. P. O. 2020. Zinc utilization and associated factors among under-five children with diarrhea in East Africa: A generalized linear mixed modeling. 15**,** e0243245.
YI, C., YU, Z., REN, Q., LIU, X., WANG, Y., SUN, X., YIN, S., PAN, J., HUANG, X. J. P. & THERAPY, P. 2020. Nanoscale ZnO-based photosensitizers for photodynamic therapy. 30**,** 101694.
YOU, Z., MADRID, L. V., SAIMS, D., SEDIVY, J. & WANG, C.-Y. J. J. O. B. C. 2002a. c-Myc sensitizes cells to tumor necrosis factor-mediated apoptosis by inhibiting nuclear factor κB transactivation. 277**,** 36671-36677.
YOU, Z., SAIMS, D., CHEN, S., ZHANG, Z., GUTTRIDGE, D. C., GUAN, K.-L., MACDOUGALD, O. A., BROWN, A. M., EVAN, G. & KITAJEWSKI, J. 2002b. Wnt signaling promotes oncogenic transformation by inhibiting c-Myc–induced apoptosis. *The Journal of cell biology,* 157**,** 429-440.
YOUNG, G. P., MORTIMER, E. K., GOPALSAMY, G. L., ALPERS, D. H., BINDER, H. J., MANARY, M. J., RAMAKRISHNA, B. S., BROWN, I. L. & BREWER, T. G. 2014. Zinc deficiency in children with environmental enteropathy—development of new strategies: report from an expert workshop. Oxford University Press.

YOUNG, L. S. & RICKINSON, A. B. 2004. Epstein–Barr virus: 40 years on. *Nature Reviews Cancer,* 4**,** 757.

ZENG, X., WINTER, D. B., KASMER, C., KRAEMER, K. H., LEHMANN, A. R. & GEARHART, P. J. 2001. DNA polymerase η is an AT mutator in somatic hypermutation of immunoglobulin variable genes. *Nature immunology,* 2**,** 537.

ZHANG, J., LI, B., WU, H., OU, J., WEI, R., LIU, J., CAI, W., LIU, X., ZHAO, S. & YANG, J. J. T. B. 2016. Synergistic action of 5Z-7-oxozeaenol and bortezomib in inducing apoptosis of Burkitt lymphoma cell line Daudi. 37**,** 531-539.

ZHANG, L., NOMIE, K., ZHANG, H., BELL, T., PHAM, L., KADRI, S., SEGAL, J., LI, S., ZHOU, S. & SANTOS, D. J. C. C. R. 2017. B-Cell Lymphoma Patient-Derived Xenograft Models Enable Drug Discovery and Are a Platform for Personalized TherapyB-Cell Lymphoma PDX Model for Personalized Therapy. 23**,** 4212-4223.

ZHOU, P., BLAIN, A. E., NEWMAN, A. M., ZAKA, M., CHAGALUKA, G., ADLAR, F. R., OFFOR, U. T., BROADBENT, C., CHAYTOR, L. & WHITEHEAD, A. 2019. Sporadic and endemic Burkitt lymphoma have frequent FOXO1 mutations but distinct hotspots in the AKT recognition motif. *Blood advances,* 3**,** 2118-2127.

ZHU, J. & EMERSON, S. G. 2002. Hematopoietic cytokines, transcription factors and lineage commitment. *Oncogene,* 21**,** 3295-3313.

ZIEGLER, J. L. J. N. E. J. O. M. 1977. Treatment results of 54 American patients with Burkitt's lymphoma are similar to the African experience. 297**,** 75-80.

ZOU, P., KAWADA, J., PESNICAK, L. & COHEN, J. I. J. J. O. V. 2007. Bortezomib induces apoptosis of Epstein-Barr virus (EBV)-transformed B cells and prolongs survival of mice inoculated with EBV-transformed B cells. 81**,** 10029-10036.

CHAPTER NINE
APPENDICES

10 Appendix A.

10.1 Materials and methods buffer and solution preparations.

10.2 Western blotting.

10.2.1 10X Running SDS buffer (for 2 litre).

Compound name	Chemical form	Volume or weight	Final compound concentration in 2 L
tris(hydroxymethyl)aminomethane (Tris) (121.14 g/mol)	powder	60 g	250 mM
Glycine (75.07 g/mol)	powder	288 g	1.92 M
Sodium dodecyl sulfate (SDS) (288.38 g/mol)	powder	20 g	34.67 mM

- All compounds are mixed in a glass bottle with dH_2O up to 2 L (keep at room temperature).

- 1X running SDS buffer was prepared by diluting 10X running SDS with dH_2O 1:10 (keep at room temperature).

10.2.2 10X Transfer buffer (for 1 litre).

Compound name	Chemical form	Volume or weight	Final compound concentration in 1 L
tris(hydroxymethyl)aminomethane (Tris) (121.14 g/mol)	powder	30 g	250 mM
glycine	powder	144 g	1.92 M

- All compounds are mixed in a glass bottle with dH_2O up to 1 L (keep at room temperature).

- 1X transfer buffer was prepared by diluting 10X transfer buffer with dH_2O 1:10 with 20% methanol (200 mL methanol + 100 mL 10X transfer buffer + dH_2O up to 1 L (keep at 4 °C).

10.2.3 1 M Tris solution (PH 7.5) (1 litre).

- 121.14 g Tris.

- 800 mL dH2O.

- Adjust PH with Hydrochloric acid (HCL) or Sodium hydroxide (NaOH).

- Add dH_2O up to 1 L (keep at room temperature).

10.2.4 Tris-buffered saline (TBS) (2 litre).

Compound name	Chemical form	Volume or weight	Final compound concentration in 2 L
1 M Tris PH 7.5	liquid	40 mL	20 mM
Sodium chloride (NaCl) 58.44 (g/mol)	Powder / granules	16 g	136.89 M

- All compounds are mixed in a glass bottle with dH_2O up to 2 L (keep at room temperature).

10.2.5 Tris-buffered saline (TBS-T) (2 litre).

- Same Tris-buffered saline (TBS) ingredients + adding 2 mL of (Tween® 20).

- All compounds are mixed in a glass bottle with dH_2O up to 2 L (keep at room temperature).

10.2.6 Tris 1.5 M (PH 8.8) (500 mL).

Compound name	Volume (mL)
tris(hydroxymethyl)aminomethane (Tris) (121.14 g/mol)	90.8 g
dH_2O	400 mL

- Mix well and adjust solution PH to 8.8 with Hydrochloric acid (HCL) or Sodium hydroxide (NaOH) then fill with dH_2O up to 500 mL (keep at room temperature).

10.2.7 Tris 1 M (PH 6.8).

Compound name	Volume (mL)
tris(hydroxymethyl)aminomethane (Tris) (121.14 g/mol)	90.8 g
dH_2O	400 mL

- Mix well and adjust solution PH to 6.8 with Hydrochloric acid (HCL) or Sodium hydroxide (NaOH) then fill with dH_2O up to 500 mL (keep at room temperature).

10.2.8 Tris-glycine SDS-polyacrylamide gel.

A- Resolving gel (10 mL).

Compound name	Volume (mL)
dH_2O	3.3
30% acrylamide mix (ProtoGel)	4
1.5 M Tris (PH 8.8)	2.5
10% SDS	0.1
10% ammonium persulphate (APS)	0.1
Tetramethylethylenediamine (TEMED)	0.004

B- Stacking gel (5 mL).

Compound name	Volume (mL)
dH_2O	3.4
30% acrylamide mix (ProtoGel)	0.83
1 M Tris (PH 6.8)	0.63
10% SDS	0.05
10% ammonium persulphate (APS)	0.05
Tetramethylethylenediamine (TEMED)	0.005

10.2.9 Radioimmunoprecipitation assay cell lysis buffer (RIPA buffer) (100 mL).

Compound name	Chemical form	Volume or weight
NP40	liquid	1 mL
Sodium deoxycholate (414.6 g/mol)	Powder	0.5 g
10% SDS	liquid	mL

- All compounds are mixed in a glass bottle with dH2O up to 100 mL (keep at 4 °C).

- Before using, 1 tablet of cOmplete™, Mini Protease Inhibitor Cocktail is added to 7 mL of RIPA buffer and then kept at -20 °C.

10.2.10 Protein gel loading buffer (4X SDS).

Compound name	Chemical form	Volume or weight
Tris PH 6.8	liquid	2 mL
Glycerol (92.09382 g/mol)	liquid	4 mL
Sodium dodecyl sulfate (SDS) (288.38 g/mol)	powder	0.8 g
β-mercaptoethano 14.7 M	liquid	0.4 mL
Ethylenediaminetetraacetic acid (EDTA) 0.5 M	liquid	1 mL
Bromophenol blue	powder	0.8 mg

- All compounds are mixed in a glass bottle with dH2O up to 8 mL (keep at -20 °C).

- Mix with protein lysate upon loading to acrylamide gel with respect to total protein concentration.

10.2.11 Tris borate buffer (TBE).

Compound name	Chemical form	Volume or weight
Tris	powder	10.8 g
Boric acid (61.83 g/mol)	Powder	5.5 g
Ethylenediaminetetraacetic acid (EDTA) 5 M PH 8	liquid	4 ml

- All compounds are mixed in a glass bottle with dH2O up to 1 L (keep at room temperature).

10.2.12 Preparation pf agarose gel (2 %).

Compound name	Chemical form	Volume or weight
Agarose	powder	2 g
1X TBE buffer	liquid	100 mL
Ethidium bromide (Added after heating the above)	liquid	5 µL

- All compounds are mixed in a glass bottle and microwave heated. Ethidium bromide was added when mixture cooled down (before solidified).

10.3 Flow cytometry fixation solution (FACS FIX).

Compound name	Chemical form	Volume or weight
Formaldehyde (37/40%)	liquid	16.6 mL
Fetal bovine serum (FBS)	liquid	10 mL
Phosphate buffered saline (PBS)	liquid	10.4 mL

- All compounds are mixed in a glass bottle and kept at 4 °C.

10.5 Cell cycle buffer.

Compound name	Chemical form	Volume or weight
Sodium chloride (NaCl)	Powder	584.4 mg
Triton	liquid	1 mL
propidium iodide (30 µg/mL)	liquid	3 mL

- All compounds are mixed in a glass bottle with dH2O up to 100 mL and kept at 4 °C.

10.6 Transfection reagents (Piggybac transfection).

10.6.1 Luria Bertanibroth (LB).

Compound name	Chemical form	Volume or weight
LB broth (L3022)	powder	10 g

- LB broth was mixed in a glass bottle with dH2O up to 500 mL.
- LB mixture was autoclaved.
- 500 µg Ampicillin ➔ (100 µg/mL).
- Bacterial growth was performed on sterile surface close to Bunsen burner.

11 Appendix B.

11.1 Vector construct.

All details are obtained from VectorBuilder spreadsheet for each plasmid construct.

11.1.1 VB200623-1116ump.

Name	Description
5' ITR	piggyBac 5' inverted terminal repeat
EF1A	Human eukaryotic translation elongation factor 1 α1 promoter
Kozak	Kozak translation initiation sequence
C-MYC	C-MYC gene
T2A	Self-cleaving 2A peptide
EGFP	Enhanced green fluorescent protein
rBG pA	Rabbit Polyadenylation signal
CMV promoter	Human cytomegalovirus immediate early promoter
Hygro	Hygromycin resistance

BGH pA	Polyadenylation signal
3' ITR	piggyBac 3' inverted terminal repeat
Ampicillin	Ampicillin resistance
pUC ori	origin of replication

11.1.2 VB900088-2218fcw.

Name	Description
5' ITR	piggyBac 5' inverted terminal repeat
EF1A	Human eukaryotic translation elongation factor 1 α1 promoter
Kozak	Kozak translation initiation sequence
EGFP	Enhanced green fluorescent protein
rBG pA	Rabbit Polyadenylation signal
CMV promoter	Human cytomegalovirus immediate early promoter
Hygro	Hygromycin resistance
BGH pA	Polyadenylation signal
3' ITR	piggyBac 3' inverted terminal repeat
Ampicillin	Ampicillin resistance
pUC ori	origin of replication

11.1.3 VB160216-10057.

Name	Description
CAG	piggyBac 5' inverted terminal repeat
Kozak	Kozak translation initiation sequence
hyPBase	piggyback transposase (PBase)
SV40 late pA	Simian virus 40 late polyadenylation signal
CMV promoter	Human cytomegalovirus immediate early enhancer/promoter
mCherry	Variant of mRFP1
BGH pA	Polyadenylation signal
pUC ori	origin of replication
Ampicillin	Ampicillin resistance

12 Appendix C.
12.1 FMC drug library full list.

Drug Name	Drug Name
prednisolone	itraconazole
amantidine hydrochloride	methyldopa
folic acid	fenofibrate,
thiamine HCL,	clofibric acid
ranitidine/zantac	clobetasol propionate
fluoxetine	paracetamol (acetaminophen),
dexamethasone	alverine citrate
DMSO	mefenamic acid
phytomenadione/ vitamin K1	prochlorperazine
carbamazepine	chlorambucil
propanolol hydrochloride	metoclopramide HCL
erythromycin	chloroquine
retinol	metformin hydrochloride
bendroflumethiazide	niclosamide
propylthiouracil	pravastatin sodium
nicotinic acid	nortriptyline
theophylline	dantrolene sodium
nicotinamide	omeprazole
ascorbic acid	diclofenac sodium
Acyclovir	ritodrine hydrochloride,
allopurinol	selegiline hydrochloride / deprenyl HCl
chlorpheniramine disodium salt	mebendazole
neostigmine	flupentixol
alpha tocopheryl acetate	acipimox
2-bromo-a-ergocryptine methanesulfonate salt/ bromocriptine	ethanol
cyclophosphamide	desferrioxamine mesilate
imatinib	imipramine
zinc acetate	artemisinin
valproic acid	propantheline bromide
rifampicin	diltiazem hydrochloride
	ampicillin sodium salt
praziquantel	methanol
flutamide	amphotericin b
clomipramine	danazol
testosterone	phenoxymethyl penicillin
calciferol/ergocalciferol	5'aminosalicyclic acid/ mesalazine
doxycycline	finasteride
tetracycline	colchicine
ibuprofen	levothyroxine sodium

norethisterone	methotrexate
cefaclor	chloramphenicol
cyanocobalamin (vitamin B12)	Bortezomib
medroxyprogesterone acetate	mifepristone
bezafibrate	phenelzine
paroxetine,	media
trimethoprim	clomiphene citrate
water	carvedilol
naloxone hydrochloride	amiodarone
simvastatin,	methylphenidate
flecainide acetate	selenium
pilocarpine HCl	meperidine phenidate
fluconazole	riboflavin
acitretin	Memantine
Magnesium Sulfate (MgSO4)	